

# **Investigations on Azide Functional Polymers as Binders for Solid Propellants**

A Thesis  
Submitted for the Degree of  
***Doctor of Philosophy***  
in the Faculty of Science

by

**S.Reshmi**



**Department of Inorganic and Physical Chemistry**

**INDIAN INSTITUTE OF SCIENCE**

**BANGALORE- 560012, INDIA**

**July, 2014**

*Dedicated to my family*

## Declaration

I hereby declare that the work presented in this thesis entitled "**Investigations on Azide Functional Polymers as Binders for Solid Propellants**" has been carried out by me under the joint supervision of Professor E. Arunan, Department of Inorganic and Physical Chemistry, Indian Institute of Science, Bangalore, India, and Dr.C.P.Reghunadhan Nair, Group Director, Vikram Sarabhai Space Centre, Thiruvananthapuram.

Date

S.Reshmi

## Certificate

We hereby certify that the work presented in this thesis entitled "**Investigations on Azide Functional Polymers as Binders for Solid Propellants**" has been carried out by Ms. S. Reshmi at the Department of Inorganic and Physical Chemistry, Indian Institute of Science, Bangalore, India and at Vikram Sarabhai Space Centre, Thiruvananthapuram, India, under our joint supervision.

Dr.C.P.Reghunadhan Nair  
(Research Supervisor)  
Group Director  
Polymers and Special Chemicals Group  
Vikram Sarabhai Space Centre  
Thiruvananthapuram, India

Prof. E. Arunan  
(Research Supervisor)  
Professor  
Dept. of Inorganic and Physical Chemistry  
Indian Institute of Science  
Bangalore, India

Date

## ACKNOWLEDGMENTS

I express my heartfelt gratitude to my research supervisors Dr. C. P. Reghunadhan Nair, Group Director, PSCG, VSSC and Prof. E. Arunan, Professor, Department of Inorganic and Physical Chemistry for their motivation and guidance. Dr.C. P. Reghunadhan Nair has taken keen interest and navigated this work amidst his busy schedules. I owe him especially for the directions shown and for the moral support extended during difficult times. I thank Prof. Arunan for the whole hearted support, encouragement and the keen interest he has taken to see that I complete my PhD work and he has been the driving force during each stage. My research supervisors have generated inquisitiveness and have guided me to basics theories and practices of chemistry which I did not know before for which I shall always be indebted to them.

I am grateful to Director, VSSC and DD, PCM (former and present) for granting permission to carry out my research work in VSSC. I thank Dean, IISc (Science Faculty), for providing the facilities, opportunity to carry out the course work as well as the support rendered during the submission phase.

I thank Chairman (former and present) and faculty members of Department of Inorganic and Physical Chemistry, IISc for the guidance during course work as well as for the subsequent reviews. I thank Prof. K. P. J. Reddy Dept. of Aerospace Engineering, for the support that he has given. I thank all my friends at IPC and Aerospace department for the help rendered during different phases of the work. I would like to specially acknowledge Shri.Devendra, IPC who has helped during the final phases of thesis preparation.

I thank Prof.S.Ramakrishan, Department of Inorganic and Physical Chemistry, Prof.Giridhar Madras, Department of Chemical Engineering and Prof.Satish Patil, Department of Solid State and Structural Chemistry Unit, IISc for the constructive suggestions given to improve the thesis.

I thank academic committee (PCM and VSSC) for the reviews and suggestions given. I thank Head, PED for the encouragement and Head, ASD for providing the required facilities. I am grateful to Dr. T. L.Varghese (former GH, PSCG) and Dr. K. N. Ninan (former DD, PCM) for providing me an opportunity to undertake PhD at IISc.

I wish to acknowledge the help rendered by Ms. Deepthi Thomas and Dr. Vijayalakshmi, ASD, VSSC for their selfless help and fruitful discussions.

I am immensely grateful to Dr. Dona Mathew, PSCD, and VSSC for her friendship and unstinting support during difficult times. Words shall not be able to express my gratitude for the valuable time which she had spared without which I would never have completed my work. I thank Shri. Salil Thomas for his timely and whole hearted help for the PhD work.

I am grateful to Dr. Korah Bina Cathrine, BMPD, VSSC and Dr. C.Gowri, LFCD, VSSC for their moral support, guidance and encouragement which were very valuable to tide over difficult periods.

I am grateful to Smt.Sadhana, Smt.Salu Jacob, Smt.Deepthi L.Sivadas, Dr.R.Rajeev, Smt.Soumyamol, Smt. Nisha Balachandran, Smt.Bhuvaneshwari, Smt.Temina Robert who have supported during different stages of the work.

I thank all my colleagues from PDS, PED, Dr. G. Santhosh, Dr. Sreejith.M, A. Mahalingam, Jeevan Thomas, Linson Paul N. Binu, E. S. Hareesh, R. Manoj for their support and cooperation. I thank the members from CTSS, PED, VSSC for the characterization support. My special thanks to Smt.S.Gayathri, Shri.Anish and Ms.Harsha, PDS, PED, for the help they have rendered during final phase of thesis work.

I thank all my friends, teachers, colleagues and relatives for their support and encouragement

I am indebted to my husband Dr. S. Suraj for his love, patience, companionship, constructive suggestions for the work; enormous amount of time that he has spent for me during thesis preparation which has facilitated the completion of the work. I thank my mother for the sacrifices and encouragement all through this journey. I thank my husband's parents for their concern, moral support and constant encouragement without which I could not have completed this work. I thank my daughter Ms. Parvathi for being patient and bearing with my busy schedules. I thank my sister for her concern and care. I am ever indebted to my father whose wisdom, guidance and advice has guided every stride of my life and is a source of motivation even in his absence. Finally I thank God almighty for the innumerable blessings that has been bestowed upon me.

# Synopsis

---

## **SYNOPSIS**

This thesis contains investigations in the area of polymers herein propellants binders are modified functionally to meet the requirements of future energetic propellants. Chapter 1 contains a broad introduction to the area of recent advances in solid propellants and the numerous applications of 'Click Chemistry'. Chapters 2 details the materials, characterization tools and the experimental techniques employed for the studies. This is followed by Chapter 3, 4, and 5 which deals with functional modification of various propellants binders, their characterisation and evaluation in propellant formulations. Chapter 6 details with the thermal decomposition of diazides and its reaction with alkenes.

The advent of modern rockets has opened a new era in the history of space exploration as well as defence applications. The driving force of the rocket emanates from the propellant – either solid or liquid. Composite solid propellants find an indispensable place, in today's rockets and launch vehicles because of the inherent advantages such as high reliability, easy manufacturing, high thrust etc. The composite propellant consisting of inorganic oxidiser like ammonium perchlorate, (AP), ammonium nitrate (AN) etc), metallic fuel (aluminium powder, boron etc) and polymeric fuel binder (hydroxyl terminated polybutadiene-HTPB, polybutadiene-acrylic acid-acrylonitrile PBAN, glycidyl azide polymer (GAP), polyteramethylene oxide (PTMO) etc. is used in igniters, boosters, upper stage motors and special purpose motors in large launch vehicles.

Large composite solid propellant grains or rocket motors in particular, demand adequate mechanical properties to enable them to withstand the stresses imposed during operation, handling, transportation and motor firing. They should also have a reasonably long 'potlife' to provide sufficient window for processing operations such as mixing and casting which makes the selection of binder with appropriate cure chemistry more challenging. In all composite solid propellants currently in use, polymers perform the role of a binder for the oxidiser, metallic fuel and other additives. It performs the dual role of imparting dimensional stability to the composite, provides structural integrity and

---

## Synopsis

---

good mechanical properties to the propellant besides acting as a fuel to impart the required energetics.

Conventionally, the terminal hydroxyl groups in the binders like GAP, PTMO and HTPB are reacted with diisocyanates to form a polyurethane network, to impart the necessary mechanical properties to the propellant. A wide range of diisocyanates such as tolylene diisocyanate (TDI) and isophorone diisocyanate (IPDI) are used for curing of these binders. However, the incompatibility of isocyanates with energetic oxidisers like ammonium dinitramide (ADN), hydrazinium nitroformate (HNF), short 'potlife' of the propellant slurry and undesirable side reactions with moisture are limiting factors which adversely affect the mechanical properties of curing binders through this route.

The objective of the present study is to evolve an alternate approach of curing these binders is to make use of the 1,3 dipolar addition reactions between azide and alkyne groups which is a part of 'Click chemistry'. This can be accomplished by the reaction of azide groups of GAP with triple bonds of alkynes and reactions of functionally modified HTPB/PTMO (azide/alkyne) to yield 1,2,3 -triazole based products. This offers an alternate route for processing of solid propellants wherein, the cured resins that have improved mechanical properties, better thermal stability and improved ballistic properties in view of the higher heat of decomposition resulting from the decomposition of the triazole groups.

GAP is an azide containing energetic polymer. The azide groups can undergo reaction with alkynes to yield triazoles. In, Chapter 3 the synthesis and characterisation of various alkynyl compounds including bis propargyl succinate (BPS), bis propargyl adipate (BPA), bis propargyl sebacate (BPSc.) and bis propargyl oxy bisphenol A (BPB) for curing of GAP to yield triazoles networks are studied. The mechanism of the curing reaction of GAP with these alkynyl compounds was elucidated using a model compound viz. 2-azidoethoxyethane (AEE). The reaction mechanism has been analysed using Density Functional Theory (DFT) method. DFT based theoretical calculations implied marginal preference for 1, 5 addition over the 1, 4 addition for the uncatalysed cycloaddition reaction between azide and alkyne group. The detailed characterisation of these systems with respect to the cure kinetics, mechanical properties, dynamic

---



## Synopsis

---

mechanical behaviour and thermal decomposition characteristics were done and correlated to the structure of the network. The glass transition temperature ( $T_g$ ), tensile strength and modulus of the system increased with crosslink density which in turn is, controlled by the azide to alkyne molar stoichiometry. Thermogravimetric analysis (TGA) showed better thermal stability for the GAP-triazole compared to GAP based urethanes. Though there have been a few reports on curing of GAP with alkynes, it is for the first time that a detailed characterisation of this system with respect to the cure kinetics, mechanical, dynamic mechanical, thermal decomposition mechanism of the polymer is being reported.

To extend the concept of curing binders through 1,3 dipolar addition reaction, the binder HTPB as chemically transformed to propargyloxy carbonyl amine terminated polybutadiene (PrTPB) with azidoethoxy carbonyl amine terminated polybutadiene (AzTPB) and propargyloxy polybutadiene (PTPB). Similarly, PTMO was converted to propargyloxy polytetramethylene oxide (PTMP). Triazole-triazoline networks were derived by the reaction of the binders with alkyne/azide containing curing agents. The cure characteristics of these polymers (PrTPB with AzTPB, PTPB with GAP and PTMP with GAP) were studied by DSC. The detailed characterisations of the cured polymers for were done with respect to the, mechanical, dynamic mechanical behaviour and thermal decomposition characteristics were done.

Propellant level studies were done using the triazoles derived from GAP, PrTPB-AzTPB, PTPB and PTMP as binder, in combination with ammonium perchlorate as oxidiser. The propellants were characterised with respect to rheological, mechanical, safety, as well as ballistic properties. From the studies, propellant formulations with improved energetics, safety characteristics, processability and mechanical properties as well defect free propellants could be developed using novel triazole crosslinked based binders.

Chapter 6, is aimed at understanding the mechanism of thermal decomposition of diazido compounds in the first section. For this, synthesis and characterisation of a diazido ester 1,6 –bis (azidoacetoxy) hexane (HDBAA) was done. There have been no reports on the thermal decomposition mechanism of diazido compounds, where one

---

## Synopsis

---

azide group may influence the decomposition of the other. The thermal decomposition mechanism of the diazido ester were theoretically predicted by DFT method and corroborated by pyrolysis-GC-MS studies. In the second section of this chapter, the cure reaction of the diazido ester with the double bonds of HTPB has been investigated. The chapter 6B reports the mechanism of Cu (I) catalysed azide-alkene reaction validated using density functional theory (DFT) calculations in isomers of hexene (cis-3-hexene, trans-3-hexene and 2-methy pentene: model compound of HTPB) using HDBAA. This the first report on an isocyanate free curing of HTPB using an azide.

Chapter 7 of the thesis summarizes the work carried out, the highlights and important findings of this work. The scope for future work such as development of high performance eco-friendly propellants based on triazoles in conjunction with chlorine-free oxidizer like ADN, synthesis of compatible plasticisers and suitable crosslinkers have been described.

This work has given rise to one patent, three international publications and four papers in international conferences in the domain.

---

## LIST OF SYMBOLS AND ABBREVIATIONS

$\alpha$	Fractional conversion
A	Pre-exponential factor
ADN	Ammonium dinitramide
AEE	Azido ethoxy ether
AMMO	3-azido methyl-3-methyl oxetane
AN	Ammonium nitrate
AP	Ammonium perchlorate
AR	Analytical Grade
ATPB	Amine-terminated polybutadiene
ATRP	Atom Transfer Radical Polymerisation
BAMO	3,3'-bis (azidomethyl) oxetane
BPA	Bispropargyl adipate
BPB	Bis propargyloxy bisphenol A
BPS	Bispropargyl succinate
BPSc	Bispropargyl sebacate
$^{13}\text{C}$ NMR	$^{13}\text{C}$ Nuclear Magnetic Resonance Spectroscopy
CBDT	2-chloro-4,6-bis (dimethylamino)-1,3,5-triazine
CDB	Cast double base
$-\text{CF}(\text{NO}_2)_2$	Fluorodinitro
CMDB	Composite modified double base
CTPB	Carboxyl terminated polybutadiene polymer
DBTDL	Dibutyl tin dilaurate
DEGBAA	Diethylene glycol bis (azido acetate)
DFT	Density functional theory
DMA	Dynamic mechanical analysis
DNCB	1-chloro-2,4-dinitrobenzene
DSC	Differential Scanning Calorimetry
E	Activation energy
EDB	Extruded double base
EGBAA	Ethylene glycol bis(azidoacetate)
EMCDB	Elastomeric modified cast double base
FeAA	Ferric acetyl acetate
FTIR	Fourier transform infrared

GAP	Glycidyl azide polymer
GC-MS	Gas chromatogram-mass spectrometer
GOX	Gaseous oxygen
$\Delta H_c$	Heat of combustion
$^1\text{H NMR}$	Proton Nuclear Magnetic Resonance
HEF 20	High Energy Fuel 20
HEM	High energy Material
HMDI	Hexamethylene diisocyanate
HMX	Cyclotetramethylene tetranitramine
HNF	Hydrazinium nitroformate
HNIW	Hexanitrohexazaisowurtzitane
HTPB	Hydroxyl terminated polybutadiene
IPDI	Isophorone diisocyanate
Isp	Specific Impulse
$\text{LF}_2$	Liquid fluorine
LOX	Liquid oxygen
MMH	Monomethyl hydrazine
$M_n$	Number average molecular weight
$M_n$	Molecular weight
MON	Mixed oxides of nitrogen
$M_w$	Average molecular weight
n	Reaction order
$\text{N}_2\text{O}_5$	Dinitrogenpentoxide
$-\text{N}_3$	Azide
NIMMO	3-nitrato methyl-3'methyl oxetane
NMR	Nuclear magnetic resonance
NTO	3-nitro-1,2,4-triazole-5-one
ONC	Octanitrocubane
$-\text{ONO}_2$	Nitrato
PBAA	Polybutadiene acrylic acid
PBAN	Polybutadiene-acrylic acid-acrylonitrile
PCP	Polycaprolactone
PECH	Polyepichlorohydrin
PEG	Polyethyleneglycol
PETKAA	Pentaerythritol tetrakis (azidoacetate)
PGA	Polyglycidyl adipate

PGN	Poly(glycidyl nitrate)
pKa	Acid dissociation constant
PMVT	Poly(methylvinyltetrazole)
PVC	Polyvinyl chloride
R	Universal gas constant
r	Burning rate
RDX	Cyclotrimethylene trinitramine
RFNA	Red fuming nitric acid
RT	Retention time
SRM	Solid Rocket Motor
SSME	Space Shuttle main engine
T	Temperature
t	Time
TDI	Toluene diisocyanate
TEGDN	Triethyleneglycol dinitrate
T <sub>f</sub>	Final temperature
T <sub>g</sub>	Glass transition
TGA	Thermal gravimetric analysis
T <sub>i</sub>	Initial temperature
T <sub>m</sub>	Peak temperatures
TMETN,	Trimethyl ethane trinitrate
TMNTA	Trimethylol nitromethane tris(azidoacetate)
TMP	Trimethylol propane
TNAZ	Trinitroazetidine
TS	Transition state
UDMH	Unsymmetrical dimethyl hydrazine
UN	United Nations
UV	Ultraviolet
X <sub>density</sub>	Crosslink density
Φ	Heating rate

## List of Tables

<i>Table</i>	<i>Titles</i>
Table 1.1	<i>Characteristics of Conventional Oxidisers</i>
Table 1.2	<i>Characteristics of energetic binders</i>
Table 1.3	<i>Characteristics of energetic oxidisers</i>
Table 1.4	<i>Thermochemical Performance of Various Energetic Formulations</i>
Table 2.1	<i>Details of Materials Used</i>
Table 3.1	<i>Phenomenological Details of Curing</i>
Table 3.2	<i>Kinetic Parameters of Curing</i>
Table 3.3	<i>Crosslink Density of GAP-BPS System</i>
Table 3.4	<i>Variation of Mechanical Properties of GAP-triazoles processed with aliphatic alkynes.</i>
Table 3.5	<i>Thermo chemical performance of aluminised AP Propellants</i>
Table 3.6	<i>Thermochemical Performance Parameters of Low aluminized Propellant</i>
Table 3.7	<i>Viscosity Build up of GAP Propellant</i>
Table 3.8	<i>Mechanical Properties of GAP Propellant</i>
Table 3.9	<i>Safety Properties of GAP Propellant</i>
Table 3.10	<i>Burn Rate of GAP Propellant</i>
Table 4.1	<i>Phenomenological Details of Curing</i>
Table 4.2	<i>Crosslink density of Cured HTPB-TDI and PrTPB-AzTPB Systems</i>
Table 4.3	<i>Mechanical Properties of Cured HTPB-TDI and PrTPB-AzTPB Systems</i>
Table 4.4	<i>Heat of combustion of PrTPB and AzTPB</i>
Table 4.5	<i>Thermochemical Performance Parameters of Propellant</i>
Table 4.6	<i>Properties of PrTPB-AzTPB Propellant</i>
Table 5.1	<i>Phenomenological Details of Curing –Effect of catalyst</i>
Table 5.2	<i>Phenomenological Details of Curing-Effect of heating rate</i>
Table 5.3	<i>Mechanical Properties of Cured PTPB and PTMP Polymer</i>
Table 5.4	<i>Heat of formation of PTPB and PTMP</i>
Table 5.5	<i>Thermochemical Performance Parameters of PTPB and PTMP Propellant</i>
Table 5.6	<i>Viscosity Build up of PTPB and PTMP Propellant</i>
Table 5.7	<i>Mechanical Properties of PTPB and PTMP Propellant</i>
Table 5.8	<i>Burn rate of PTPB and PTMP Propellant</i>
Table 6b.1	<i>Computed heat of reaction and activation barrier of Hexene-HDBAA reactions</i>
Table 6b.2	<i>Computed energy parameters for the formation of Cu [CH<sub>3</sub>CN, Hexene, HDBAA]<sup>+</sup> and its decomposition to triazolines.</i>

## List of Schemes

<i>Scheme</i>	<i>Titles</i>
<i>Scheme 1.1</i>	<i>Free radical synthesis of HTPB</i>
<i>Scheme 1.2</i>	<i>Synthesis of GAP</i>
<i>Scheme 1.3</i>	<i>Reaction of isocyanate with hydroxyl group</i>
<i>Scheme 1.4</i>	<i>Formation of biuret, allophanate and tetrazoline-5-one</i>
<i>Scheme 1.5</i>	<i>Proposed catalytic cycle for the CuI-catalysed ligation</i>
<i>Scheme 1.6</i>	<i>Proposed catalytic cycle for the Ru-catalysed ligation</i>
<i>Scheme 1.7</i>	<i>Three types of alkyne homocouplings</i>
<i>Scheme 3.1</i>	<i>a. Urethane formation reaction of hydroxyl GAP telechelic with diisocyanate b. Reaction of isocyanate with water.</i>
<i>Scheme 3.2</i>	<i>Reaction of azide with isocyanate</i>
<i>Scheme 3.3</i>	<i>Cycloaddition reaction between alkyne and azide compounds</i>
<i>Scheme 3.4</i>	<i>Curing of GAP-BPS through 1,3 dipolar cycloaddition reaction between azide and propargyl groups</i>
<i>Scheme 3.5</i>	<i>Pyrolysis pathway for GAP-triazole giving rise to anhydride</i>
<i>Scheme 4.1</i>	<i>Synthesis scheme for PrTPB</i>
<i>Scheme 4.2</i>	<i>Synthesis scheme for AzTPB</i>
<i>Scheme 4.3</i>	<i>Curing of mixture of PrTPB with AzTPB</i>
<i>Scheme 4.4a</i>	<i>Mechanism of decomposition of PrTPB-AzTPB cured network and products</i>
<i>Scheme 4.4b</i>	<i>Cleavage of urethane in PrTPB-AzTPB to yield alcohol and isocyanate along with triazole group breakdown</i>
<i>Scheme 4.4c</i>	<i>Cleavage of urethane in PrTPB-AzTPB to yield alkene and amine along with triazole group cleavage</i>
<i>Scheme 5.1</i>	<i>Typical synthesis scheme for PTPB</i>
<i>Scheme 5.2</i>	<i>Typical synthesis scheme for PTMP</i>
<i>Scheme 5.3</i>	<i>Cycloaddition reaction between PTMP and GAP giving triazole</i>
<i>Scheme 5.4</i>	<i>Low temperature decomposition of PTMP triazole with AP a) General scheme b) Step 1 c) Step 2</i>
<i>Scheme 6a.1</i>	<i>Imine formation in azides by 1,2 H shift</i>
<i>Scheme 6a.2</i>	<i>Decomposition mechanism of an azido carboxylic acid</i>
<i>Scheme 6a.3</i>	<i>Synthesis scheme of HDBAA</i>
<i>Scheme 6a.4</i>	<i>Mechanism for thermal decomposition of HDBAA</i>
<i>Scheme 6b.1</i>	<i>Azide-alkene 1,3 dipolar cycloaddition</i>
<i>Scheme 6b.2</i>	<i>Proposed reaction pathway for Cu(I)catalysed HTPB curing using HDBAA</i>
<i>Scheme 6b.3</i>	<i>Elimination of nitrogen from triazoline</i>

## List of Figures

S.No.	Title
Figure 1.1.	Molecular structure of energetic nitro plasticisers
Figure 1.2.	Molecular structure of energetic azide plasticisers
Figure 1.3.	Molecular structure of Epoxy HTPB
Figure 1.4.	Molecular structure of Nitrated HTPB
Figure 1.5.	Molecular structure of HTPB reacted with thiols
Figure 1.6.	Molecular structure of acetylated HTPB
Figure 1.7.	Molecular structure of carboxyl terminated HTPB
Figure 1.8.	Molecular structure of isocyanate end capped HTPB
Figure 3.1.	Molecular Structure of a) BPS b) BPA c) BPB and d) BPSc
Figure 3.2	Optimized structures of transition states for (a) tetrazolin- 5-one (b) urethane
Figure 3.3.	(a) Transition states for the 1,4- and (b) 1,5-cycloaddition between AEE and BPS. Bond lengths are given in Å. Transition state structures calculated at B3LYP/6-31G** level of DFT
Figure 3.4.	for 1, 5 cycloaddition (b) 1,4 cycloaddition
Figure 3.5.	DSC trace of GAP-BPS for different heating rates
Figure 3.6	Kissinger plot for determination of activation energy (E)
Figure 3.7.	Coats Redfern Plot for GAP-BPS system
Figure 3.8.	Predicted and experimental isothermal cure profile of GAP-BPS at 60° C FTIR spectra of (a) GAP-BPS mixture-before curing (b) GAP-BPS mixture-after curing
Figure 3.9.	Dependence of enthalpy of reaction on the stoichiometry of reactants (GAP to BPS, azide to propargyl)
Figure 3.10.	DSC curves for GAP curing with BPS, BPA and BPSc
Figure 3.11.	Evolution of storage modulus as a function of temperature for GAP-BPB System
Figure 3.12.	Tan $\delta$ vs temperature of GAP triazoles and GAP urethane system
Figure 3.13	Variation of storage modulus with molar equivalence for GAP-triazole and GAP-urethane
Figure 3.14	Tan $\delta$ vs temperature of GAP-BPA and GAP-BPSc triazoles
Figure 3.15	Effect of reactant stoichiometry on (a) tensile strength and elongation (b). Young's Modulus of GAP-BPS system
Figure 3.16	Variation of modulus with $X_{density}$
Figure 3.17	SEM images of the fractured surface of (a)GAP cured using TDI (GAP-Urethane) (b)GAP cured by BPS (GAP-triazole)
Figure 3.18	TG curves of GAP, GAP- urethane and GAP-triazole
Figure 3.19	Pyrograms of GAP-Triazole (1:1) at 350°C and 500°C
Figure 3.20	Effect of solid loading on the adiabatic flame temperature of GAP-AP propellant
Figure 3.21a	Effect of solid loading on the Isp of GAP-AP propellant
Figure 3.21b	TGA of GAP-urethane and GAP-triazole propellant
Figure 4.1	FTIR spectra of a)PrTPB b)AzTPB c)ITPB



- Figure 4.2 <sup>1</sup> H NMR spectrum of a) PrTPB b)AzTPB
- Figure 4.3 GPC chromatogram of a)PrTPB b)AzTPB c)HTPB
- Figure 4.4 DSC traces of curing of a)PrTPB with AzTPB b)Self curing of AzTPB  
Kissinger plot for determination of activation energy PrTPB-AzTPB system
- Figure 4.5 Prediction of isothermal cure profile (at 60 ° C) for PrTPB-AzTPB
- Figure 4.6 FTIR spectrum of cured PrTPB-AzTPB
- Figure 4.7
- Figure 4.8 Rheogram of a) PrTPB- AzTPB b) HTPB-TDI (uncatalysed) at 80 ° C
- Figure 4.9 a)Tan δ vs temperature of HTPB-TDI urethane and triazoles b) Storage modulus of HTPB-TDI urethane and PrTPB-AzTPB triazoles  
SPM Images of a) Morphological changes during heating of cured network from 40 to 50 ° C
- Figure 4.10 a)TGA trace of PrTPB-AzTPB triazoles and HTPB-TDI b) Pyrogram of PrTPB-AzTPB triazoles at 300°C
- Figure 4.11 Effect of solid loading on the Isp of PrTPB-AzTPB and HTPB propellant
- Figure 4.12 Thermal decomposition of PrTPB-AzTPB propellant
- Figure 4.13
- Figure 5.1 FTIR spectrum of a. PTPB
- Figure 5.2 <sup>1</sup> H NMR spectrum of PTPB
- Figure 5.3 FTIR spectrum of PTMP
- Figure 5.4 <sup>1</sup> H NMR spectrum of PTMP
- Figure 5.5 GPC chromatogram of HTPB and PTPB
- Figure 5.6 GPC chromatogram of PTMO and PTMP  
DSC Traces of Curing of PTPB with GAP a) Azide-alkyne equivalence (1:1) b) Azide-alkyne equivalence (1:0.1)
- Figure 5.7 DSC Traces of Curing of PTMP with GAP  
Kissinger plot for determination of activation energy PTMP-GAP system
- Figure 5.8 Prediction of Isothermal Cure Profile for PTMP-GAP System (at 60 ° C)
- Figure 5.9 FTIR Spectra of cured PTMP-GAP
- Figure 5.10 Rheogram of PTPB with GAP at 80 ° C
- Figure 5.11 Rheogram of PTMP with GAP at 80 ° C
- Figure 5.12 Tan δ and Storage modulus of Cured PTPB-GAP Polymer
- Figure 5.13 a)TGA-DTG trace of PTPB triazoles b)Pyrogram of PTBP -GAP at 500°C
- Figure 5.14 a)TGA-DTG trace of PTMP triazoles b)Pyrogram of PTMP -GAP at 500°C
- Figure 5.15 Pyrogram of PTMP triazole-AP at 500°C
- Figure 5.16 Variation of Isp with solid loading for PTPB, PTMP and HTPB propellant
- Figure 5.17 TGA of PTPB, PTMP-AP and HTPB-TDI-AP propellant
- Figure 6a.1 Structure of the HDBAA
- Figure 6a.2 TGA curve of HDBAA (Heating rate 5 ° C/min)

- Figure 6a.3 Pyrogram of HDBAA at (a) 230° C and (b) at 500° C  
(a)TS1 for elimination of first N<sub>2</sub> from HDBAA and (b) TS2 for the  
Figure 6a.4 elimination of N<sub>2</sub> from mono-imine intermediate.
- Figure 6a.5 Energy profile diagram of N<sub>2</sub> elimination reactions of HDBAA
- Figure 6a.6 (a) TS3 & (b) TS4 for elimination of two CO<sub>2</sub> molecules from HDBIA  
Energy profile diagram for decomposition reaction of HDBIA to  
Figure 6a.7 octadiimine  
TS5 B) TS6 C) TS 5a for elimination of CO<sub>2</sub> and CH<sub>2</sub>NH from HDBIA  
(d) Energy profile diagram for the formation of 1,5 hexadiene from  
Figure 6a.8 HDBIA.  
Formation of CO and HCN via (a) TS7 and (b) TS8. (c) Energy profile  
Figure 6a.9 diagram for 1, 6-hexanediol formation from HDBIA.
- Figure 6b.1 HTPB and HDBAA crosslinked to yield triazoline
- Figure 6b.2 Mesomeric structure of azide
- Figure 6b.3 Types of double bonds in HTPB  
Optimized Structure of cis-3 hexene, trans 3-hexene, 2methyl  
Figure 6b.4 pentene
- Figure 6b.5 Transition state for Monoadduct of cis-3-hexene with HDBAA  
Transition states located for 1, 4 and 1,5 cycloadditions of 2 methyl  
Figure 6b.6 pentene  
Schematic orbital description of Cu-alkene coordination (b)
- Figure 6b.7 optimized structure of Cu [CH<sub>3</sub>CN, Cis3Hexene]<sup>+</sup>
- Figure 6b.8 Ternary complex of Cu(I) acetonitrile, trans-3- hexene and HDBAA.
- Figure 6b.9 FTIR spectra of HTPB-HDBAA Cured polymer
- Figure 6b.10 Pyrogram of HTPB cured using HDBAA (300° C)

## Table of Contents

Sl no	Title	Page No
<b>1</b>	<b>Chapter 1</b>	<b>1</b>
	Abstract	2
1.1	Introduction	3
1.2	Chemical Propellant Classification	3
1.2.1	Solid Propellants	3
1.2.2	Liquid Propellants	3
1.2.3	Hybrid Propellants	4
1.3	Solid Propellant Classification	4
1.3.1	Double base/Homogenous Propellants	5
1.3.2	Composite (Heterogenous) propellant	5
1.4	Major Components of Composite Solid Propellants	9
1.4.1	Oxidiser	9
1.4.2	Binder	9
1.4.3	Metallic fuel	9
1.4.4	Other Additives	10
1.4.4.1	Crosslinking Agents and Curing Agents	10
1.4.4.2	Plasticisers	10
1.4.4.3	Burn rate modifier, antioxidant, Cure catalyst	12
1.5	New Energetic Materials	12
1.5.1	Energetic Binders	13
1.5.2	Energetic Oxidisers	13
1.5.3	Energetic Solid propellants	15
1.6	Role of the binder	16
1.7	Properties of an ideal binder	17
1.8	Types of polymeric binders	18
1.8.1	Linear binders	18
1.8.2	Crosslinked binders	19
1.8.3	Polyurethane binders	19
1.9	HTPB	20
1.9.1	Synthesis of HTPB	20
1.9.2	Characterization studies on HTPB	21
1.9.3	Thermal properties of HTPB	21
1.9.4	Functional modification of HTPB	22
1.10.	GAP	25
1.10.1	Synthesis of GAP	25
1.10.2	Curing of GAP	27
1.10.3	Thermal properties of GAP	27
1.10.4	GAP based propellants	29
1.11	Curing reactions in HTPB and GAP	30
1.12	Reaction of isocyanate with water	30
1.13	Click chemistry	32

1.13.1	Cycloaddition of Azides and Terminal Alkynes	32
1.13.2	Limitations of Copper catalysed click reaction	34
1.13.3	Synthesis of polymers with azide and alkyne groups	35
1.14	Scope and Objective of the Present work	37
1.15	References	39
<b>2</b>	<b>Chapter 2</b>	<b>49</b>
	Abstract	50
2	Materials	51
2.1	Characterisation techniques	52
2.1.1	Fourier Transform Infrared Spectroscopy (FTIR)	52
2.1.2	Nuclear Magnetic Resonance Spectroscopy (NMR)	53
2.1.3	Gel Permeation Chromatography (GPC)	53
2.1.4	Differential Scanning Calorimetry (DSC)	54
2.1.4.1	Cure kinetics	55
2.1.5	Pyrolysis Gas Chromatography-Mass Spectrometer (Pyrolysis GC-MS) and thermogravimetry -mass spectrometer	55
2.1.6	Crosslink Density by Dynamic Mechanical Analysis (DMA)	56
2.1.7	Mechanical and rheological Properties	56
2.1.8	Morphological studies	57
2.2	Determination of Burn rate, heat of Combustion and safety characteristics	57
2.3	Chemical Analysis	58
2.3.1	Isocyanate content	58
2.3.2	Hydroxyl value	58
2.4	Computational calculations	59
2.5	References	60
<b>3</b>	<b>Chapter 3</b>	<b>62</b>
	Abstract	63
3.1	Introduction	64
3.2	Experimental	66
3.2.1	Materials and measurement	66
3.2.2	Instrumental	67
3.2.3	Synthesis of the aliphatic alkynes	67
3.2.4	Curing of GAP with alkyne curing agent	69
3.2.5	Curing of GAP with diisocyanate	69
3.2.6	Computational calculations	70
3.2.7	Propellant Processing	70
3.3	Results and Discussion	71
3.3.1	Synthesis of alkyne compounds and curing of GAP	71
3.3.2	Theoretical aspects of cure reaction	71
3.3.3	Cure optimisation	74
3.3.3.1	DSC analysis	74
3.3.3.2	Cure kinetics	75
3.3.3.3	Prediction of isothermal cure time	77

3.3.3.4	Effect of reactant stoichiometry on curing	79
3.3.3.5	DSC analysis of higher alkne homologues	80
3.3.4	Rheological Characteristics	80
3.3.5	Dynamic mechanical characterisation	81
3.3.6	Mechanical properties	84
3.3.7	Thermal decomposition studies	87
3.3.8	Pyrolysis GC-MS studies	89
3.3.9	Theoretical performance analysis of Propellant	90
3.3.10.	Propellant studies:Processability, mechanical properties, burn rate and safety	93
3.4	Conclusions	96
3.5	References	97
<b>4</b>	<b>Chapter 4</b>	<b>104</b>
	Abstract	105
4.1	Introduction	106
4.2	Experimental	107
4.2.1	Methods and Materials	107
4.2.2	Instrumental	107
4.2.3	Synthesis	108
4.2.3.1	Synthesis of Isocyanate-Terminated Prepolymer (ITPB)	108
4.2.3.2	Synthesis of propargyl carbamate terminated polybutadiene (PrTPB)	108
4.2.3.3	Synthesis of azidoethoxy carbamate terminated polybutadiene (AzTPB)	108
4.2.4	Curing Procedure	109
4.2.5	Swelling Studies	109
4.2.6	Determination of cross link density	109
4.2.7	Propellant processing	109
4.3	Results and Discussion	110
4.3.1	Characterisation of PrTPB and AzTPB polymers	110
4.3.2	Cure optimisation	114
4.3.2.1	DSC analysis	114
4.3.3	Cure kinetics	117
4.3.4	Determination of cross link density	120
4.3.5	Mechanical properties	121
4.3.6	Dynamic mechanical characterisation	122
4.3.7	Thermal decomposition studies	123
4.3.8	Propellant Studies	127
4.3.8.1	Thermochemical measurements	127
4.3.8.2	Propellant processability, mechanical properties and burn rate	129
4.3.8.3	Thermal decomposition of the propellant	130
4.4	Conclusions	131
4.5	References	133
<b>5</b>	<b>Chapter 5</b>	<b>135</b>
	Abstract	136
5.1	Introduction	137
5.2	Experimental	138

5.2.1	Materials	138
5.2.2	Instrumental	138
5.2.3	Synthesis	139
5.2.3.1	Synthesis of propargyl oxyterminated poly butadiene (PTPB)	139
5.2.3.2	Synthesis of propargyl terminated poly tetramethylene oxide (PTMP)	139
5.2.4	Curing Procedure	139
5.2.5	Propellant Studies	140
5.3	Results and Discussion	140
5.3.1	Functionalisation of HTPB and PTMO	140
5.3.2	Cure Characterization	144
5.3.2.1	PTPB- GAP curing	144
5.3.2.2	PTMP-GAP Curing	146
5.3.3	Cure kinetics	147
5.3.4	Mechanical properties	150
5.3.5	Dynamic mechanical characterisation	151
5.3.6	Thermal decomposition studies	152
5.3.7	Propellant Studies	158
5.3.7.1	Thermochemical measurements	158
5.3.7.2	Propellant processability, mechanical properties, thermal decomposition and burn rate	160
5.4	Conclusions	163
5.5	References	165
<b>6A</b>	<b>Chapter 6a</b>	<b>169</b>
	Abstract	170
6A.1	Introduction	171
6A.2	Experimental	172
6A.2.1	Materials	172
6A.2.2	Instrumental	172
6A.2.3	Synthesis and characterization of HDBAA	173
6A.2.4	Computational calculations	173
6A.3	Results and Discussion	174
6A.3.1	Synthesis scheme of HDBA	174
6A.3.2	Thermal decomposition studies of HDBAA	175
6A.3.3	Pyrolysis GC-MS Studies	175
6A.4	Conclusions	181
6A.5	References	182
<b>6B</b>	<b>Chapter 6b</b>	<b>184</b>
	Abstract	185
6B.1	Introduction	186
6B.2	Experimental Section	186
6B.2.1	Materials	186
6B.2.2	Instrumental	186
6B.2.3	Synthesis and characterization of HDBAA	187
6B.2.4	Curing of HTPB with HDBAA	187
6B.2.5	Computational calculations	187

6B.3	Results and Discussion	187
6B.3.1	Reaction of HDBAA with HTPB	187
6B.3.2	Uncatalyzed cycloaddition of HDBAA with Hexene	188
6B.3.3	Catalyzed cycloaddition of HDBAA with Hexene	191
6B.4	Conclusions	195
6B.5	References	196
<b>7</b>	<b>Chapter 7</b>	<b>199</b>

*Chapter 1*

**Solid Propellants and Polymeric Binders –An  
Overview**

---



### **Abstract**

*Solid propellants are widely used for launch vehicle and missile applications. This chapter gives an overview of the current developments and future directions in the area of solid propellants focusing on high performance, environment friendly propellants. The polymeric fuel binder is a critical ingredient of a composite solid propellant. It acts as the matrix for holding together the oxidiser, metallic fuel and other additives and also imparts structural integrity and mechanical properties to the propellant. In recent years, the impetus has been to improve the energetics by the use of binders with energetic functional groups. The chapter reviews the evolution of binders, energetic binders, functional modification of binders for improving the cure characteristics, thermal decomposition aspects, mechanical and ballistics properties of solid propellants derived thereof.*

## 1.1. INTRODUCTION

The advances in modern rocketry during the past few decades are principally due to the developments in the realms of chemical propellants. Propellants, either solid or liquid are the driving force of a rocket. The main function of the propellant is to impart kinetic energy to the rocket by imparting a regulated thrust or impulse.<sup>1</sup>

The performance of propellants is assessed based on the parameter 'specific impulse' (Isp). It is a measure of the fuel efficiency of the rocket. It is an important index of the energetics, defined as the thrust produced per unit mass flow rate of the propellant.

## 1.2. CHEMICAL PROPELLANTS CLASSIFICATION

*Chemical propellants are broadly classified as solid and liquid propellants.*

### 1.2.1 Solid propellants

A solid propellant is a mixture of fuel and oxidizer which burn without the requirement of oxygen from other sources and generates hot gases at high pressure.<sup>2-7</sup> The quantum leap achieved in the area of propellants have led to the development of safer, more powerful and more reliable solid propellant for advanced launch vehicles and defence applications. Solid propellants find widespread use in launch vehicles owing to their ruggedness, safety, high thrust, simplicity, reliability, lower cost of production and storage capabilities.

### 1.2.2. Liquid propellants

In a liquid propellant, the fuel and the oxidiser are both in liquid state. Liquid propellants may be classified into cryogenic, semi cryogenic and earth storable propellants. Well known cryogenic fuels are liquid hydrogen, methane etc. with oxidisers such as liquid oxygen (LOX) and fluorine (LF<sub>2</sub>). The popular cryogenic engines<sup>9</sup> are Space Shuttle Main Engine (SSME), HM-7B, Vulcan engines of Ariane, CUS engine of Geosynchronous Satellite Launch Vehicle (GSLV) etc. Semi cryogenic engine uses hydrocarbon fuels like kerosene which are storable. They are used in combination with LOX. The F1 engine in Saturn V, the Russian RD170 etc. are engines which use storable hydrocarbon fuels in combination with LOX. Examples of storable

propellants are hydrazine, unsymmetrical dimethyl hydrazine (UDMH), monomethyl hydrazine (MMH) which are fuels and are used with oxidisers like mixed oxides of nitrogen (MON-10, with 10% nitric oxide, MON-3 with 3% nitric oxide) etc while oxidisers are nitrogen tetroxide (NTO/N<sub>2</sub>O<sub>4</sub>) and red fuming nitric acid (RFNA). The Aestus engine, Viking engine of Ariane, Vikas engine of ISRO, CZ-2F engine of China use earth storable liquid propellants.<sup>9-10</sup> In liquid propellant rocket, the fuel and oxidiser are stored separately and injected into the combustion chamber as fine droplets. These systems generally have higher performance and specific impulse than solid propellants, but they require complicated technology with high speed pumps and numerous precision valves and regulators to obtain accurate metering of the oxidiser and fuel.

### **1.2.3. Hybrid propellants**

A hybrid propellant usually contains a solid fuel and a liquid or gas oxidizer. Eg: cured HTPB with liquid oxygen (LOX) or gaseous oxygen (GOX). Here, the liquid oxidizer can make it possible to throttle and restart the motor just like conventional liquid propellants. Hybrid rockets offer more efficient and controllable alternatives among other two. Some recent launch vehicles use hybrid motors like the SpaceShip-1, a sub orbital manned vehicle which achieved an altitude of 120 km with a human pilot.<sup>9</sup> However, rockets based on hybrid propellants have not found wide applications, mainly because of lack of suitable hypergolic propellants, low recovery of theoretical impulse and low regression rates achieved in these systems.

### **1.3. SOLID PROPELLANTS -CLASSIFICATION**

Solid propellants find widespread use in launch vehicles. They are also used in boosters as well as for specific tasks such as ignition, spin-off rockets, and assistance in separation of spent stages, providing means for escape in manned missions as well as interplanetary missions.<sup>11-13</sup>

Solid propellant may be categorised as double base (also known as homogenous) and composite (also known as heterogeneous) propellants.

### 1.3.1. Double base/Homogenous solid propellants

In homogeneous propellant, the oxidising and reducing functions are contained in the same molecule. It can be single or double base, depending on whether it contains one or two components<sup>6,8</sup>. Examples are nitrocellulose (single base) used in guns, nitrocellulose and nitroglycerine (double base) used mostly for missiles, and nitrocellulose, nitroglycerine and nitroguanidine (triple base), used specifically for smokeless and flash less missiles.

Amongst homogenous propellants, there are four sub categories<sup>11</sup>:

1. Extruded double base (EDB) (prepared by impregnation of nitrocellulose with nitroglycerine in water to form a paste).
2. Cast double base (CDB)-similar to EDB, but are obtained by casting a mixture of nitroglycerine inert plasticiser and nitrocellulose.
3. Composite modified double base (CMDDB) derived from CDB with better mechanical properties.
4. Elastomer modified cast double base (EMCDB) propellants, which are improved versions of CDB with better mechanical properties.

### 1.3.2. Composite (Heterogeneous) solid propellants

Composite solid propellants form the base of all modern developments of solid rocket propulsion systems. For space faring, the composite solid propellants are the prime choice due to the higher performance in terms of high specific impulse, lower hazard and ease of processing. The space launch industry looks for the safety characteristics and associated hazards of the propellant during the entire lifecycle and hence composite solid propellant belonging to the United Nations (UN) hazard class 1.3 is the choice. Today, large boosters with propellant capacity of 200-500 T are used in launch vehicles such as GSLV MK III, Ariane 5, Space Shuttle etc<sup>9</sup>.

Basic ingredients of composite propellants are:

1. Inorganic oxidiser (62-70%) which serves as a source of oxygen, e.g.: salts of perchloric acid or nitric acid. E.g.: ammonium perchlorate (AP) or ammonium nitrate (AN).

2. Powdered metallic fuel (2-20% by weight) which acts as a source of thermal energy, e.g.: aluminium, boron, magnesium.
3. Polymeric fuel binder (9-20% by weight) acts as a fuel (by supplying elements such as carbon and hydrogen required for combustion) and as matrix (after curing) to hold oxidiser, metallic fuel and other additives together they also impart the required mechanical properties to the propellant (e.g.: polyethers, polyesters or polybutadienes with reactive functional groups. It provides the carbon and hydrogen required for combustion.
4. Propellant additives (0.1-5% by weight) like stabilisers, ballistic modifier, high energy fuel additives, plasticizers etc are also added in small quantities to modify the physical, mechanical and ballistic propellants of the propellant.

The invention of the first composite propellant by Parsons<sup>14</sup> was a fundamental breakthrough in solid-propellant rocketry where asphalt was the binder and potassium perchlorate the oxidizer. This was later on modified by using AP as the oxidizer and polysulphide polymer as binder, which gave better performance.

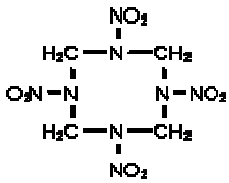
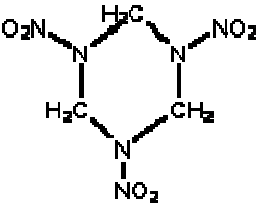
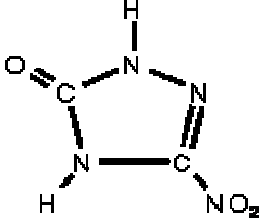
The composite solid propellants have evolved from low energetic asphalt binder to polyester-polystyrene, polyvinyl chloride (PVC) plastisol and polysulphide. These are used with ammonium perchlorate (AP) as oxidizer. Though the processability is easy; the propellant does not have rubbery and high elongation characteristics needed for case bonding and find application in small free standing grains. Hence, it was necessary to develop crosslinked binder systems. Research conducted at Thiokol in the mid-1950's evolved a liquid copolymer of butadiene and acrylic acid namely polybutadiene acrylic acid (PBAA). The drawback of poor mechanical properties for PBAA was improved by using polybutadiene acrylic acid- acrylo nitrile (PBAN) which is still used today by National Aeronautical and Space Administration (NASA). Carboxyl terminated polybutadiene polymer (CTPB) was developed by Thiokol. It gave significantly better mechanical properties for making case bonded motors. Retro-motor of Surveyor used for Moon landing<sup>9</sup> in 1966 was based on CTPB. However, CTPB did not find much application due to its high cost. Finally hydroxyl terminated polybutadiene (HTPB) was synthesised leading to the development of HTPB based

polyurethane propellant systems.<sup>11,14-17</sup> HTPB propellant developed by Societe Nationale des Poudres et des Explosifs (SNPE) was chosen for Ariane V in Europe and H-II series in Japan. China also has developed a series of composite solid propellant using PBAA, CTPB and HTPB with AP as oxidizer and other oxidizers like nitramines (HMX) as additives.<sup>18-21</sup> In Indian Space Research Organisation (ISRO), there were a series of development in the area of composite solid propellant starting with PVC based propellants for the sounding rockets, lactone terminated polybutadiene (high energy fuel, HEF20) which use an epoxy curing agent for the Augmented Satellite Launch Vehicle (ASLV). Later, it was replaced by ISRO polyol, a polyester polyol based on castor oil and stearic acid and HTPB<sup>22</sup>. Now, HTPB is the workhorse binder along with AP and aluminium powder is the state-of-the-art composite solid propellant for the solid rocket motors (SRM's) of Polar Satellite Launch Vehicle (PSLV) and GSLV of ISRO.<sup>23</sup>

The Isp of a solid propellant is decided by the combination of the fuel (binder and metallic fuel) and oxidiser chosen<sup>5-6</sup>. The first oxidiser used in composite propellant was potassium perchlorate<sup>3</sup>. It is stable, compatible and relatively insensitive, but has poor performance due to the evolution of potassium chloride (KCl) which has high molecular weight and difficult to vaporise. This was replaced by AP, which is now extensively used in solid propellants for launch vehicle and missile programs. Ammonium nitrate is considered as an environment friendly alternative to AP. But, its low specific impulse, multiple phase transitions, hygroscopicity and poor ignition characteristics impede its wide spread use. It is used for specialized applications such as gas generators and pyrogen igniters. 3-nitro-1, 2, 4-triazole-5-one (NTO), cyclotetramethylene tetranitramine (HMX) and cyclotrimethylene trinitramine (RDX) are high energy additives with poor oxygen balance. Oxygen balance<sup>4</sup> is the concentration of oxygen within an explosive or oxidiser and can be defined as the amount of oxygen remaining after the oxidation of carbon, hydrogen and metals. However, the presences of N-NO<sub>2</sub> groups in these molecules confer the energetic characteristics to these molecules. They have been used as partial replacement for AP to improve performance in terms of specific impulse (Isp), while substituting AP with 10-12% HMX/RDX<sup>24</sup>. However, beyond 12%, RDX/HMX is not recommended by international law for

civilian applications as propellant UN hazard class change from 1.3 to 1.1 and their compatibility with conventional propellant ingredients is a problem<sup>25-26</sup>. NTO and transition metal complexes of NTO have been reported<sup>27</sup> as ballistic modifiers, but there has been no significant increase in Isp. The properties of the common oxidizers/energetic additives are given in Table 1.1

**Table. 1.1** Characteristics of Conventional Oxidisers  
(Ref. ICT database of thermo chemical values)

Sl.No.	Oxidiser	Structure	Oxygen Balance (%)	Density (g/cm <sup>3</sup> )	$\Delta H_f$ (kJ/mol)
1	AP	$\text{NH}_4\text{ClO}_4$	34.0	1.82	-150.6
2	AN	$\text{NH}_4\text{NO}_3$	19.9	1.87	-72.0
3	KP	$\text{KClO}_4$	46.2	2.04	381.2
4	HMX		-21.6	1.84	33.6
5	RDX		-21.6	1.82	70.3
7	NTO		-24.6	1.93	-111.8

The discovery at Atlantic Research Corporation (ARC)<sup>11</sup> that the use of large amount of aluminium powder (14-20% by weight of propellant) increases the specific impulse and density impulse of composite solid propellant and the benefits of

aluminium in suppressing destructive acoustic instability in the rocket motor was a breakthrough in solid propellant research.<sup>15</sup>

#### **1.4. MAJOR COMPONENTS OF COMPOSITE SOLID PROPELLANTS**

Composite propellants<sup>5, 6</sup> are made of a polymeric matrix, loaded with an oxidiser and possibly a metal powder that plays the role of a secondary fuel component. A certain number of properties such as burning rate, rheology and mechanical behaviour are directly related to this composite character.

##### **1.4.1. Oxidiser**

Oxidisers are molecules that can provide the necessary oxygen, for the combustion reaction to take place. Oxygen can be introduced into the system by incorporation of materials containing bound oxygen. The most important solid propellant oxidisers are nitrates, e.g.: ammonium nitrate, sodium nitrate, potassium nitrate, perchlorates-e.g.: potassium perchlorate and ammonium perchlorate.

The characteristics of a good oxidiser are the capability to supply excess oxygen to burn the fuels (metallic fuel and binders) with maximum heat of combustion.

##### **1.4.2. Binder**

Binders in composite solid propellant are the matrix that holds together solid oxidiser particles and metal particles. They impart the necessary mechanical strength to the propellant besides acting as a fuel. Functionally terminated polymers such as PBAN, HTPB or CTPB are the most commonly used binders. Their enthalpy of formation should be more positive, and on combustion, the binder must produce low molecular weight gases thereby leading to high specific impulses.

##### **1.4.3. Metallic fuel**

Metallic fuels are substances that release a large amount of heat during the oxidation process in the presence of oxidisers. They are used as spherical powders, with small diameters so as to suit for high loading. The most common metallic fuel is aluminium powder. Apart from aluminium, boron, beryllium and lithium have also been



used in very specific applications. In view of the increased cost, toxicity, long term instability and toxic combustion products, the latter fuels are not used.

#### **1.4.4. Other Additives**

##### **1.4.4.1. Crosslinking Agents and Curing Agents**

Crosslinking agent facilitates curing of the prepolymer molecules by forming a crosslinked network. It plays a critical role in kinetics of the curing reaction and in achieving the desired mechanical properties of the propellant. Examples are trimethylol propane (TMP), glycerol etc. In addition to crosslinking agents, curing agents like tolylene diisocyanate (TDI), isophorone diisocyanate (IPDI) or hexamethylene diisocyanate (HMDI) are used, which react with the terminal functional groups of the binder and crosslinking agent to give rigid matrix with desired mechanical properties to the propellant.

##### **1.4.4.2. Plasticisers**

Plasticisers have an essential role in reducing the viscosity of the propellant slurry and in improving the mechanical properties by lowering the glass transition ( $T_g$ ). Glass transition temperature is the temperature at which the motion of molecules are locked in or frozen and the polymer becomes brittle and hard. Plasticizers can be energetic or non-energetic. Non-energetic plasticizers are effective in improving mechanical properties, but degrade the output of the formulation by reducing the overall oxygen balance. The common non energetic plasticizers include dioctyl adipate, dioctyl azelate, isodecyl pelargonate, dioctyl phthalate etc. Energetic plasticizers not only contribute towards enhancement of structural properties, but also improve energetics due to the presence of energetic moieties like nitro (Fig.1.1) or azido groups (Fig 1.2). Examples for energetic plasticisers are nitrate ester plasticisers like trimethylol ethane trinitrate (TMETN), triethyleneglycol dinitrate (TEGDN)ethylene glycol dinitrate (EGDN), 1,2,4-butanetriol trinitrate (BTTN) etc and azido plasticisers like diethylene glycol bis (azido acetate) (DEGBAA), trimethylol nitromethane tris (azidoacetate) or azido plasticisers like ethylene glycol bis(azidoacetate) (EGBAA), diethyleneglycol bis(azidoacetate) (DEGBAA), trimethylol nitromethane tris(azidoacetate) (TMNTA), pentaerythritol tetrakis (azidoacetate) (PETKAA).<sup>28-29</sup>

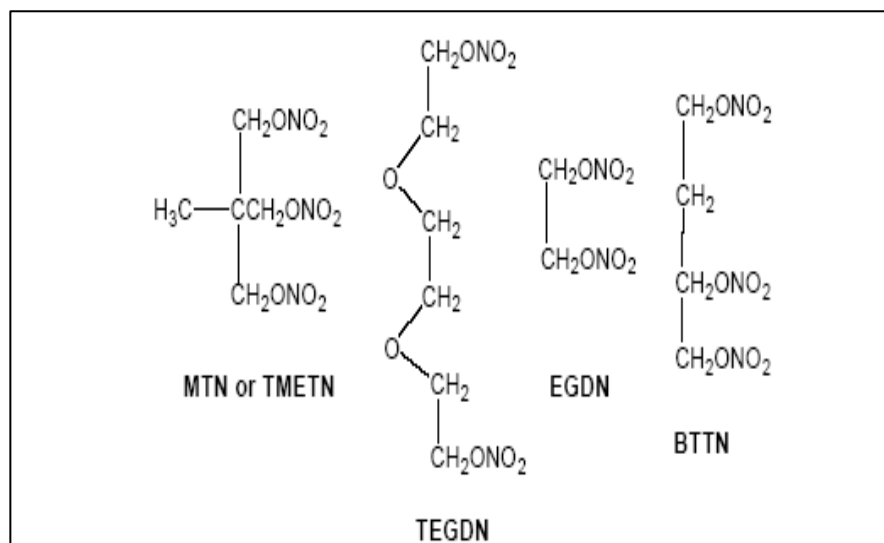


**Figure. 1.1** Molecular structure of energetic nitro plasticisers (Adapted from ; *Energetic Polymers and Plasticisers for Explosive Formulations. A Review of Recent Advances, DSTO-TR-0966*)

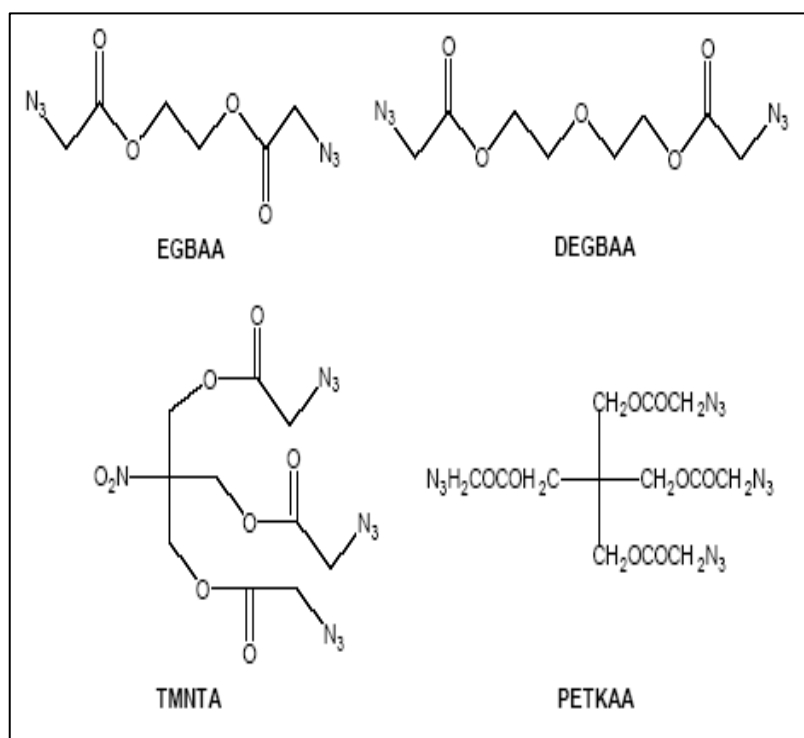


**Figure. 1.2** Molecular structure of energetic azide plasticisers (Adapted from; *Energetic Polymers and Plasticisers for Explosive Formulations. A Review of Recent Advances, DSTO-TR-0966*)

### 1.4.4.3. Burn rate modifier, Antioxidant, Cure catalyst

Apart from the above mentioned ingredients, few other liquid or solid products are added in small quantities to the propellant. Their function is to modify the characteristics of the propellant. Burning rate modifiers are used to modify the propellant burning rate of the propellant grain. Examples include copper chromite, ferric oxide, ferrocene, n-butyl ferrocene, oxamide, lithium fluoride, ammonium oxalate etc.

Antioxidants are essential to ensure satisfactory ageing of the propellant in ambient conditions. Examples are phenyl-b-naphthyl amine, ditertiary butyl paracresol, 2, 2-methylene bis (4methyl-6-tertiary-butyl phenol) etc.

Catalysts are often necessary to reduce the curing time of the propellant. They have a significant impact on the mechanical properties giving direction to the formation of the polymer network. They are usually salts of transition metals. Examples include triphenyl bismuth, dibutyltin diluarate, lead octoate, iron acetyl acetonate, lead chromate etc.<sup>9</sup>

## 1.5. NEW ENERGETIC MATERIALS

In the late 1990's subjects like environmental impact as a resultant of propellant combustion as well as the demand for better performance have led to the development of new technologies and triggered research on new energetic materials which are capable of delivering better performance than the conventional HTPB and AP based systems

This has led to the development of compounds that minimise pollution, safe for handling, assuring performance reliability and reproducibility, cost minimisation and so on. The search for environment friendly molecules is focused on chlorine free propellant compositions as perchlorate contamination as well as hydrochloric acid contamination is becoming a more widespread concern.<sup>25-26</sup>

The present attempts are to synthesise new compounds, specifically for use as energetic binders and oxidisers. This is being done by incorporation of energetic groups such as nitrate (-ONO<sub>2</sub>), azide (N<sub>3</sub>-) or fluorodinitro CF(NO<sub>2</sub>)<sub>2</sub> as side chain on to the existing polymer backbone.

### 1.5.1. Energetic Binders

Glycidyl azide polymer (GAP), 3,3'-bis (azidomethyl) oxetane (BAMO), 3-nitrato methyl-3'methyl oxetane (NIMMO), 3-azido methyl-3-metyl oxetane (AMMO), copolymer of BAMO-THF, polyglycidyl nitrate (PGN) etc are some of the energetic binders. Recently, polymer based on tetrazoles such as poly(methylvinyltetrazole) (PMVT), is quoted as under development in Russia. Other polymers such as polyethyleneglycol (PEG), polycaprolactone (PCP) and polyglycidyl adipate (PGA) are also reported for missile applications.<sup>30</sup> Characteristics of these energetic binders are given in Table 1.2.

### 1.5.2. Energetic oxidisers

The main characteristics of energetic oxidisers are higher density, high enthalpy of formation, high oxygen balance and absence of chlorine. New energetic ingredients such as heaxnitrohexazaisowurtzitane (HNIW)<sup>31</sup>, ammonium dinitramide (ADN)<sup>32-33</sup>, hydrazinium nitroformate (HNF)<sup>34</sup>, trinitroazetidine (TNAZ)<sup>35-36</sup>, octanitrocubane (ONC)<sup>34</sup>, 1,1,-diamino-2,2-dinitroethylene (FOX-7)<sup>34</sup> etc. have been synthesized for this purpose. The structures and properties of these energetic compounds are given in Table 1.3.

ADN and HNF<sup>29-31</sup> are powerful chlorine free oxidisers. Although, ADN and HNF have relatively less oxygen balance compared to AP, these have substantially higher heat of formation than AP leading to superior Isp. Moreover, they undergo highly exothermic combustion reactions near the surface leading to efficient heat feedback to the deflagrating surface enhancing the burning rates. ADN was synthesized in Zelinsky Institute of Russia and recently in Europe pilot-scale production of crystalline, prilled<sup>40</sup>, and coated ADN has commenced. Work on HNF was carried out mainly at TNO, Netherlands, and, today it is produced by Aerospace Propulsion Products (APP), Netherlands. Both the compounds are of importance all over the globe. However, severe hygroscopicity of ADN and higher sensitivity of HNF, particularly mechanical stimuli<sup>41</sup> are cause of concern. These compounds are also beset with the problem of low melting temperature (92°C and 123°C). Various approaches are attempted to overcome these drawbacks. Change in particle morphology is also recommended by various researchers to improve the sensitivity problems. However,

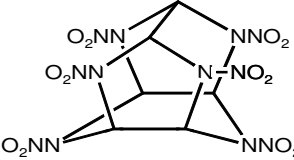
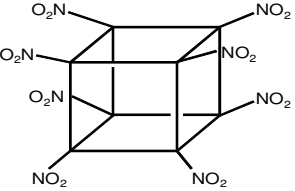
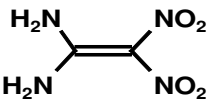
ADN propellants<sup>42</sup> are produced in Russia and are reported to be used in TOPOL-M intercontinental ballistic missile and few other formulations which are non-aluminised for tactical missile applications. However, with increase in solid loading above 78%, the hazard classification changes from 1.3 to 1.1 and this aspect is being addressed for large scale processing of these propellants.<sup>42-45</sup>

**Table 1.2. Characteristics of energetic binders**  
(Adapted from: ICT database of thermo chemical values)

Binder	Heat of formation (kJ/mol)	Density (g/cm <sup>3</sup> )	Tg(°C)	Structure
GAP	+117.2	1.3	-50	$\text{HO} - \left[ \begin{array}{c} \text{H} \\   \\ \text{CH}_2 - \text{C} - \text{O} \\   \\ \text{CH}_2\text{N}_3 \end{array} \right]_n - \text{H}$
BAMO	+413	1.3	-39	$\text{HO} - \left[ \begin{array}{c} \text{CH}_2\text{N}_3 \\   \\ \text{CH}_2 - \text{C} - \text{O} \\   \\ \text{CH}_2\text{N}_3 \end{array} \right]_n - \text{H}$
pNIMMO	-334.7	1.26	-25	$\text{HO} - \left[ \begin{array}{c} \text{CH}_3 \\   \\ \text{CH}_2 - \text{C} - \text{O} \\   \\ \text{CH}_2\text{ONO}_2 \end{array} \right]_n - \text{H}$
PGN	-284.5	1.39	-35	$\text{HO} - \left[ \begin{array}{c} \text{H} \\   \\ \text{CH}_2 - \text{C} - \text{O} \\   \\ \text{CH}_2\text{ONO}_2 \end{array} \right]_n - \text{H}$

**Table.1.3** Characteristics of Energetic Oxidisers

(Adapted from: ICT database of thermo chemical values)

Oxidiser	Structure	Oxygen Balance (%)	Density (g/cm <sup>3</sup> )	$\Delta H_f$ (kJ/mol)
ADN	$\text{NH}_4^+ \text{N}(\text{NO}_2)_2^-$	25.80	1.82	-150.6
HNF	$\text{N}_2\text{H}_5^+ \text{C}^-(\text{NO}_2)_3$	13.10	1.87	-72.0
HNIW (CL-20)		-10.95	2.04	381.2
ONC		0	2.10	413.8
FOX-7		-21.61	1.86	-133.9

### 1.5.3. Energetic Solid propellants

Future solid propellants shall be using the above mentioned energetic binders and oxidiser for both improving the energetic and for minimising environmental impact. A detailed thermochemical performance evaluation was carried, for selection of oxidiser-binder combinations with high Isp. The computations were carried out for a motor operating pressure of 6.93MPa and area ratio of 10 and given aluminium content of 18% (by weight) using NASA-CEA<sup>46</sup> software. The results are given in Table 1.4. From the table, it is clear that HNF is the superior oxidiser amongst the known choice of new oxidisers wherein, BAMO-HNF and BAMO-ADN are the best combination of advanced binder and oxidiser with Isp of 280-282 s. This is followed by GAP-ADN with 275 s as against the conventional HTPB-AP propellant with an Isp of 265s. The

vacuums Isp (V.Isp) of these propellants are also 10-15s higher than conventional HTPB-AP propellant with high density impulse as well as flame temperature. But, BAMO is a solid, and the problems related to the high sensitivity and crystal shapes of HNF are major concerns. GAP-HNIW gives high density impulse due to the high density of 2.01 g/cc of HNIW. However, HNIW has low oxygen balance and hence, an Isp increase is observed at high solid loadings of 90%, which causes difficulties while processing the propellant. Hence, GAP-ADN is the best choice with high Isp and high density impulse (Table 1.4).

**Table. 1.4** *Thermochemical Performance of Various Energetic Formulations*  
(Pressure: 6.93 MPa, Area ratio: 10)

Parameters	Propellant						
	HTPB	GAP	BAMO	PLN	GAP	BAMO	GAP
Binder	HTPB	GAP	BAMO	PLN	GAP	BAMO	GAP
Oxidiser	AP	ADN	ADN	HNF	HNF	HNF	HNIW
Solid loading (%)	86	82	76	84	84	84	90
Isp (s)	265	275	277	274	280	282	266
V.Isp (s)	290	300	302	298	305	307	290
Flame temperature (K)	3485	3787	3819	3786	3985	3936	3749
Density Impulse (s.g.cm <sup>-3</sup> )	513	537	529	533	561	565	583

## 1.6. ROLE OF THE BINDER

A binder<sup>47</sup> in the composite propellant acts as a matrix for holding together the oxidiser, metallic fuel and other additives and imparts the required dimensional stability. Thus it imparts structural integrity and mechanical properties to the propellant besides acting as a fuel by itself<sup>48-49</sup>. Large propellant grains or rocket motors in particular must have adequate mechanical properties to enable them to withstand the stresses imposed during curing, handling, transportation and motor ignition<sup>50-51</sup>. They must also withstand thermal stresses produced during long term storage and cycling at

temperature extremes. Although it contributes only about 10-15% by weight of the propellant formulation, it is the continuous binder phase that provides the elastic properties necessary for the solid propellant to withstand the stresses and strains imposed during motor processing, storage, ignition and flight. The binder containing mostly carbon and hydrogen can act as reducing agent (fuel), liberating gaseous products on combustion. The binder also forms chemical linkages with the liner and insulation interface of the rocket case and provides the required interface properties. The binder is essentially a liquid prepolymer with capability for chemical reaction with curing agents to give a crosslinked network. They retain the fluid consistency even when filled with seven to nine times by weight of solid materials (oxidiser and metallic fuel).

The mechanical properties of the propellant depend on the number of crosslinks and chains of the polymer<sup>52-54</sup>. The degree of crosslinking must be adequate to provide strength to the polymer. The addition of tri-functional to bi-functional units stabilises the number of branch points in the polymer and prevents excessive crosslinking. The random interchain connection along with crosslinking ensures the dimensional stability to propellant. The mechanical properties depend primarily on the characteristics of the binder, curing agents, the percentage of solids present (often referred to as solid loading) and the particle size distribution of the solids.

### **1.7. PROPERTIES OF AN IDEAL BINDER**

A partially polymerised liquid is ideal as binder because it cures with a minimum of shrinkage and heat release. The liquid form is required since it facilitates formation of a homogenous mixture of oxidiser and fuel as a paste, enabling the flow of the propellant slurry from mixing vessel to the rocket motor chamber. The constituents of the mixture should not be volatile to withstand the high vacuum used during mixing and casting operations.

The binder should have reasonable viscosity (in the range ~1-10 Pa.s). Very high viscosity of the binder renders it difficult to disperse the oxidiser uniformly and to process and cast at reasonable rates. Very low viscosities cause the oxidiser to settle rapidly in the uncured mix. The binder should also have chemically reactive functional groups preferably at the ends, which can be cross linked to an elastomer on curing. It



should have a reasonably long pot-life after addition of curative in propellant mixing to provide sufficient time for processing and casting of defect free grains.

It must be capable of accepting very high solid loading (up to 80-90% by weight) and must form strong adhesive bond with the rocket chamber materials such as insulations and inhibitions. It should preferably cure at low temperature and have low exothermic heat release to minimise the stresses while curing of the grain. It must have minimum shrinkage of curing to avoid severe stresses and debonding at liner-insulation- propellant interface while cooling. It should not evolve any volatile products and by-products on curing since the by-products may produce voids in the propellant grain and result in spongy propellant or can lead to undesirable post curing reactions. The curing reaction of propellant slurry should also give slow and gradual viscosity build-up in order to form a tough rubbery mass. The binder should have low glass transition temperature ( $T_g$ ) to give the propellant adequate properties to meet the physical and mechanical requirements at low temperatures. Generally,  $T_g$  is lower for polymers with hydrocarbon backbone structure than that with heteroatomic backbone (binders with oxygen, nitrogen or polar groups). The binder must be capable of bonding to rubber insulating material in addition to having similar coefficient of thermal expansion.

The binder should be physically and chemically stable in the presence of oxidisers and fillers, otherwise it will result in deterioration of propellant properties. The binder must release large amount of heat during combustion. From thermodynamic considerations, the binder must have high positive heat of formation and must contain mainly carbon and hydrogen elements in the polymeric backbone to produce low molecular weight gases and stable products on combustion.

### **1.8. TYPES OF POLYMERIC BINDERS**

All binders could be broadly classified<sup>55</sup> into linear (thermoplastic) and crosslinked (thermosetting) binders.

#### **1.8.1. Linear binders**

These are linear polymer chains exhibiting plastic properties. They are softened or even melted with heat and therefore they can be moulded to a desired shape after

mixing with other ingredients. Examples are the asphalt type of binder, polyisobutylene, polyvinylchloride etc. Although they offer the advantages of simplicity and lack of hazard from reaction exotherm or toxic curing agents, they suffer from the disadvantages of lack of dimensional stability, low performance and narrow working temperature limits, brittle and poor mechanical properties.

### **1.8.2. Crosslinked binders**

Polymeric liquid resins that can chemically crosslink during the curing process without the formation of gaseous products and solidify to become tough, insoluble, infusible substances are currently in use as binders. They have often superior physical and mechanical properties and the ability to bond to the rocket chamber wall with good adhesive properties. Commonly used chemically crosslinked propellant binders and the curing agents are discussed.

- ❖ Unsaturated polyesters cured using styrene or vinyl monomers with peroxide curative.
- ❖ Hydroxyl terminated polyether like polypropylene glycol (PPG), hydroxyl terminated polyester like polyester polyol (PEP), hydroxyl terminated natural rubber (HTNR), hydroxyl terminated polybutadiene (HTPB) etc. cured using diisocyanates
- ❖ Copolymer of butadiene and acrylic acid (PBAA), terpolymer of butadiene, acrylic acid and acrylonitrile (PBAN), carboxyl terminated polybutadiene (CTPB), lactone terminated polybutadiene (high energy fuel/HEF 20) etc. with curing agent as di/tri epoxy aziridine.

### **1.8.3. Polyurethane binders**

This binder system is formed from the quantitative reaction of prepolymers containing functional hydroxyl groups with diisocyanates. Polyesters with terminal hydroxyl groups were the first of this class to be introduced. Polyesters are not favoured for propellant formulations because of their low specific impulse, high viscosity and poor low temperature properties.

Polyethers with terminal hydroxyl groups were subsequently introduced as the prepolymer for polyurethane binder systems. The structurally different polyether diols mainly used were polyethylene glycol (PEG), polypropylene glycol (PPG) and polytetramethylene oxide (PTMO). Terminal hydroxyl groups are either primary or secondary, which have different reaction rates during curing with diisocyanates. The main disadvantages of the polyether polyols are low viscosity and improper rate of cure. However, the presence of oxygen in the backbone through ether or ester function is accompanied by a decrease in heat of combustion and thus, the specific impulse of these binders is low, compared to hydrocarbon binders. But these binders are widely used for gas generators and pyrogen igniter propellant applications.

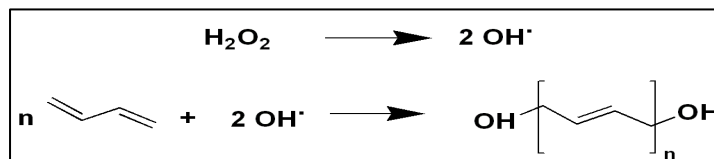
Polybutadiene containing terminal hydroxyl groups or HTPB based polyurethane binder began to be used in propellants about four decades ago and still remains the workhorse today as it has significant advantages over propellants based on CTPB, PBAN etc. in terms of increased specific impulse, superior mechanical and ballistic properties. HTPB propellants also have long term storage stability, proven by chemical and structural ageing studies.<sup>55-56</sup>

## **1.9. HTPB**

### **1.9.1. Synthesis of HTPB**

In literature<sup>57</sup> three processes are reported for the synthesis of HTPB, viz. free radical polymerization<sup>57-58</sup>, anionic polymerization<sup>59-60</sup> and by degradation of high molecular weight butadiene<sup>61</sup>. Anionic mechanism involves a living polymer chain of butadiene derived from a catalyst like metal naphthalene (Na or Li naphthalene). The chain is terminated using alkene oxide, aldehyde or ketone. For the synthesis, polar solvents are found to favour 1, 2-addition resulting in polymer with higher vinyl content (>90%) and non-polar solvent, the vinyl content is <15%. Anionic HTPB has narrow dispersity and has a functionality of two.

Free radical synthesis of HTPB involves a free radical mechanism employing initiators like azo compounds, peroxides and redox systems. The initiators are cleaved into free radical giving rise to hydroxyl substituents by heat, light or redox systems<sup>62</sup>. The synthesis scheme for free radical polymerisation of HTPB is given in Scheme 1.1



*Scheme 1.1. Free radical synthesis of HTPB*

### 1.9.2. Characterization studies on HTPB

HTPB has been characterized for the type of hydroxyl groups by chemical methods, spectrometric method like Nuclear Magnetic Resonance Spectroscopy (NMR),<sup>63-64</sup> UV visible spectroscopy,<sup>65</sup> Fourier Transform Infrared Spectroscopy (FTIR)<sup>66</sup>, and other indirect methods like column chromatography<sup>67</sup>. The structure and nature of hydroxyl groups namely primary and allylic are elucidated by NMR spectroscopy. In UV spectrum, absorption peak at 280 nm is attributed to transition of trans microstructure of HTPB. The presence of IR peaks at 723, 910 and 968  $\text{cm}^{-1}$  correspond to *cis*-1, 4, vinyl-1, 2, and *trans*-1, 4 microstructures, respectively.  $^1\text{H}$  NMR spectrum in the region of 5.2–6.2 and 4.8–5.0 ppm correspond to *cis/trans*-1, 4 and vinyl-1, 2 microstructure configurations, respectively. Conventional techniques such as end group analysis, vapor pressure osmometry, and gel permeation chromatography are used to determine the molecular weight and its distribution of HTPB. Detailed investigations on the functionality distribution of HTPB and microstructure of HTPB have also been reported.<sup>68</sup> HTPB is chemically crosslinked using isocyanates to form polyurethanes and this reaction has been investigated in detail by many researchers<sup>69-77</sup>.

### 1.9.3. Thermal properties of HTPB

The thermal decomposition kinetics of HTPB resin has been reported<sup>78-81</sup>. HTPB undergoes a two-step thermal degradation in nitrogen atmosphere. The first stage of reaction is exothermic and occurs in the range of 300 to 410°C. The reaction is primarily depolymerization, cyclization, crosslinking and partial decomposition of the cyclized products. Major gaseous products produced are hydrocarbons namely 1, 3-butadiene, cyclopentene, cyclohexadiene, and 4-vinylcyclohexene. The second stage of reaction is endothermic and occurs in the range of 410 to 510°C. The processes are dehydrogenation and decomposition of the cyclized products formed in the first stage. Panicker et al.<sup>80</sup> have studied the effect of molecular weight on thermal decomposition

temperature. As molecular weight decreases, it is reported that there is an increase in weight loss. This is due to the formation of greater number of cyclized products. The second stage is not influenced by the molecular weight of the sample. During flash pyrolysis of HTPB, six major products namely butadiene, 4-vinyl-1-cyclohexene, trans butadiene oligomers, ethylene, 1, 5-hexadiene and cyclopentene are reported. The decomposition chemistry and kinetics of HTPB and polyurethanes based on diisocyanate crosslinked HTPB were determined by thermogravimetric analysis (TGA), differential scanning calorimetry (DSC) and infra red (IR) spectroscopy. The first step (300-400°C) for polyurethane decomposition is fission of the urethane bonds. The diisocyanate crosslinking agent is vaporized to an extent that is controlled by its vapour pressure. The thermal decomposition of solid propellants based on HTPB with AP as oxidiser has been studied by Rocco et al.<sup>81</sup>. The combustion and thermal decomposition of HTPB-HNIW and HTPB-ADN have been reported wherein, a correlation between burning rate and pressure, effect of additives etc have been established. The flash pyrolysis studies on AP-HTPB mixture by Brill et al.<sup>78, 79</sup> gives a comprehensive report on the pyrolysis of AP-HTPB mixtures which is an important input for modeling of decomposition of conventional propellants.

#### 1.9.4. Functional modification of HTPB

One problem is that HTPB is an inert binder with lower overall energy output and which gives moderate performance in the rocket propellant. A significant number of efforts have been demonstrated in the literature<sup>82</sup> for modification. Phase-transfer catalytic epoxidation of HTPB by hydrogen peroxide was investigated by Wang et al.<sup>83</sup> Barcia et al.<sup>84</sup> have reported epoxy resin networks by pre-reacting functionalized polybutadiene with the epoxy resin Epoxidized HTPB (Fig. 1.3) is useful as toughening agent for epoxy resins, which are otherwise brittle at room temperature<sup>85</sup>.

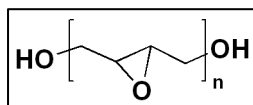


*Figure 1.3. Molecular structure of Epoxy HTPB*

Nitrated HTPB (NHTPB) acts as energetic binder. NHTPB is synthesized by epoxidizing HTPB and then nitrating with dinitrogenpentoxide (N<sub>2</sub>O<sub>5</sub>)<sup>86-89</sup> (Fig. 1.4).

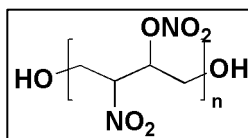


**Figure 1.4.** Molecular structure of Nitrated HTPB

Thiols react with double bonds of HTPB to give functional derivatives (Fig. 1.5) and 2-mercaptoethanol can be grafted to HTPB<sup>90</sup> to increase hydroxyl functionality and to saturate the 1, 2-double bonds.

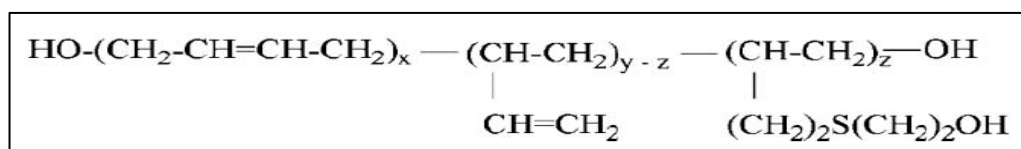


**Figure 1.5** HTPB reacted with thiols (Adapted from Ref: *J. Macromolecular Science, Part A: Pure and Applied Chemistry*, 2012, 50, 128-138)

HTPB based poly (glycidyl azide) graft copolymer can be prepared by from 4, 4-azobis (4-cyanopentanoyl chloride) and poly (glycidyl azide) using triethyl amine and benzene as solvent. This graft copolymer is an energetic binder because poly (glycidyl azide) is capable of self-burning at elevated pressures as it contains energetic pendant azide groups.<sup>90-91</sup> The hydroxyl groups of HTPB can be derivatised by different methods. Acetylation reaction was carried out by reacting HTPB with acetic anhydride in pyridine solution at 95-98°C for 3 hours or alternatively, HTPB can be refluxed with acetic anhydride<sup>93</sup>(Fig. 1.6).

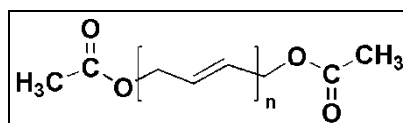


**Figure 1.6.** Molecular structure of acetylated HTPB

Carboxyl terminated polybutadiene (CTPB) is prepared from HTPB (Fig. 1.7) by reacting HTPB with maleic anhydride.<sup>94-95</sup> CTPB can be used for preparing block copolymers by reacting with epoxy resin using triphenyl phosphine as catalyst. These block copolymers help increase the compatibility between HTPB and epoxy matrix and also provides better interfacial adhesion. Compatibility and adhesion obtained using CTPB based block copolymer are higher than those obtained with epoxidized HTPB. Ester derivatives of HTPB such as acrylates and methacrylates can be prepared by

reacting with respective carboxylic acids, acid chlorides and anhydrides or by transesterification.

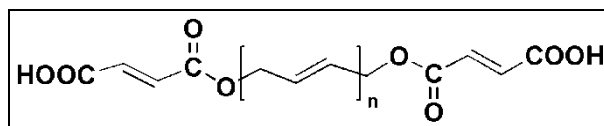


**Figure 1.7.** Molecular structure of carboxyl terminated HTPB

Isocyanate end-capped HTPB<sup>96</sup> is prepared by reacting one mole of HTPB with two moles of tolylenediisocyanate (TDI) using stannous octoate or dibutyl tin dilaurate as catalyst (Fig. 1.8). Different crosslinking density of HTPB can be prepared by varying the amount of TDI. Increase in hardness, tensile and tear strength, tensile modulus and decrease in elongation at break are observed with increase in the amount of TDI. Coupling reaction of isocyanate end capped HTPB with diglycidyl ether based epoxy resin yields epoxy resin–polybutadiene block copolymers. Alternatively, by reacting isocyanate end capped HTPB with 2-hydroxyethyl methacrylate, urethane methacrylate is obtained.

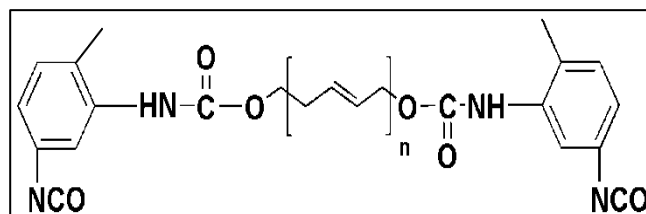


**Figure 1.8.** Molecular structure of isocyanate end capped HTPB

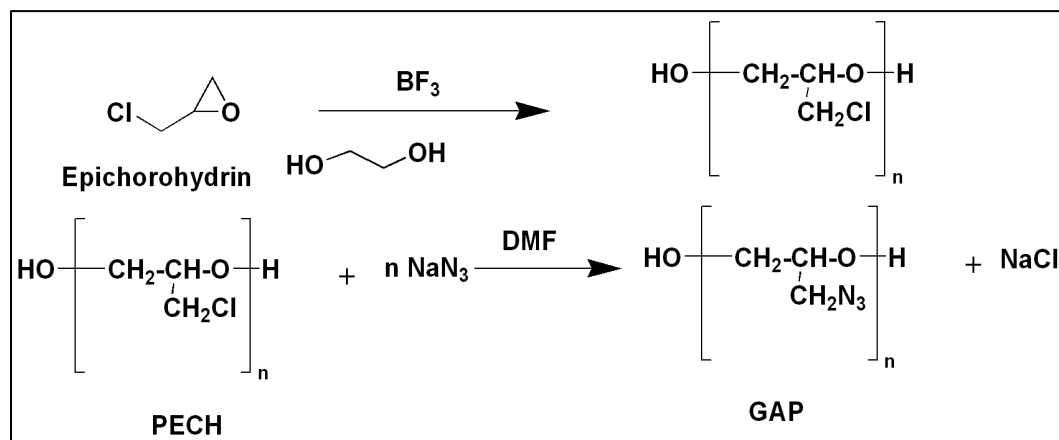
Amine-terminated polybutadiene (ATPB)<sup>97</sup> having one or two terminal amino groups, is prepared by cyanoalkylating HTPB by Michael addition of acrylonitrile in the presence of a base, forming nitrile terminal groups which are further reduced. . Functionalisation at the carbon atoms of HTPB backbone is reported to be carried out by covalently attaching 2-chloro-4,6-bis (dimethylamino)-1,3,5-triazine (CBDT) and 1-chloro-2,4-dinitrobenzene (DNCB) to the terminal carbon atoms of the HTPB.<sup>98-101</sup> Subramanian et al.<sup>102</sup> have grafted a burn rate catalyst iron pentacarbonyl to the double bonds of HTPB. The synthesis of 2-(ferrocenylpropyl) dimethylsilane (FPDS)-grafted hydroxyl-terminated polybutadiene and burning rate of ferrocene grafted HTPB based propellant have also been reported.<sup>103-104</sup>

However, in spite of these modifications, the overall energy output could not be improved and this has led to the need for in the development of new energetic binders by introducing energetic groups such as nitrate ( $-\text{ONO}_2$ ), azide ( $-\text{N}_3$ ) or fluorodinitro  $\text{CF}(\text{NO}_2)_2$  as side chain on to existing polymer backbone. Amongst these, GAP is the most popular binder with desirable features of positive heat of formation and reasonable thermal stability. It is widely used for various applications like gas generators or pyrogen igniter applications as well as used in conjunction with advanced energetic oxidizers like ammonium dinitramide as mentioned previously for realising solid propellants with improved performance.

## 1.10. GAP

### 1.10.1. Synthesis of GAP

Ever since it has been demonstrated that organic azido compounds offer great potential for producing a new generation advanced propellant, the scope of the currently available candidates were explored.<sup>105</sup> Consequently, work was initiated in 1976 for the preparation of a hydroxyl terminated azido prepolymer from the reaction of polyepichlorohydrin (PECH) with sodium azide in dimethylformamide medium at  $0^\circ\text{C}$  under nitrogen atmosphere<sup>106</sup>. PECH is formed from epichlorohydrin by using  $\text{BF}_3$ -etherate catalysts in the presence of low molecular weight diols to produce hydroxyl terminated polyepichlorohydrin as given in (Scheme 1.2). The reaction proceeds by cationic mechanism. Ethylene glycol acts as a co-catalyst and chain transfer agent.



*Scheme 1.2. Synthesis of GAP from PECH*



For the synthesis of GAP triol, PECH triol was synthesized<sup>107</sup> by the polymerization of epichlorohydrin (EM) using glycerol as initiator followed by reaction with sodium azide. Preparation of GAP containing various initiative diol units in the polymer chain have been reported by Mohan et al.<sup>108</sup> Branched glycidyl azide polymer (GAP) and glycidyl azide-ethylene oxide copolymer (GEC) have been reported to be prepared by a degradation process using different polyols. The characterization of physico-chemical properties of glycidyl azide polymer (GAP), specifically deuterated analogs was investigated by Ringuette et al.<sup>109</sup> Liu et al.<sup>110</sup> have reported a series of novel polymers, glycidyl 4-functionalized 1,2,3-triazole polymers (functionalized GTP) by click functionalisation of glycidyl azide polymer (GAP). With an objective of preparation of an OH-terminated amorphous polymer with energetic content higher than that of glycidyl azide homopolymer, glycidyl azide-(3,3-bis(azidomethyl)oxetane) copolymers were synthesized by cationic copolymerization of epichlorohydrin and 3,3-bis(bromomethyl)oxetane, using butane-1,4-diol as an initiator and boron trifluoride etherate as a catalyst, followed by azidation of the halogenated copolymer. Bui et al.<sup>111</sup> and Mohan et al.<sup>108</sup> have prepared copolymers of glycidyl azide with ethylene oxide and tetrahydrofuran, respectively and the resultant copolymer elastomers exhibited good mechanical properties because of their improved backbone flexibility. Subramanian et al.<sup>112</sup> have synthesized a triblock copolymer polyglycidylazide-b-polybutadiene-b-polyglycidylazide (GAP-PB-GAP) with the flexibility of polybutadiene and energetics of GAP. Khalifa et al.<sup>113</sup> have reported a glycidyl azide polymer with pendent N,N-diethyl dithiocarbamate groups (GAP-DDC) by the reaction of poly(epichlorohydrin) (PECH) with pendent N, N-diethyl dithiocarbamate groups (PECH-DDC) and sodium azide ( $\text{NaN}_3$ ) in dimethylformamide (DMF). It was then used as a macro-photoinitiator for the graft polymerization of methyl methacrylate (MMA). Brochu<sup>114</sup> have synthesized an isotactic GAP and a GAP-poly(BAMO) poly(bis(azidomethyl)oxetane)] copolymer and tried to improve mechanical properties of GAP elastomer through polymer recrystallisation forming a microphase separation. Manzara et al.<sup>115</sup> have patented higher molecular weight, primary-hydroxyl terminated GAPs, which, in comparison with lower molecular weight GAP, have improved GAP mechanical properties.

### 1.10.2. Curing of GAP

GAP is terminated with hydroxyl groups and the ideal curative is a polyisocyanate. The curing of a glycidyl azide polymer (GAP) with a triisocyanate, was followed by measuring the hardness and viscosity as well as quantitative FTIR spectroscopy. The thermal behaviors of the cured samples were investigated by a differential scanning calorimeter (DSC) and thermal gravimetric analysis (TGA) was done by Ozkar et al.<sup>116</sup> Reactions between hydroxyl-terminated glycidyl azide polymer (GAP) and different isocyanate curatives such as toluene diisocyanate (TDI), isophorone diisocyanate (IPDI), and methylene diisocyclohexyl isocyanate (MDCI) at various temperatures were followed by Fourier transform infra red spectroscopy<sup>117</sup>. Copolymerization and block copolymerization, polymer blends or interpenetrating polymer network have also been reported by Manu et al.<sup>118</sup> wherein mechanical and thermal characterization cross-linked glycidyl azide polymer (GAP) and GAP–hydroxyl terminated polybutadiene (HTPB) networks have been reported.

Change in the surface free energy of poly(glycidyl azide) (PGA) networks prepared with different reactive systems was investigated using contact-angle measurement in order to estimate their wettability properties. Min et al.<sup>119</sup> have used composite curing agents and prepared GAP/polyethylene glycol and GAP/polycaprolactone interpenetrating network elastomers. The morphologies of energetic block copolymers based GAP was investigated by particle dynamics simulation. The results show that the morphologies could be used to qualitatively explain the variation in the mechanical properties of poly(glycidyl azide-b-butadiene) diblock copolymers and that bicontinuous phases could effectively improve the mechanical properties.<sup>120-122</sup>

### 1.10.3. Thermal properties of GAP

Thermal decomposition reactions and decomposition products of glycidyl azide polymer (GAP) have been investigated by direct insertion mass spectrometry and evolved gas analyses by FTIR spectroscopy techniques. It has been observed, that the thermal degradation of GAP begins with cleavage of the side groups. Evolved gas analyses by FTIR spectroscopy confirmed formation of small molecular weight species

such as CO, CH<sub>4</sub>, C<sub>2</sub>H<sub>2</sub>, HCOOH, and NH<sub>3</sub>.<sup>123</sup> The combustion characteristics viz. burning rates, temperature profiles, kinetic parameters for the thermal decomposition of uncrosslinked GAP and cured GAP were determined by Korobeinichev et al..<sup>124</sup> The pyrolysis of a 50:50 mixture of RDX-GAP-diol cured with the Desmodur N-100 (HMDI-based isocyanate), and a 70:21:9 mixtures. of RDX-BTTN-GAP-polyol cured with HMDI were studied by Brill et al..<sup>125</sup> The mechanism for the thermal decomposition of a model GAP compound CH<sub>3</sub>CH(CH<sub>2</sub>N<sub>3</sub>)CH<sub>2</sub>OH, was elucidated<sup>126</sup> by means of a quantum chemical calculations with the hybrid d.-functional theory. The result reveals the following three low-energy pathways for the decomposition involving evolution of nitrogen, formation of imine and rearrangement of the imine formed with activation barriers of 39.9, 41.9, and 57.2 kcal/mol respectively. Differential scanning calorimetry (DSC) and thermo gravimetric analysis (TGA) were used to investigate the thermal behavior of glycidyl azide polymer (GAP) and GAP-based urethanes and GAP in the presence of plasticizers dioctyl adipate (DOA) and bis-2,2-dinitropropyl acetal or formal (BDNPA/F).<sup>127</sup> The thermal decomposition and burning rate of GAP mixed with metals Al, Mg, B, Ti, and Zr were studied by Kuwahara et al..<sup>128</sup> Simultaneous temperature and species measurements were performed to investigate thermal decomposition of cured GAP.<sup>129</sup> Experiments were conducted at atmospheric pressure in argon with heat fluxes of 50, 100, and 200 W/cm<sup>2</sup> delivered by CO<sub>2</sub> laser. It was found that the species and temperature were insensitive to the heat flux level. The mole fractions of the observed species at a heat flux 100 W/cm<sup>2</sup> were almost the same as those at a heat flux of 200 W/cm<sup>2</sup>, and the surface temperature was approximately 1050 K at both heat fluxes. The thermal decomposition of branched GAP was studied using DSC and TGA.<sup>130</sup> The variable heating rate and isothermal techniques were used for obtaining kinetic results for branched GAP having one, two, or three terminal -OH groups were flash pyrolyzed (dT/dt = 800 K/s) to 540-600 K at 2 atmosphere in Ar by.<sup>131</sup> The volatile products identified from the condensed phase were CH<sub>4</sub>, HCN, CO, C<sub>2</sub>H<sub>4</sub>, NH<sub>3</sub>, CH<sub>2</sub>O, CH<sub>2</sub>CO, H<sub>2</sub>O, N<sub>2</sub>, and GAP oligomers. Decomposition reactions of glycidyl azide polymer (GAP) and poly(glycidyl nitrate) (PGN) have been investigated by pulsed IR laser pyrolysis and UV laser photolysis of thin films at 17-77 K.<sup>132-135</sup> The initial step of chemical reaction initiated by laser-generated shock waves was observed in glycidyl azide polymer (GAP) in the condensed phase. Shocks were generated by pulsed laser vaporization of thin aluminum films and launched into adjacent films of

GAP at 77 K. Comparison of FTIR spectra obtained before and after shock passage shows that initial reaction involves elimination of molecular nitrogen ( $N_2$ ) from the azide functional groups of the polymer. The mechanism and energetics of the thermal decomposition of GAP triol, a non-linear glycidyl azide polymer used as the starting material to produce a binder in composite propellants, were examined by differential scanning calorimetry, thermogravimetry (TGA), and accelerating rate calorimetry.<sup>132</sup> The thermal decomposition of polyglycidyl azide (GAP) and bis(azidomethyl)oxetane-tetrahydrofuran copolymer (BAMO/THF),<sup>131</sup> studied by TGA and DSC showed overall first-order kinetics for the decomposition of these compounds. Additional azide groups at the terminal positions in GAP decomposed independently and increased the rate of decomposition and the decomposition kinetics was less affected by the additional azide groups in the main chain. A mass spectrometric study of thermal decomposition was made on four azido polymers BAMO, AMMO, azidooxetane polymer (AZOX) and GAP. The primary decomposition mechanism for all the polymers was the rupture of the azide bond to release  $N_2$ . Activation energies obtained were 42.7 kcal/mol for BAMO, 43.6 kcal/mol for AMMO, 40.1 kcal/mol for AZOX, and 42.2 kcal/mol for GAP.

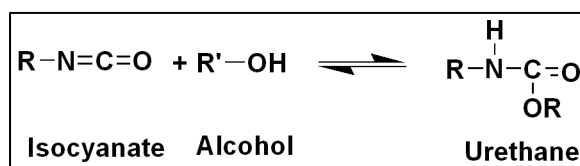
#### 1.10.4. GAP based propellants

Yuan et al.<sup>136</sup> have described the combustion characteristics of GAP gumstock propellants in the presence of burn rate modifiers like catocene, n-butyl ferrocene etc. The burning rate and flame structure of GAP based composite propellants were examined in order to obtain a wide spectrum of burning rates<sup>137-138</sup>. A study has been conducted on droplet combustion of liquid GAP with metals and oxidisers to clarify the reaction with GAP.<sup>139</sup> Suppression of HCN emission from GAP-HTPB cured polymers was studied by Panda et al.<sup>140</sup> for ramjet applications. The steady-state combustion of mixtures of RDX/GAP has been modeled using a one dimensional, three-phase numerical model, with detailed chemical kinetics.<sup>141</sup> Numerical simulation of HMX/GAP pseudo-propellant combustion has been performed with detailed chemical kinetics and it is reported that burning rate decreases with the addition of GAP at low pressures, even though the burn rate of GAP itself is much higher than pure HMX.<sup>139</sup> The performance of gas generator propellants based on bisdinitropropyl acetal/formal as plasticiser with phase stabilised ammonium nitrate (PSAN) /guanidine trinitrate

(TAGN) as oxidisers also have been reported.<sup>142-144</sup> Landsem et al.<sup>145</sup> have reported the preparation, friction and impact sensitivity and mechanical properties of several smokeless propellant formulations based on prilled ADN and isocyanate cured and plasticized GAP or polycaprolactone-polyether. They have also reported the synthesis and use of a new aromatic alkyne curing agent, in smokeless propellants based on GAP using either octogen (HMX) and prilled ADN as energetic filler materials.

### 1.11. CURING REACTIONS IN HTPB AND GAP

HTPB and GAP are conventionally cured with isocyanates like tolylene diisocyanate (TDI) or isophorone diisocyanate (IPDI) to form polyurethane networks. The formation of polyurethane an addition reaction between an isocyanate with an alcohol as shown in Scheme 1.3. The reaction is strongly influenced by catalysts; e.g. acid compounds (mineral acid, acid halide etc.) slow the reaction, whereas basic compounds (tertiary amines) and metal compounds (Sn, Zn, and Fe salts) accelerate the reaction.<sup>146</sup>



*Scheme 1.3. Reaction of isocyanate with hydroxyl group*

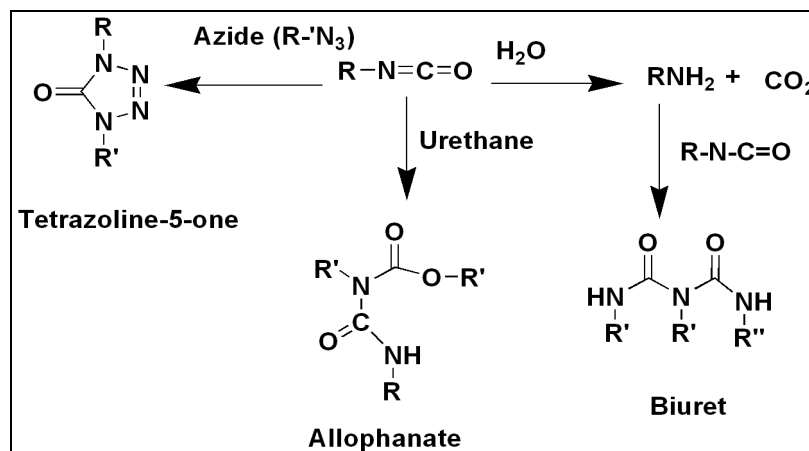
Among the isocyanates, the aromatic ones are more reactive than the aliphatic ones. This is because, the electron withdrawing groups increase the reactivity of the –NCO groups while the electron donating groups decrease the reactivity against hydrogen active compounds.

However, the urethane formation has several draw backs because of other side reactions as described below.

### 1.12. REACTION OF ISOCYANATE WITH WATER

The primary product of the reaction with water is a substituted carbamic acid, which breaks down into an amine and carbon dioxide. The amine then reacts with further isocyanate to yield the substituted urea. Thus to avoid this reaction, complete

exclusion of water from the reaction is essential. The liberation of  $\text{CO}_2$  results in voids in the polymer during curing and results in deterioration in properties. In addition, isocyanates can react with diamines. Other secondary reactions of isocyanate are with the active hydrogen atoms of the urethane and urea linkages to form allophanate and biuret linkages, respectively. Both reactions are cross-linking reactions, and occur to an appreciable rate over the temperature intervals of  $100\text{-}150^\circ\text{C}$  and  $120\text{-}150^\circ\text{C}$ , respectively. The reaction of isocyanates with urea groups is significantly faster than that with urethane groups. However, these linkages are thermally reversible, and dissociate at higher temperatures into starting components. The extraneous side reaction of isocyanates with other ingredient leads to problems during propellant processing. Moreover, the azido group in GAP can also react with isocyanates leading to the formation of tetrazoline-5-one<sup>147</sup> as shown below in Scheme 1.4.



**Scheme 1.4** Formation of biuret, allophanate and tetrazoline-5-one

A fast cure process that rapidly depletes the isocyanate groups has been employed to attempt to overcome this problem. These fast cure reactions lead to short propellant pot-lives which make propellant processing and motor casting more difficult. Additionally, the cure catalysts often contain metal ions which are known to decompose organic azides.

Hence, a need has been felt to explore an alternate methodology for curing HTPB and GAP. One such alternate route is ‘Click chemistry’ which is the focus of the thesis.

### 1.13. CLICK CHEMISTRY

Click chemistry is a versatile and fast emerging tool for the design of molecules with diverse characteristics. The term 'click chemistry' was introduced by Sharpless et al.<sup>148-151</sup> and is defined as "a reaction that is modular, wide in scope, high in yield, has little side products that are easily isolated using simple methods, is stereo specific, uses simple reaction conditions, is not sensitive to oxygen or water, uses easily accessible reagents, requires no solvent or a solvent that is easily removed, enables simple product isolation, has a high thermodynamic driving force (greater than 20 kcal/mol) and goes rapidly to completion". Most of the click chemistry reactions are carbon-heteroatom bond forming reactions, for example:

- Cycloadditions of unsaturated molecules
- Nucleophilic substitution, especially ring-opening reactions of heterocyclic electrophiles that have high ring-strain
- Carbonyl chemistry (except for the "aldol")-type reactions
- Certain 'Michael Type' addition reaction
- Oxidizing reactions like aziridination, dihydroxylation and epoxidation.

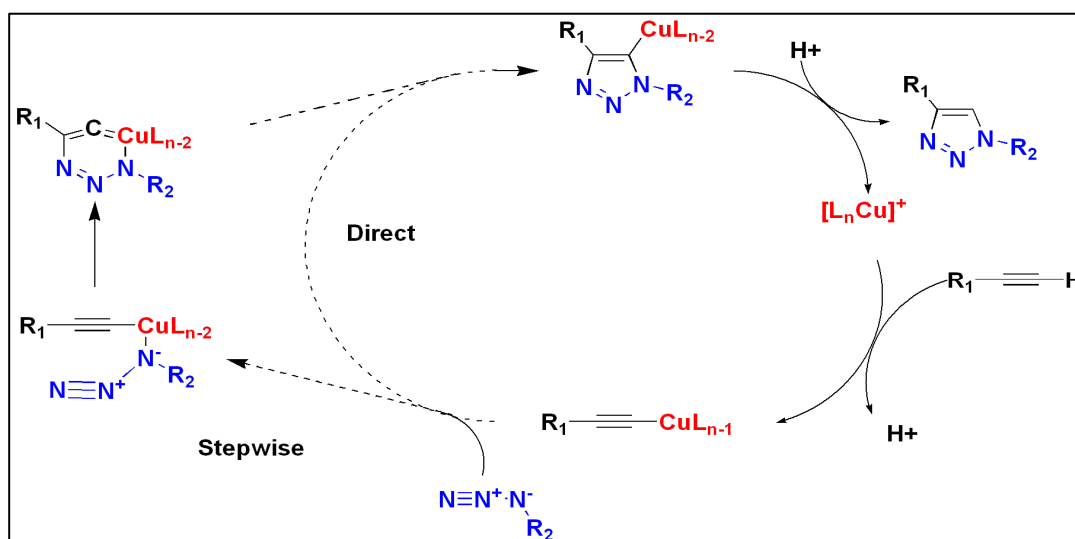
Reports on click chemistry are mostly on the CuI catalyzed Huisgen 1, 3-dipolar cycloaddition reaction.<sup>152</sup> This reaction is part of the hetero-Diels-Alder family and is considered to be the most reliable (due to the stability of compounds namely azides and alkynes used in the reaction) and powerful due to the wide variety, accessibility and relative inertness (towards other organic reactions) of the starting compounds.

#### 1.13.1. Cycloaddition of Azides and Terminal Alkynes

The Huisgen reaction<sup>152</sup> using azides as dipoles with alkynes and azides as diophile resulting in 1,4 and 1,5 regioisomer of 1,2,3-triazoles were reported. This reaction gained interest after the copper catalyzed version was introduced by Meldal et al.<sup>153</sup> and Sharpless et al.<sup>154</sup>. It was reported that acceleration of the thermal process by CuI salts, occurs at ~25°C in quantitative yields with high regioselectivity yielding 1, 4 regioisomer of 1, 2, 3-triazoles. Later, Sharpless<sup>155-156</sup> reported the formation of 1, 2, 3-triazoles by the CuI-catalyzed Huisgen reaction between non-activated alkynes and alkyl/aryl azides based on a concerted mechanism via a Cu acetylide intermediate. The

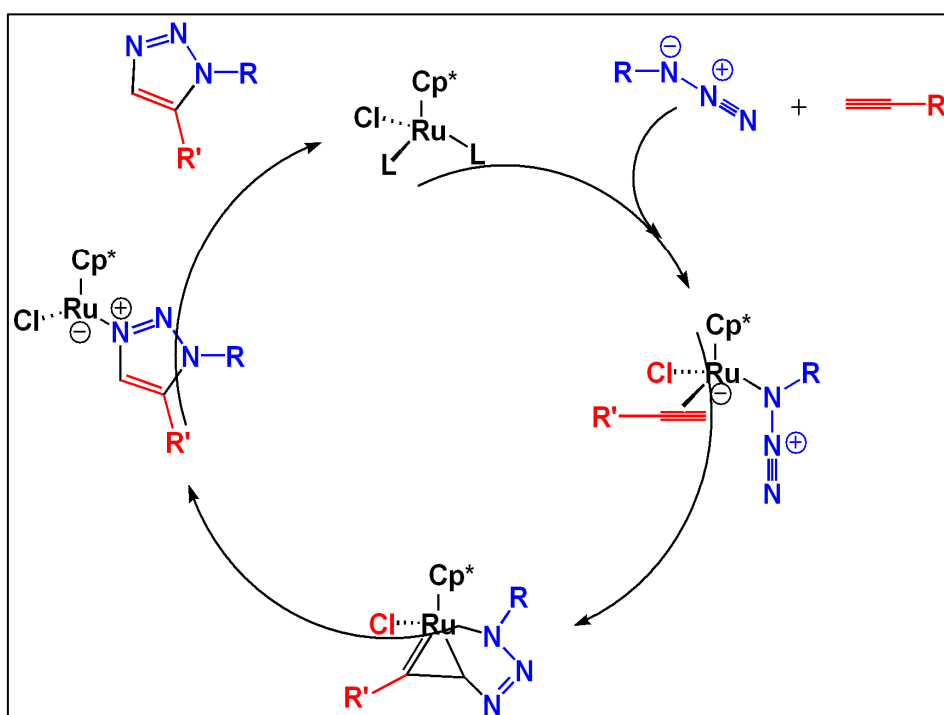
critical ‘invention’ of this process is the transformation of a purely thermal 1,3-dipolar cycloaddition process (Scheme 1.5) to a 1,3- dipolar cycloaddition process catalyzed by metal salts (mostly CuI salts, but recently also Ru, Ag, Ni, Pd, and Pt salts) which runs at ambient temperature and is solvent insensitive (Scheme 1.6).<sup>157-159</sup>

In general, cycloadditions proceed through a concerted mechanism. However, experimental kinetic data and molecular modeling performed on the reaction seem to favor a stepwise reaction pathway. Cu (I) can readily get inserted into terminal alkynes to form Cu acetylide by forming of  $\pi$ -complexes between Cu (I) and alkynes. In this process, pKa value of the terminal alkyne decreases by as much as 9.8 pH units, indicating an increase in acidity of terminal carbon. Thus, C-H bond will break, leading to deprotonation of the terminal hydrogen and formation of Cu-acetylide. The mechanism involves formation of a bond between nitrogen and one of the Cu in the Cu acetylide complex with a metallocycle intermediate followed by formation of triazole (Scheme 1.5). The Cu dimer will dissociate from the 1, 2, 3 triazole on protonation. Most methods use Cu (I) salts directly, other methods generate the copper(I) species by reduction of Cu (II) salts using sodium ascorbate or metallic copper. Recently, the use of copper clusters of Cu/Cu oxide nanoparticles, (sized 7–10 nm), as well as copper clusters of diameter 2 nm, with a specific surface area of 168 m<sup>2</sup>/g have been described<sup>160</sup>. There have been reports on the formation of 1, 5 regioisomer using Ru catalyst based on a mechanism given in Scheme 1.9.



**Scheme 1.5** Proposed catalytic cycle for the CuI-catalyzed ligation. (Adapted from: *J. Am. Chem. Soc.*, 2005, 127, 210-216)



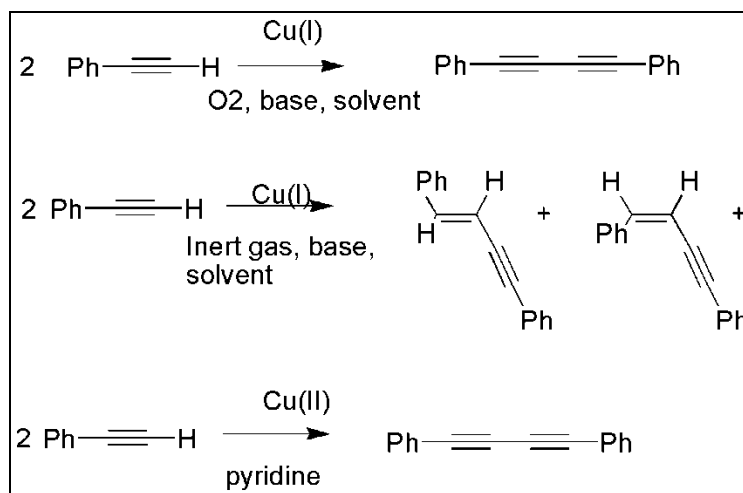


**Scheme 1.6** proposed catalytic cycles for the Ru-catalyzed ligation yielding 1, 5 regioisomer (Adapted from: *J. Am. Chem. Soc.*, 2008, 130, 8923-8930)

### 1.13.2. Limitations of Copper Catalysed Click Reaction

Cu (I)-catalyzed Huisgen 1, 3-dipolar cycloaddition of terminal alkynes and azides does not always give high yields irrespective of the nature of the reactants. If the diene (the azide in the case) is highly electron deficient, the energy of its ground state configuration is far too low for it to interact with a dienophile (the terminal alkyne) and likewise, if the dienophile is highly electron rich, reaction will not occur.

A more common problem is alkyne homocoupling. This occurs when an alkyne reacts with a second alkyne instead of the azide as shown in Scheme 1.6. There are several alkyne homocoupling side reactions that can occur such as those reported by Glaser<sup>161</sup>, Straus<sup>162</sup>, and Eglinton couplings.<sup>163</sup> Some of these require a Cu<sup>+1</sup> catalyst (Glaser and Straus), while others require Cu<sup>+2</sup> (Eglinton). Some need the presence of oxygen to react (Glaser) while others can continue in inert atmosphere (Straus). Most of these reactions, though, can be minimized by using a sterically hindering bulky base.



*Scheme 1.7: Three types of alkyne homocouplings*

Another problem encountered is saturation of the coordination sphere of Cu (I). For click reaction to occur, the CuI-acetylide complex intermediate has to be in close proximity with the azide. However, if the complex is closely surrounded by terminal alkynes, then there is a chance that the alkynes will chelate with the complex, thereby “saturating” the coordination sphere of copper. This effectively prevents any azide functional groups from reaching the complex. Cu (I) saturation is rare, as it requires a dienophile that contains multiple terminal alkynes that can coordinate to a single location. One such notable example is reported by Zhao et al.<sup>164</sup> A substrate containing four terminal alkynes in close proximity was unable to undergo a copper catalysed click reaction. However, when the alkynes were replaced with azide functional groups, the substrate readily reacted.

The click reaction was not widely pursued due to the explosive nature of sodium azide as well as that of low molecular weight organic azides. However, with the advent of advanced synthetic methodologies these problems have been circumvented and ‘click chemistry’ is now widely used in all realms of chemistry as well as biology.

### 1.13.3. Synthesis of polymers with azide and alkyne groups

Pendant functional polymers can be synthesized from monomers bearing clickable groups, initiators or by introducing clickable functional group on to the polymer backbone. The clickable monomer can be homopolymerized or copolymerized to obtain versatile random or block copolymers.

The syntheses of alkyne-functionalised polymers have been reported and synthesis of monomers involves the esterification of (meth) acryloyl chloride with propargyl alcohol or propargyl amine for (meth) acrylates<sup>165-168</sup> and acrylamides<sup>169</sup> respectively. Multifunctional initiators (bearing more than one alkyne functionality) can be used to create two or three dimensional architectures such as star polymers or networks<sup>170</sup>. Atom transfer radical emulsion polymerization in water to synthesize crosslinked nanoparticles of styrene and vinylbenzyl azide has been reported.<sup>171</sup> It is reported that polymerization of styrene without protecting the second alkyne moiety that resulted in a ‘‘tadpole-shaped’’ architecture has been realized by using alkyne-functionalized initiator for correlating with azide functional poly(ethyleneglycol) (PEG).<sup>172</sup>

The cycloaddition counterparts of the alkyne-functionalized polymers are azide-functionalized ones and the common procedure for their synthesis is the functionalisation of a basic framework with (i) an azide group via substitution reaction of an alkyl halide with sodium azide and (ii) with  $\alpha$ -haloisobutyrate as the ATRP initiating fragment via esterification of an amine or alcohol function<sup>173</sup>. The substitution of halides with sodium azides is also frequently used in polymer chemistry<sup>174</sup>. Telechelic halide functional polymers are readily obtained via ATRP. The subsequent substitution of the halide with sodium azide yields a polymer with high azide chain-end functionality.<sup>175-176</sup> The azide moiety is used without protection during polymerization, although some side reactions: such as (i) Cyclisation reactions between the azide and the propagating radical that causes low initiator efficiency<sup>177-178</sup> (ii) 1,3-cycloaddition of azides with the double bond of the monomer in the absence of a catalyst at high temperatures and long reaction times, at which the propensity decreases in the order of acrylates > acrylamides >> methacrylates > styrenes was described.<sup>179</sup> To restrict the side reactions to a minimum, short reaction times and low temperatures<sup>180</sup> are preferably used. It was shown that the polymerization at room temperature completely suppressed side reactions involving the azide moiety<sup>181</sup>. Synthesis of 1, 2, 3-triazoles on a polystyrene support has been reported.<sup>176</sup> Matyjaszewski et al.<sup>177</sup> have reported the direct ATRP of an azide-functionalized monomer, 3-azidopropyl methacrylate and the click reaction of the corresponding polymers in presence of mono substituted alkynes. Haddleton<sup>178</sup> and co-workers used the azide-functionalized initiator for the random

copolymerization of methyl methacrylate (MMA). Mespouille et al.<sup>179</sup> reported the synthesis of poly [(N, N-dimethylamino-2-ethyl methacrylate-g poly (caprolactone)] amphiphilic and environmental responsive polymer networks (DMAEMA-g-PCL) by Click chemistry from an azido-functionalised backbone. Johnson et al.<sup>180</sup> reported crosslinked polyacrylates, synthesized by atom transfer radical polymerization (ATRP), via the “click chemistry” concept to obtain a star polymer. A similar synthetic strategy using the acetylene-telechelic macro monomer in reaction with an azido-poly (ethylene glycol) was reported by Opsteen.<sup>175</sup> Polystyrene, poly(tert-butyacrylate) and poly methyl methacrylate (PMMA) containing azide and triisopropylsilyl protected alkyne end groups have been synthesized and clicked together sequentially. Click chemistry was used to graft a variety of groups on the surface, including a fluorescent dye to yield fluorescent polymers.<sup>181</sup> Densely grafted polymers were obtained by click reaction of azido polymers with alkyne functionalised polymers have been reported.<sup>182</sup> Acrylate copolymers with pendant azide groups were introduced by copolymerization of an azide containing monomer, viz. azido methacrylate AZMA with MMA.<sup>183-184</sup> Eight – shaped copolymers were obtained when a difunctional ATRP initiator with two hydroxyl groups was used for ROP and ATRP and subsequently click cyclization.<sup>185</sup> Recently there have been reports on azide and alkyne end functionalisation of polymers for various applications also.<sup>186-187</sup>

There are a few reports wherein ‘Click chemistry has been extended for the functional modification of solid propellant binders also<sup>188-193</sup>. However, in these the authors have not addressed the aspects of propellant energetic, the processability aspects, mechanical properties and ballistics and hence, warrant a systematic study in this direction which is the scope of this thesis.

### **1.14. SCOPE AND OBJECTIVE OF THE PRESENT WORK**

The foregoing review of literature details the current trends in development of energetic binder and requirements of alternate curing methodologies, to replace the existing isocyanate based curing of polymeric binders. The objective of this thesis is to investigate the possibility of exploring ‘Click chemistry’ for curing of binders namely GAP, HTPB and PTMO, resulting in triazole based crosslinked networks. Interestingly most of the acceptable binders are hydroxy telechelics based on butadiene, azidoalkyl

ether, alkyl ethers etc. which are crosslinked through reaction with a diisocyanate. These isocyanates are highly reactive, thus imposing limitations on pot-life of the propellant mix. Yet another problem is the incompatibility of promising energetic oxidisers like ADN and HNF with binders like GAP, HTPB or PTMO. This necessitates the need for evolving an isocyanate free curing reaction in propellant processing. This thesis is an attempt towards achieving this objective. ‘Click chemistry’ has been explored to effect the crosslinking of selected propellant binders like HTPB, GAP, PTMO etc. The thesis describes the synthesis in relevant cases of the binders, their ‘click’ reaction, cure optimisation etc both experimentally and by theoretical modelling. The properties of the cured resin and in few cases of their propellants have been described and correlated to the structural and crosslinking features. The research work done in this perspective, has been presented in different chapters. The initial two chapters discuss the current trends in solid propellant oxidisers and binders followed by the experimental techniques used for the processing and characterisation of the binders, oxidisers and propellants. In the subsequent chapter, the synthesis and characterisation of alkynyl compounds namely bis propargyl succinate (BPS), bis propargyl adipate (BPA), bis propargyl sebacate (BPSc.) and bis propargyloxy bisphenol A (BPB) for curing of GAP, yielding triazole networks is described. This is followed by characterisation of the triazoles formed from the reaction of GAP with these curing agents as well as evaluation of propellant properties. In chapter 4, the synthesis and characterisation of HTPB with ‘Clickable’ groups, viz., propargyloxy carbonyl amine terminated polybutadiene (PrTPB) and azidoethoxy carbonyl amine terminated polybutadiene (AzTPB), their crosslinking and property evaluation are described. The cure characteristics, thermal and mechanical properties of these polymers are reported and propellant level studies are described. Chapter 5 deals with the synthesis and characterisation of propargyl terminated polybutadiene (PTPB) and propargyl terminated PTMO (PTMP). Investigations on the cure kinetics of PTMP with GAP, the mechanical properties of the cured triazoles and propellant level evaluation are described. In chapter 6, in the first section, the synthesis and characterisation of an ester diazide, its thermal decomposition mechanism is described. In the second section of this chapter, investigations on the 1, 3 -dipolar addition reaction of this diazide with HTPB to form 1, 2, 3-triazolines are dealt with. The last chapter summarises the results of the preceding chapters and indicates prospects of future work in this area.

---

**1.15. REFERENCES**

1. Sutton, GP; *Rocket Propulsion Elements*, 8<sup>th</sup> Edition, John Wiley & Sons Inc, New York, **2010**.
2. Hunley, JD; AIAA Paper 99-2925, 35<sup>th</sup> AIAA, ASME, SAE, ASEE *Joint Propulsion Conference and Exhibit*, Los Angeles, California, June 20–24, **1999**.
3. Urbanski, T; *Chemistry and Technology of Explosives*, Vol. 1-4, Pergamon press, **1984**.
4. Roth, J; Carpenter E.L, *Encyclopedia of explosives and Related Items*, Vol.8, US Army Armament Research and Development Command, New Jersey, **1978**.
5. Ilimas, FA; Barrere, M; Huang, NC, *Fundamental Aspects of Solid Propellant Rockets*, Advisory Group for Aerospace Research and Development of N.A.T.O. Technivision Services, USA, **1969**.
6. Mastrolia, EJ; Klager, K; *Propellants: Manufacture, Hazards and Testing*, eds. Boyars, C; Klager, K; ACS, Vol. 88,122–164, **1969**.
7. Akhavan, J; *The Chemistry of Explosives*, *The Royal Society of Chemistry*, Cambridge, UK, **1998**.
8. Linder, V; *Explosives and Propellants - Encyclopedia of Chemical Technology*, Kirk Othmer (ed.), 3rd ed., John Wiley, New York, 9, **1980**.
9. Bruno, C; Accettura, AG; *Advanced Propulsion Systems and Technology Today to 2020*, Vol.223, AIAA, Reston, VA, **2008**.
10. Turner, MJL; *Rocket and Spacecraft Propulsion: Principles, Practice and New Developments*, 3<sup>rd</sup> Edition, Springer, Newyork, **2009**.
11. Davenas, A. *J. Propulsion and Power*, **2003**, 19, 1108-1128.
12. Caveny, LH; Geisler, RL; Ellis RA, Moore TL, *J. Propulsion and Power*, **2003**, 19, 1038-1066.
13. Lipanov, AM. *J. Propulsion and Power*, **2003**, 19, 1067-1088
14. Mcgrath, DK; Carr II, CE.AIAA paper 1998-3844 AIAA/SAE/ASME/ASEE *Joint Propulsion Conference*, 34<sup>th</sup> OH, USA June 24-26, **1998**.
15. Hamilyn, K. AIAA paper, 91-1853, AIAA/SAE/ASME/ASEE *Joint Propulsion Conference*, 27<sup>th</sup> Sacramento, CA, June 24-26, **1991**.
16. Moore, TL. AIAA paper, 2002-3750, AIAA/SAE/ASME/ASEE *Joint Propulsion Conference*, 38<sup>th</sup> Reston, VA, June 24-26, **1991**.
17. Zimmerman, CA. *Acta Astonautica*, **1980**, 7, 277-292.

18. Roger D. Launius, RD, *To Reach the High Frontier: A History of U.S. Launch Vehicles*, Jenkins DR, The University Press of Kentucky, Kentucky, USA, **2002**.
19. Pekkanen,S; Umezu,PK. *In Defense of Japan: From the Market to the Military in Space Policy*, Stanford University Press, Stanford, USA, **2010**.
20. Angelo, JA. *Encyclopedia of Space and Astronomy*, Facts on File, Inc.Infobase publishing, NY, USA, **2006**.
21. Angelo, JA. *ARIANE- Rockets*, Facts on File, Inc.Infobase publishing, NY, USA, **2006**.
22. Nagappa, R; Kurup, MR; Muthunayagam, AE. *Acta Astonautica*, **1989**, 19, 681-697.
23. Abraham, PJ; Easwaran, V; Srinivasan, M; Narayanamoorthy, N; Ramakrishnan, S. IAC paper, IAC-10.C4.2.1, *International Astronautical Federation*, **2010**.
24. Muthiah, R; Varghese, TL; Ninan, KN; Krishnamurthy, VN. *Propellants, Explos.Pyrotech.* 1998,23, 90-93
25. Guery, JF; Chang, IS; Shimada ,T; Glick ,M; Boury ,D; Robert, E; Napior, J; Wardle, R; Perut ,C; Calabro, M; Glick ,R; Habu ,H; Sekino, N; Vigier, G; d'Andrea, B. *Acta Astronautica*, **2010**, 66, 201-219.
26. Agrawal, JP, *High Energy Materials*, Wiley-VCH, Weinheim, **2010**.
27. Singh, G; Felix, SP. *Combustion and Flame*, **2003**, 132, 2003, 422–432
28. Wingborg, N; Eldsäter, C; *Propellants, Explos.Pyrotech.*, **2002**, 27, 314-319
29. Damse, RS; Singh, A. *Def. Sci. J.*, **2008**, 58, 86-93.
30. Provatas, A. *Energetic Polymers and Plasticisers for Explosive Formulations. A Review of Recent Advances*, DSTO-TR-0966, DSTO, Aeronautical and Maritime Research Laboratory, Australia, April, **2000**.
31. Yang, R; Hongmei, A; Huimin, T. *Combustion and Flame*, **2003**, 135, 463–473
32. Badgujar, DM; Talawar, MB; Asthana, SN; Mahulikar, PP. *J. Hazardous Materials*, **2008**, 151, 289–305.
33. Jones, DEG; Kwok, QSM; Vachon, M; Badeen, C; Ridley, W. *Propellants, Explos.Pyrotech*, **2005**, 30, 140-147.
34. Schoyer, HFR; Welland-Veltmans, WHM; Louwers ,J; Korting, PAOG; Heijden, AEDM-V; Keizers ,HLJ; Van den Berg, RP. *J. Propulsion and Power*, **2002**, 18, 131-145.
35. Wan der Heijden, AEDM; Leeuwenburgh, AB. *Combustion and Flame*, **2009**, 156, 1359–1364

36. Zhang, M; Eaton , PE; Gilardi ,R. *Angew.Chem.Int.Ed.*,**2000**, 39, 401-404.
37. Eaton, PE; Gilardi, RL; Zhang, M. *Adv. Mater*, **2002**, 12, 1143-1148.
38. Evers, J; Gobel, M; Klapotke, TM; Mayer, P; Oehlinger, G; Wlch, JM. *Propellants, Explos.Pyrotech* , **2007**, 32, 478-495.
39. Herve, G. *Propellants, Explos.Pyrotech*, **2009**, 34, 444-451
40. Heintz, T; Pontius, H; Aniol, J; Birke, C; Leisinger, K; Reinhard, W. *Propellants, Explos.Pyrotech*, **2009**, 34, 231-238.
41. Athar, J; Ghosh, M; Dendage,PS; Damse RS; Sikder, AK. *Propellants, Explos.Pyrotech*, **2010**,35, 153-158.
42. Rahm,M. *Green Propellants*, Stockholm, Sweden; PhD Thesis, Royal Institute of Technology, **2010**.
43. Abhay, MK; Devendra, PD. *Res.J.Chem.Envirion*, **2010**, 14, 94-103.
44. Nair, UR; Asthana SN, Rao AS, Gandhe BR. *Def. Sci. Journal*, 60, **2013**, 137-151.
45. Cumming, AS. *J. Aerospace Tech. Manag.* , **2009**, 1, 161-166.
46. Gordon, S; McBride, BJ. *Computer Programme for Calculation of Complex Chemical Equilibrium Compositions and Applications II*, NASA reference publication, NASA RP-1311-P2, Lewis Research Center, Cleveland,Ohio, USA, **1994**.
47. Stacer, RG; Husband, DM. *Propellants, Explos.Pyrotech.*, **1991**, 16, 167-176
48. Al-Harhi, A; Williams, A. *Fuel*, **1998**, 77, 1451–1468.
49. Tingfa, D. *Thermochim. Acta*, **1989**, 138, 189–197.
50. Gligorijevi, N, Rodi, V; Jeremi, R; Živkovi, S; Suboti,S. *Scientific Technical Review*, **2011**, 61,1-9
51. Wang, DT; Shearly, RN. AIAA paper 86-1415, AIAA/SAE/ASME/ASEE *Joint Propulsion Conference*, 26<sup>th</sup> Huntsville, Alabama, June 16-18, **1986**
52. Rao, R; Scariah, KJ; Varghese, A; Naik, PV; Swamy, KN; Sastri, KS. *European. Polym J.*, **2000**, 36, 1645–1651.
53. R. Manjari, V. C. Joseph, L. P. Pandureng and T. Sriram, *.J.Appl.Polym.Sci.*, **1993**, 48, 271-278
54. Smith, T. *Ind.Eng.Chem*, **1960**, 52, 776-780.
55. Catherine, KB. *Thermoanalytical investigations on curing and decomposition of polyol binders*. Thiruvananthapuram: University of Kerala. India; **2003**.



- 
56. Manjari, R; Pandureng, LP; Somasundaran, UI; Sriram, T, *J. Appl. Polym. Sci*, 1994, 51435–442
  57. Burke, OW; Davis, P; Kizer, JA. *Polymerization process*, US3673168 A, **1972**
  58. Verdol, J; Ryan, P. *Low molecular weight diene polymers using aqueous hydrogen peroxide and cyclohexanol(one)medium*, US3796762, **1974**.
  59. Zelinsky, RP; Hsieh, HL. *Branched polymers prepared from monolithium-terminated polymers and compounds having at least three reactive sites*, US 3281383 A, **1966**
  60. Kaita, S; Yamanaka, M; Horiuchi AC; Wakatsuki, Y. *Macromolecules*, **2006**, 39 1359–1363
  61. Brandt,HD; Nentwig, W; Rooney, N, LaFlair RT, Wolf,UU; Duffy, J, , Puskas, JE, Kaszas, G;, Drewitt, M; Glander, S, *Rubber, 5. Solution Rubbers" Ullmann's Encyclopedia of Industrial Chemistry*, Wiley-VCH,Weinheim **2011**,
  62. Reed Jr, SF. *J.Polym.Sci.Part A:Polym.Chem*, **1971**, 9, 2029-2038.
  63. Zymona, J; Santte, E; Harwood, H. *Macromolecules*, **1973**, 6,129- 133
  64. Quack, G; Fetters, LJ. *Macromolecules*, **1978**, 11, 369–373.
  65. Sadeghi, GMM, Morshdedian, J; Barikani, M; Taromi, FA. *Iran.polym.J*, 2003,12,515-521.
  66. Frankland, J A.; Edwards, HG M.; Johnson, AF; Lewis, IR, Poshyachinda, S. *Spectrochimica Acta.*, 1991, .47A,1511-1524
  67. Panicker, SS; Ninan, KN. *J.Appl. Polym.Sci.***1995**, 27, 1797-1804
  68. Panicker, SS; Ninan, KN. *Polym. Int.***1995**, 37, 255-259
  69. Burel, F; Feldman, A; Bunel, C. *Polymer*, **2005**, 46, 15–25.
  70. Kincal, D; Özkar, S. *J. Appl. Polym. Sci.*, **1997**, 66, 1979–1983.
  71. Sekkar, V; Devi, KA; Ninan, KN; *J. Appl. Polym. Sci.*, **2001**, 79, 1869–1876.
  72. Bina, C; Kannan, KG; Ninan, KN, *J. Thermal Analysis Calorimetry*, **2004**, 78, 753–760.
  73. Hailu K, Guthausen, G; Becker, W; KÖnig A, Bendfeld A, Geissle E. *Polymer Testing*, **2010**, 29, 513–519.
  74. Sekkar, V; Krishnamurthy, VN; Jain, SR. *J. Appl.Polym. Sci.*, **1997**, 66, 1795–1801.
  75. Sekkar, V; Venkatachalam, S; Ninan, KN. *Eur. Polym. J*, **2002**, 38,169–178.
  76. Fages, G; Pham, QT. *Makromol. Chem*, **1978**, 179, 1011–1023.
-

- 
77. Bresler, LS; Barantsevich, EN; Polyansky, VI; Ivantchev, SS. *Makromol. Chem.*, **1982**, 183, 2479–2489.
  78. Arisawa, H; Brill, TB. *Combust. Flame*, **1996**, 106, 131–143.
  79. Chen, JK; Brill, TB. *Combust. Flame*, **1991**, 87, 217-232
  80. Panicker, SS; Ninan, KN. *Thermochim. Acta*, **1997**, 290, 191–197
  81. Rocco, JAFF; Lima, JES; Frutuoso, AG; Iha, K; Ionashiro, M; Matos, JR; Suarez-ha, MEV. *J. Thermal Analysis and Calorimetry*, **2004**, 75,, 551-557.
  82. Gopala Krishnan, PS; Ayyaswamy, K; Nayak, SK. *J. Macromolecular Science, Part A: Pure and Applied Chemistry*, **2012**, 50, 128-138.
  83. Wang, Y; Hillmyer, MA. *Macromolecules*, **2000**, 33, 7395-7403
  84. Barcia, FL; Amaral, TP; Soares, BG. *Polymer*, **2003**, 44, 5811–5819
  85. Latha, PB; Adhinarayanan, K; Ramaswamy, R. *Int.J. Adhes. Adhes*, **1994**, 14, 57–61.
  86. Zhou ,Y; Long, X P; Zeng, QX. *J.Appl. Polym. Science*, **2012**, 125, 1530-1537
  87. Millar, RW; Colclough, ME; Golding, P; Honey, PJ; Paul, NC; Sanderson, AJ; Stewart, MJ. *Phil. Trans. R. Soc. Lond. Ser. A. Math. Phys. Eng. Sci.*, **1992**, 339, 305–319.
  88. Colclough, ME; Paul, NC; ACS Symp. Seri., **1996**, 623, 97–102, Colclough, ME; Golding, P; Paul, NC; Proceedings of the 14th International Pyrotechnics Seminar, Jersey, Channel Islands, Great Britain, Sept 18–22, **1989**, Henry Ling Press, Dorset, 105–111.
  89. Santhosh, NM; Bannerji, S; Khanna, PK. *Propellants..Explos.Pyrotech*, **2013**, 38,748-753
  90. Boutevin, G; Ameduri, B; Boutevin, B; Joubert, JP. *J.Appl. Polym. Sci.*, **2000**, 75, 1655–1666.
  91. Hazer, B. *Macromol. Chem. Phys*, **1995**, 196, 1945–1952.
  92. Eroglu, MS; Hazer, B; Guven, O. *Polymer. Bull*, **1996**, 36, 695–701.
  93. Nigam, V; Setua, DK; Mathur, GN. *J. Appl. Polym.Sci.*, **1998**, 70, 537–543.
  94. Lira, CH; Nicoini, LF; Poinsky, MCB. *Ann.Magn.Reason*. **2006**, 5, 22-27.
  95. Nair, PR, Nair, CPR; Francis, DJ. *J. Appl. Polym.Sci*, **1999**, 71, 1731-1738
  96. Dusek, K; Lednicky, F; Lunak, S; Mach, M; Duskova, D; *Rubber-Modified Thermoset Resins*, Review, Gilham, C Keithview; J. K., Eds. ACS Publications: Washington DC, Vol. 208, 27–35, **1984**.
-

- 
97. Chao, H; Tian, N; Drexler, A; Schmidhauser, J. *Amino-terminated polybutadienes*, US Patent 6 831 136, **2004**.
  98. Mohan, YM. *Designed Monomers Polymers*, **2005**, 8, 159-175
  99. Shankar, RM; Roy ,TK; Jana, T. *J. Appl. Polym. Sci.*, **2009**, 114, 732–741.
  100. Sankar, RM; Saha, S; Meera, KS; Jana, T. *Bull. Mater. Sci.*, **2009**, 32, 5, 45-49
  101. Muralisankar, R; Roy, TK; Jana, T. *Bull. Mater. Sci.*, **2011**, 34, 69-75, 745-754 .
  102. Subramanian, K; Sastri, KS. *J. Appl. Polym. Sci.*, **2003**, 90, 2813-2823
  103. Cho, BS; Noh, ST. *J. Appl. Polym. Sci*, **2011**, 121, 3560-3568.
  104. Saravanakumar, D; Sengottuvelan, N; Narayanan, V; Kandaswamy, M; Varghese, TL. *J. Appl. Polym. Sci*, **2011**, 119, 2517-2524
  105. Frankel, M; Grant, L; Flanagan, J; AIAA Paper 89-2307, AIAA/SAE/ASME/ASEE 25<sup>th</sup> Joint Propulsion Conference, July, **1989**.
  106. Ross, IW. *Glycidyl azide polymer (GAP) synthesis by molten salt method*, EP0453642A1, **1991**.
  107. Gaur, B; Lochab, B; Choudhary, V; Varma, IK. *J. Macromol. Sci. Part C—Polymer Reviews*, **2003**, 43, 505–545.
  108. Mohan, YM; Raju, MP; Raju, KM. *J. Appl. Polym. Sci*, **2004**, 93, 2157–2163.
  109. Ringuette, S; Dubois, C; Stoe, RA; Charlet, G. *Propellants. Explos. Pyrotech.*, **2006**, 31, 131-138.
  110. Liu, D; Zheng, Y; Steffen, W; Wagner, M; Butt, HJ; Ikeda, T. *Macromol. Chem. Phys.*, **2013**, 214, 56–61.
  111. Bui, VT; Ahad, E; Rheume, D; Raymond, MP. *J. Appl. Polym. Sci*, **1996**, 62, 27-32.
  112. Subramanian, K. *Eur. Polym. J.*, **1999**, 35, 1403-411
  113. Khalifa, Al-K; Ampleman, G. *Macromolecules*, **1995**, 28, 5230-5239.
  114. Brochu, S; Ampleman, G. *Macromolecules*, **1996**, 29, 5539-5545
  115. Manzara, AP; Johanssen, B. *Non-detonable poly(glycidyl azide) product*, US 5565650A, **1996**.
  116. Keskin, S; O'zkar, S. *J. Appl. Polym. Sci*, **2001**, 81, 918–923.
  117. Manu, SK; Sekkar, V; Scariah ,KJ; Varghese, TL; Mathew, S. *J. Appl. Polym. Sci*, **2008**, 110, 908–914.
  118. Manu, SK; Varghese, TL; Mathew, S; Ninan, KN. *J. Appl. Polym. Sci*, **2009**, 114, 3360–3368.
-

119. Min, BS. *Propellants.Explos.Pyrotech*, **2008**, 33, 131-138.
120. Zhai,J; Shan, Z; Li, J; Li, X; Guo, X; Yang, R. *J. Appl. Polym. Sci.*, **2013**, 128, 2319–2324.
121. Zhou, Y; Long, XP; Zeng, QX. *J. Appl. Polym. Sci*, **2012**, 125, 1530–1537.
122. Dogan, M; Mehmet, S; Eroglu, H; Erbil, Y. *J. Appl. Polym. Sci* , **1999**, 74, 2848–2855.
123. Hatice, F; Jale, H. *J. Analy.Appl. Pyrolysis*, **2002**, 63, 327-338.
124. Korobeinichev, OP; Kuibida, LV; Volkov , EN; Shmakov, AG. *Combustion and Flame*, **2002**, 129, 136-150.
125. Brian, RD; Brill, TB. *Propellants.Explos.Pyrotech*, **2001**, 26, 213-220
126. Lin, M; C. Chakraborty, D; Xia, W. JANNAF 36th Combustion Subcommittee Meeting, **1999**, 1, 325-331.
127. Selim, K; Ozkar, S; Yilmaz, L. *J. Appl. Polym. Sci*, **2000**, 77, 538-546.
128. Kuwhara, T; Takizuka, T; Onda; Kubota, N. Proceedings of the 25<sup>th</sup> International Pyrotechnics Seminar, **1999**, 2, 457-467.
129. Ching-Jen, T; Youngjoo, L; Litzinger, TA. *Combustion and Flame*, **1999**, 117, 244-256.
130. Feng, HT; Mintz, K J; Augsten , RAG; Jones, DE. *Thermochimica Acta*, **1998**, 311, 105-111.
131. Arisawa, H; Brill, TB. *Combustion and Flame*, **1998**, 112, 533-544.
132. Ping, L; Charles, AW. *J. Phys. Chem. B*, **1997**, 101, 2126-2131.
133. David, EGJ; Laurence, M; Rainer, A. *Thermochimica Acta*, **1994**, 242, 187-94.
134. Yoshioo, O. *Prop.Expos.Pyrotech*, **1992**, 17, 226-231.
135. Milton,F; Harris, SP; Srivastava, RD. *Combustion and Flame*, **1984**, 55, 203-211.
136. Yuan, LY; Liu, TK; Cheng, SS. AIAA-96-3235, AIAA joint propulsion conference 32<sup>nd</sup>, Buena vista, FL; **1996**.
137. Kim, ES; Yang, V; Liau, YC.AIAA paper, 2001-0341, 39th AIAA Aerospace Sciences, Meeting & Exhibit, 8-11 January, Reno, NV, **2001**.
138. Kubota, N; Sonobe, TA; Yamamoto, J; Shimizu, H. AIAA-88-3251 , July 11-13, AIAA/ASME/SAE/ASEE 24<sup>th</sup> AIAA/ASME/SAE/ASEE Joint Propulsion Conference, Boston, Massachusetts, **1988**.

- 
139. Helmy, AM; Teledyne, MKS; Hollister, CA. AIAA-87-1725, AIAA/SAE/ASME/ASEE 23rd Joint Propulsion Conference, June 29-July 2, San Diego, California. **1987**
  140. Panda, S; Thakur, J; Sahu,S. AIAA 2000-3200, 36th AIAA/ASME/SAE/ASEE Joint Propulsion Conference and Exhibit 16-19 July, **2000**.
  141. Yamauchi, S; Kuwahara,T. AIAA 2012-3972, 48th AIAA/ASME/SAE/ASEE Joint Propulsion Conference & Exhibit, 30 July - 01 August, Atlanta, Georgia, **2012**.
  142. Puduppakkam, KV; Tanner, MW; Beckstead ,MW. AIAA 2006-4926, 42<sup>nd</sup> AIAA/ASME/SAE/ASEE Joint Propulsion Conference & Exhibit, 9 - 12 July, **2006**, Sacramento, California.
  143. Li, J; Litzinger, TA. *J.Propulsion.Power*, **2007**, 23, 166-174.
  144. Puduppakkam, KV; Beckstead, MW. AIAA 2001-3429, 37<sup>th</sup> AIAA/ASME/SAE/ASEE Joint Propulsion Conference, 9-11 July, **2001**.
  145. Landsem, E; Jensen, TL; Kristensen, TE; Hansen, FK; Benneche, T; Unneberg, E. *Propellants.Explos.Pyrotech*, **2013**, 38, 75 – 86.
  146. Woods, G; *The ICI Polyurethanes Book*, John Wiley and Sons, New York, **1990**.
  147. Hassner, A. *Synthesis of Heterocycles via Cycloadditions I*, Topics in *Hetrocyclic Chemistry*, Springer-Verlag, Berlin, Heidelberg, **2008**.
  148. Kolb, HC; Finn, MG; Sharpless, KB. *Angew. Chem. Int. Ed.*, 2001, 40. 2004-2021.
  149. Sharpless, KB; *Angew. Chem. Int. Ed.*, **2002**, 41. 2024-2032.
  150. Rostovtsev, VV; Green, LG; Fokin, VV; Sharpless, KB. *Angew. Chem. Int. Ed.*, **2002**, 41.2596-2599.
  151. Binder, WH; Sachsenhofer, R. *Macromol. Rapid Commun.*, **2007**, 28, 15-54.
  152. Huisgen, R; Knorr, R; Mobius, L; Szeimies, G. *Chem. Ber.*, **1965**, 98. 4014-4021.
  153. Tornoe, CW; Christensen, C; Meldal, M. *J. Org. Chem.*, **2002**, 67. 3057-3064.
  154. Himo, F; Lovell, T; Hilgraf, R; Rostovtsev, VV; Noodleman, L; Sharpless, KB; Fokin, VV. *J. Am. Chem. Soc.*, **2005**, 127. 210-216.
  155. Rodionov VO, Fokin VV, Finn MG. *Angew. Chem., Int. Ed.*, **2005**;44:2210–2215
  156. Rostovtsev VV, Green LG, Fokin VV, Sharpless KB. *Angew. Chem., Int. Ed.*, **2002**;41:2596–2599
  157. Bore, BC; Narayan, S; Rasmussen, K; Zhang, ; Zhao, H; Lin, Z; Jia, G; Fokin, VV. *J. Am. Chem. Soc.* 2008, 130, 8923–8930.

- 
158. Zhang, L; Che, X; Xue, P; Sun, HY; Williams. ID; Sharpless, KP; Fokiv, VV; Jia, G, *J. Am. Chem. Soc.* **2005**, 127 15998–15999
  159. McNulty, J.; Keskar, K; Vemula, R, *Chemistry - A European Journal*, **2011**, 17, 14727–14730.
  160. Woo, H; Hang, H; Kima, A; Jnag, S; Park, JC; Park, S; Kim, BS, Song, H; Park, KH. *Molecules* .**2012**, 17,13235-13252.
  161. Glaser, C; Ber. *Dtsch. Chem. Ges.* **1869**, 2, 422-424.
  162. Straus, F; Liebig, J. *Ann. Chem.* **1905**, 342, 190–265.
  163. Eglinton, G; Galbraith, AR. *Chem. Ind.* **1956**, 737–738.
  164. Ryu, EH; Zhao, Y. *Org. Lett*, **2005**, 7, 1035–1037.
  165. Ladmiral, V; Mantovani, G; Clarkson, GJ; Cauet, S; Irwin ,JL; Haddleton, DM. *J.Am.Chem. Soc.*, **2006**, 128, 4823–4830
  166. Quemener, D; Hellaye, ML; Bissett ,C; Davis, TP; Kowollik, B; Stenzel ,MH. *J. Polym. Sci., Part A: Polym. Chem.*, **2008**, 46, 155–173.
  167. Damiron, d; Desorme, M; Ostaci, RV; Akhras, SA; Drockenmuller, E. *J.Polym.Sci. Part A. Polym Chem*, **2009**, 47, 3803-3813.
  168. Ladmiral, V; Legge, TM; Zhao ,Y; Perrier, S. *Macromolecules*, **2008**, 41, 6728–6732.
  169. Huang, CJ; Chang, FC. *Macromolecules*, **2009**, 42, 5155–5166
  170. Wiltshire, JT; Qiao , GG. *J. Polym. Sci., Part A: Polym. Chem.*, **2009**, 47, 1485–1498
  171. Xu, LQ; Yao, F; Fu, GD; Shen, L. *Macromolecules*, **2009**, 42, 6385–6392
  172. Dong, YQ; Tong ,YY; Dong ,BT; Du ,F-S; Li, Z-C. *Macromolecules*, **2009**, 42, 2940–2948
  173. Brase S, Gil, C; Knepper, K; Zimmermann, V. *Angew. Chem., Int. Ed.*, **2005**, 44, 5518-5240.
  174. Li ,Y; Yang ,JW; Benicewicz ,BC. *J. Polym. Sci., Part A: Polym. Chem.*, **2007**, 45,4300–4308.
  175. Opsteen ,JA ; Hest ,JCM-V. *Chem. Commun.*, **2005**, 6, 57–59.
  176. Gouault, N; Cupif,JF; Sauleau ,A; David ,M. *Tetrahedron Letts*, **2000**, 41, 7293 – 7297.
  177. Tsarevsky, NV; Sumerin, BS; Matyaszewski, K. *Macromolecules*, **2007**, 40,4439-4445.
-

178. Chen, G; Tao, L; Mantovani, G; Ladmiral, V; Burt, DP; Macpherson, JV; Haddleton, DM. *Soft Matter*, **2007**, 3, 732–739.
179. Mespouille, L; Coulembier, O; Paneva, D; Degee, P; Rashkov, I; Dubois P, J. *Polym. Sci., Part A: Polym. Chem.*, **2008**, 46, 4997-5013.
180. Johnson, JA; Lewis, DR; Diaz, DD; Finn, MG; Koberstein, JT; Turro, NJ. *J. Am. Chem. Soc.*, **2006**, 128, 6564–6565.
181. Cummins, D; Duxbury, CJ; Quaedflieg, PJLM; Magusin, PCMM; Koning, CE; Heise, A. *Soft Matter*, **2009**, 5, 804-811.
182. Gao, H; Matyjaszewski, K. *J. Am. Chem. Soc.*, **2007**, 129: 6633-9.
183. Hu, D; Zheng, S. *Eur. Polym. J.*, **2009**, 45, 3326-3338.
184. Van Camp, W; Germonpre, VL; Mespouille, P; Dubois; Du Prez FE; Goethas EJ. *React. Funct. Polym.*, **2007**, 67, 1168-1180.
185. Shi, GY; Yang, LP; Pan, CY. *J. Polym. Sci., Part A: Polym. Chem.*, **2008**, 46, 6496-6508
186. Smitha, CS; Sunitha, K; Mathew, D; Nair, CPR. . *J. Appl. Polym. Sci.* **2013**, doi: 10.1002/APP, 39295
187. Sunitha, K; Santhosh Kumar, KS; Mathew, D, Nair, CPR, *Material Letters*, **2013**, 101-104
188. Aronson ‘*The synthesis and characterization of energetic materials from sodium azide*, PhD Thesis, Georgia Institute of Technology; **2004**.
189. H. Jung, Y.G. Lim, K.H. Lee, B. T. Koo, *Tetrahedron Lett.* **2007**, 48, 6442-6448
190. Keicher, T; Kuglstatler, W; Eisele, S; Wetzel, T; Krause, H. *Propellants, Explos. Pyrotech.*, **2009**, 34, 210-217
191. Cerri, S; Bohn, MA; Menke, K; Galfett, L. *Propellants, Explos., Pyrotech.*. **2010**, 35, 1-12
192. Rahm, M; Malmstrom, E; Eldsater, C. *J. App. Polym. Sci.*, **2011**, 122, 1-11
193. Ding, Y; Hu, C; Guo, X; Che, Y; Huang, J. *J. Applied Polymer Science* **2014**, doi: 10.1002/APP 40007

*Chapter 2*

**Materials and Characterisation  
Techniques**

---



***Abstract***

*This chapter gives a brief description of the various chemicals and materials used for the synthesis of azide and propargyl functional monomers and polymers during functionalisation. Analytical techniques employed for the characterisation of these monomers and polymers are also described. The spectral, chromatographic, thermal and thermo-analytical, mechanical, morphological characteristics and ballistics properties in terms of burn rate measurements are included.*

## 2.0 Materials

A series of compounds were used for the synthesis of azide and propargyl functional monomers and triazoles. The polymers used for the study are hydroxyl terminated polybutadiene (HTPB), polytetramethylene oxide (PTMO) and glycidyl azide polymer (GAP). Their structures, source of procurement etc. are given below in Table 1.

*Table 1 Detail of Materials Used*

<b>Chemical</b>	<b>Properties</b>	<b>Remarks</b>
Succinic Acid	Purity > 99% Melting point: 184°C Used after recrystallisation	M/s Merck.
Adipic Acid	Purity > 99% Melting point: 152°C Used after recrystallisation	M/s Merck.
Sebacic Acid	Purity > 99% Used after recrystallisation	M/s Merck.
Bisphenol-A	Purity > 99% Melting point: 158°C Used after recrystallisation	M/s Merck.
Tolylene diisocyanate (TDI)	Purity > 99% Used as received	M/s Bayer
Hydroxyl Terminated Polybutadiene (HTPB)	Hydroxyl vaue:41.3 mgKOH/g Molecular weight (VPO)-2800 Used after drying at 80°C (3 hrs)	VSSC
Hydroxyl Terminated Glycidyl azide polymer (GAP)	Hydroxyl vaue:55.0 mgKOH/g Molecular weight (VPO)-2500 Used after drying at 50°C (3 hrs)	VSSC
Polytetramethylene oxide (PTMO)	Hydroxyl vaue:52.0 mgKOH/g Molecular weight (VPO)-2000 Used after drying at 50°C (3 hrs)	M/s Aldrich
Sodium hydride	Purity ~60% Dispersion in mineral oil	M/s Alfa Aeser

Chemical	Properties	Remarks
2-Chloro ethoxy ethanol	Purity > 99% Distilled prior to use	M/s Aldrich
1,6- Hexane diol	Purity > 99% Used after drying at 80°C (3 hrs)	M/s Merck
Chloroacetic acid	Purity > 99% Used as received.	M/s Merck
Ammonium perchlorate	Purity > 99% Average Particle size: 45 microns	VSSC
Aluminium powder	Purity > 99% Particle size: 15 microns	M/s MEPCO
Dibutyl tin diluarate	Purity >99% Used as received	M/s Aldrich
Toluene-4-sulphonic acid	Purity >99% Used as received	M/s Fischer
Cuprous Iodide	Purity >99%	M/s Aldrich
Propargyl bromide	Purity: 80% solution in toluene	M/s Merck
Propargyl alcohol	Purity: 98% Distilled prior to use	M/s Spectrochem
Sodium azide	Purity: 99%	M/s SD Fine

All the solvents used were analytical (AR) grade. The synthesis and structures of the derivatives are described in the respective chapters.

The chemical structure evaluation and property evaluation of the monomers and polymers were performed by various analytical techniques which are elaborated below.

## 2.1 Characterisation techniques

### 2.1.1. Fourier Transform Infrared Spectroscopy (FTIR)

The use of infrared spectroscopy for the characterisation of the polymeric materials has experienced tremendous growth in recent years, primarily because a variety of sampling techniques and experimentations are now available. Interaction of electromagnetic radiation with molecular vibrations gives rise to absorption bands

throughout most of the IR region of spectrum. Identification of composition and morphology of polymers and their blends, curing studies, diffusion and oxidation studies, degradation of polymers, orientation of polymers etc. are some of the areas where it finds extensive use. In this research work, Fourier transform infra red (FTIR) spectra were obtained with a Perkin Elmer spectrum GXA spectrophotometer in the range of 4000-400  $\text{cm}^{-1}$  at a resolution of 4  $\text{cm}^{-1}$ . The sampling techniques viz. smearing of sample on sodium chloride (NaCl) crystals as well as attenuated total reflectance (ATR) accessory has been used for recording the IR spectra.<sup>1-2</sup>

### **2.1.2. Nuclear Magnetic Resonance Spectroscopy (NMR)**

NMR spectroscopy is an important analytical tool which is extensively used to study the structure and purity of monomers/polymers<sup>3</sup>. The solution NMR has emerged as one of the premier methods for polymer characterisation because of the high resolution and sensitivity. The chemical shifts are sensitive to polymer microstructure, including polymer stereochemistry, regioisomerism and the presence of branches and defects. Proton ( $^1\text{H}$ ) and  $^{13}\text{C}$  NMR were recorded with a Bruker Avance Spectrometer (300 MHz). Tetra methyl silane (TMS) is the internal standard used for comparing the NMR signals. The samples were prepared in  $\text{CDCl}_3$ , while deuterated acetone was also used in the case of insolubility of samples in  $\text{CDCl}_3$ .

### **2.1.3. Gel Permeation Chromatography (GPC)**

The molecular weight and molecular weight distribution of a polymer is determined by a versatile and the most popular technique known as gel permeation chromatography (GPC). The technique of GPC is based on the permeation of polymer molecules according to their size in solution through a 'permeation column'. The column material, generally styrene-divinyl benzene gel, of different pore sizes is packed suitably. Large-size molecules elute early while small sized molecules elute later. Thus, each polymer molecule has a specific hydrodynamic volume in solution for a given solvent under physical conditions. In this work, GPC (GPC, Waters model 600) in conjugation with differential refractive index detectors and Waters HR3 and HR4 microstyragel columns were used for determination of molecular weight distribution of the sample. The columns were calibrated using polystyrene standards. Tetrahydrofuran (THF) was used as the solvent at a flow rate of 1 ml/min. Number average ( $M_n$ ) and weight average ( $M_w$ ) molecular weights and

poly dispersity index ( $M_w/M_n$ ) were obtained from the chromatograms. These values are based on polystyrene standard and

#### **2.1.4 Differential Scanning Calorimetry (DSC)**

DSC is based on the principle of measuring the energy necessary to establish zero temperature difference between the test sample and reference material against either time or temperature under specified environment. Constant energy input is provided to heat both the sample and reference material at a constant rate. The sample may evolve or absorb energy against the reference material, depending on the type of change, which can be exothermic and endothermic. The heat flow vs. temperature (thermogram) is recorded for the run. Thermal decomposition was studied using a simultaneous TG-DSC (SDT Q600) in this work. Kinetic investigations are one of the most important applications of thermal analysis. A common goal of kinetic studies is to define the time-temperature dependence of conversion, that is  $\alpha = f(t, T)$ , where  $\alpha$  is the fractional conversion,  $t$  is time and  $T$  is the temperature of the reaction. The kinetic analysis included determination of the reaction mechanism or appropriate kinetic equation for the system being analysed and measurement of parameters viz. reaction orders, activation energies and pre-exponential factor of the specified reactions. Another important purpose of the kinetic analysis is modelling of polymer cure behaviour for process design and control. Accurate time-temperature-degree of conversion relationships are of great practical utility in establishing cure schedules. Kinetic analysis is also used to characterise the cure, aging or degradation of polymer systems. Still another purpose is for comparison purposes, for example to compare the effectiveness of different catalyst on cure and degradation reactions, to compare the effects of fillers, additives, thermal history and environmental factors. In DSC, the rate of change of properties namely  $dH/dt$  respectively is measured as a function of time, where  $H$  is the reaction enthalpy. The thermodynamic (reaction enthalpy) and kinetic (activation parameters and kinetic model) can be determined simultaneously. This is one of the major advantages of the DSC method. In this work, curing was monitored using differential scanning calorimeter (DSC), TA Instruments Q 20.

### 2.1.4.1. Cure kinetics

Non-isothermal DSC analysis was employed to study the curing reaction based on varying heating rates. With increase in heating rate, the peak cure exotherm shifted to higher temperature regime.

The kinetics of cure reaction was evaluated by the variable heating rate method of Kissinger<sup>4</sup> based on the temperature peak maxima ( $T_m$ ) in DSC. The final forms of Kissinger equation, used for finding the activation parameters are given in equation 1.

#### Kissinger equation

$$\frac{d \log(\phi/T_m^2)}{d(1/T_m)} = -\frac{E}{2.303R} \quad \text{---1}$$

where  $\phi$ =heating rate,  $E$ =activation energy,  $R$ =universal gas constant,  $T_m$ =peak maximum temperature in DSC in absolute scale. From the slope of the linear plot of  $\log(\phi/T_m^2)$  against  $1/T_m$ ,  $E$  can be calculated.

The pre-exponential factor ( $A$ ) was calculated using Kissinger method based on the relation given in equation 2.

$$A = \phi E e^{E/RT_m} / RT_m^2 \quad \text{--- 2}$$

Where,  $T_m$  is the average of the  $T_{max}$  for average  $\phi$ .

### 2.1.5 Pyrolysis Gas Chromatography-Mass Spectrometer (Pyrolysis GC-MS) & Thermogravimetry- Mass Spectrometer (TG-MS)

The pyrolysis GC-MS studies are useful for predicting the reaction mechanism involved during the decomposition of a polymer or cured polymer network. In the present work, pyrolysis GC-MS studies were conducted using a Thermo Electron Trace Ultra GC directly coupled to a Thermo Electron Polaris Q (Quadrupole ion trap) mass spectrometer and SGE pyrolyser. GC is equipped with 30m, 0.25 mm ID capillary column (PDMS with 5% phenyl). Samples were taken in capillary tube and inserted in to the pyrolyser furnace set at the desired temperature. The pyrolysis-GC-MS conditions were set as follows: Ion source temperature 200°C, electron energy 70eV, Inlet temperature 250°C, column flow 1ml/min, split

20ml/in, column temperature programme 40-250°C with a heating rate of 10<sup>0</sup>C/min, transfer line temperature 280°C. TG-MS studies were conducted using Perkin Elmer Pyres 1 TGA attached with Claus SQ8 Quadruple mass spectrometer at heating rate of 5<sup>0</sup>C/min.

### 2.1.6. Crosslink Density by Dynamic Mechanical Analysis (DMA)

DMA is used for determination of dynamic mechanical properties such as storage modulus, viscoelastic nature of polymeric material, determination of glass transition temperature ( $T_g$ ), identification of low temperature transitions (beta, gamma transitions) and investigation of multiphase morphology. Compared to other physical tests such as stress-strain testing, DMA has the advantage of being easy to use in a temperature-scanning mode. Using the data from DMA and from the theory of rubber elasticity, the crosslink density of a cured polymer can be determined by the following equation

$$G' = \Phi \nu RT = \Phi \rho RT / M_c$$

Where  $G'$  is the shear storage modulus of the cured polymer in the rubbery plateau region above  $T_g$  ( $T_g + 40^\circ\text{C}$ ),  $\Phi$  is front factor,  $R$  is the gas constant,  $T$  is the absolute temperature in Kelvin,  $\rho$  is the polymer density and  $M_c$  is the average molecular weight between cross links. The cross link density is known as concentration of network chains and defined as the number of network chains per unit volume of the cured polymer. It is related to the storage modulus based on equation given below

$$\log_{10} G' = 7 + 293 X_{\text{density}} = 7 + 293 / (\rho / M_c)$$

Here  $G'$  is in dynes/cm<sup>2</sup>, crosslink density,  $X_{\text{density}}$  is denoted for cross link density<sup>5-6</sup>. Dynamic mechanical analysis (DMA) was done using 01 db Metravib Viscoanalyser (Model VA 2000) using rectangular specimens of dimension (25x15x5 mm).

### 2.1.7. Mechanical and Rheological Properties

The mechanical properties of plastics can be broadly classified as short term, long term and surface properties. The short term properties are measured at a constant rate of stress or strain in different modes like tension, flexural,

compression, shear etc. Mechanical properties were measured in a computer controlled Universal Testing Machine, Instron. Mechanical properties viz. tensile strength, elongation and modulus were evaluated using Universal Testing Machine (INSTRON Model 4469). Dumbbell specimens conforming to ASTM-D-412 (equivalent to IS3600) were used for these tests. The sample size being an overall length of 110 mm, width (at ends)  $25 \pm 1$  mm, length of narrow parallel portion  $33 \pm 2$ , grips  $60 \pm 2$  mm, width of narrow parallel portion  $6 \pm 0.4$  mm and the tests were performed at a temperature of  $30 \pm 2^\circ\text{C}$  at a cross head speed of 50 mm/min. All the measurements were taken at room temperature. Minimum four specimens were analysed for each case and standard deviation were computed.<sup>6</sup>

Viscosity build up was monitored using Brookfield viscometer (HBDV II+). Rheological analysis was done using a Bohlin Gemini 2 rheometer with 20 mm parallel plate assembly in oscillation mode at a frequency of 1 Hz and controlled strain of 1%. The gap between the plates was 0.5 mm. The isothermal experiments were done by measuring the storage ( $G'$ ) and loss modulus ( $G''$ ) at different intervals.

### **2.1.8. Morphological studies**

Microstructure was examined using Scanning Electron Microscope (SEM) Philips XL 30 at 10kV for studying morphological characteristics of the cured polymer. The biphasic morphology exhibited by the cured polymer was studied using Scanning Probe Microscopy. The equipment used for the present study was Agilent 5500 Scanning Probe Microscope (SPM) with a scan size: 90 x 90 microns, with a scan speed of 2.0 lines/ s in contact and tapping mode.

### **2.2. Determination of burn rate, heat of combustion and safety characteristics**

Propellant strands of size 6 x 6 x 80 (mm) are ignited electrically by a hot wire and burned under water in a stainless steel bomb by acoustic emission technique. The burn rate is computed as length of sample burn time. The burn rate law is computed using St. Robert's Law<sup>7</sup>:  $r = a p^n$ , where  $r$  = burn rate,  $a$  = constant known as temperature coefficient,  $p$  = pressure and  $n$  = pressure index.

Heat of combustion was measured using bomb calorimeter, Parr Instrument (Make 6201). The pressure inside the bomb was fixed at 3MPa to perform the analysis. The bomb constant was determined from benzoic acid pellets weighing



approximately 1g. A nichrome wire was used to initiate the combustion. Five tests were performed for each sample and the average value was taken.

Impact sensitivity was evaluated used BAM drop hammer method. (Make: R&P, REICHEL & Partner, GmbH). Friction sensitivity was evaluated using Julius Peter's apparatus.

### 2.3. Chemical Analysis

#### 2.3.1. Isocyanate Content

The purity of the commercial isocyanate curatives used in this study was determined from the isocyanate content by a titrimetric method using n-butyl amine in dioxane as reagent.<sup>8</sup> A known excess of the reagent was added to a weighed amount of the isocyanate. Isocyanates react readily with primary amines to yield substituted urea. The excess amine is titrated with standard alcoholic hydrochloric acid. A blank experiment is also performed simultaneously.

$$\text{Isocyanate content (I}_{\text{exp}}) = (B-V) N \times 42/WX10$$

Where B = mL of acid solution required for blank titration,

V= mL of acid solution required for sample titration

N= normality of acid solution

W= weight of the sample in grams

#### 2.3.2. Hydroxyl value

An accurate knowledge equivalent weight of the polyol is required for calculating the quantity of crosslinker needed for cure.

**Equivalent weight of polyol = 56100/hydroxyl value in mg KOH/g**

Hydroxyl values of the binders were determined by acetylating method using acetic anhydride-pyridine mixture. The reaction mixture was refluxed on a water bath for about four hours. Excess acetic anhydride was hydrolysed to acetic acid and the total free titrated against sodium hydroxide solution using phenolphthalein indicator. A control or blank experiment was also performed simultaneously.<sup>9</sup>

The acid value<sup>10</sup> was determined to correct for the free acid present in the sample. For this, the binder was dissolved in a 3:2 mixture of toluene and methanol

and the resulting single phase solution titrated against standard alcoholic KOH using phenolphthalein indicator.

$$\text{Hydroxyl value} = (B-A) \times N \times 56.1/W$$

Where B mL of NaOH solution required for the blank titration

A = mL of NaOH solution required for the sample titration

N= normality of NaOH solution and W= weight of the sample in grams

#### **2.4. Computational calculations**

Mechanistic aspects of the curing and decomposition reactions have been investigated theoretically. All the structures of reactants, products and transition states were optimized at B3LYP/6-31G\*\* level of Density Functional Theory (DFT)<sup>11-17</sup>, using Gaussian 09 suite of programs.<sup>18</sup> All the stationary points were confirmed by means of frequency analysis, and all the transition states were characterized by the determination of a single imaginary frequency.

The theoretical performance analysis of the propellant was done using NASA-CEA programme<sup>19</sup> at an operating pressure of 6.93 MPa and area ratio of 10:1

---

## 2.5. REFERENCES

1. Griffiths, PR; Hasth, DJ. *Fourier Transform Infrared Spectroscopy*. Wiley and Sons, New York, **1986**
2. Colthup, NB; Aly, D; Wiberley, LH. *Introduction to IR and Raman Spectroscopy*. Academic Press, 3<sup>rd</sup> Edition, Boston, **1990**.
3. Bovey, FA; Jelinski, L; Mirau, PA. *Nuclear magnetic resonance spectroscopy*. 2<sup>nd</sup> Edition. San Diego, Academic Press, **1988**.
4. Kissinger, HE. *J. Res. Natl. Bur. Stand.* **1956**, 57, 217-221
5. Murayam, T. *Dynamic Mechanical Analysis of Polymeric Material, Material Science Monographs* 1<sup>st</sup> Edition, Elsevier, New York, **1978**.
6. Ward, IM; Hadley, DW. *An Introduction to the Mechanical Properties of Solid Polymers*, Wiley, New York, 1993.
7. Sutton, GP. *Rocket Propulsion Elements*, 8<sup>th</sup> Edition, John Wiley & Sons Inc, New York, **2010**.
8. Siggia, S. *Quantitative organic analysis via functional groups*, John Wiley and Sons, Inc. New York, **1963**.
9. ASTM D 2849-69 'Urethane foam polyol raw materials testing', **1980**.
10. ASTM D-1980, 'Fatty acids and polymerised fatty acids'. **1980**.
11. Rae, AIM. *Quantum Mechanics*, IOP Publishing Ltd, Cornwall, **2002**.
12. Szabo, A; Ostlund, NS. *Modern Quantum Chemistry*, Dover Publications, Inc, New York, **1996**.
13. Levine, IN. *Quantum Chemistry*, Pearson Education, Inc, New Jersey, **2009**.
14. Becke, AD. *Phys. Rev. A*, **1988**, 38, 3098-3100.
15. Lee, C; Yang, W; Parr, RG. *Phys. Rev. B*. **1988**, 37, 785-789.
16. Becke, AD. *J. Chem. Phys.* **1993**, 98, 1372-1377.
17. Curtiss, LA; Redfern, PC; Raghavachari, K. *J. Chem. Phys.* **2005**, 123, 124107/1-124107/12.
18. Frisch, M; Trucks, GW; Schlegel, HB; Scuseria, GE; Robb, MA; Cheeseman, JR; Scalmani, G; Barone, V; Mennucci, B; Petersson, GA; Nakatsuji, H; Caricato, M; Li, X; Hratchian, HP; Izmaylov, AF; Bloino, J; Zheng, G; Sonnenberg, JL; Hada, M; Ehara, M; Toyota, K; Fukuda, R; Hasegawa, J; Ishida, M; Nakajima, T; Honda, Y; Kitao, O; Nakai, H; Vreven, T; Montgomery J; Peralta, JE; Ogliaro, F; Bearpark M; Heyd, JJ; Brothers, E; Kudin, KN; Staroverov, V; Kobayashi, R; Normand, J; Raghavachari, K; Rendell, A; Burant, JC; Iyengar, SS; Tomasi, J; Cossi, M; Rega, N; Millam, J M; Klene, M; Knox, J E; Cross, JB; Bakken, V; Adamo, C; Jaramillo, J; Gomperts, R; Stratmann, RE;

Yazyev, O; Austin, AJ; Cammi, R; Pomelli, C; Ochterski, JW; Martin, RL; Morokuma, K; Zakrzewski, VG; Voth, GA; Salvador, P; Dannenberg, JJ; Dapprich, S; Daniels, AD; Farkas, O; Foresman, JB; Ortiz, J V; Cioslowski, J; Fox, DJ. *Gaussian 09*. Revision A02; Gaussian, Inc. Wallingford, CT **2009**.

19. Gordon, S; McBride, BJ. *Computer Programme for Calculation of Complex Chemical Equilibrium Compositions and Applications II*, NASA reference publication, NASA RP-1311-P2, Lewis Research Center, Cleveland, Ohio, USA, **1994**.

*Chapter 3*

**Triazole Crosslinked Glycidyl Azide  
Polymer as Propellant Binders**

---

*A part of the results from this chapter has been published in*

1. **Reshmi,S;** Vijayalakshmi,KP; Thomas,D; Arunan, E; Nair, CPR, Glycidyl Azide Polymer Crosslinked Through Triazoles by Click Chemistry: Curing, Mechanical and Thermal Properties *Propellants, Explosives, and Pyrotechnics*, **2013**, 35, 525-532.
2. **Reshmi, S;** Gayathri, S; Nair, CPR. Indian Patent, “A process for high burn rate solid propellants based on azide polymer binder crosslinked through triazoles”: *submitted*.

## Abstract

*This chapter describes the detailed investigations on crosslinking of glycidyl azide polymer (GAP) through 'Click chemistry'. Conventionally isocyanates are used for curing GAP resulting in urethanes. However, incompatibility of isocyanates with energetic oxidisers like ammonium dinitramide (ADN) and extraneous side reactions of isocyanates necessitate development of an alternate cure methodology. This was achieved by the reaction of the azide group in GAP with compounds containing alkyne groups through a 1, 3 dipolar cycloaddition reaction to form 1,2,3-triazole networks. For this, four alkynes compounds namely bispropargyl succinate (BPS), bispropargyl adipate (BPA), bispropargyl sebacate (BPSc) and bispropargyl oxybisphenol A (BPB) were synthesised, characterised and curing of GAP was effected using these.*

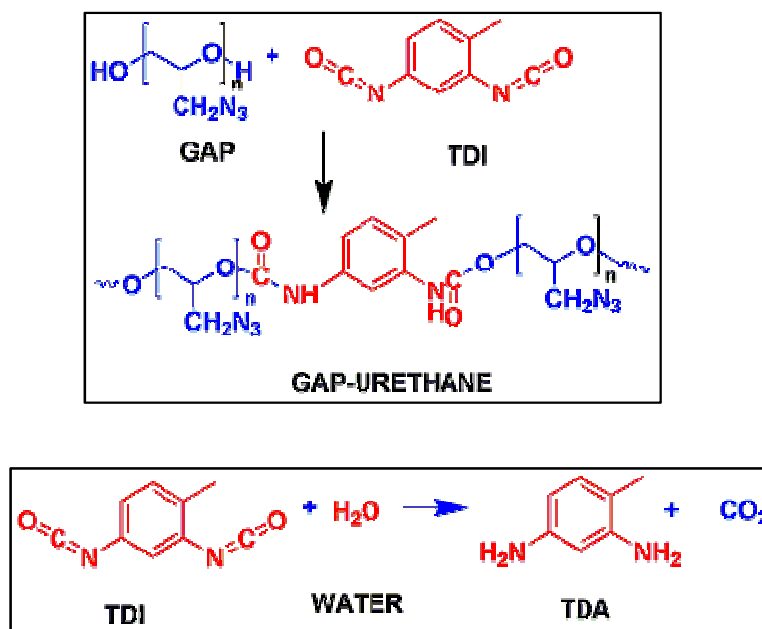
*The properties of GAP based triazole networks are compared with those of the urethane cured GAP systems. The glass transition temperature ( $T_g$ ), tensile strength and modulus of the system increased with crosslink density, controlled by the azide to propargyl ratio. The GAP-triazole imparts higher  $T_g$  in contrast to the GAP-urethane system and the networks exhibit biphasic transitions. The triazole curing was studied using Differential Scanning Calorimetry (DSC) and the related kinetic parameters enabled predicting the cure profile at a given temperature. Density functional theory (DFT) based theoretical calculations implied marginal preference for 1, 5 addition to the 1, 4 addition for the cycloaddition between azide and propargyl group. Thermogravimetric analysis (TG) showed better thermal stability for the GAP-triazole and the mechanism of decomposition was elucidated using pyrolysis GC-MS studies.*

*Propellant level properties of GAP-triazole and GAP-urethane systems were evaluated and compared. The studies revealed that GAP-triazole confers better mechanical properties, processability, improved ballistic properties and safety characteristics yielding defect free propellants than the GAP - urethane based propellant systems.*

### 3.1. INTRODUCTION

Glycidyl azide polymer (GAP) is an energetic binder commonly used in solid propellant formulations<sup>1-3</sup> in combination with oxidizers such as ammonium perchlorate (AP), ammonium dinitramide (ADN) and hydrazinium nitroformate (HNF). The energetic property of GAP originates from the azide group which decomposes exothermically with an associated enthalpy change of  $\sim 1170$  kJ/kg<sup>1</sup>.

The terminal hydroxyl groups in GAP can react with diisocyanates to form polyurethane networks, which imparts the necessary mechanical properties to the propellant. A wide range of diisocyanates such as tolylene diisocyanate (TDI) and isophorone diisocyanate (IPDI) are used for curing of GAP (Scheme 3.1a). However, curing of GAP with an isocyanate leading to polyurethane has the drawback of extraneous reactions with moisture causing evolution of gaseous products like carbon dioxide that induce voids in the system (Scheme 3.1 b).

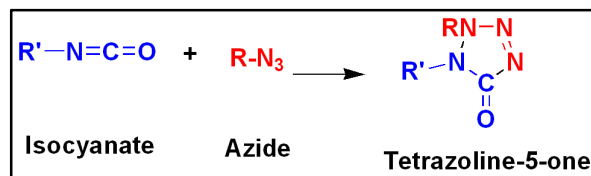


**Scheme.3.1. a.** Urethane formation reaction of hydroxyl telechelic GAP with diisocyanate **b.** Reaction of tolylene diisocyanate (TDI) with water yielding tolylene diamine (TDA) and carbon dioxide

The hydroxyl groups in GAP are secondary in nature.<sup>4</sup> In order to enhance the reactivity of these secondary hydroxyl groups during curing with an isocyanate, use of cure catalyst like ferric acetyl acetonate (FeAA)/dibutyl tin diluarate (DBTDL) is warranted. The propellant level studies using this catalysed route revealed that

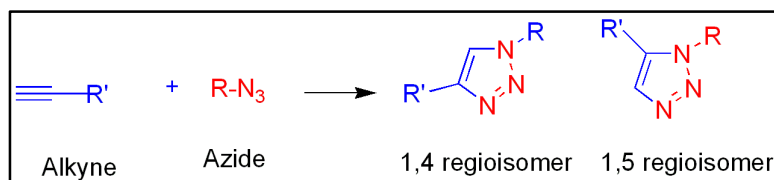
viscosities of the propellant slurry are to the tune of 2500 Pa.s. This is beyond the castable range for a propellants. Moreover, ADN and HNF undergo spontaneous degradation in the presence of isocyanates. Hence, new curing agents are essential for processing high energy propellants based on these oxidisers<sup>5</sup>.

In addition, the azide groups in GAP have a tendency to react with NCO groups to form tetrazoline-5-one as given in Scheme 3.2. All these warrant a new route for curing of GAP in propellant formulation.



*Scheme 3.2 Reaction of azide with isocyanate*

An alternate approach is to exploit the 1, 3 dipolar addition reactions between azide group of GAP and triple bonds of alkynes yielding 1, 2, 3- triazole. These reactions are nowadays an important part of ‘click chemistry’.<sup>5-12</sup> The most extensively studied compounds are azides reacting with alkynes giving rise to 1,4 and 1,5 regioisomers<sup>5</sup> as shown in Scheme 3.3.



*Scheme 3.3 Cycloaddition reaction between alkyne and azide compounds*

Earlier studies on curing of GAP with an alkyne such as bispropargyl succinate (BPS) and 1, 4-bis (1-hydroxypropargyl) benzene (BHPB) to form triazole networks have been reported.<sup>14-19</sup> The reports elaborate on the mechanical properties, swelling characteristics and crosslink densities of the system. However, there have been no reports on the detailed characterisation of this system with respect to the cure kinetics, mechanical, dynamic mechanical, thermal decomposition mechanism of the polymer and those of the propellant.

The present chapter details the curing of GAP with various aliphatic alkynes (Fig 3.1) such as bispropargyl succinate (BPS), bispropargyl adipate (BPA),



bispropargyl sebacate (BPSc) and aromatic alkyne bispropargyl oxybisphenol A (BPB). The properties of GAP based triazole networks are compared with the urethane cured GAP. The detailed characterisation of this system with respect to the cure kinetics, mechanical, dynamic mechanical and thermal properties were carried out. The cure characteristics and dynamic mechanical property of the triazole network have been correlated to the stoichiometry, extent of crosslinking and nature of alkyne curing agent. Further, the mechanism of the curing reaction of GAP with alkynes to yield triazoles was studied using a model compound viz. 2-azidoethoxyethane (AEE) and the reaction mechanism has been analysed using density functional theory (DFT) method for two systems, both aliphatic and aromatic alkynes. The thermal decomposition characteristics and mechanism of GAP-triazole decomposition have also been elucidated. Further, propellant level studies of GAP-BPSc system with ammonium perchlorate as oxidiser have been undertaken. The mechanical properties, thermal decomposition characteristics, burn rate and safety characteristics of the propellant have been determined.

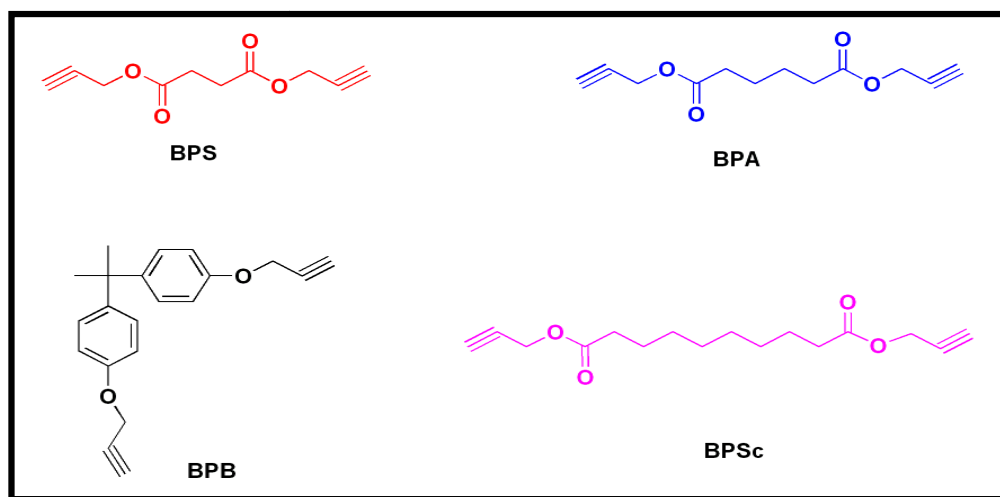


*Figure 3.1 .Molecular Structure of a) BPS b) BPA c) BPB and d) BPSc*

## 3.2. EXPERIMENTAL

### 3.2.1. Materials and measurements

Hydroxyl terminated GAP, ammonium perchlorate, aluminium powder, succinic acid, adipic acid, sebacic acid, bisphenol-A (2,2-bis-[4-hydroxy phenyl]propane), propargyl bromide, propargyl alcohol, toluene-4-sulphonic acid

monohydrate and toluene were the materials used for the studies and their characteristics are described in Chapter 2.

### 3.2.2. Instrumental

The methods and equipments used for characterisation are described in Chapter 2. FTIR,  $^1\text{H}$  and  $^{13}\text{C}$  NMR analyses of the samples were done. Curing was monitored using differential scanning calorimeter. Thermal decomposition was studied using a simultaneous TG-DSC. Mechanical properties viz. tensile strength, elongation and modulus were evaluated using Universal Testing Machine. Dynamic mechanical analysis (DMA) was done. Microstructure of GAP-BPS system was examined using Scanning Electron Microscope (SEM). Rheological analysis was done using a Bohlin Gemini 2 rheometer with 20 mm parallel plate assembly in dynamic mode. GC-MS studies were conducted using a Thermo Electron Trace Ultra GC directly coupled to a mass spectrometer and SGE pyrolyser. TG-MS studies were conducted using TGA attached with Quadruple mass spectrometer at heating rate of  $5^\circ\text{C}/\text{min}$  for cured polymer and at  $2^\circ\text{C}/\text{min}$  for the propellant samples. Heat of combustion were measured using bomb calorimeter. Burn rate measurements were done using acoustic emission technique mentioned. Impact sensitivity was evaluated used BAM drop hammer method (Make: R&P, REICHEL & Partner, GmBH). Friction sensitivity was evaluated using Julius Peter's apparatus.

### 3.2.3. Synthesis of the aliphatic alkynes

**Bispropargyl succinate (BPS):** was synthesised by the esterification reaction of succinic acid with propargyl alcohol in toluene in the presence of a catalyst namely toluene-4-sulfonic acid based on a reported procedure.<sup>15</sup> In a flask equipped with reflux condenser with a Dean-Stark water trap, 59.05 g (0.5 mol) of succinic acid, 140.15 g (2.5 mol) of propargyl alcohol, 1.25 g (6.6 mmol) of toluene-4-sulfonic acid-monohydrate in 150 ml toluene was taken. The mixture was heated under reflux until no more azeotrope from toluene –water – propargyl alcohol mixture separated in the Dean – Stark trap. Then the reaction mixture was cooled down to room temperature and washed with 5% sodium bicarbonate solution, five times with water, and dried with sodium sulfate. Then, the solvent was removed by distilling under vacuum. Yield: 87%.

FTIR (NaCl plates):  $3291\text{cm}^{-1}$  ( $\text{HC}\equiv\text{C}$ -),  $2947\text{cm}^{-1}$  (-CH),  $2129\text{cm}^{-1}$  (-C $\equiv$ C),  $1739\text{cm}^{-1}$  (-COO).  $^1\text{H NMR}$  (300 MHz  $\delta$ , ppm,  $\text{CDCl}_3$ ): 2.52 ( $\text{HC}\equiv\text{C}$ -); 2.75 (- $\text{CH}_2$ - $\underline{\text{CH}}_2$ -COO-); 4.75 (- $\text{CH}_2$ -O).  $^{13}\text{C NMR}$  (300 MHz,  $\delta$ , ppm,  $\text{CDCl}_3$ ): 29.1 (-OOC- $\underline{\text{C}}\text{H}_2$ ); 52.6 ( $\text{HC}\equiv\text{C}$ - $\underline{\text{C}}\text{H}_2$ ); 75.5 ( $\text{HC}\equiv\text{C}$ - $\text{CH}_2$ ); 77.9 ( $\text{HC}\equiv\text{C}$ - $\underline{\text{C}}\text{H}_2$ ) and 171.6 (- $\text{CH}_2$ - $\underline{\text{C}}\text{H}_2$ -COO-).

**Bispropargyl adipate (BPA):** The synthesis of BPA was carried out using the similar experimental set up mentioned above. For this, 73 g (0.5 mol) of adipic acid, 70 g (1.25 mol) propargyl alcohol, 1.25 g (6.6 mmol) toluene-4-sulfonic acid-monohydrate in 150 ml toluene were taken in a flask. The mixture was heated under reflux until no more azeotrope from toluene –water – propargyl alcohol separated in the Dean – Stark trap. Then the reaction solution was cooled down to room temperature and washed with 5% sodium bicarbonate solution, five times with water, and dried with sodium sulfate. Then the solvent was removed by distilling under vacuum. Yield: 72%.

FTIR (NaCl plates):  $3291\text{cm}^{-1}$  ( $\text{HC}\equiv\text{C}$ -),  $2947\text{cm}^{-1}$  (-CH),  $2129\text{cm}^{-1}$  (-C $\equiv$ C),  $1740\text{cm}^{-1}$  (-COO).  $^1\text{H NMR}$  (300 MHz  $\delta$ , ppm,  $\text{CDCl}_3$ ): 2.25 ( $\text{HC}\equiv\text{C}$ -); 2.51 (- $\text{CH}_2$ - $\underline{\text{C}}\text{H}_2$ -COO-); 4.75 ( $\text{CH}_2$ -O).  $^{13}\text{C NMR}$  (300 MHz,  $\delta$ , ppm,  $\text{CDCl}_3$ ): 24.0 (-OOC- $\underline{\text{C}}\text{H}_2$ ); 51.7 ( $\text{HC}\equiv\text{C}$ - $\underline{\text{C}}\text{H}_2$ ); 74.7 ( $\text{HC}\equiv\text{C}$ - $\text{CH}_2$ ); 77.0 ( $\text{HC}\equiv\text{C}$ - $\underline{\text{C}}\text{H}_2$ ) and 172.1 (- $\text{CH}_2$ - $\underline{\text{C}}\text{H}_2$ -COO-).

**Bispropargyl sebacate (BPSc):** The synthesis of BPSc was carried out using the similar experimental set up mentioned above. For this, in a flask equipped with reflux condenser with a Dean-Stark water trap, 87 g (0.5 mol) of sebacic acid, 70 g (1.25 mol) propargyl alcohol, 7 g (30.8 mol) toluene-4-sulfonic acid-monohydrate in 150 ml toluene were taken. The mixture was heated under reflux until no more azeotrope from toluene –water – propargyl alcohol excess separated in the Dean – Stark trap and the toluene circulated as a clear homogeneous phase. Then the reaction solution was cooled down to room temperature and washed with 5% sodium bicarbonate solution, five times with water, and dried with sodium sulfate. Then the solvent was removed by distilling under vacuum. Yield: 92%.

FTIR (NaCl plates):  $3292\text{cm}^{-1}$  ( $\text{HC}\equiv\text{C}$ -),  $2947\text{cm}^{-1}$  (-CH),  $2129\text{cm}^{-1}$  (-C $\equiv$ C),  $1742\text{cm}^{-1}$  (-COO).  $^1\text{H NMR}$  (300 MHz  $\delta$ , ppm,  $\text{CDCl}_3$ ): 2.25 ( $\text{HC}\equiv\text{C}$ -); 2.60 (- $\text{CH}_2$ - $\underline{\text{C}}\text{H}_2$ -COO-); 4.78 ( $\text{CH}_2$ -O).  $^{13}\text{C NMR}$  (300 MHz,  $\delta$ , ppm,  $\text{CDCl}_3$ ): 24.6 (-OOC- $\underline{\text{C}}\text{H}_2$ -COO-); 4.78 ( $\text{CH}_2$ -O).

$\underline{\text{C}}\text{H}_2$ ); 51.6 ( $\text{HC}\equiv\text{C}-\underline{\text{C}}\text{H}_2$ ); 74.6 ( $\text{HC}\equiv\text{C}-\text{CH}_2$ ); 77.7 ( $\text{HC}\equiv\text{C}-\text{CH}_2$ ) and 172.7 ( $-\text{CH}_2-\text{CH}_2-\underline{\text{C}}\text{OO}-$ ).

**Bispropargyloxy bisphenol A (BPB)** was synthesised based on a reported procedure.<sup>20</sup> Bisphenol-A (25 g, 0.11 mol) was dissolved in 100 ml freshly distilled DMF to which a solution of 10 g (0.25 g) sodium hydroxide in 20 ml distilled water. To this, solution of propargyl bromide (28 g, 0.23 mol) in 25 ml DMF was added drop wise under agitation at room temperature. After the addition, the reaction was kept under agitation for 5 hrs at RT followed by agitation at 70°C for 8 hrs. The product was isolated by precipitating the mixture into cold water. The product was filtered and dried under reduced pressure. The product was recrystallised from methanol to obtain a pale yellow solid (m.p 81°C). Yield: 80%. FTIR (NaCl plates): 3272 $\text{cm}^{-1}$  ( $\text{HC}\equiv\text{C}-$ ), 2947  $\text{cm}^{-1}$  ( $-\text{CH}$ ), 2225  $\text{cm}^{-1}$  ( $-\text{C}\equiv\text{C}$ ), 1742  $\text{cm}^{-1}$  ( $-\text{COO}$ ). <sup>13</sup>C NMR(300 MHz,  $\delta$ , ppm,  $\text{CDCl}_3$ ): 31.4 ( $-\text{C}-\text{CH}_3$ ); 42.7 ( $\text{Ar}-\text{C}$ ); 56.3 ( $\text{O}-\text{CH}_2$ ); 79.2 ( $\text{HC}\equiv\text{C}-\text{CH}_2$ ), 75.8 ( $\text{HC}\equiv\text{C}-\text{CH}_2$ ); 114.7 ( $\text{Ar}-\text{C}$ ), 128.2 ( $\text{Ar}-\text{C}$ ), 144.3 ( $\text{Ar}-\text{C}$ ), 155.9 ( $\text{Ar}-\text{C}$ ).

#### 3.2.4. Curing of GAP with alkyne curing agent

GAP was cured to obtain triazole networks by mixing GAP with BPS in varying molar equivalence ratio (with respect to azide and alkyne groups) from 1:0.1 to 1:1. GAP triazoles from higher aliphatic alkyne homologues and aromatic alkyne were also prepared in similar way with azide and alkyne groups in the molar equivalence ratio of 1: 1. The mixtures were then cast in aluminium moulds and the curing reaction was carried out by keeping the system at 30°C for 2 days and then at 60°C for a period of 5 days.

#### 3.2.5. Curing of GAP with diisocyanate

GAP was also cured by reacting with TDI to yield GAP urethane. A mixture of 1,4- butanediol and 1,1,1, trimethylol propane was added to crosslink the system (3% by weight of binder) and to impart necessary strength. The stoichiometric ratio of 1:1 (w.r.t isocyanate and hydroxyl, NCO: OH) was used for curing at 60°C for 2 days.

### 3.2.6. Computational calculations

The mechanistic aspects of the urethane formation as well as the side reaction invoking formation of tetrazoline-5-one formation in GAP while curing with a diisocyanate was analysed by DFT method. The investigations were done using a model compound 1-azido-3-methoxypropan-2-ol (AMP) with TDI.

Thermodynamic aspects of the curing reaction between azides and alkynes were investigated theoretically using 2-azido ethoxyethane (AEE) as a model compound of GAP with bispropargyl succinate (BPS) and bispropargyloxy bisphenol A (BPB).

All the structures of reactants, products and transition states were optimized with B3LYP/6-31G\*\* level of DFT, using Gaussian 09 suite of programs.<sup>21-22</sup> All the stationary points were confirmed by means of frequency analysis, and all the transition states were characterized by the determination of a single imaginary frequency.

The theoretical performance analysis of the propellant was done using NASA-CEA programme<sup>23</sup> at an operating pressure of 6.93 MPa and area ratio of 10:1

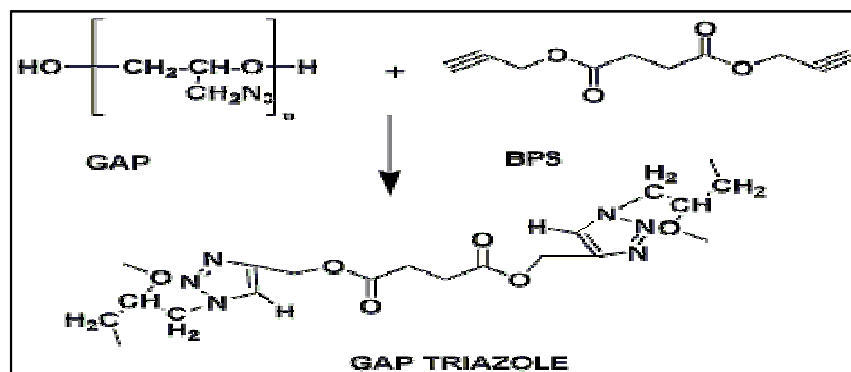
### 3.2.7. Propellant processing

Propellant batches were processed in a 1 kg scale in a Guitard horizontal mixing system at 40°C and average mixing time of three hours. A typical solid propellant formulation consisting of GAP as binder, aluminium as metallic fuel (2% by weight) and ammonium perchlorate as oxidiser (75% by weight) was chosen for the studies. BPSc was used as curing agent. For comparison, HTPB with TDI as curing agent was also processed in the same manner. End of mixing (EOM) viscosity and build up values were measured using Brookfield Viscometer (Model:HBDV II+). The samples were cured 30°C for 2 days followed by curing at 60°C for 5 days. The cured propellant samples (110x6x5 mm) were tested for mechanical properties. The burn rates were measured using acoustic emission technique at an operating pressure range of 2.94- 6.93 MPa using cured strands (80x6x6 mm). The bomb was pressurised using nitrogen and burning was detected by acoustic emission detector. Impact and friction sensitivity tests were also done for the samples.

### 3.3 RESULTS AND DISCUSSION

#### 3.3.1 Synthesis of alkynes compounds and curing of GAP

Alkyne compounds BPS, BPA, BPSc and BPB were synthesised and characterised. In a typical reaction, the azide group of GAP undergoes curing with alkyne containing compound like BPS to form triazole networks as shown in Scheme 3.4.



*Scheme 3.4 Curing of GAP-BPS through 1, 3 dipolar cycloaddition reaction between azide and alkyne (propargyl) groups*

#### 3.3.2 Theoretical aspects of cure reaction

The cure reaction between GAP and TDI is believed to proceed via the hydroxyl (-OH) to isocyanate (-NCO) reaction. In literature, there are numerous reports on curing of GAP through this route like curing of a glycidyl azide polymer (GAP) with a triisocyanate and diisocyanate and investigations on the related kinetic parameters.<sup>24-25</sup> The presence of azide (-N<sub>3</sub>) groups makes probable a likely reaction between -N<sub>3</sub> and -NCO group. This has been overlooked in previous research works. The mechanistic aspects of the urethane formation as well as the side reaction invoking formation of tetrazoline-5-one formation in GAP on curing with a diisocyanate was analysed using density functional theory (DFT) method. For this, the reaction of a model compound 1-azido-3-methoxypropan-2-ol (AMP) with TDI was theoretically followed. Transition states were located for both urethane and tetrazolin-5-one cured products as depicted in Figure 3.2. The calculated activation barriers are 28.4 kJ/mol and 185.2 kJ/mol respectively for urethane and tetrazoline-5-one products. This indicates that, there is no possibility of latter reactions at

ambient conditions. Though, the propensity for this reaction is lower than that of hydroxyl groups, it is to be noted that the relative concentration of azide to hydroxyl in GAP is 20:2. Thus, we propose that, there is good probability for crosslinking to happen via addition of diisocyanate to azide also. Hence, it is important to evolve new curing routes for GAP.

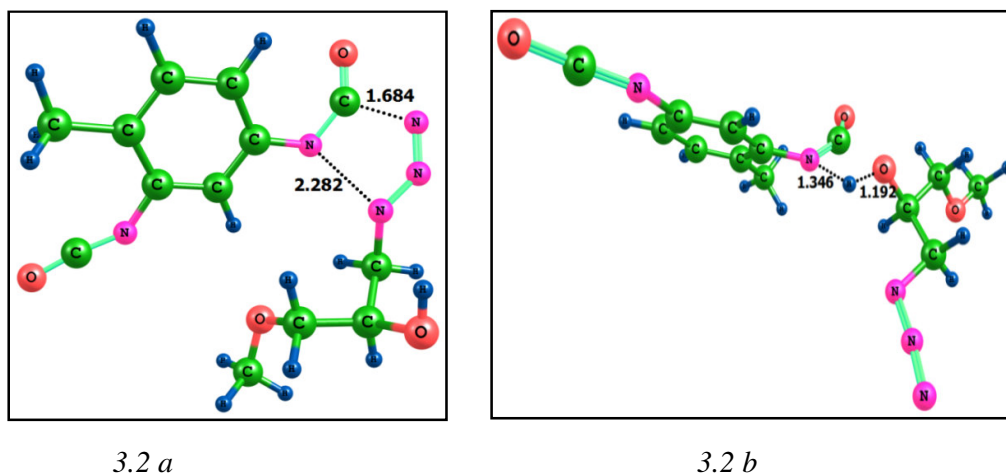


**Figure 3.2** .Optimized structures of transition states for (a) tetrazoline- 5-one (b) urethane (AMP ith TDI), Bond lengths are given in Å.

To shed some light on the mechanistic aspects of azide-alkyne reaction, the reaction of a model compound AEE with BPS was theoretically followed by calculating two possible ‘click’ cycloaddition pathways. In the first case, simultaneous interaction leading to bond formation between terminal nitrogen of AEE (N3) and terminal carbon (C1) of one of the triple bonds of BPS as well as N1 of AEE and C2 of BPS is modelled to locate the transition state. This gives a 1, 4-cycloaddition mechanism and the transition state for such a reaction is given in Figure 3.3. In the second case, simultaneous bond formation between N3 of AEE and C2 of BPS as well as N1 of AEE and C1 of BPS can occur. This yields transition state for 1, 5-cycloaddition mechanism (Figure 3.3b). In both type of reactions, the resulting product is a monoadduct of AEE and BPS. The activation energy for the 1, 4 addition is 60 kJ/mol and that for 1, 5 addition is 58 kJ/mol. In both cases, the monoadducts are formed with release of 313 kJ/mol for 1, 4-addition and 320 kJ/mol for 1, 5 addition respectively. The computed structural parameters as well as the activation barrier are in close agreement with the reported experimental and theoretical values of typical 1, 3 dipolar addition reaction transition state structures<sup>26</sup>. The unreacted CC triple bond in the monoadducts can further undergo cycloaddition with AEE. The second stage of this reaction was also modelled by

locating transition states for 1, 4- and 1, 5- type cycloaddition pathways. The activation barrier (58 to 60 kJ/mol) was same as that observed for monoadduct formation. Thus, the DFT study clearly suggests a facile reaction of the azide groups with both the triple bonds of the BPS. Since both ends of the BPS can react with almost equal probability with the azide group, the BPS will be incorporated in the polymer as a very effective networking agent. The theoretical study validates formation of a completely triazole incorporated GAP-BPS system that is also observed experimentally.

The curing mechanism of GAP with BPB was also studied theoretically by DFT, using AEE.

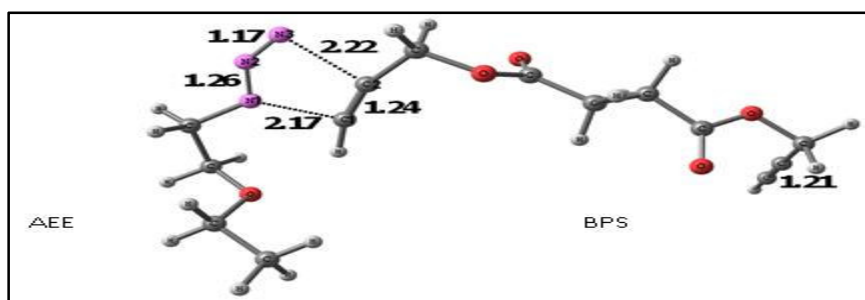


Fig. 3.3 a

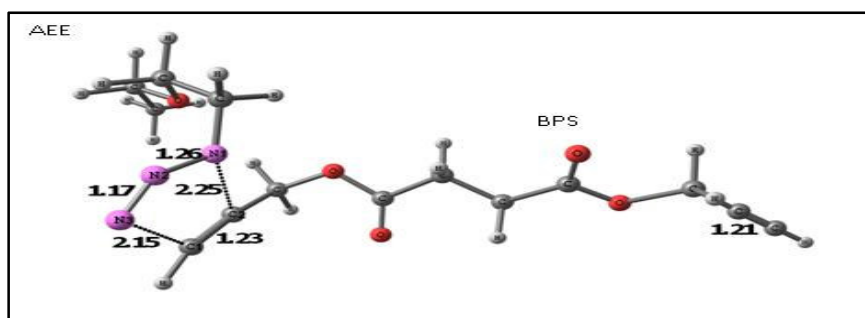


Fig. 3.3 b

**Fig 3.3** (a) Transition states for the 1, 4 and (b) 1, 5 cycloaddition between AEE and BPS. Bond lengths are given in Å.

The reaction of AEE and BPB also follows a cycloaddition mechanism leading to two different monoaddition products. In the first case, simultaneous interaction of terminal nitrogen of AEE (N3) and terminal carbon of one of the triple bonds of BPB (C1) as well as N1 of AEE and C2 of BPB can occur. This occurs through 1,5cycloaddition mechanism and the TS for such a reaction is given in Figure 3.4a. In the second case, simultaneous bond formation takes place between



N1 of AEE and C1 of BPB. This follows 1, 4 cycloaddition mechanism and the transition state (TS) for the same is depicted in Figure 3.4b. The calculated activation barrier for 1,4 and 1,5 addition reaction are 68.6 kJ/mol and 65.2 kJ/mol respectively implying almost equal probability for both additions. The reaction is found to be highly exothermic and the heats of reaction are 308.3 and 302.6 kJ/mol for 1,4 and 1,5 addition respectively.

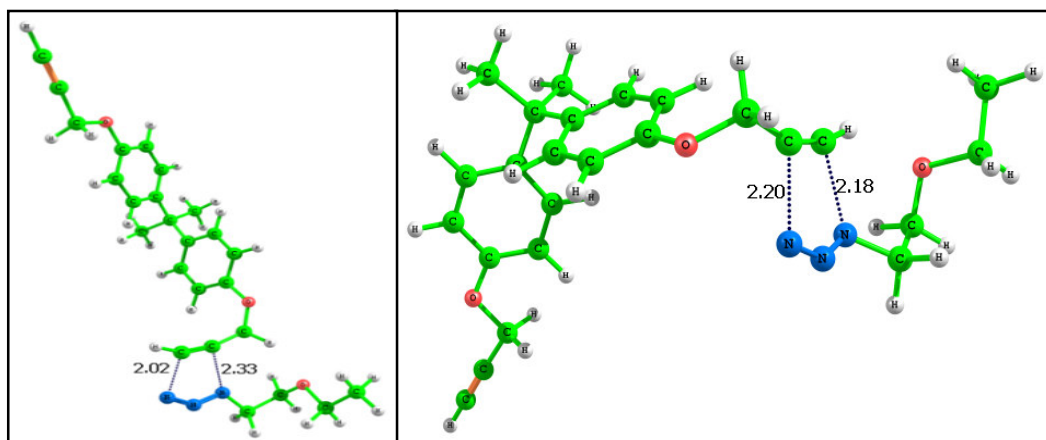


Fig. 3.4 a

Fig. 3.4 b

**Figure 3.4** Transition state structures calculated at B3LYP/6-31G\*\* level of DFT for (a) 1, 5 cycloaddition (b) 1,4 cycloaddition (AEE-BPB system, bond lengths are given in Å.)

In a similar manner, one more AEE can be added to the second C≡C bond in the BPB either through 1, 4 or 1, 5 cycloaddition pathways. The activation energy for second addition is slightly lower than for the first addition. The second addition further stabilizes the system with high exothermic reaction energy 623.8, 625.5 and 610.8 kJ/mol respectively for 1,4 -1,4; 1,5- 1,5 and 1,4-1,5 cycloadditions. The activation energy for this reaction is marginally higher than that for the curing reaction of the aliphatic curing agent bispropargyl succinate with AEE. This may be due to the reduced mobility of the aromatic curing agent.

### 3.3.3 Cure optimisation

#### 3.3.3.1 DSC analysis

Non-isothermal DSC analysis based on varying heating rates of 1, 2, 3 and 5°C/min was employed to study the curing reaction of GAP with BPS (Fig 3.5). The cure reaction occurs in the temperature range of 64-172 °C for GAP with BPS. The curing is associated with higher enthalpy change of 1250±30 J/g compared to the

GAP-isocyanate system 30 J/g.<sup>27</sup> The DSC studies revealed that a cure catalyst is not required for GAP-alkyne curing as the reaction proceeds in the temperature regime normally used for propellant curing.

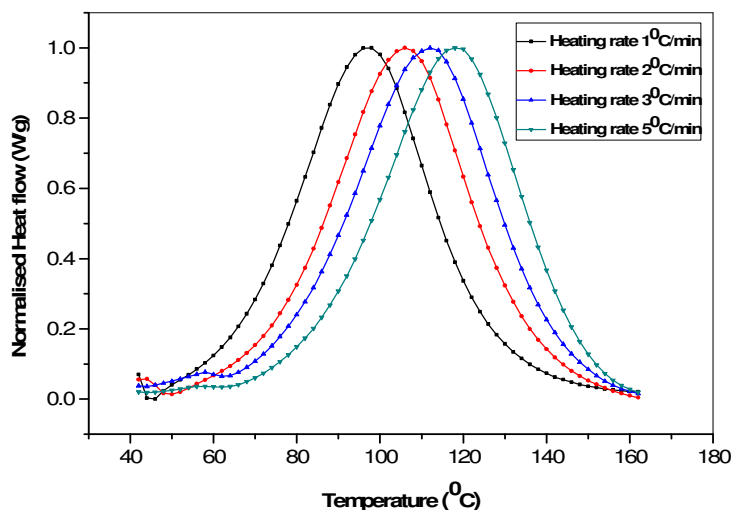


*Fig.3.5 DSC trace of GAP-BPS for different heating rates ( $N_2$  atmosphere)*

### 3.3.3.2. Cure kinetics

The cure kinetics was also followed by the non-isothermal method based on varying heating rates of 1, 2, 3 and 5 °C/min (Fig.3.6). With an increase in heating rate, the peak cure exotherm shifted to higher temperature regime. The peak temperatures ( $T_m$ ) are 97, 103, 113 and 118 °C for heating rates of 1, 2, 3 and 5 °C/min respectively (Table 3.1).

*Table 3.1. Phenomenological Details of Curing*

<i>Heating rate</i> (°C/min)	<i>Initial temperature</i> $T_i$ (°C)	<i>Peak temperature</i> $T_m$ (°C)	<i>Final temperature</i> $T_f$ (°C)
1	45	97	156
2	50	103	168
3	62	113	169
5	64	118	170

The kinetics of GAP-BPS cure reaction was evaluated by the variable heating rate method of Kissinger<sup>28</sup> based on the temperature peak maxima ( $T_m$ ) in DSC. The final form of Kissinger equation, used for finding the activation parameters is given in equation 1.

**Kissinger equation**

$$\frac{d \log(\phi/T_m^2)}{d(1/T_m)} = -\frac{E}{2.303R} \quad \text{--- 1}$$

where  $\phi$  =heating rate, E= Activation energy, R= Universal gas constant,  $T_m$ = Peak maximum temperature in DSC in absolute scale. From the slope of the linear plot of  $\log (\phi/T_m^2)$  against  $1/T_m$ , E can be calculated. The kinetic plot of Kissinger method is shown in Fig.3.6 respectively.

The pre-exponential factor (A) was calculated using equation 2.

$$A = \phi E e^{E/RT_m} / RT_m^2 \quad \text{--- 2}$$

$T_m$  is the average of the  $T_{max}$ . The activation energies (E) computed by Kissinger methods is  $85.1 \pm 7.4$  kJ/mol. The E values calculated are higher than those calculated by theoretical model (58 kJ/mol). Using the pre-exponential factor (A) and E, rate constant (k) at a temperature of 60 °C was computed (by the relation  $k=Ae^{-E/RT}$ ) and the value is  $5.84 \times 10^{-5} \text{ s}^{-1}$  respectively with a correlation coefficient of 0.9925. In the model, we take into account the chemically controlled reaction only while; DSC data is comprehensive of the overall reaction including the diffusion controlled phenomenon. Thus, the former has higher E.

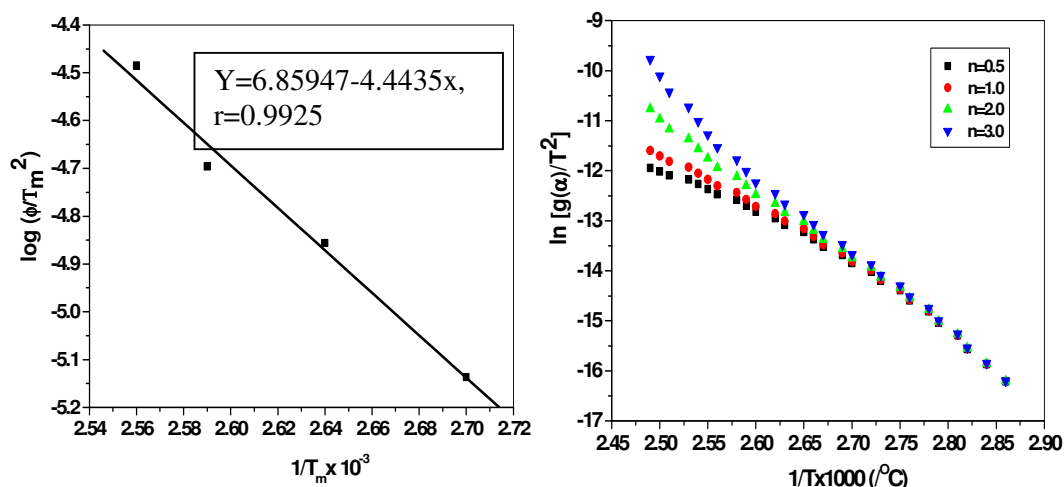


**Fig.3.6** Kissinger plot for determination of activation energy (E) for GAP-BPS

**Fig.3.7** Coats Redfern Plot for GAP-BPS system

The order parameter 'n' was evaluated using the Coats Redfern (CR) equation<sup>29</sup> as given in equation. 3, using iteration method.

$$\ln \left[ \frac{g(\alpha)}{T^2} \right] = \ln \left[ \frac{AR}{\phi E} \left( 1 - \frac{2RT}{E} \right) \right] - \frac{E}{RT} \quad \text{---- 3}$$

Where  $g(\alpha) = \frac{1-(1-\alpha)^{1-n}}{1-n}$ ,  $g(\alpha)$  for all values of  $n$  ( $n$ =order of reaction), except  $n=1$  for which  $g(\alpha) = -\ln(1-\alpha)$ ,  $\phi$  =heating rate,  $R$ =universal gas constant,  $T$ =temperature in absolute scale.

Kinetic plots were drawn from the plot of  $[\ln (g(\alpha)/T^2)]$  vs  $1/T$  for different values of 'n' ranging from 0.5 to 3.0 (Fig 3.7). The value of 'n' corresponding to the best-fit curve was chosen as the order parameter and found to have a value close to 2. This matches with the molecularity of the reaction, invoking both  $C \equiv C$  and  $N_3$  groups in the transition step.

### 3.3.3.3. Prediction of isothermal cure time

From the  $E$  and  $A$  values obtained through the kinetic studies, it was possible to predict the cure behaviour under isothermal conditions. The time necessary for the resin to reach a certain conversion at a fixed temperature can be determined. The cure time was thus optimised based on these results. The equation relating time ( $t$ ), temperature ( $T$ ) and fractional conversion ( $\alpha$ ) is given as equation 4,

$$\alpha = 1 - \{1 - A(1-n) t e^{-E/RT}\}^{1/1-n} \quad \text{----- 4}$$

$n$ =order reaction,  $E$ =activation energy,  $R$ =universal gas constant,  $T$ =temperature in absolute scale. The time-conversion profile for the isothermal cure at  $60^\circ\text{C}$  of the system is shown in Fig 3.8.

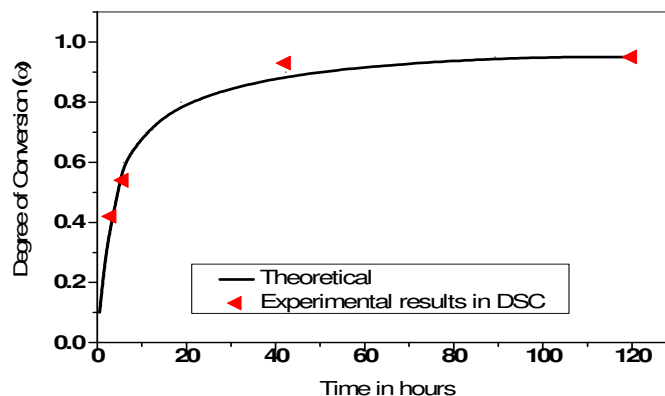
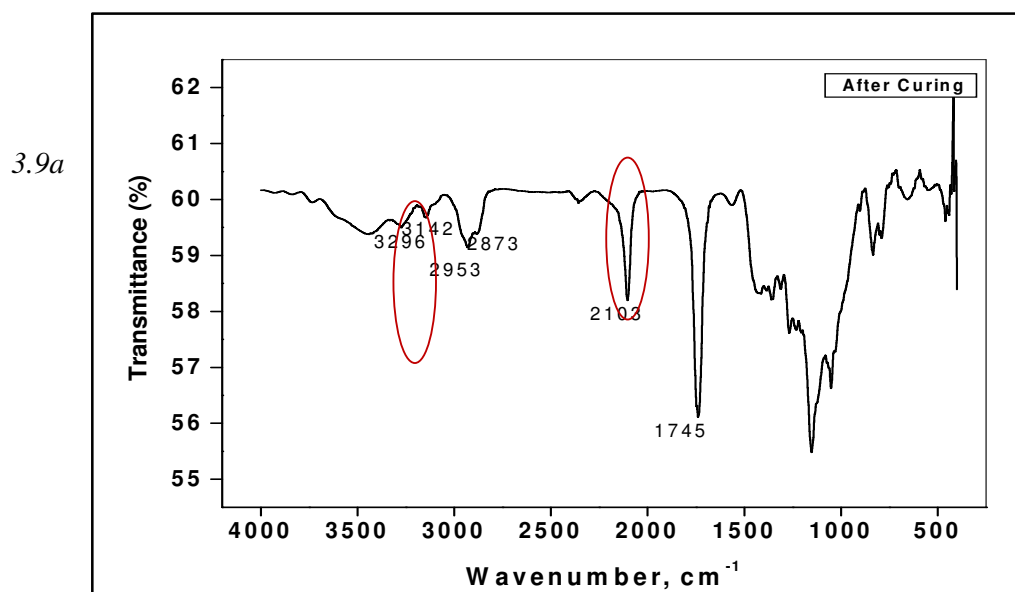


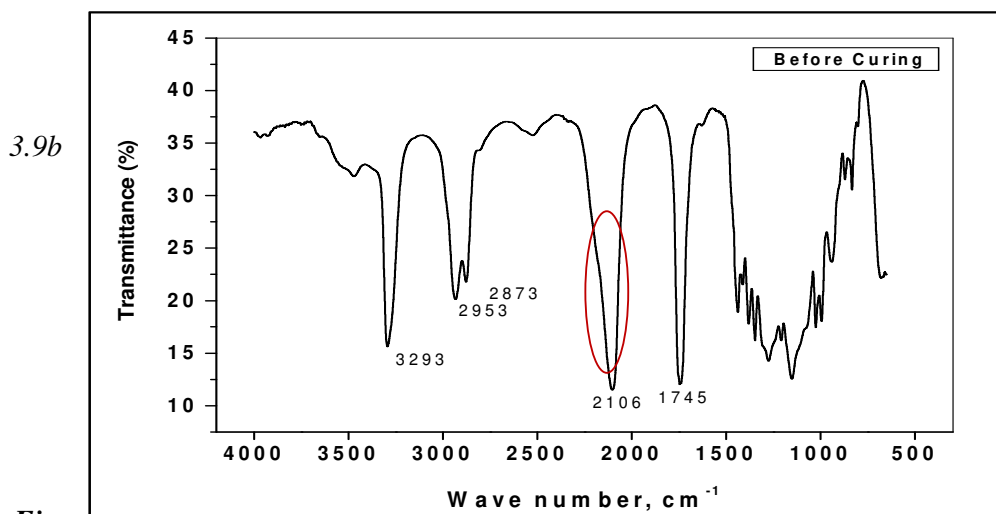
**Fig 3.8** Predicted and experimental isothermal cure profile of GA-BPS at  $60^\circ\text{C}$

The extent of curing at different time intervals calculated as per equation 4 is shown in Fig.3.8 and the experimental conversion data conform to the theoretical within experimental limits, validating the accuracy of the kinetics. The conversion at different time intervals was calculated by FTIR (monitoring the absorbance at 2106  $\text{cm}^{-1}$  due to azide group) and DSC techniques. The carbonyl absorption at 1745  $\text{cm}^{-1}$  was used as internal standard. The studies reveal that 95% conversion is achieved in 5 days which is in agreement with the calculation by the cure kinetic studies. For all practical proposes, this extent of curing is adequate for the crosslinked system. The FTIR spectra of the uncured resin and that of 95% cured resin are shown in Fig 3.9 (a) and (b).

The triazole formation is confirmed by the appearance of the peak at 3142  $\text{cm}^{-1}$  owing to the C-H stretching in triazole group in the FTIR spectra of GAP-BPS mixture<sup>30</sup> (Fig 3.20b).

Since the enthalpy of cure reaction is high, the cure schedule recommended for safe operations is at 30°C for 2 days, (after reaching a conversion of ~54%) followed by curing at 60°C for 5 days.





Fig

3.9 FTIR spectra of (a) GAP-BPS mixture-before curing (NaCl plates)  
(b) GAP-BPS mixture-after curing (ATR)

#### 3.3.3.4. Effect of reactant stoichiometry on curing

GAP and BPS were mixed at various molar equivalences viz. 1:0.1, 1:0.3, 1:0.7 and 1:1 and DSC studies were done at a heating rate of 5°C/min. The enthalpy of curing (with respect to the moles of the BPS) for the GAP-BPS system is given in Fig 3.10. The proportion of GAP in the system being constant, it is seen that heat liberated is proportional to the concentration of BPS in the system. The enthalpy increases linearly with increase in the concentration of BPS in the system. This confirms that the exotherm is exclusively due to triazole formation. From the slope of the graph the heat of reaction was calculated to be 251 kJ/mol. This matches with the enthalpy of azide-alkyne cure reaction reported in literature.<sup>6</sup>

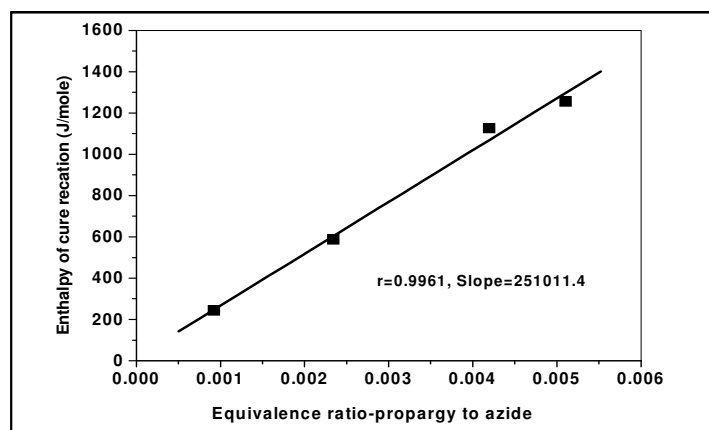
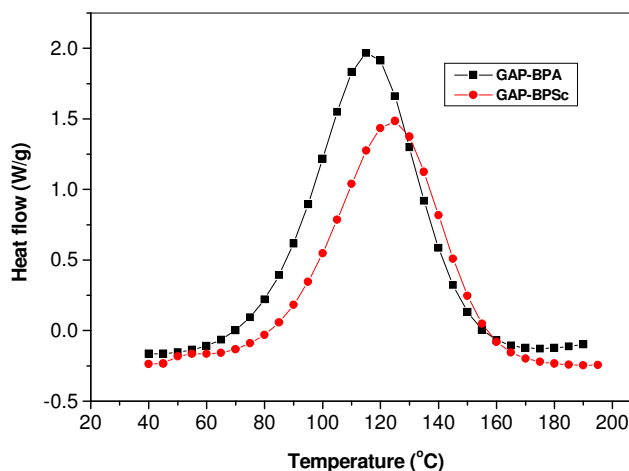


Fig 3.10 Dependence of enthalpy of reaction on the stoichiometry of reactants (GAP to BPS, azide to propargyl)

### 3.3.3.5. DSC analysis of higher alkyne homologues

Non-isothermal DSC analysis was employed to study the curing reaction of GAP with BPA and BPSc which are higher alkyne homologues. The cure reaction occurs in the temperature range of 52-175°C for GAP with BPA associated with an enthalpy change of  $1100 \pm 20$  J/g and for GAP with BPS it occurs in the temperature range of 45-178°C with an associated enthalpy change of  $940 \pm 25$  J/g (Fig.3.11).



**Figure 3.11** DSC curves for GAP curing with BPA and BPSc (Heating rate 5°C/min)

Curing reaction of GAP with BPB occurs in the temperature range 80-172°C with peak reaction temperature ( $T_m$ ) at 123°C. The curing of GAP with the aromatic alkyne BPB is associated with an enthalpy change of  $750 \pm 30$  J/g. The use of cure catalyst CuI (0.3% by wt of binder) lowered the reaction temperature range to 78-156°C with  $T_m$  at 114°C for GAP-BPB system. The curing enthalpy of GAP-BPB is lowest among the various aliphatic counterparts.

### 3.3.4. Rheological Characteristics

For a typical case, the rheological characteristics were studied. Fig.3.12 depicts the dynamic storage modulus curves as a function of temperature for the uncatalysed and catalysed for GAP-BPB systems. The storage modulus attains a maximum and follows a plateau after certain time intervals, which is considered as the time for complete cure. The catalyst lowers the cure to 120°C in comparison to the uncatalysed system which initiates at 140°C. The ultimate modulus is also higher for the catalysed system. The catalysed system effectively

increases the extent of reaction causing an increase in crosslinking and consequently the higher modulus.

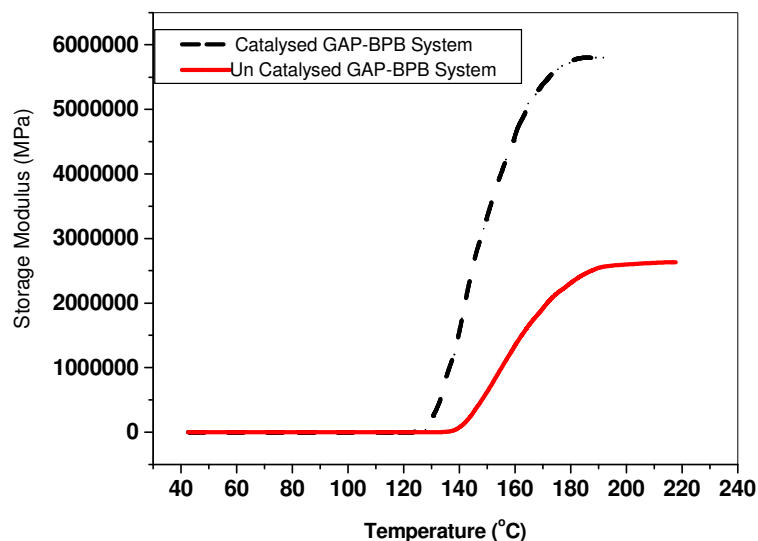


*Figure 3.12 Evolution of storage modulus as a function of temperature for GAP-BPB system*

### 3.3.5 Dynamic mechanical characterisation

DMA of the GAP triazole formed from GAP-BPS (equivalence of 1:1) shows a biphasic transition with two glass transitions ( $T_g$ ) occurring at 61°C and 85°C (Fig 3.13). These two transitions were manifested in DSC also. The glass transition temperature of GAP-urethane is at -20°C and in the GAP-triazole network, it is shifted to a positive regime. The observation that there is an increase in  $T_g$  of triazole based system than urethane system is in line with literature data.<sup>15,19</sup> The biphasic behaviour is manifested when the triazole content attains the maximum. This was confirmed by carrying out DMA studies of GAP cured at various azide to propargyl equivalence of 1: 0.3, 1: 0.5, 1:0.7 and 1:1. At low crosslink density (equivalence ratio 1:0.3) the matrix shows only a single phase with a  $T_g$  at 5°C.



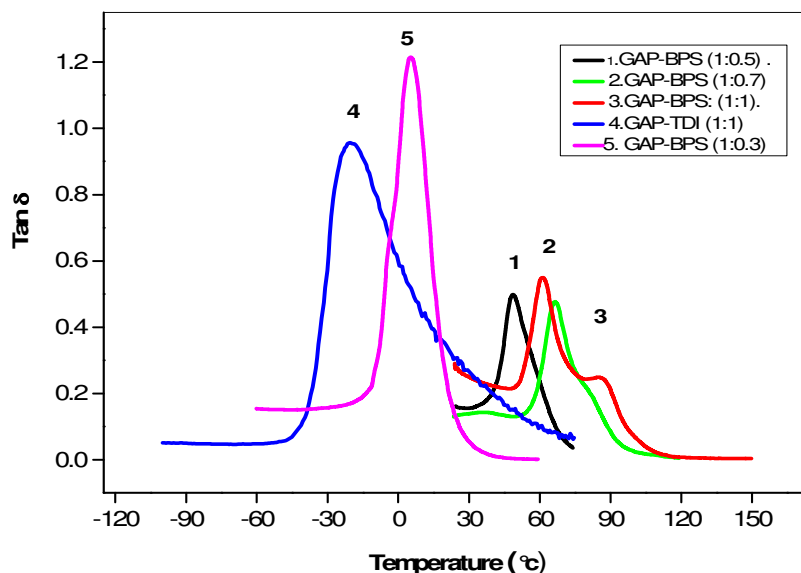


**Fig 3.13** *Tan  $\delta$  vs temperature of GAP triazoles and GAP urethane system*

As the reactant stoichiometry is enhanced to 1:0.5,  $T_g$  increases to 48°C and at the equivalence ratios of 1:0.7,  $T_g$  becomes 66°C and there is a signature of the biphasic behaviour. The two transitions may be attributed to the existence of two phases; the one at lower temperature due to the polyether backbone and the other at higher temperature due to the triazole networks.

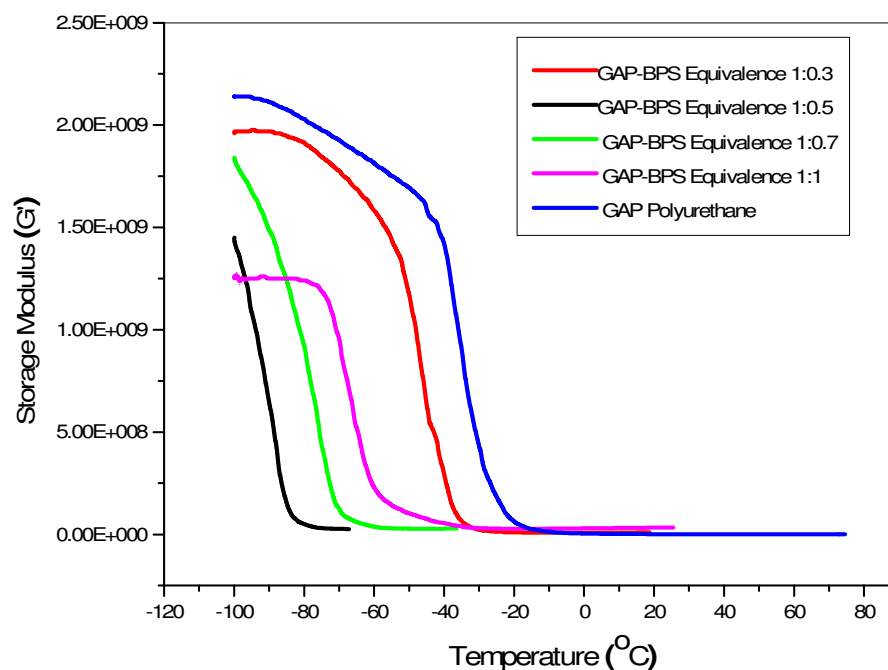
The glass transitions ( $T_g$ ) and crosslink density ( $X_{\text{density}}$ ) are the characteristic properties of a thermosetting system. The  $X_{\text{density}}$  of the system was calculated from the DMA data. A semi empirical equation<sup>31</sup> has been used for calculating crosslink density of highly crosslinked system.

$$\log_{10}G' = 7 + 293 X_{\text{density}} \quad \text{--- 5}$$

Where  $G'$  is the storage modulus of the cured polymer in the rubbery plateau region (in dynes/cm<sup>2</sup>) above  $T_g$  (i.e.  $T_g + 40^\circ\text{C}$ ),  $X_{\text{density}}$  is the cross link density of the cured polymer. The crosslink density showed a systematic increase with increase in azide to propargyl (alkyne) equivalent ratios for the GAP-BPS system, as did the  $T_g$  (Table 3.3). The variation of storage modulus with equivalence ratio is given in Fig.3.14. With increase in the azide to alkyne ratio, storage modulus also increases.

**Table 3.3** Crosslink density of GAP-BPS system

Azide : alkyne ratio	T <sub>g</sub> (°C)	Storage modulus (MPa) at T <sub>g</sub> + 40°C	Crosslink density (mol/m <sup>3</sup> )	Theoretical crosslink density (mol/m <sup>3</sup> )
1:0.3	5.0	9.7	3370	2540
1:0.5	48.2	26.7	4850	3250
1:0.7	66.0	28.1	4900	4030
1:1	85.0	34.6	5920	4710

**Fig.3.14** Variation of storage modulus with molar equivalence for GAP-triazole and GAP-urethane

DMA of the GAP triazole with GAP-BPS equivalence of 1:1 shows a biphasic transition with the glass transitions occurring at 61°C and 85°C as described earlier. However, for GAP-BPA and GAP-BPSc based triazole networks, the T<sub>g</sub> decreases to 51°C and 54°C respectively for an azide to alkyne equivalence ratios of 1:1. GAP-BPA system exhibits biphasic transition at 72°C. But in GAP-BPSc system biphasic transition is not observed, which may be due to the increase in the number of methylene spacing between triazoles wherein phase segregation is not facilitated. (Fig.3.15).

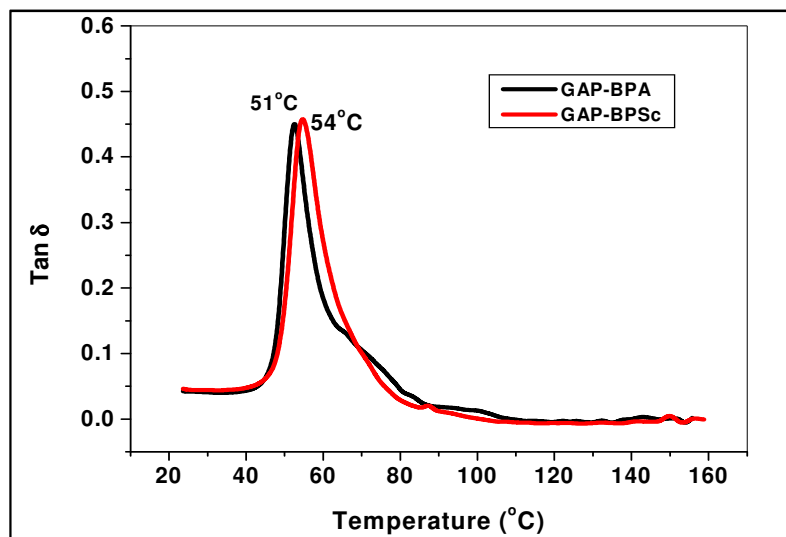
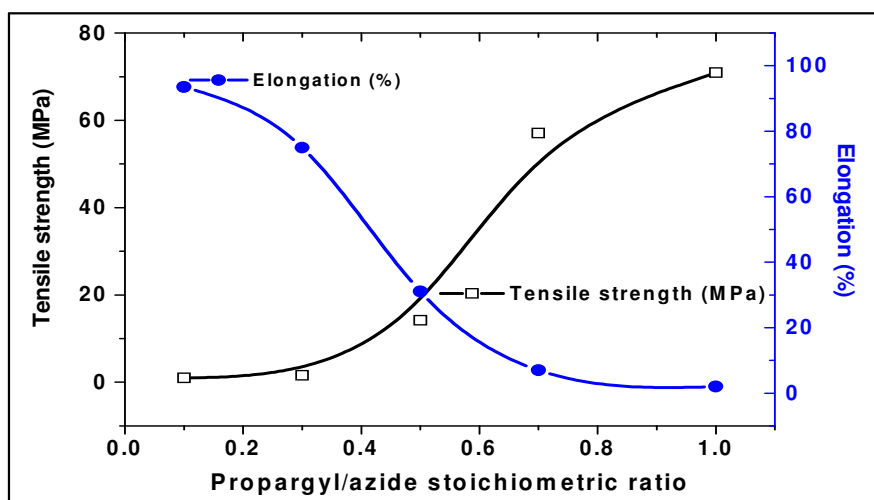


Fig.3.15 Tan  $\delta$  vs temperature of GAP-BPA and GAP-BPSc triazoles

### 3.3.6 Mechanical properties

The mechanical properties viz. tensile strength and elongation of the cured resin were determined. It is observed that as the azide to propargyl stoichiometry was varied from 1: 0.1 to 1: 1, the tensile strength increased from 0.2 to 72.5 MPa and elongation at break decreased from 120 to 2%, as depicted in Fig. 3.16a. This is a natural consequence of increased cohesion on increasing the crosslink density.



3.16a

Fig 3.16 (a) Effect of reactant stoichiometry on tensile strength and elongation

3.16b

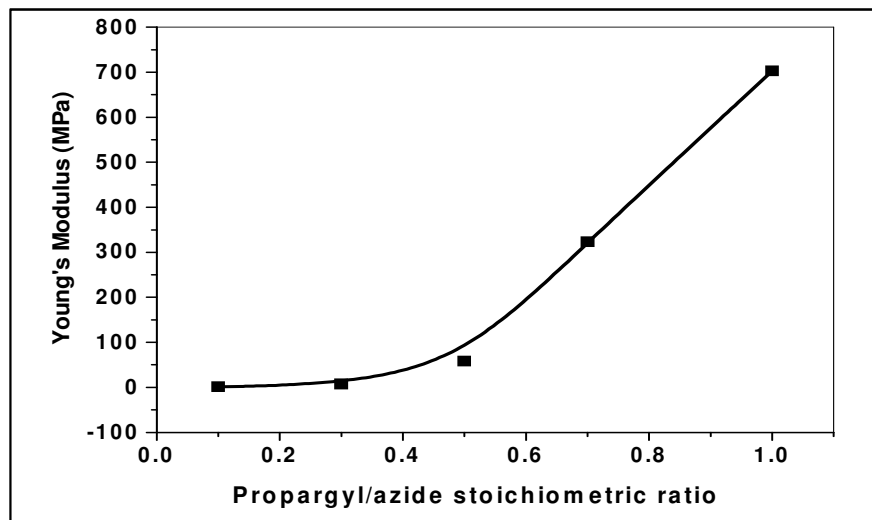


**Fig 3.16 b)** Effect of reactant stoichiometry on Young's Modulus of GAP-BPS triazoles

Tensile strength increases and the elongation decreases almost exponentially with increase in the reactant stoichiometry. The modulus also showed similar trend exhibiting a higher sensitivity for stoichiometries beyond 0.5 (Fig.3.16b). The highest properties were achieved at 1:1 stoichiometry as this ratio ensured maximum crosslinking. The  $X_{\text{density}}$  values (Table.3.3) also support this. The logarithmic relation between modulus and crosslink density ( $X_{\text{density}}$ ) is shown in Fig.3.17. The modulus can be related to the crosslink density using an empirical equation  $M = 10^{-27} X_d^{8.33}$  and modulus increases exponentially with crosslinking. For propellant level studies, it is preferable to maintain an azide-alkyne stoichiometry of 1:0.3 for obtaining optimum mechanical properties.

Keicher et al.<sup>15</sup> have reported that tensile strength and modulus increases with BPS content due to increase in crosslink densities of the cured polymer. However, as they have investigated for very low stoichiometries of BPS based on the equivalent weights used for GAP that are derived based on hydroxyl end groups, the elongation at break obtained are higher than our values. Similar observation is reported by Bin et al.<sup>16</sup> wherein a dual cure system using isocyanate and dipolarophile is reported.

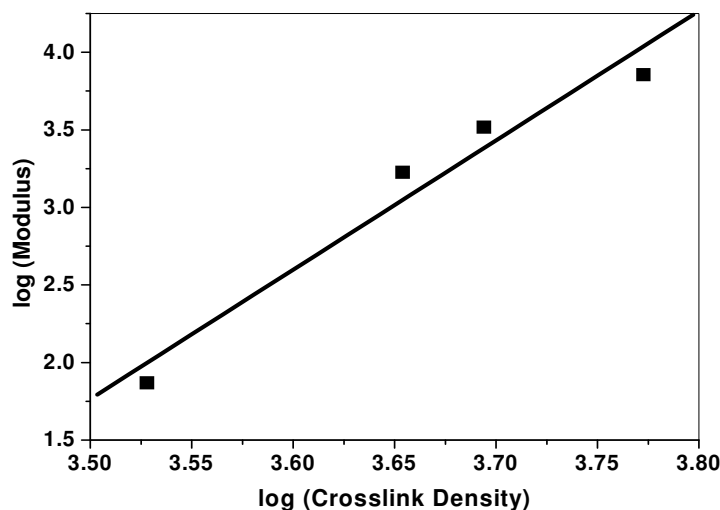


*Fig 3.17 Variation of modulus with  $X_{density}$*

The mechanical properties of GAP triazole obtained from BPA and BPSc (azide-alkyne equivalence, 1:1) are given in Table 3. For the GAP urethane system (for an isocyanate-hydroxyl equivalence of 1:1, and cross linker content of 3.0% by weight of binder) the tensile strength achieved is 0.8 MPa with an elongation of 225% and modulus of 0.9 MPa. The mechanical properties achieved for GAP triazole is superior to that of GAP-urethane.

The surface morphologies of GAP urethane (Fig.3.18a) and GAP triazole (Fig 3.18b) were studied by SEM analysis using freshly fractured surface of the cured polymers. The micrographs of the GAP urethane system indicates the presence of voids, indicative of the side reaction of isocyanate with moisture releasing carbon dioxide that affect the quality of the cured matrix.

The morphology of GAP triazole indicates a brittle failure due to rigid crosslinked triazole networks. The matrix was free of any voids, as there are no side reactions giving rise to volatile products (generating CO<sub>2</sub> with moisture) during curing by click reaction in contrast to urethane curing. Thus, defect-free gumstock slabs and propellants can be realised by curing GAP with BPS. The biphasic nature deduced from DMA was not clearly visible in the micrographs. Probably, the domains are not distinguishable.

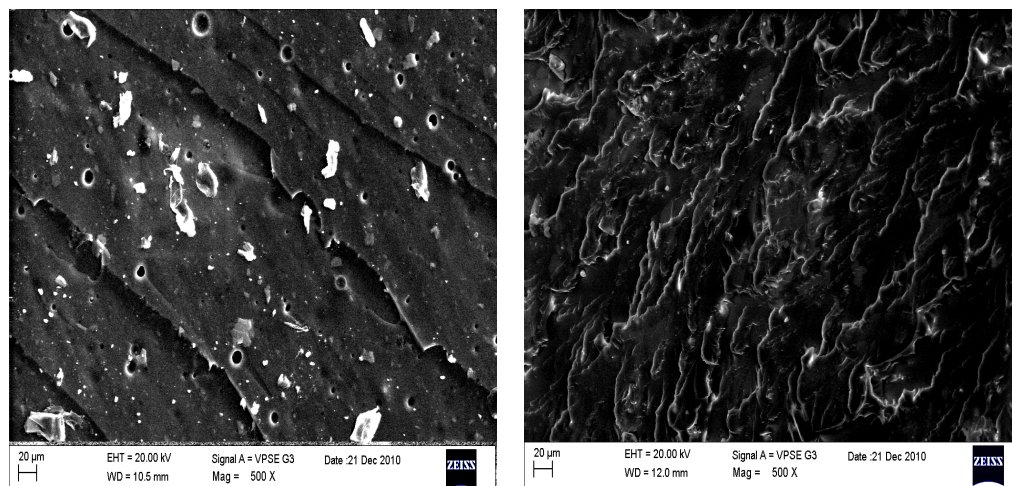


**Fig 3.18** SEM images of the fractured surface of (a) GAP cured using TDI (GAP-Urethane) (b)GAP cured by BPS (GAP-triazole)

The mechanical properties viz. tensile strength and elongation at break of the cured resin (GAP-BPA and GAP-BPSc) were determined. It is observed that tensile strength and Young's modulus decrease with marginal increase in elongation (Table 3.4). The cured slabs of GAP-BPB were very brittle and mechanical properties could not be evaluated. In the present study we have found that excellent properties can be obtained by choosing the proper alkyne homologues and dual curing method involving isocyanate is not necessary.

**Table 3.4.** Variation of mechanical properties of GAP –triazoles processed using aliphatic alkynes

<i>Sample ID</i>	<i>Tensile Strength (MPa)</i>	<i>Elongation (%)</i>	<i>Young's Modulus (MPa)</i>
GAP-BPS	75	2	715
GAP-BPA	66	7	682
GAP-BPSc	45	11	599

### 3.3.7 Thermal decomposition studies

The thermal decomposition (TG) characteristics of GAP, GAP-urethane and GAP -triazoles are given in Fig 3.19. TG was done at a heating rate of 5°C/min in nitrogen (N<sub>2</sub>) atmosphere. GAP resin shows a two-stage decomposition which is in concordance with reported literature.<sup>32-34</sup> The first stage is exothermic and occurs in the temperature range of 186-270 °C. It involves cleavage of azide group with the release of N<sub>2</sub>. The weight loss up to 270°C is ~40 % which is in agreement with the

azide content of GAP. The second stage decomposition occurs in the temperature range 270-450 °C and corresponds to degradation of the polymer backbone with a weight loss of 25%. A residue of 35% is obtained which corresponds for carbonaceous matter.

GAP urethane also undergoes two-stage decomposition in the temperature range of 160-270°C with scission of azide group. The weight loss for this stage is ~39%. The second stage decomposition occurs in the temperature range of 272-450° C. The residue of ~32% at 600°C is obtained.

The triazole crosslinks confers better thermal stability to the system in contrast to GAP-urethane system. The first stage decomposition occurs in the temperature range of 214-343°C with a weight loss of 29%. The second stage decomposition occurs in the temperature range of 344-575°C with a weight loss of 39%. The enthalpy of decomposition of azide group in GAP resin is 3200 J/g (317 kJ/mol of azide) and that of triazole is 3370 J/g (418 kJ/mol of triazole). The heat of combustion of GAP-triazole (azide-alkyne molar equivalence 1:1) was evaluated and found to be 20.8 kJ/g as against GAP-urethane 20.9 kJ/g (isocyanate:hydroxyl ratio 1:1). This also indicates that conversion of azide groups to triazole does not lower the heat of combustion as the enthalpy of decomposition of triazole groups are higher than azide groups. The higher heat of decomposition of GAP-triazole renders it a better propellant binder property than GAP-polyurethane. The mechanisms of decomposition for both the stages were investigated by pyrolysis GC-MS and TG-MS studies. The studies revealed that the first stage decomposition involves the cleavage of ester link and in the second stage; the triazole cleavage was followed by degradation of polymer backbone.

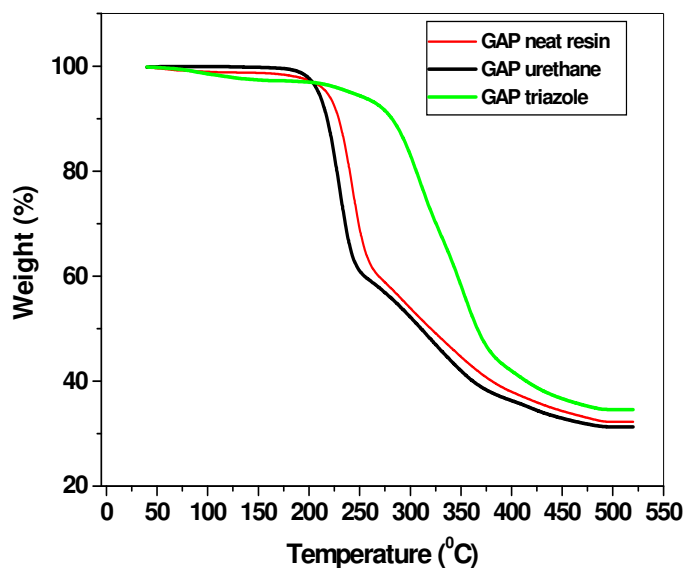


*Fig. 3.19. TG curves of GAP, GAP-urethane and GAP-triazole (in N<sub>2</sub> at heating rate of 5°C/min)*

### 3.3.8. Pyrolysis GC-MS

The thermal decomposition mechanism of GAP-triazole and GAP-urethane was studied by pyrolysis-GC-MS and TG-MS. For this, pyrolysis of GAP-triazole was carried out 350 °C. The major products obtained is succinic anhydride (retention time, RT 8.09) due to cleavage of ester link in GAP-triazole with traces of succinimide (RT 9.91) due to the unreacted azide present in the system (Fig.3.20). There was no indication of the breaking of the triazole ring at this temperature and probable reaction mechanism is given in Scheme 3.5, which was further confirmed by TG-MS studies. Pyrolysis of GAP-urethane at the same temperature (350°C), on the other hand gives N<sub>2</sub> and CO<sub>2</sub> as the major products (RT 1.36) along with butanediol (RT 6.93) and trimethylol propane (RT 12.02) as reported in literature<sup>35</sup>. The butane diol and trimethylol propane are additives used for crosslinking GAP in GAP - polyurethane.

Pyrolysis of GAP-triazole at higher temperature (500°C) shows N<sub>2</sub> as major pyrolysis product indicating the cleavage of triazole ring with evolution of nitrogen (RT 1.36) along with propenol (RT 1.63), pyridone (RT 3.70), methyl pyridine (RT 5.38), 8-azabicyclo (RT 3.2.10) carboxyl aldehyde) (RT 10.93) and succinic anhydride. Low molecular weight species are formed at the higher temperature of 500°C which is desirable for a propellant binder.



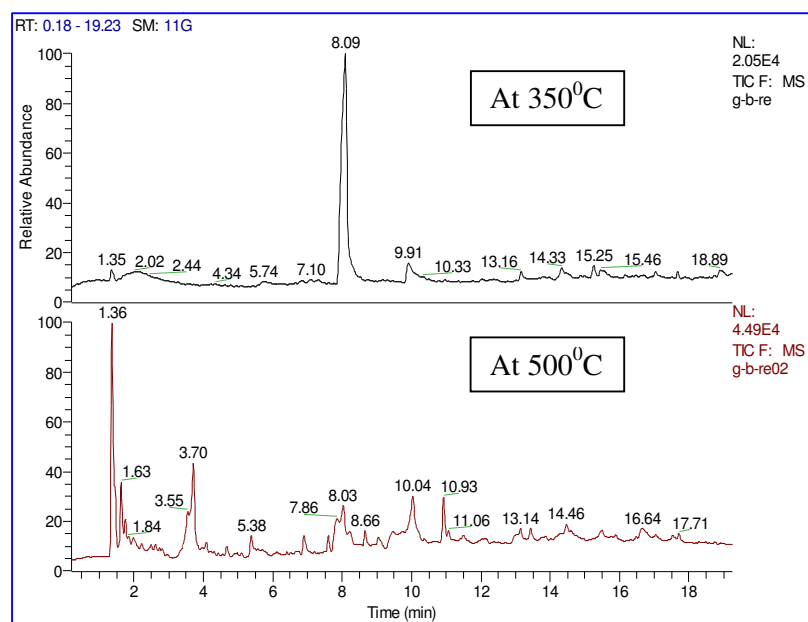
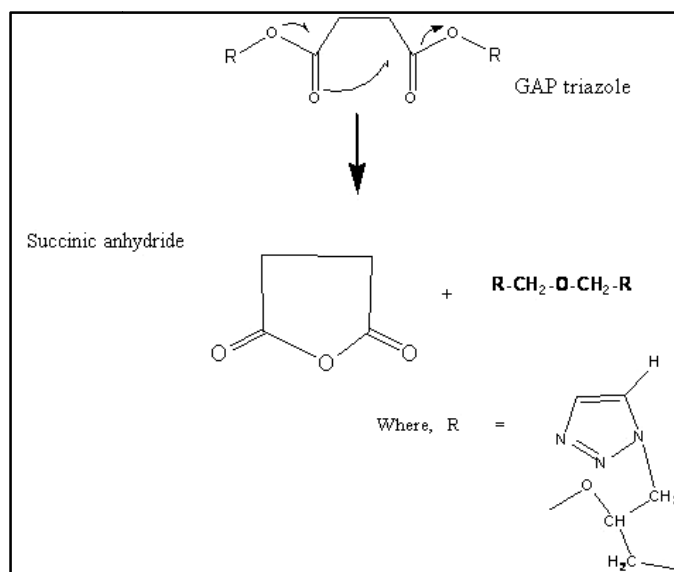


**Fig 3.20 a.** Pyrograms of GAP-Triazole (1:1) at 350<sup>o</sup>C and 500<sup>o</sup>C



**Scheme 3.5** Pyrolysis pathway for GAP-triazole giving rise to anhydride

### 3.3.9. Theoretical performance analysis of the propellant

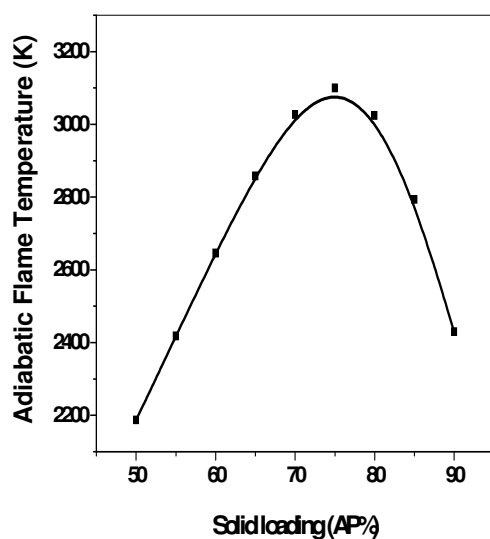
GAP in combination with ADN oxidiser (aluminised) gives ~10s improvement in specific impulse (Isp) than HTPB-AP propellant system (Table 3.6). However, as ADN is a 1.1 class explosive, exploring the advantages of GAP in combination with a less sensitive oxidiser like ammonium perchlorate is important to be investigated. In addition, GAP in combination with AP is a potential candidate for fast burning propellant for use in pyrogen igniters or gas generator applications

due to high regression rates offered by GAP. These applications usually warrant the use of low aluminium content. Though reports<sup>37-38</sup> are available on aluminised GAP-AP propellant, detailed characterisation of fast burning propellant using low aluminium content has not been reported. Theoretical performance evaluation using NASA CEA programme for low aluminised (with 2% aluminium) GAP-AP propellant at various AP solid loadings was done and the output parameters namely the Isp, adiabatic flame temperature (Tc) and combustion products were analysed. The effect of solid loading on Isp and adiabatic flame temperature of GAP-AP propellant is given in Fig.3.21a and 3.21b. It is observed that optimum Isp and Tc is obtained at a solid loading of 75%. A comparison of HTPB-AP propellant and GAP-AP propellant containing 2% aluminium are given in Table 3.5. Theoretical performance analysis of GAP-triazole and GAP-urethane are not separately presented.

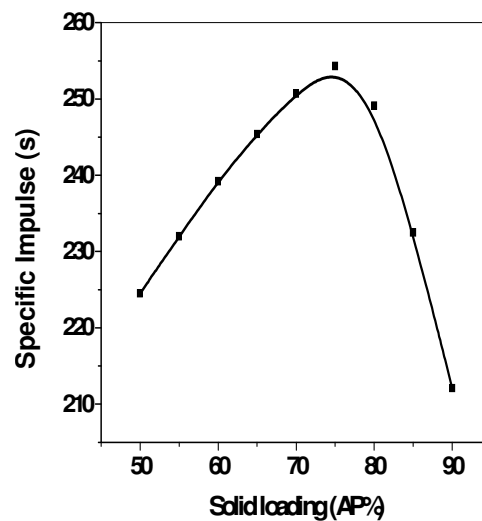
**Table.3.5.** Thermo chemical performance of aluminised AP Propellants  
Area ratio: 10:1 at 6.93 MPa pressure

<b>Propellant</b>	<b>HTPB-AI-AP</b>	<b>GAP- AI- AP</b>
Solid loading %	14-18-68	28-18-54
Sea level Isp (s)	265	275
Vacuum Isp (s)	290	300

In the present work, the characteristics of low aluminised GAP-AP propellant are described. A typical propellant formulation with solid loading of 75%, containing 2% aluminium by weight with unimodal distribution of AP was chosen for the study as the peak performance is obtained at this solid loading. The theoretical Isp of the system was 257s. A comparison of GAP-AP propellant with HTPB-AP propellant is given in Table 3.6 which indicates a higher flame temperature of 3184K, high mass percentage of gaseous products namely CO<sub>2</sub> and N<sub>2</sub>.



3.21. a



3.21. b

*Fig. 3.21. a. Effect of solid loading on the adiabatic flame temperature of GAP-AP propellant*

*Fig.3.21.b. Effect of solid loading on the Isp of GAP-AP propellant*

**Table 3.6. Thermochemical Performance Parameters of Propellant (Aluminium content 2%)**

<i>Parameters</i>	<i>HTPB-AP</i>	<i>GAP-AP</i>
Isp (s)	241.4	257.0
V.Isp (s)	224.0	279.0
Flame temperature (Chamber) K	2123	3184
<b>Combustion products</b> (Mass %)		
CO	42.5	10.7
CO <sub>2</sub>	0.9	16.5
HCl	15.5	20.4
H <sub>2</sub>	5.1	0.4
H <sub>2</sub> O	1.6	24.5
N <sub>2</sub>	6.3	19.1
Al <sub>2</sub> O <sub>3</sub>	8.2	3.5

### 3.3.10. Propellant studies: processability, mechanical properties, burn rate and safety

The propellant level studies were conducted using GAP-triazole (azide-alkyne molar stoichiometry of 1:0.3, with GAP-BPSc system) as binder, with ammonium perchlorate as oxidiser and aluminium powder as metallic fuel. For comparison, the properties of propellant processed using GAP-TDI polyurethane as binder were also evaluated. The processability, mechanical properties at ambient temperature and burn rate of the two propellants are given in Table 3.

The GAP triazole propellant system tends to exhibit better processability than GAP-urethane propellant as expected. The unloading viscosity is 150 Pa.s for GAP-triazole propellant as against 624 Pa.s for GAP-urethane propellant which brings out the obvious advantage of the new azide-alkyne curing reaction over the conventional diisocyanate-hydroxyl reactions. The viscosity (Table 3.7) after 3 hrs for GAP-urethane propellant is very high (2784.4 Pa.s) compared to 280.0 Pa.s for GAP-triazole propellant. The mechanical properties (Table 3.8) of GAP-triazole are comparable to GAP-urethane at an azide-alkyne equivalence was 1:0.3. It is observed that on increasing the alkyne content, the modulus increases. The impact sensitivity and friction sensitivity of GAP-triazole propellant is observed to be higher than GAP-urethane (Table3.9) which is due to the partial conversion of free azides to triazole resulting in a reduced sensitivity and better safety characteristics.

*Table 3.7 Viscosity build up propellant*

Time (hrs)	Viscosity in Pa.s at 40°C	
	GAP-triazole	GAP-Urethane
0	150.0	624.0
2	172.5	1460.2
3	280.0	2784.8

*Table 3.8 Mechanical properties of propellant*

Mechanical Properties	GAP-triazole	GAP-Urethane
Tensile strength, (MPa)	0.39	0.69
Elongation at break (%)	20	39
Young's Modulus (MPa)	2.94	2.65

**Table 3.9** Safety properties of propellant

<b>Propellant</b>	<b>Impact Sensitivity (kg-cm)</b>	<b>Friction sensitivity (kgf)</b>
GAP-Urethane	50	9.6
GAP-triazole	70	16.8

The burn rate of the GAP-triazole propellant was evaluated using a cured strand by acoustic emission technique for different pressure ranging from 2.94 to 6.93 MPa and the burn rate varies from 19.02 to 24.6 mm/s over this range (Table 3.10). The burn rate law was computed to be  $r$  (cm/sec) =  $0.672 P^{0.306}$ .

The mechanical properties of GAP-ADN and GAP-AP propellants have been reported by Menke et al.<sup>38</sup> and Cerri et al.<sup>39</sup> for oxidiser content in the range of 55-63% for non-aluminised propellant and the values that we have obtained for aluminised (2%) formulation with oxidiser content of 73% is comparable. The burn rates reported are in the range of 22-25 mm/s at 10 MPa. But, the formulation reported by us provides a higher burning rate of 24.6 at 6.93 MPa with lower pressure index. This could be due to the fact that the propellant system that we report has higher triazole content with only AP fine (with average particle size of 45 microns) as oxidiser. This could be contributing to the increase in burning rates at lower pressures thereby reducing the pressure index of burn rate. The burning rate of GAP-urethane propellant at 6.93 MPa is 23 mm/s.

**Table 3.10** Burn rate of the propellant  
(Five strands tested at each pressure)

<b>Pressure (MPa)</b>	<b>Burn rate (mm/s)</b>
2.94	19.0±0.02
3.92	22.5±0.08
5.52	23.6±0.1
6.93	24.6±0.06

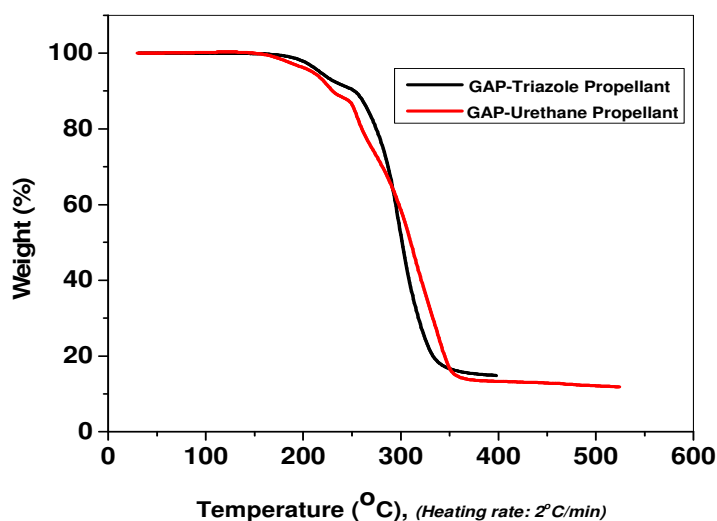


**Fig. 3.22.** TG curves of GAP- urethane and GAP-triazole propellant (in  $N_2$  at heating rate of  $2^\circ C/min$ )

The thermal decomposition of GAP urethane and GAP-triazole propellant was studied by TG-DSC at a heating rate of  $2^\circ C/min$  (Fig.3.22). GAP-urethane propellant undergoes a three-stage decomposition. The first stage decomposition occurs in the range of  $182-229^\circ C$  with peak decomposition temperature of  $250^\circ C$  due to the scission of azide group with a weight loss of 3 %. The second stage decomposition occurs in the temperature range of  $230-258^\circ C$  where decomposition of urethane linkage and AP occurs with a weight loss of 34%. The third stage decomposition occurs in the temperature range of  $259-350^\circ C$  with a weight loss of 52% and the residue obtained at  $370^\circ C$  is 11%. GAP triazole propellant undergoes a two-stage decomposition. The first stage occurs in the range of  $191-243^\circ C$  with peak decomposition temperature of  $215^\circ C$  due to the cleavage of ester group in triazole network. The second stage decomposition occurs in the temperature range of  $244-361^\circ C$  with a weight loss of 75% where AP decomposition and triazole decomposition is complete. The residue obtained at  $370^\circ C$  is 15%. Landsem et al.<sup>17</sup> have reported the thermal decomposition of GAP-AP-HMX based propellant using DSC technique. The temperature of initiation for decomposition reported is  $\sim 170^\circ C$ , which is lower than the present values. This could be due to the fact the reported formulations contain HMX as an additive which could be affecting the thermal stability of the propellant.

### 3.4. CONCLUSIONS

GAP could be crosslinked through ‘Click chemistry’ by reacting with various alkyne homologues like BPS, BPA, BPSc and BPB. The curing of the system was monitored by DSC studies and the derived kinetic parameters were used for predicting the cure profile of the system. DFT studies done using a model compound showed marginal preference for 1, 5 addition over 1, 4 addition. DFT studies on competitive curing reaction invoking hydroxyl/azide groups with isocyanates were also studied which indicated that competitive reactions can occur on thermal activation. The enthalpy of curing of GAP-BPB is lower than that of the aliphatic counterpart BPS, BPA and BPSc. Rheokinetic studies indicate that the use of a catalyst enhances the rate of reaction substantially and leads to complete curing as indicated by a higher storage modulus. For the GAP-triazole systems, the tensile strength and modulus increased while elongation decreased on increasing the crosslinking and yielded defect-free polymer as evident from SEM analysis. DMA of the GAP-triazole based on GAP-BPS showed a biphasic transition with both transitions occurring at higher temperatures (61°C and 85°C) compared to the GAP-urethane system which is monophasic. It is also observed that the biphasic behavior characteristics decreases for triazoles based on higher alkyne homologues. The thermal decomposition studies indicate a higher thermal stability for triazole crosslinked GAP in comparison to pristine GAP and GAP-urethane. Pyrolysis GC-MS and TG-MS studies indicated that the first stage decomposition of GAP-triazole is primarily due to cleavage of ester linkage of the curing agent and triazole cleavage occurs at higher temperature substantiating the better thermal stability of the triazole crosslinks. The study showed that curing of GAP through ‘click chemistry’ offers an alternate route for processing of this propellant binder, wherein the cured resins have better thermal stability and could offer ballistic advantages in view of the higher heat of decomposition due to the triazole groups and generation of low molecular weight species during thermal decomposition. The propellant has the advantages of improved ‘pot-life’ as indicated by the end of mix viscosity along with a slow build up rate, good mechanical properties, higher thermal stability as well as better safety characteristics with higher impact and friction sensitivity than the GAP-urethane propellant.

**3.5. REFERENCES**

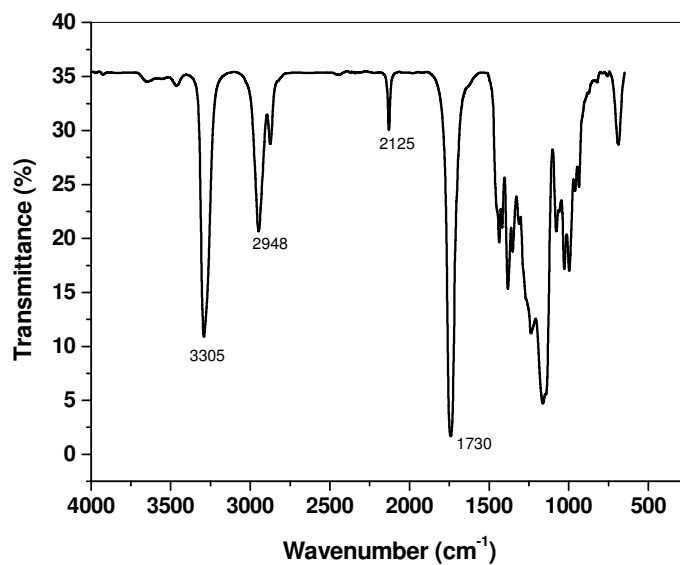
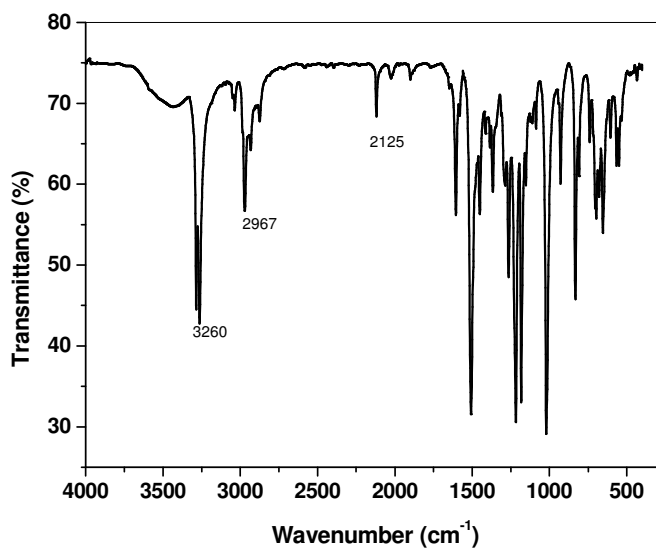
1. Frankel, M; Grant, ; Flanagan, JE. *J. Propulsion and Power*, **1992**, 8, 560-563.
2. Guery, J-F; Chang, IS; Shimada, T; Glick, M; Boury, D; Robert, E. *Acta Astronautica*, **2010**, 66, 201-219.
3. Rahm, M. *Green Propellants*, Stockholm, Sweden.: Royal Institute of Technology; **2010**.
4. Cheng, HN; Smith DA. *J.Appl.Polym.Sci*,**1987**, 34, 909-912.
5. Huisgen, R. *In 1,3-Dipolar Cycloaddition Chemistry*. New York: Wiley; **1984**.
6. Kolb HC, Finn MG, Sharpless KB. *Angew. Chem. Int. Ed.* **2001**, 40, 2004-2021.
7. David, D; Diaz, SP; Holzer, P; Mcpherso, AK; Sharpless, KB; Fokin, VV; Finn, MG. *J. Polymer Science: Part A: Polymer Chemistry*, **2004**, 42, 4392-4403.
8. Binder, WH; Sachsenhoer,R. *Macromol.Rapid Commun*, **2007**, 28, 15-54.
9. Wei ,JJ; Jin, L; Wan, K; Zhou, CH. *Bull Korean ChemSoc*, **2011**, 32, 229-238
10. Odlo, K; Hansen, TV. *Tetrahedron Letters*, **2007**, 48, 2097-2099.
11. Wu P, Feldman AK, Nugent AK, Hawker CJ, Scheel A, Voit B, Pyun J, Fréchet, JMJ; Sharpless, KB; Fokin, VF. *Angew Chem, Int Ed.*, **2004**, 43, 3928-3932.
12. Thompson, CM; Hergenrother, PM. *High Perform. Polym.* **2001**, 13, 313-322.
13. Lodge, TP. *Macromolecules*, **2009**, 42, 3827-3829.
14. Jung,JH; Lee,KH; Koo, BT. *Tetrahedron Letters*, **2007**, 48, 6442-6448.
15. Keicher, T; Kuglstatter, W; Eisele, S; Wetzels, T; Krause, H. *Propellants, Explos.Pyrotech.*, **2009**, 34, 210-217.
16. Min, BS; Park, YC; Yoo, JC. *Propellants, Explos.Pyrotech.*, **2012**, 37, 59-68
17. Landsem E, Jensen TL, Kristensen TE, Hansen FK, Benneche T, Unneberg E. *Propellants, Explos.Pyrotech.*, **2013**, 38, 75-86
18. Reshmi, S; Vijayalakshmi, KP; Thomas, D; Arunan, E; Nair, CPR. *Propellants, Explos.Pyrotech.* **2013**, 38, 525-532.
19. Hu, C; Guo, X; Jing, Y; Chen,,J;, Zhang, C; Huang, J. *J.Appl.Polym.Sci.*, **2014**, 131-135
20. Nair, CPR; Krishnan, K; Ninan,KN.*Thermochimica Acta*, **2000**, 359, 61-67
21. Becke, AD. *J. Chem Phys*, **1993**, 98, 5648-5652.



22. Frisch, M; Trucks, GW; Schlegel, HB; Scuseria, GE; Robb, MA; Cheeseman, JR; Scalmani, G; Barone, V; Mennucci, B; Petersson, GA; Nakatsuji, H; Caricato, M; Li, X; Hratchian, HP; Izmaylov, AF; Bloino, J; Zheng, G; Sonnenberg, JL; Hada, M; Ehara, M; Toyota, K; Fukuda, R; Hasegawa, J; Ishida, M; Nakajima, T; Honda, Y; Kitao, O; Nakai, H; Vreven, T; Montgomery, J; Peralta, JE; Ogliaro, F; Bearpark, M; Heyd, JJ; Brothers, E; Kudin, KN; Staroverov, V; Kobayashi, R; Normand, J; Raghavachari, K; Rendell, A; Burant, JC; Iyengar, SS; Tomasi, J; Cossi, M; Rega, N; Millam, J M; Klene, M; Knox, J E; Cross, JB; Bakken, V; Adamo, C; Jaramillo, J; Gomperts, R; Stratmann, RE; Yazyev, O; Austin, AJ; Cammi, R; Pomelli, C; Ochterski, JW; Martin, RL; Morokuma, K; Zakrzewski, VG; Voth, GA; Salvador, P; Dannenberg, JJ; Dapprich, S; Daniels, AD; Farkas, O; Foresman, JB; Ortiz, J V; Cioslowski, J; Fox, DJ. *Gaussian 09*. Revision A02; Gaussian, Inc. Wallingford, CT **2009**.
23. Gordon, S; McBride, BJ. *Computer Programme for Calculation of Complex Chemical Equilibrium Compositions and Applications II*, NASA reference publication, NASA RP-1311-P2, Lewis Research Center, Cleveland, Ohio, USA, **1994**.
24. Keskin, S; Ozkar, S. *J. Appl. Polym. Sci*, **2001**, 81, 918–923
25. Manu, SK; Sekkar, V; Scariah, KJ; Varghese, TL; Mathew, S. *J. Appl. Polym. Sci*, 2008, **110**, 908–914
26. Ess, DH; Houk, KN. *J. Phys. Chem A*, **2005**, 109, 9542-9553
27. Catherine, KB. *Thermoanalytical investigations on curing and decomposition of polyol binders*. Thiruvananthapuram: University of Kerala. India; **2003**.
28. Kissinger, HE. *J Res Nat Bur Stand*, **1956**, 57, 217-221.
29. Coats, AW; Redfern, J. *Nature*, **1964**, 201, 68-69.
30. Sun, S; Wu, P. *J Phys Chem A*, **2010**, 114, 8331-8336.
31. Ward, IM; Sweeney, J. *An introduction to the mechanical properties of solid polymers*. New York: Wiley; **2004**.
32. Eroglu, MS; Guven, O. *J. Appl. Polym. Sci*, **1996**, 60, 1361-1367.
33. Ling, P; Wight, CA. *J. Physical Chemistry B*, **1997**, 101, 12, 2126-2131.
34. Fazlıođlu, H; Hacalođlu, J. *J. Analyt. Appl. Pyrol.*, **2002**, 63, 327-338.
35. Korobeinichev, OP; Volkov, EN; Shmakov, AG. *Combustion and Flame*, **2002**, 129, 136-150.
36. Bruno, C; Accettura, AG. *Advanced Propulsion Systems and Technology Today to 2020*, Vol. 223, AIAA, Reston, VA, **2008**
37. Nguyen, C; Morin, F; Hiernard, Guengant Y, Proc. *Insensitive Munitions & energetic Materials Technology Symposium*, Munich, Germany, **2010**.

38. Menke, K; Heintz, T; Schweikert, W; Keicher, T; Krause, H. *Propellants, Explos. Pyrotech.*, **2009**, 34, 218-230.
39. Cerri, S; Bohn, MA; Menke, K; Galfett, L. *Propellants, Explos., Pyrotech.* **2010**, 35, 1-12.

## SUPPORTING INFORMATION

*Fig.3.1A. FTIR Spectrum of BPA**Fig. 3.2 A. FTIR Spectrum of BPB*

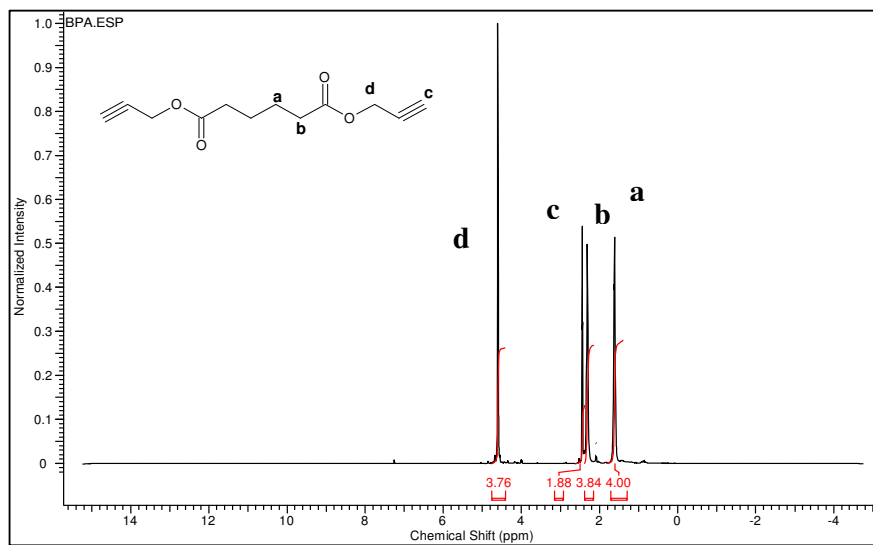


Fig.3.3 A.  $^1\text{H}$  NMR Spectrum of BPA (in  $\text{CDCl}_3$ )

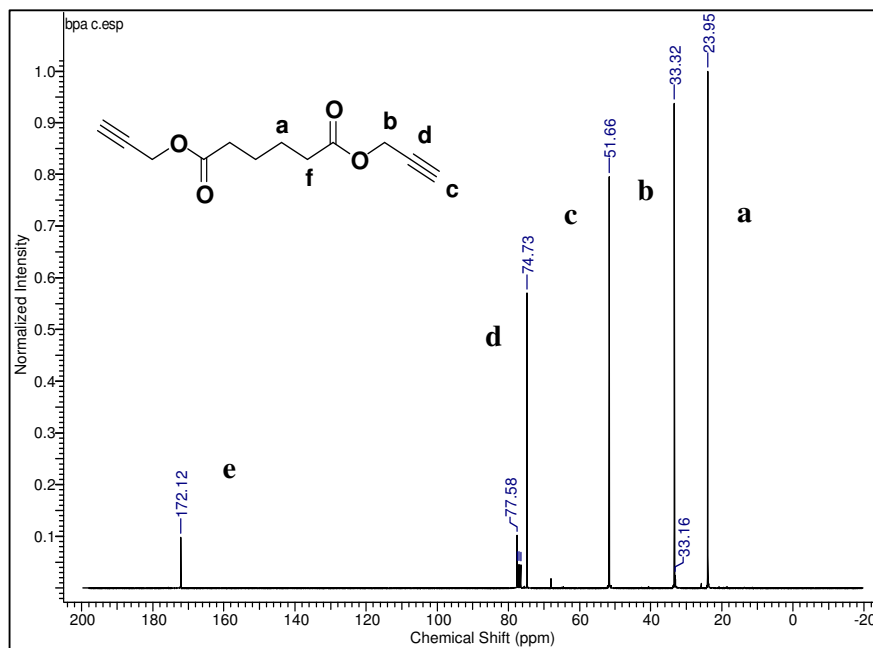
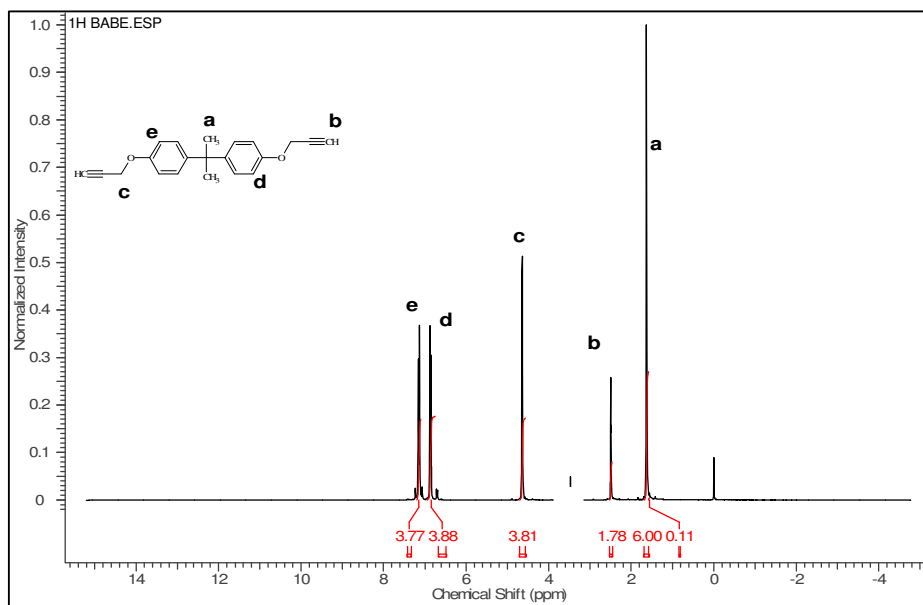
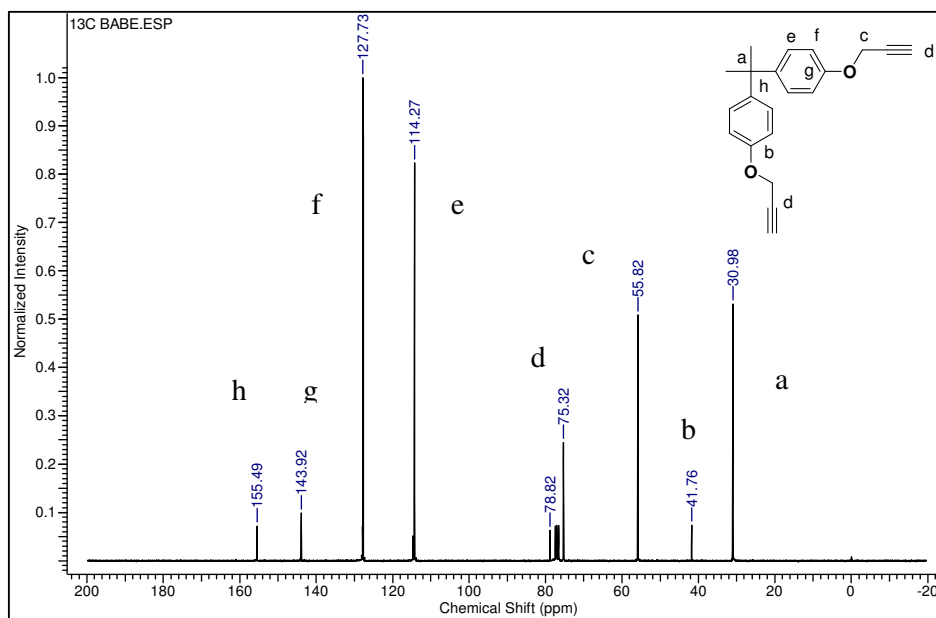


Fig. 3.4 A.  $^{13}\text{C}$  NMR Spectrum of BPA (in  $\text{CDCl}_3$ )



*FTIR 3.5 A. <sup>1</sup>H NMR Spectrum of BPB (in CDCl<sub>3</sub>)*



*Fig. 3.6 A. <sup>13</sup>C NMR Spectrum of BPA (in CDCl<sub>3</sub>)*

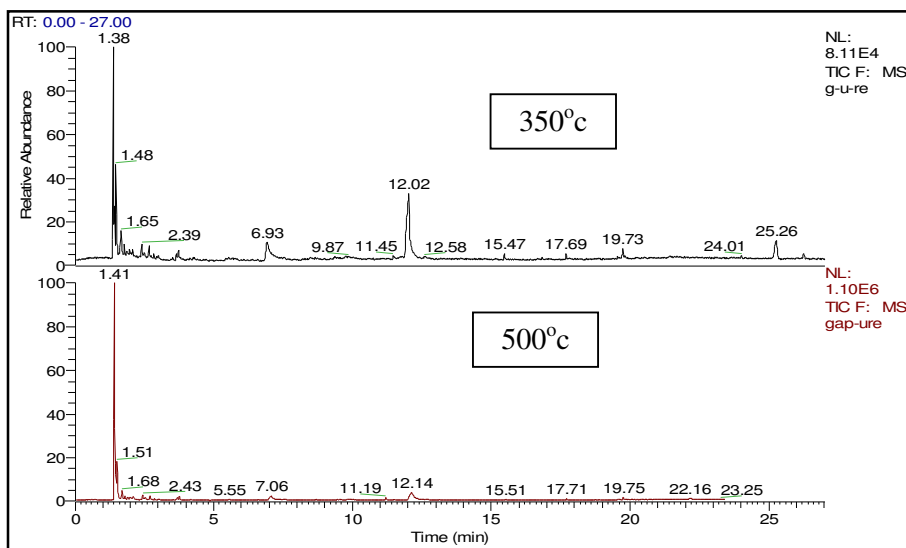


*Fig 3.7A. Pyrograms of GAP-Urethane (1:1) at 350°C and 500°C*

*Chapter 4*

**Azide-Alkynes End Capped Polybutadienes:  
Synthesis, Characterisation and Propellant  
Studies**

---

*A part of the results from this chapter*

***Reshmi, S; Nair, CPR; Arunan, E.** Azide and Alkyne Terminated Polybutadiene Binders: Synthesis, Crosslinking and Propellant Studies, *Industrial and Engineering Chemistry Research*, **2014**, 453, 16612–16620.*

---

**Abstract**

*Amongst the different types of polymeric binders used in composite solid propellants, hydroxyl terminated polybutadiene (HTPB) is considered as the most versatile. HTPB is conventionally cured using isocyanates to form polyurethanes. However, the undesirable side reactions and incompatibility of isocyanates with energetic oxidisers like ammonium dinitramide (ADN), hydrazinium nitroformate (HNF) described in previous chapters are limiting factors for its use as curing agents for future solid propellants.*

*With an aim of resolving these problems, HTPB was chemically transformed to azidoethoxy carbonyl amine terminated polybutadiene (AzTPB) and propargyloxy carbonyl amine terminated polybutadiene (PrTPB) by adopting appropriate synthesis strategies and were characterised by spectroscopic and chromatographic techniques. The blend of these two polymers underwent curing under mild temperature (60°C) conditions through 1, 3-dipolar cycloaddition reaction resulting in 1, 2, 3-triazoles. It was also observed that the azide groups in AzTPB can undergo a competitive addition reaction to the unsaturation in polybutadiene backbone to yield 1,2,3-triazoline networks. The curing parameters were studied using Differential Scanning Calorimetry (DSC). The cure profile at a given temperature was predicted using the derived kinetic parameters. Rheological studies revealed that the gel time for curing through the 1, 3 -dipolar addition is higher than that for curing through the urethane route. The mechanical properties of the resultant cured polybutadiene network were superior to those of polyurethanes. This is the first report on 1, 3-dipolar cycloaddition reaction involving azide and alkyne end groups for crosslinking HTPB.*

*The cured triazoline-triazole polymer network exhibited biphasic morphology with two glass transitions ( $T_g$ ) in contrast to the polyurethane which exhibited a single transition. This was corroborated by associated morphological changes observed by Scanning Probe Microscopy (SPM).*

*Novelty of this work lies in exploring the well-known 1,3 -dipolar reaction for crosslinking of HTPB, resulting in propellants with improved processability and superior mechanical as well as safety properties without risking the ballistic properties.*



---

## 4.1. INTRODUCTION

Large composite solid propellant grains or rocket motors in particular, demand adequate mechanical properties to enable them to withstand the stresses imposed during operation, handling, transportation and motor firing. They should also have a reasonably long 'pot-life' to provide sufficient window for processing operations such as mixing and casting which makes the selection of binder with appropriate cure chemistry more challenging. In all composite solid propellants currently in use, polymers perform the role of a binder for the oxidiser, metallic fuel and other additives. It performs the dual role of imparting dimensional stability to the composite, provides structural integrity and good mechanical properties to the propellant. Hydroxyl terminated polybutadiene (HTPB) is the most popular hydrocarbon binder used in composite solid propellants<sup>1-10</sup> which is normally cured by reaction with diisocyanates like tolylene diisocyanate (TDI) or isophorone diisocyanate (IPDI) to form polyurethane networks. However, this reaction is highly susceptible to spurious reaction with moisture, leading to deterioration in properties of the propellant<sup>10-11</sup>. In addition, the high reactivity of isocyanate group limits the 'pot-life' of the propellant. The inherent incompatibility of isocyanates with energetic oxidisers like ammonium dinitramide (ADN) and hydrazinium nitroformate (HNF) also warrants new cure methodologies to be evolved for processing high energy propellants using HTPB as binder.

Several reports exist on the modification of HTPB<sup>11-14</sup> such as grafting of energetic groups such as poly(glycidyl azide),<sup>15</sup> anchoring of iron pentacarbonyl,<sup>16</sup> grafting of 2-(ferrocenylpropyl) dimethylsilane (FPDS), functionalisation by attaching polyazido groups through cyanuric chloride etc.<sup>17-22</sup>. Most of these are aimed at improving the ballistic performances of HTPB based propellants. A comprehensive approach of achieving improved processability and superior mechanical properties for the propellant without compromising its ballistics is essential to meet the future requirements.

1,3-dipolar cycloaddition reaction of an organic azide with an alkyne (Huisgen reaction) resulting in triazoles is a versatile tool in polymer chemistry for realising crosslinked networks in good yield without any side reactions.<sup>23-29</sup> Though there have been a few reports on azide-alkyne reactions for crosslinking glycidyl azide polymer<sup>30-32</sup>, synthesis of triazole based binders<sup>33</sup> and alkyne terminated HTPB<sup>34</sup>, there have been practically no reports on the functional modification of

---

HTPB with azide and alkyne groups which are further subjected to curing through 1,3-dipolar addition reaction.

In the present chapter, a novel approach for functionalisation of HTPB to derive azidoethoxy oxy carbonyl amine terminated polybutadiene (AzTPB) and propargyloxy carbonyl amine terminated polybutadiene (PrTPB) by chemical transformation of the hydroxyl groups is reported. The blend of the resultant polymers viz. ATPB and PrTPB was subsequently crosslinked via 1,3-dipolar addition reaction. The chapter describes the details of synthesis, characterization, cure studies, mechanical, dynamic mechanical and morphological characteristics of the crosslinked polymers and propellant level studies.

## **4.2. EXPERIMENTAL**

### **4.2.1 Methods and Materials**

HTPB, TDI (2,4 : 2,6 isomer, 80:20), propargyl alcohol, 2-(2-chloro ethoxy) ethanol, sodium azide, propargyl bromide, dibutyl tin diluarate (DBTDL), ammonium perchlorate (AP) and aluminium powder were used for the studies. The solvents namely methanol, toluene and tetrahydrofuran (THF) of high purity (AR grade) were used. The characteristics of the materials are described in Chapter 2.

### **4.2.2 Instrumental**

The methods and equipments used for characterisation are described in Chapter 2. FTIR,  $^1\text{H}$  and  $^{13}\text{C}$  NMR analyses of the samples were done. Curing was monitored using differential scanning calorimeter. Rheological analysis was done using a Bohlin Gemini 2 rheometer with 20 mm parallel plate assembly. Isothermal experiments were done by measuring the storage ( $G'$ ) and loss modulus ( $G''$ ) at different intervals at 80°C. Thermal decomposition was studied using a simultaneous TG-DSC. Mechanical properties viz. tensile strength, elongation and modulus were evaluated using Universal Testing Machine. Dynamic mechanical analysis (DMA) was done. The morphological studies of the sample were carried out using a Scanning Probe Microscope (SPM). GC-MS studies were conducted using a Thermo Electron Trace Ultra GC directly coupled to a mass spectrometer and SGE pyrolyser. TG-MS studies were conducted using TGA attached with Quadruple mass spectrometer at heating rate of 5°C/min for cured polymer and at 2°C/min for the propellant samples. Heat of combustion were measured using bomb calorimeter.

---

Burn rate measurements were done using acoustic emission technique. Impact sensitivity was evaluated using BAM drop hammer method (Make: R&P, REICHEL & Partner, GmBH). Friction sensitivity was evaluated using Julius Peter's apparatus.

### **4.2.3. Synthesis**

#### **4.2.3.1 Synthesis of Isocyanate-Terminated Prepolymer (ITPB)**

The isocyanate-terminated prepolymer of HTPB (ITPB) was synthesised based on a reported procedure<sup>35</sup> by reacting HTPB with excess TDI. In a typical reaction, 10 g (0.004 mol) of HTPB containing the catalyst (a few drops of dibutyl tin dilaurate, DBTDL) was added drop wise under nitrogen purging to 1.21g (0.007 mol) of TDI (isocyanate-hydroxyl molar ratio 2:1) at 40°C and was kept under stirring for 5 hrs. The resultant resin was used as such for subsequent reaction. FTIR (NaCl plates): 2266  $\text{cm}^{-1}$  (-NCO), 1740  $\text{cm}^{-1}$  (-NH-COO-, carbonyl), 3368  $\text{cm}^{-1}$  (-NH). Isocyanate content of 2.7 % in the polymer<sup>36</sup> corresponds to the theoretical value. The isocyanate value and FTIR analysis confirmed the complete reaction of hydroxyl group to generate equal concentration of isocyanate end groups.

#### **4.2.3.2 Synthesis of propargyloxy carbonyl amine terminated polybutadiene (PrTPB)**

The propargyloxy carbonyl amine terminated polybutadiene (PrTPB) was synthesized by reacting ITPB with propargyl alcohol. About 6ml (0.107 mol) of propargyl alcohol was added drop by drop to 10 g (0.004 mol) of ITPB (from above reaction). The reaction was carried out in bulk in the presence of DBTDL as catalyst at 80°C for 4 hrs, (in nitrogen atmosphere) under magnetic stirring. The product was dissolved in THF and was precipitated into excess methanol. The product was washed with methanol and dried under reduced pressure at 60°C for 3hrs. Yield ~89%.

#### **4.2.3.4. Synthesis of azidoethoxy carbonyl amine terminated polybutadiene (AzTPB)**

Azidoethoxy carbonyl amine terminated polybutadiene (AzTPB), was obtained by reacting ITPB with 2-(2-azido ethoxy) ethanol. For this, 2-(2-azido ethoxy) ethanol was synthesized as per a reported procedure.<sup>37</sup> About 50 g (0.4 mol) of chloro ethoxy ethanol and 40 g (0.6 mol) of sodium azide was accurately weighed and

---

transferred into a flask containing 900 ml DMF. The above mixture was mechanically stirred at 100°C for 15 hrs and 2-(2-azido ethoxy) ethanol was recovered from DMF by distillation under vacuum.

For the synthesis of AzTPB, about 6g (0.046 mol) of 2-(2-azido ethoxy) ethanol was dissolved in 20 ml toluene and was added drop by drop to the previously prepared ITPB (10g, 0.004 mol). The reaction was carried out at 60°C for 5 hrs in the presence of DBTDL as the catalyst. The mixture was dissolved in THF and the product was isolated by precipitating in excess methanol, washing with methanol and drying under reduced pressure at 60°C for 3hrs. Yield: ~84%.

#### **4.2.4. Curing Procedure**

The PrTPB and AzTPB were cured at an alkyne:azide molar ratio of 1: 0.75, 1:0.85 and 1:1. The mixtures were then cast in aluminium moulds and the curing reaction was carried out at 60°C for a period of 5 days. For comparison, HTPB-TDI urethanes (stoichiometric ratio of 1:0.75, 1:0.85 and 1:1 (with respect to isocyanate and hydroxyl, NCO: OH) were also prepared and evaluated.

#### **4.2.5. Swelling Studies**

To investigate the cross-linking density of the cured samples, triazoles based on PrTPB-AzTPB, the cured sample of varying alkyne:azide ratios viz. 0.7, 0.85 and 1.0 were cut into pieces of approximately 5 x 5 x 5 mm and soaked in toluene for 72 hrs. The soaked sample was weighed after 72 hrs after gently wiping off the solvent. The same was repeated for HTPB-TDI urethane samples also.

#### **4.2.6. Determination of crosslink density**

To evaluate the cross-link density, the cured polymer samples were cut into pieces of approximately 5 x 5 x 5 mm sizes and soaked in toluene for 72 hrs. The soaked sample was weighed after 72 hrs after gently wiping off the solvent. From the swell ratio, the crosslink density was calculated using Flory Rehner equation<sup>38</sup>.

#### **4.2.7. Propellant processing**

Propellant batches were processed in a 1 kg scale in a Guitard horizontal mixing system at 40°C and average mixing time of three hours. The typical solid propellant formulation consisting of PrTPB-AzTPB as binder in THF solvent,

---

aluminium as metallic fuel (2% by weight) and ammonium perchlorate as oxidiser (77% by weight) was chosen. For comparison propellant based on, HTPB with TDI as curing agent was also processed in the same manner. End of mixing (EOM) viscosity and build up values were measured using Brookfield Viscometer (Model: HBDVII+). The samples were cured at 60°C for 5 days without adding a catalyst. The cured propellant samples were tested for mechanical properties. The burn rates were measured using acoustic emission technique at an operating pressure of 6.93MPa using cured propellant strands (size: 80x6x6mm). Impact and friction sensitivity tests were also done for the samples.

### 4.3. RESULTS AND DISCUSSION

#### 4.3.1. Characterisation of PrTPB and AzTPB polymers

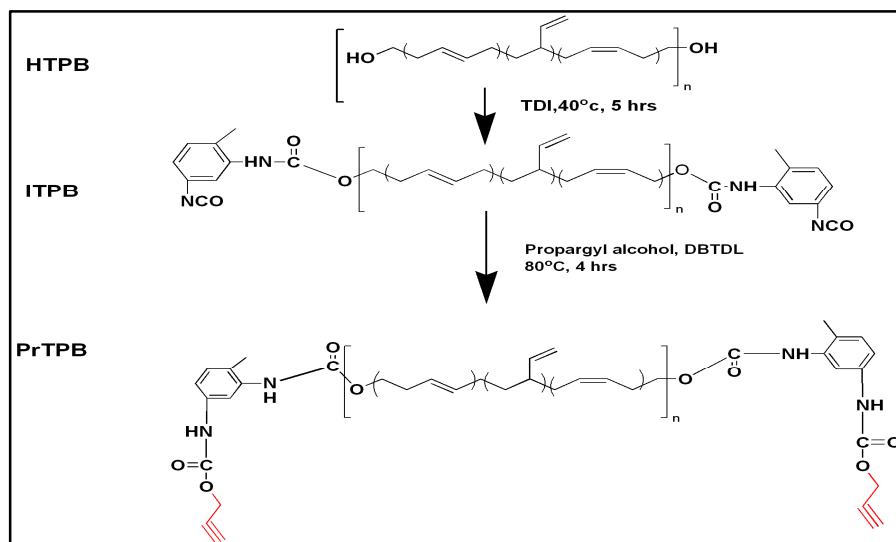
Azide and propargyl end functional polybutadiene were synthesised by the chemical transformation of terminal hydroxyl groups of HTPB. Hydroxyl groups were first reacted with excess TDI for end-capping with isocyanate groups. Subsequently the terminal groups were reacted with propargyl alcohol or 2-(2-azido ethoxy) ethanol as per Scheme 4.1&4.2. The isocyanate content of intermediate polymer (ITPB) was determined to be 2.7 % which matched with the theoretical value required for the complete reaction of hydroxyl groups to form isocyanate terminated polymer (ITPB). For the synthesis of PrTPB, ITPB was reacted with excess propargyl alcohol. The propargyl end capping took place completely. Though an isocyanate:hydroxyl ratio of 2:1 was used for the first step, chain extension by coupling of isocyanate terminated polybutadiene with hydroxyl terminated polybutadiene occurred to some extent. This caused an increase in molecular weight of the endcapped polymer. AzTPB was synthesised by reaction of ITPB with 2-(2-azido ethoxy) ethanol. Both the polymers were characterised.

FTIR analysis (Fig. 4.1a, b and c) of PrTB showed complete conversion of NCO group (disappearance of NCO absorption at 2270 $\text{cm}^{-1}$ , Fig 4.2 1c). The sharp peak centred at 3305  $\text{cm}^{-1}$  corresponds to the C-H (stretching) of propargyl group (-C≡C-C-H) and N-H (stretching) of urethane group. In AzTPB, the peak at 2108  $\text{cm}^{-1}$  indicates the presence of azide groups in addition to the -C=O peaks of urethane, at 1740  $\text{cm}^{-1}$ . The characteristic peaks of polybutadiene<sup>39</sup> (966  $\text{cm}^{-1}$  for 1, 4 trans, 911  $\text{cm}^{-1}$  for 1, 2-vinyl and 724  $\text{cm}^{-1}$  for 1, 4-cis) remained unchanged in both the polymers.

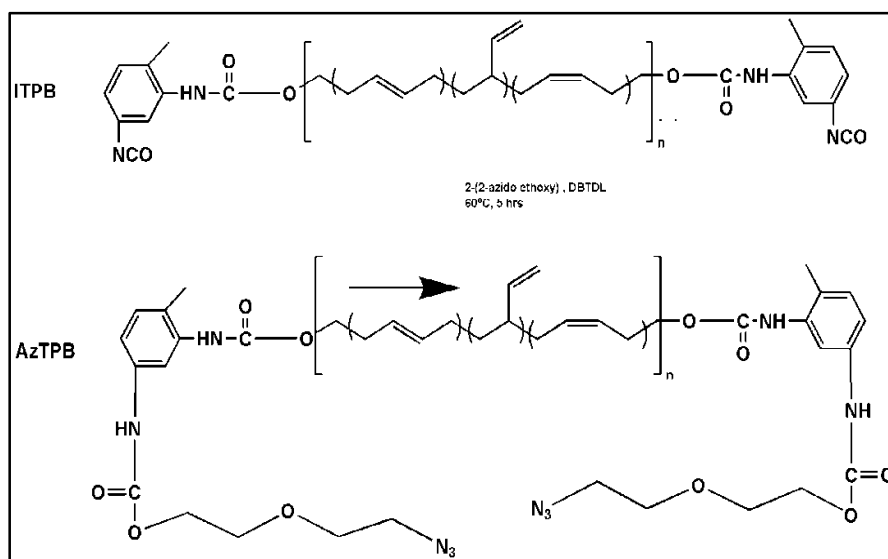
---

$^1\text{H}$  NMR of PrTPB (Fig.4.2 a) showed all the chemical shifts characteristic of HTPB<sup>40</sup>. The signal at 1.8 ppm is due to  $-\text{CH}_2-$ , at 2.5ppm due to  $-\text{C}\equiv\text{C}-\text{H}$  and the one at 4.8 ppm due to  $\text{O}-\text{CH}_2-$  bonded to the propargyl group. Protons on the aromatic ring appeared at 7.1 ppm and  $-\text{CH}_3$  groups in aromatic ring at 1.6 ppm.

$^1\text{H}$  NMR of AzTPB (Fig.4.2.b) showed signals corresponding to HTPB. In addition to the chemical shifts at 1.8 ppm due to  $-\text{CH}_2-$ , two singlets at 2.8-2.9 ppm due to  $-\text{CH}_2$  bonded to azide and the one at 4.8 ppm due to  $\text{O}-\text{CH}_2-\text{C}-$  confirmed its structure. The protons in the tolyl group appeared similar to PrTPB. The spectra conformed to the expected structures.



*Scheme 4.1. Synthesis Scheme for PrTPB*



*Scheme. 4.2. Synthesis Scheme for AzTPB*

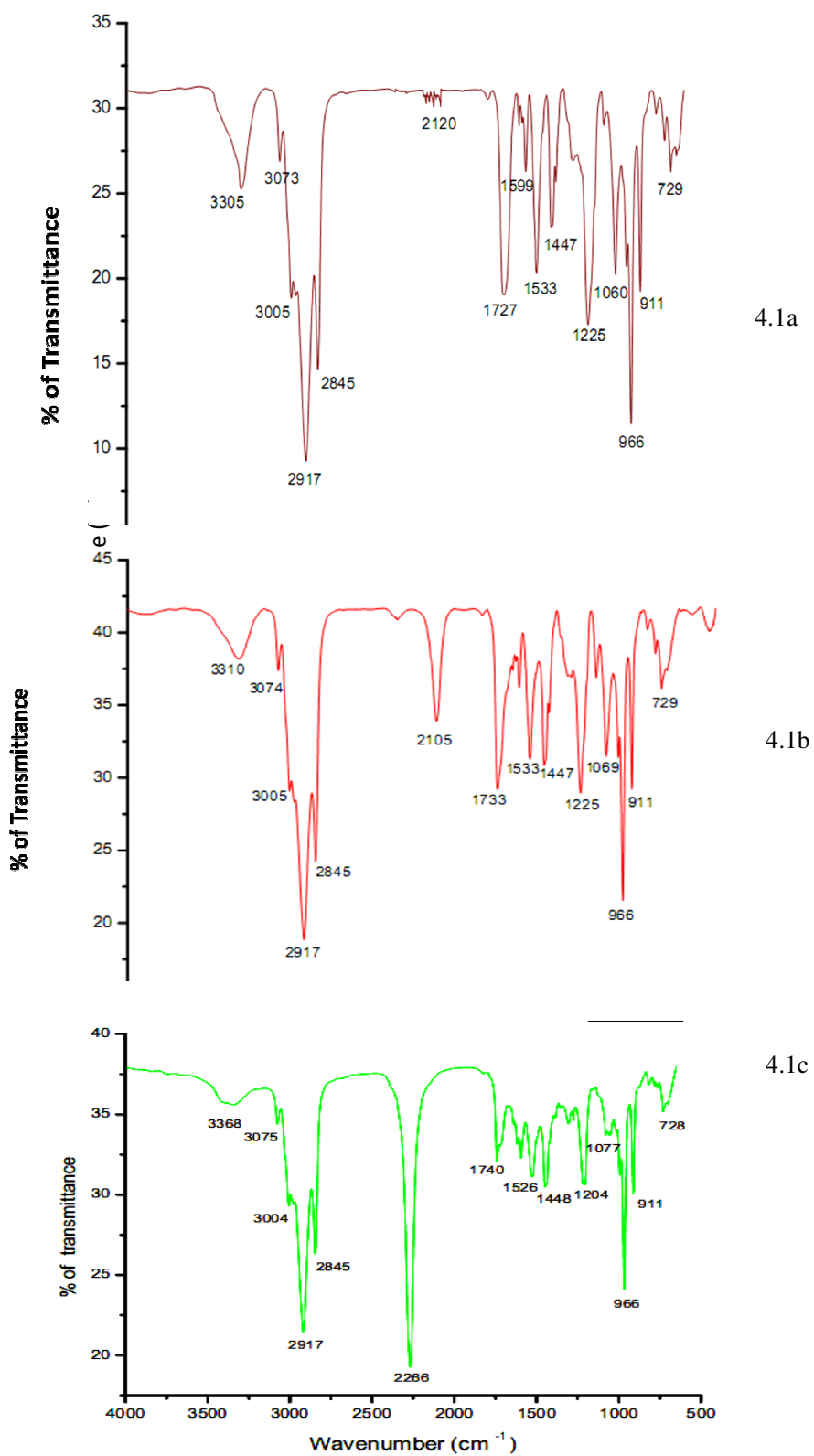


Fig .4.1. FTIR spectra of a) PrTPB b) AzTPB and c) ITPB

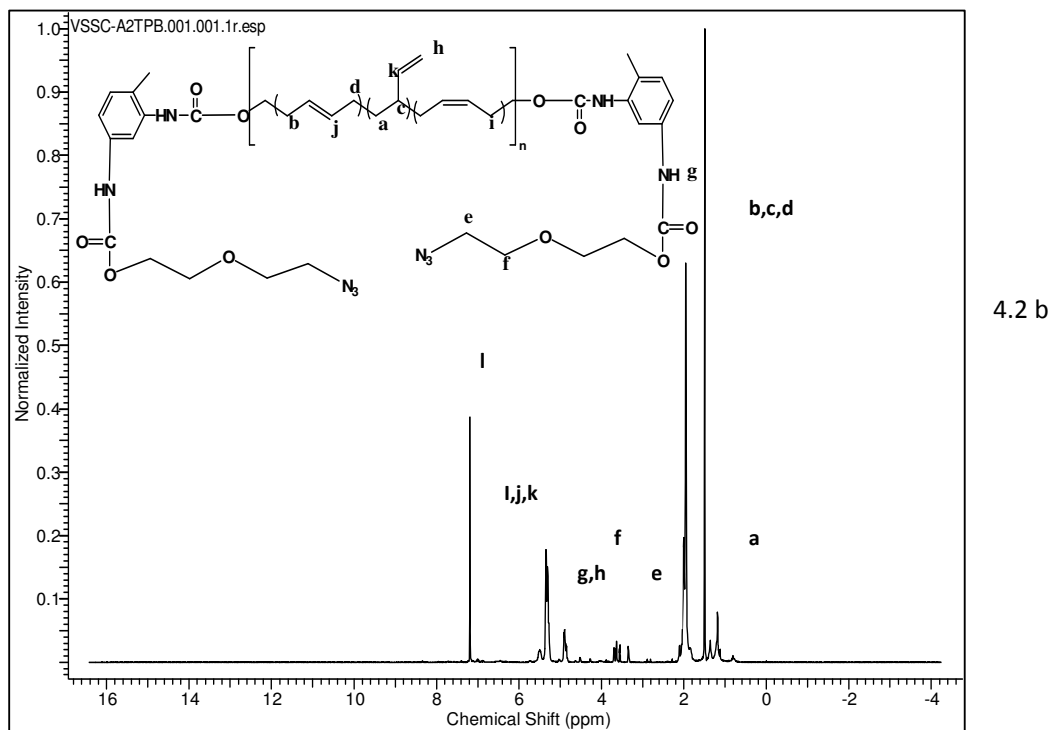
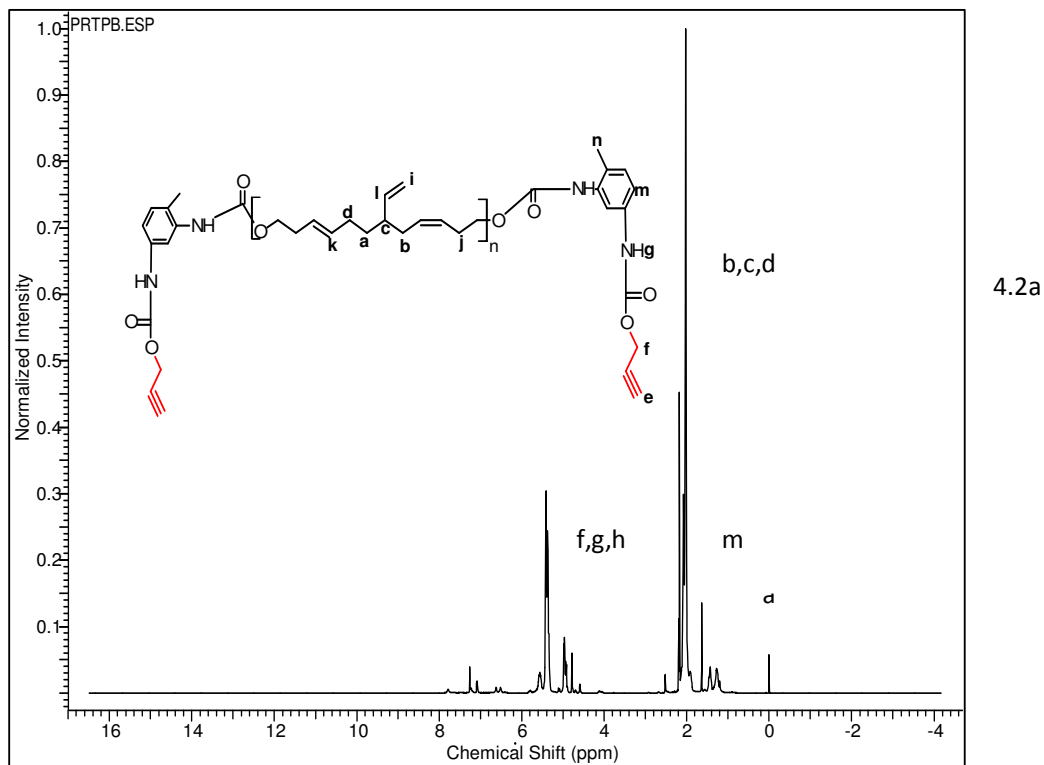
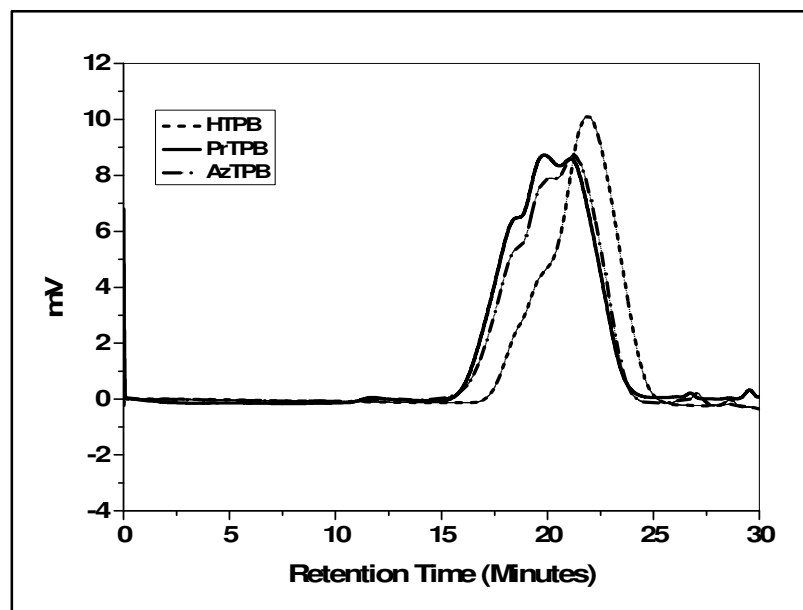


Fig.4.2. <sup>1</sup>H NMR spectrum of a) PrTPB b) AzTPB (in CDCl<sub>3</sub>)





*Fig. 4.3. GPC chromatograms of a) PrTPB and b) AzTPB c) HTPB*

GPC traces of the HTPB, PrTPB and AzTPB are given in Fig.4.3. The calculated number average molecular weight ( $M_n$ ) corrected for hydrodynamic volume (using universal calibration) are 3450, 6330 and 7460. While, weight average molecular weight  $M_w$  is 8530, 20060 and 24720, and the polydispersity indices (PDI) are 2.5, 3.2 and 3.3 respectively for HTPB, PrTPB and AzTPB. The increase in molecular weight for PrTPB and AzTPB in comparison to HTPB is due to partial chain extension during TDI coupling

### 4.3.2 Cure Optimisation

#### 4.3.2.1 DSC analysis

PrTPB reacts with AzTPB to yield triazoles (Scheme 4.3). Since HTPB is known to contain polyhydroxyl functional groups,<sup>40-41</sup> its derivatives are also expected to contain polyfunctional groups (propargyl and azide), accounting for cross linking. The cure reaction was monitored by non-isothermal DSC analysis at heating rates of 5, 7 and 10 °C/min. DSC shows that the cure reactions of PrTPB with AzTPB occur in the temperature range of 70-165 °C with an enthalpy change of 75 ± 2 J/g. This is followed by decomposition of the residual azide in the temperature range of 167-215 °C with an apparent enthalpy change of ~6 J/g (Fig.4.4a). However, AzTPB can undergo a self curing reaction through the addition

of azide groups on to the double bond of polybutadiene yielding 1, 2, 3-triazoline. The reaction of azide group with olefinic unsaturation is known.<sup>42</sup> This reaction is confirmed by the DSC analysis (Fig.4.4b) of AzTPB, where an exotherm corresponding to the azide-ethylenic unsaturation reaction was observed in the temperature regime of 88 to 153°C with an enthalpy change of ~23 J/g. DSC also shows decomposition of azide in the temperature range of 153-215°C with an enthalpy change of ~91 J/g. This was further confirmed by the FTIR analysis of cured AzTPB which indicated the disappearance of peaks due to azide groups at 2108 cm<sup>-1</sup> and change in the appearance of peak in the range 1599-1639 cm<sup>-1</sup>.<sup>43</sup> In order to avoid the addition of azide to the unsaturation, AzTPB was stored in refrigerated condition (~5°C).

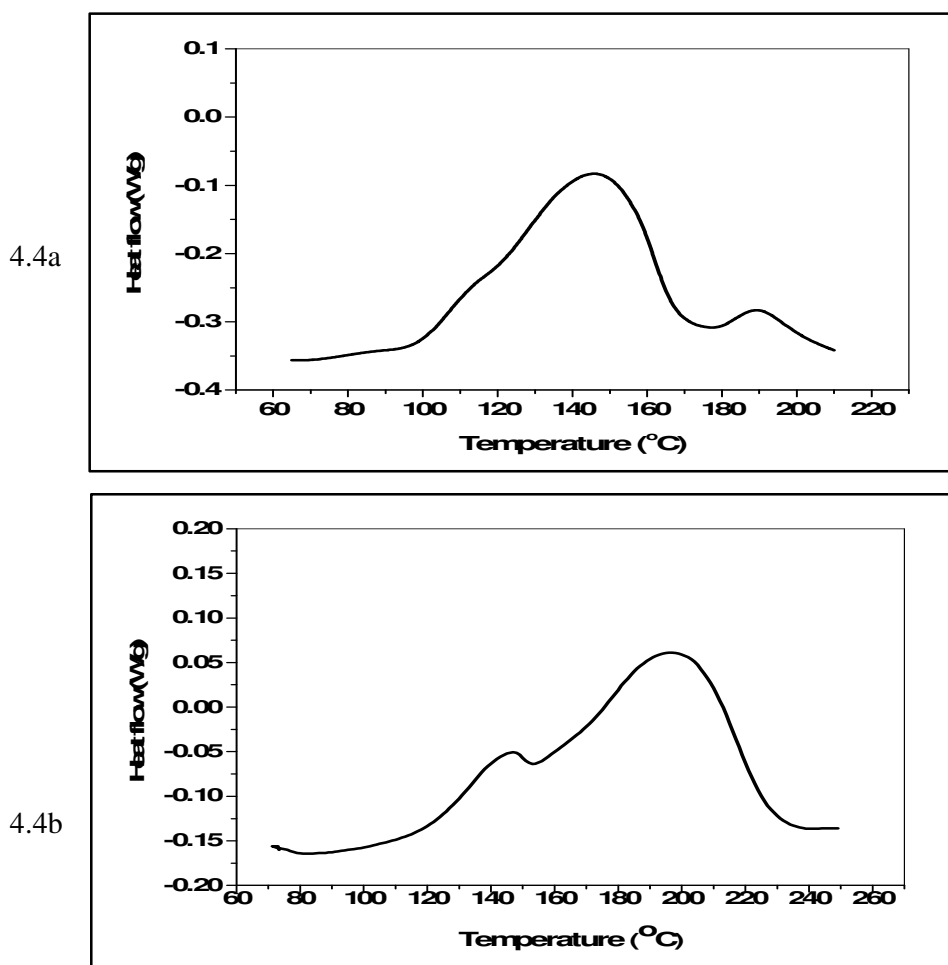
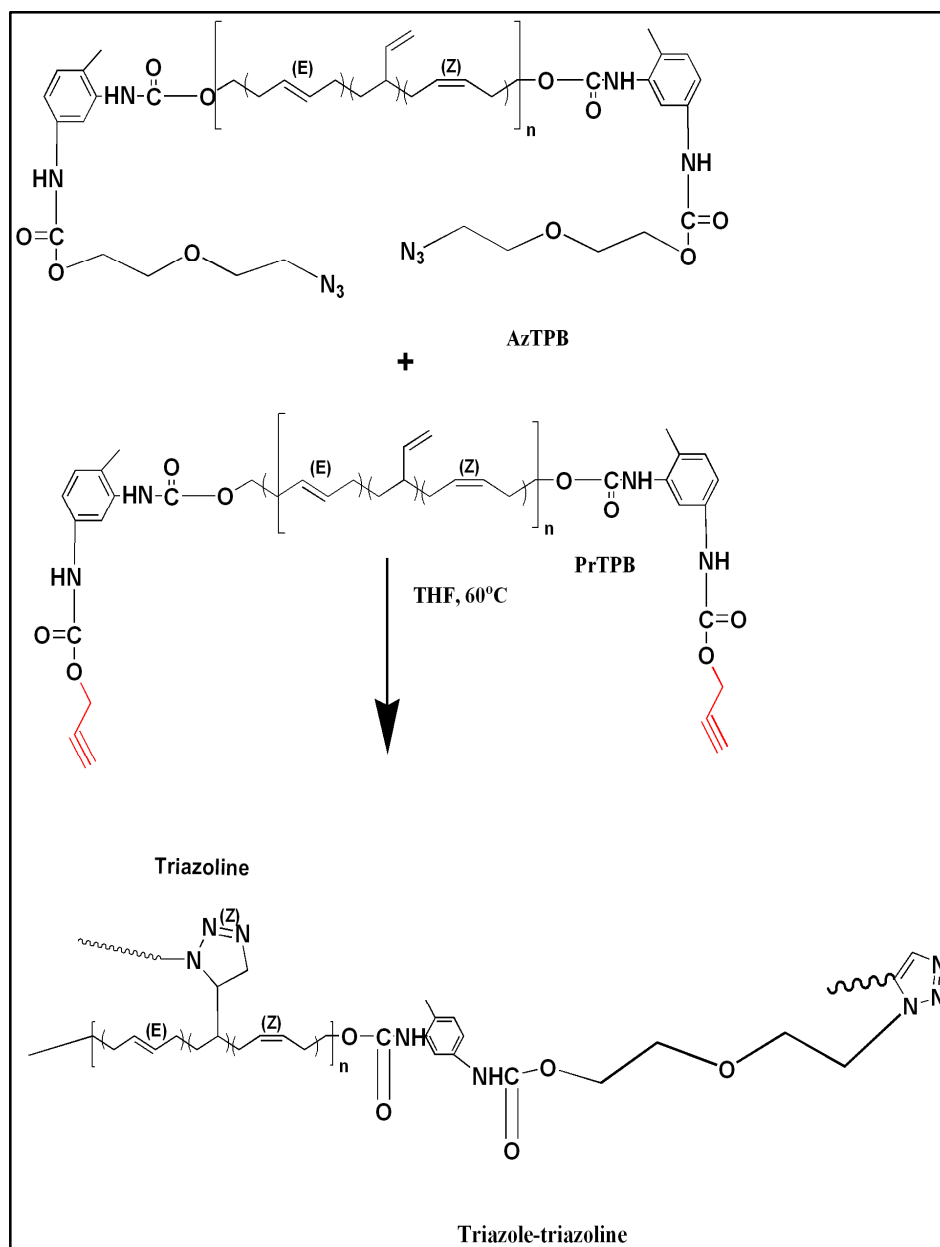


*Fig. 4.4. a) DSC Traces of Curing of PrTPB with AzTPB b) DSC Traces of Self Curing of AzTPB (Heating rate 5°C/min)*



**Scheme 4.3** Curing of mixture of PrTPB with AzTPB

The propensity of the azide groups for addition to double bond is lower when compared to that for ethynyl groups<sup>42</sup>. However, the relative concentration of double bonds in PrTPB is almost 100 times of triple bonds. Hence, there is good probability for addition of azide to the olefinic unsaturation of polybutadiene resulting in crosslinking. The enthalpy calculated from the exotherm in DSC for the AzTPB-PrTPB blend corresponds to the overall enthalpy of formation of triazoline and triazole groups. Since, the system is uncatalysed, the decomposition of the azide

groups initiates before the completion of the cure reaction. As a result the exotherm comprising of unreacted azide group appear with a peak reaction temperature ( $T_m$ ) at 190 °C.

### 4.3.3 Cure kinetics

The cure kinetics was followed by the non-isothermal DSC method based on varying heating rates of 5, 7 and 10 °C/min. The peak reaction temperatures ( $T_m$ ) obtained are 135, 141 and 145 °C for heating rates of 5, 7 and 10 °C respectively and the phenomenological details of the curing at different heating rates is given in Table 4.1.

*Table 4.1. Phenomenological Details of Curing*

Heating rate (°C/min)	Initial temperature, $T_i$ (°C)	Peak temperature, $T_m$ (°C)	Final temperature, $T_f$ (°C)
5	98	135	156
7	103	141	169
10	105	145	170

The kinetics of cure reaction was evaluated by the variable heating rate method of Kissinger<sup>44</sup> based on heating rate as a function of the temperature maxima ( $T_m$ ) in DSC. E is obtained from the slope of the plot of  $\log(\phi/T_m^2)$  against  $1/T_m$  (Fig.4.5). The pre-exponential factor (A) was calculated using the relation given in equation. 1 .

$$A = \phi E e^{E/RT_m} / RT_m^2 \text{ ----- 1}$$

$T_m$  is the average of the  $T_{max}$ . The activation energy (E) computed by Kissinger method is 107.6 kJ/mol. The pre-exponential factor (A) is  $2.79 \times 10^{12} \text{ s}^{-1}$  and rate constant at a temperature of 60 °C is  $3.64 \times 10^{-5} \text{ s}^{-1}$ .

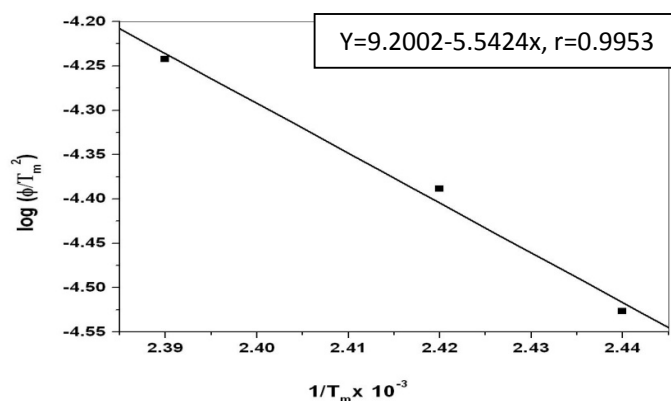


**Fig. 4.5.** Kissinger plot for determination of activation energy ( $E$ ) for PrTPB-AzTPB System

From the  $E$ ,  $A$  and  $k$  values, the isothermal cure profile for the system could be predicted for any given temperature using equation 2, relating time ( $t$ ), temperature ( $T$ ) and fractional conversion ( $\alpha$ ) for a second order reaction. A time-conversion profile is predicted for  $60^\circ\text{C}$  as shown in Fig.4.6. As per this, a conversion of 95% is achieved in 70 hrs. However, for practical purposes, cure duration of 5 days at  $60^\circ\text{C}$  was employed. This was confirmed by FTIR, from the complete disappearance of azide peak at  $2108\text{ cm}^{-1}$  and appearance of a peak at  $1637\text{ cm}^{-1}$ , due to  $\text{C}=\text{C}$  double bond of triazole, which is absent in the pre-polymers viz. PrTPB and AzTPB (Fig.4.7).

$$\alpha = 1 - \{1 - A(1-n) t e^{-E/RT}\}^{1/1-n} \quad \text{--- 2}$$

$n$ =order reaction,  $E$ =activation energy,  $R$ =universal gas constant,  $T$ =temperature in absolute scale.

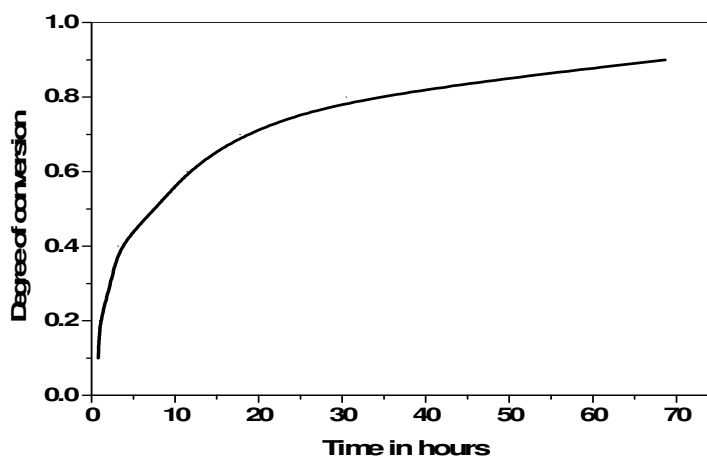


**Fig. 4.6.** Prediction of Isothermal Cure Profile (at  $60^\circ\text{C}$ ) for PrTPB-AzTPB

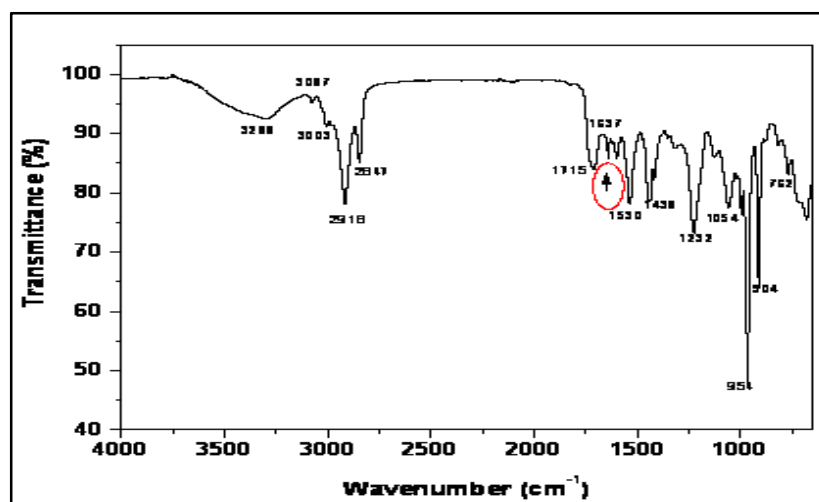
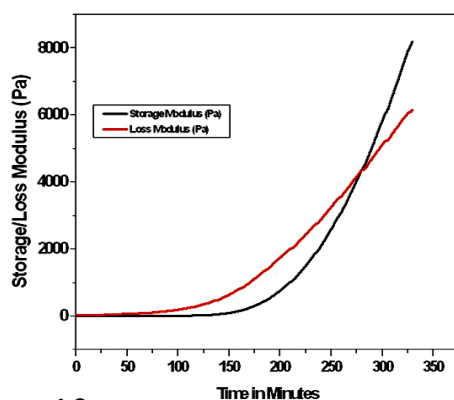
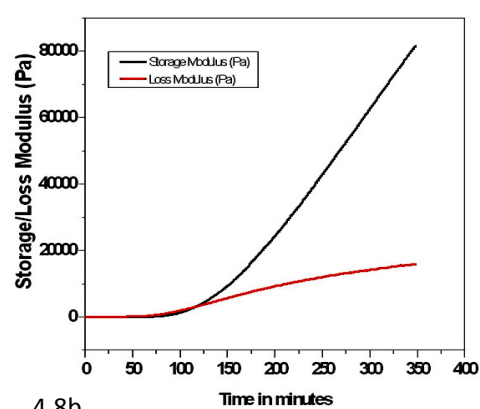


Fig 4.7. FTIR Spectrum of Cured PrTPB-AzTPB

The rheological behaviour of the curing reaction of PrTPB with AzTPB was investigated at 80°C and the results were compared with HTPB-TDI system at the same temperature. The isothermal evolution of storage modulus ( $G'$ ) and loss modulus ( $G''$ ) with reaction time for the curing reaction is given in Fig 4.8. Both the moduli (storage and loss) increase as a result of the increase in crosslinking, as observed in the rheogram. The cross over point of loss modulus with storage modulus is considered as the gel point. The gel point for PrTPB-AzTPB system occurs after 280 minutes and for HTPB-TDI system (Figs. 4.8a and 4.8b), it occurs after 120 minutes indicating a faster rate of curing for the urethane reaction. Thus, reaction invoking hydroxyl-isocyanate has shorter 'pot-life'.



4.8a



4.8b

Fig 4.8. Rheogram of a. PrTPB-AzTPB, b. HTPB-TDI at 80°C (uncatalysed)

#### 4.3.4. Determination of crosslink density

The crosslink density of the cured sample was calculated using Flory Rehner equation<sup>38</sup>. The soaked sample was weighed after 72 hrs after gently wiping off the solvent ( $w_s$ ). The swollen sample was dried in vacuum oven at 100 °C for 5 hrs and the weight was noted ( $w_{ds}$ ). The swell ratio (Q) of the sample was calculated using the equation 3.

$$Q = \frac{w_s}{w_{ds}} - 1 \quad \text{----- 3}$$

The swell ratio is used to find the weight fraction of the polymer ( $w_2$ ) and weight fraction of the solvent ( $w_1$ ). Q is related to  $w_2$  and  $w_1$  by the following equations 4 and 5.

$$W_2 = \frac{1}{(1+Q)} \quad \text{----- 4}$$

$$W_1 = (1 - W_2) \quad \text{-----5}$$

Flory- Rehner relation is used to calculate the cross-link density ( $X_{\text{density}}$ ) of the polymer (equation 6)

$$X_{\text{density}} = -[\ln(1-V_2) + V_2 + \chi V_2^2] \div V_s (V_2^{1/3} - V_2/2) \quad \text{----- 6}$$

Where  $V_2$  is the volume fraction of the polymer in swollen specimen;  $V_s$  is the molar volume of the solvent and  $\chi$  is the polymer-solvent interaction parameter.  $V_2$  is computed from the equation 7

$$V_2 = [w_2/\rho_2] \div [(w_2/\rho_2) + (w_1/\rho_1)] \quad \text{----- 7}$$

In the above equation,  $\rho_1$  and  $\rho_2$  are the densities of solvent and polymer weight fraction of the polymer ( $w_2$ ) and weight fraction of the solvent ( $w_1$ ) respectively. A value of 0.43 is taken<sup>45</sup> for  $\chi$  (for HTPB-toluene interaction). It was presumed that  $X_{\text{density}}$  is unaffected by the small concentration of triazole or triazoline groups. In fact the spacing between functional groups in case of AzTB and PrTPB are more than those of HTPB due to chain extension during chemical transformation and the crosslink density was expected to be less than that of HTPB-TDI urethane system. In literature<sup>46</sup> the crosslink densities of HTPB-IPDI based urethanes have been reported and the values are in the range  $0.5\text{-}0.55 \times 10^{-4}$  mol/cm<sup>3</sup> for isocyanate to hydroxyl ratio of 1:1 which matches with the values that we have obtained ( $0.62 \times 10^{-4}$

mol/cm<sup>3</sup>). The values are marginally higher due to the aromatic nature of curing agent that we have used. However, a higher crosslink density of the triazole polybutadiene than the analogous urethane network confirms that additional crosslinking take place through reaction of the azide group with the unsaturation on the backbone of polybutadiene (Table 4.2).

**Table. 4.2.** Crosslink density of cured HTPB-TDI and PrTPB-AzTPB systems

Equivalence Ratio (alkyne/azide)/(NCO/OH)	Crosslink density (mol/cm <sup>3</sup> ) (Cured PrTPB-AzTPB )	Crosslink density (mol/cm <sup>3</sup> ) (cured HTPB-TDI)
1:0.7	1.20 x 10 <sup>-8</sup>	0.65 x 10 <sup>-8</sup>
1:0.85	3.43 x 10 <sup>-6</sup>	0.27 x 10 <sup>-6</sup>
1:1	2.86 x 10 <sup>-4</sup>	0.62 x 10 <sup>-4</sup>

#### 4.3.5. Mechanical properties

The mechanical properties viz. tensile strength, elongation at break and stress at 100% for the cured polymers were compared with those for HTPB based polyurethanes. The tensile strength of the triazole-triazoline system increased from 0.99 to 1.52 MPa, while the elongation at break increased from 480 to 660 % and the stress at 100% elongation varied from 0.31 to 0.50 MPa as the alkyne to azide stoichiometry evolved from 1: 0.7 to 1: 1. The properties of PrTPB-AzTPB systems are superior to those of HTPB-TDI (Table 4.3). At comparable stoichiometry, the triazole-triazoline crosslinked system provided better tensile strength and elongation (at comparable modulus) vis- a- vis the polyurethanes. In literature<sup>46-47</sup> different crosslinkers are added to improve the tensile strength of HTPB-isocyanate urethanes. However, our studies reveal that the properties can be improved by functional modification of HTPB and further co-curing by 1,3-dipolar addition without any additional crosslinkers.



**Table 4.3.** Mechanical Properties of Cured HTPB-TDI and PrTPB-AzTPB

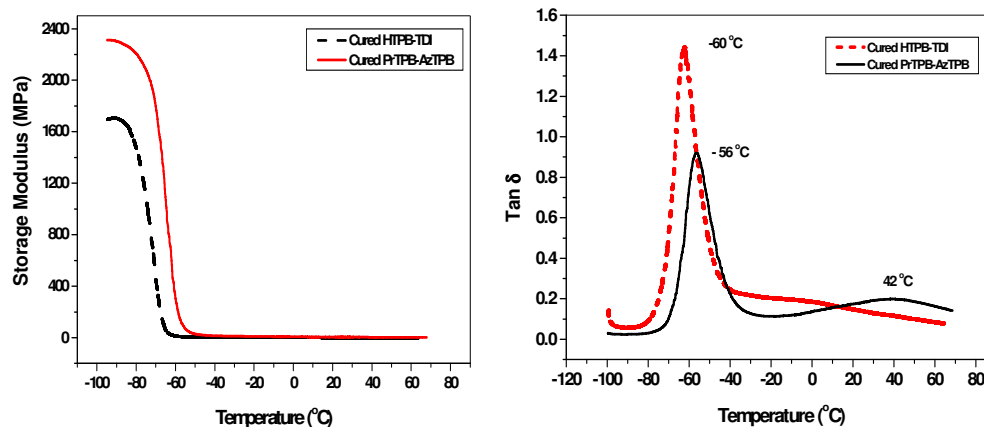
Equivalence Ratio (-C≡CH/-N <sub>3</sub> ) or (NCO/OH)	Mechanical Properties (Cured HTPB-TDI)			Mechanical Properties (Cured PrTPB-AzTPB)		
	TS (MPa)	Elong. (%)	Stress (100% elong.) (MPa)	TS (MPa)	Elong. (%)	Stress at (100% elong.) (MPa)
1:0.7	0.45	920	0.12	0.99	480	0.31
1:0.85	0.64	460	0.28	1.29	520	0.42
1:1	0.86	240	0.52	1.52	660	0.50

(TS=tensile strength, Elong.=elongation at break )

The fracture energy<sup>48</sup> of the cured polymers, PrTPB-AzTPB (alkyne: azide=1:1) and HTPB-TDI (NCO:OH 1:1) was computed from the stress - strain graph. The fracture energy for PrTPB-AzTPB system is 3.33 J/cm<sup>2</sup> which is marginally higher than that for HTPB-TDI system (3.03 J/cm<sup>2</sup>).

#### 4.3.6. Dynamic mechanical characterisation

DMA of triazoles for an alkyne to azide equivalence of 1:1 shows a biphasic transition with two glass transitions ( $T_g$ ) occurring at -56°C which corresponds to butadiene-polyurethane backbone and the second one at 42°C probably due to the triazoline-triazole network (Fig.4.9a).

**Fig. 4.9a** Tan  $\delta$  vs. temperature of cured HTPB-TDI and PrTPB-AzTPB**Fig. 4.9b.** Storage modulus of cured HTPB-TDI and PrTPB-AzTPB

DMA studies reveal that storage modulus of triazole-triazoline network is higher than that of cured HTPB-TDI urethanes as expected (Fig.4.9b) due to the higher crosslink density of the polymer networks. The biphasic behaviour observed in DMA analysis is corroborated by morphological changes in the scanning probe microscopy (SPM) analysis of the cured PrTPB-AzTPB samples. When the samples are heated in the temperature range of 40-50°C, morphological change occurs which is an evidence for segmented motion in the sample. (Fig.4.10).

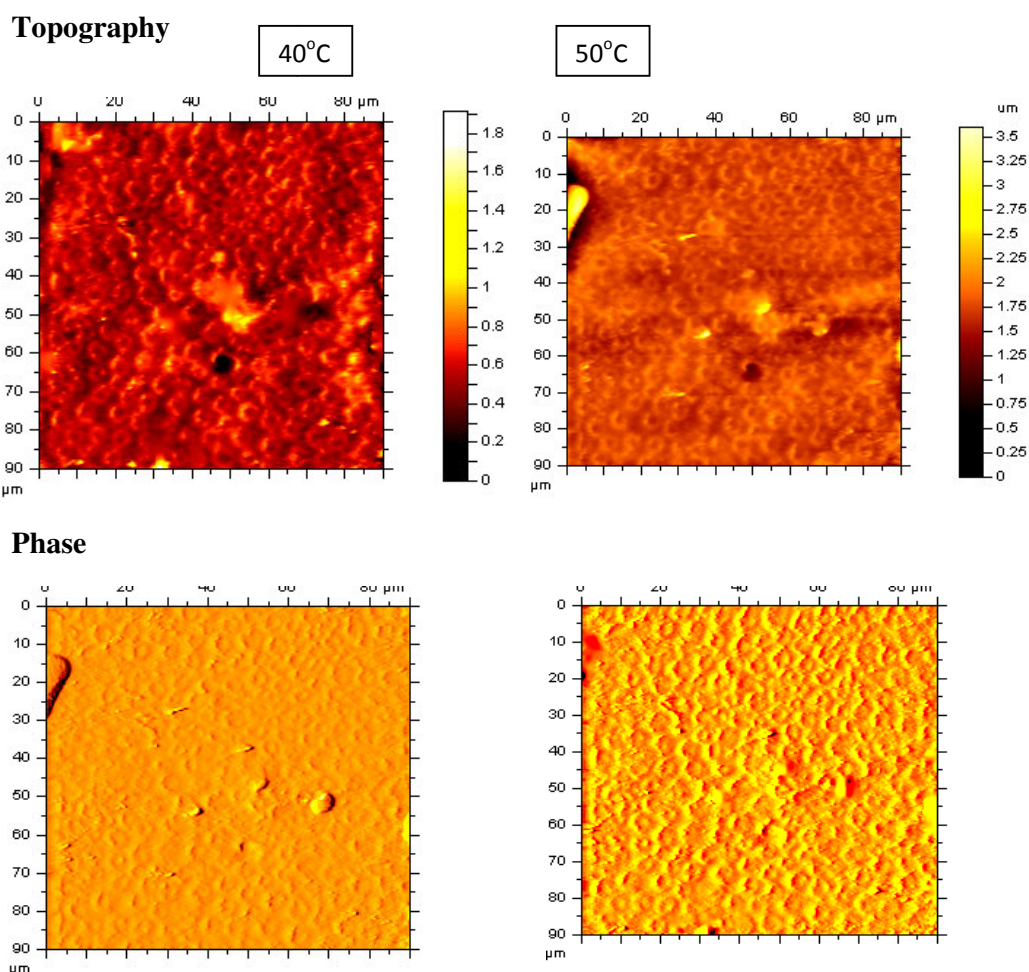


*Fig.4.10. SPM Images of Morphological changes during heating of cured network from 40 to 50°C*

#### 4.3.7. Thermal decomposition studies

The thermal decomposition characteristics of cured PrTPB-AzTPB were studied using thermo gravimetric analysis (TGA) and the results were compared with

---

polyurethane based on HTPB-TDI. TGA was done at a heating rate of 5°C/min in nitrogen atmosphere. The cured polymer undergoes a two-stage decomposition (Fig.4.11a). The first stage decomposition occurs in the temperature range of 215-315°C with a weight loss of ~10%. To understand the mechanism of decomposition, pyrolysis GC-MS was done at 300°C (Fig 4.11b). The studies revealed that the major products of decomposition are N<sub>2</sub>, CO<sub>2</sub> (retention time, RT 1.37), 3-isocyanato-4-methylbenzenamine (retention time, RT 13.62), TDI (retention time, RT 12.82), propargyl alcohol (RT 1.87) and 2-(vinyl oxy)ethanimine RT 8.56). The products indicate that both polyurethane and triazole –triazoline groups are cleaved during the process and this was further confirmed by TG-MS studies. The proposed mechanism is given in Scheme 4.4a. It is evident that the polyurethane cleavage occurs through two different routes as reported in literature<sup>49-51</sup>. In the first pathway (Scheme 4.4b) the reversal of polyurethane formation occurs, i.e. alcohol and diisocyanate are regenerated. The second pathway is through an internal elimination mechanism wherein an amine and alkene are formed with liberation of carbon dioxide (Scheme 4.5c). Lattimer *et al.*<sup>52</sup> have also reported that in the different decomposition pathways for urethane, the first one is mainly due to dissociation to isocyanate and alcohol and the second one being dissociation to amine, olefin, and carbon dioxide. The latter reaction was reported to be favourable at higher decomposition temperatures of 300°C. In the present case, during cleavage of urethane, triazole –triazoline groups also decompose resulting in elimination of nitrogen, propargyl alcohol and imine (Scheme 4.5c). The second stage decomposes in the temperature range of 315- 500°C with peak temperature at 460°C with an associated weight loss of 84% due to polybutadiene backbone decomposition. The residue left over at 600°C is 6%. HTPB-TDI polyurethane undergoes two- stage decomposition with the first stage decomposition with initial temperature (T<sub>i</sub>) of 260°C, peak decomposition temperature of T<sub>m</sub> of 315°C and final decomposition temperature, (T<sub>f</sub>) of 340°C. The first stage decomposition corresponds to breakage of polyurethane linkages, followed by second stage decomposition by polybutadiene back bone degradation as reported in literature.<sup>53</sup> This way, crosslinked HTPB releases the curing agent and further the polymer fragments appear. However, in the present case due to the difference in nature of crosslinking, the reaction mechanism is more complex.

---

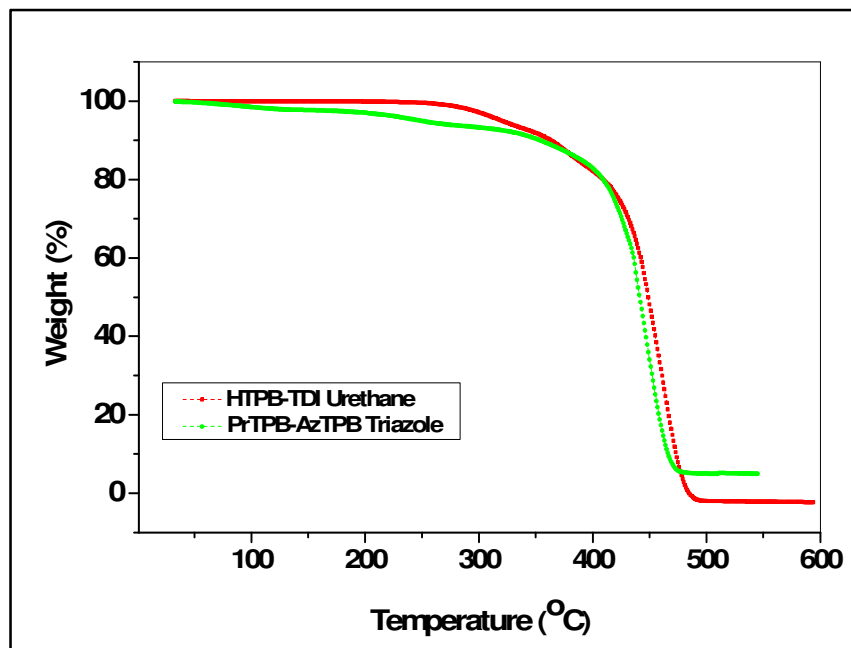


*Fig 4.11a. TGA trace of cured PrTPB-AzTPB and HTPB-TDI urethane (Heating rate 5°C/min)*

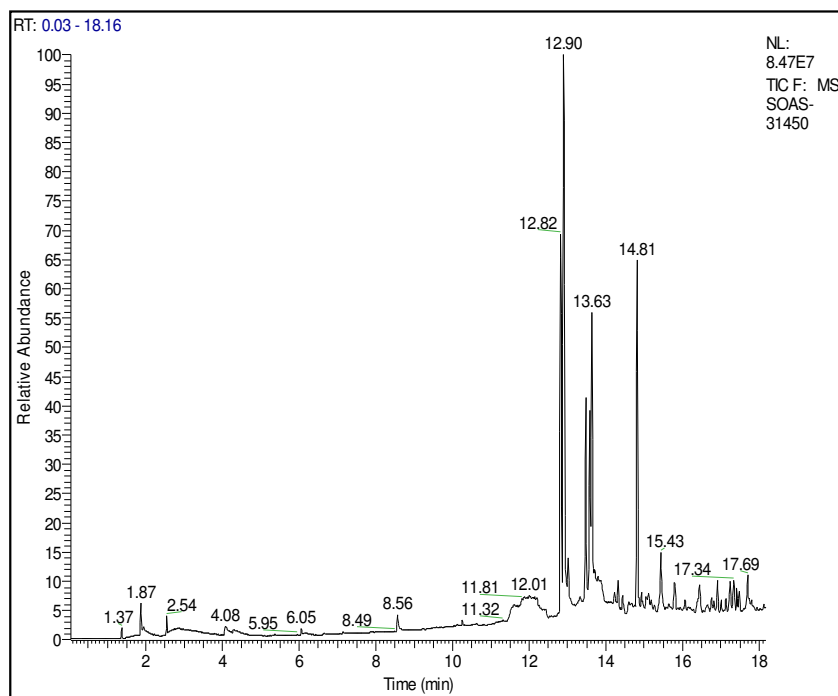
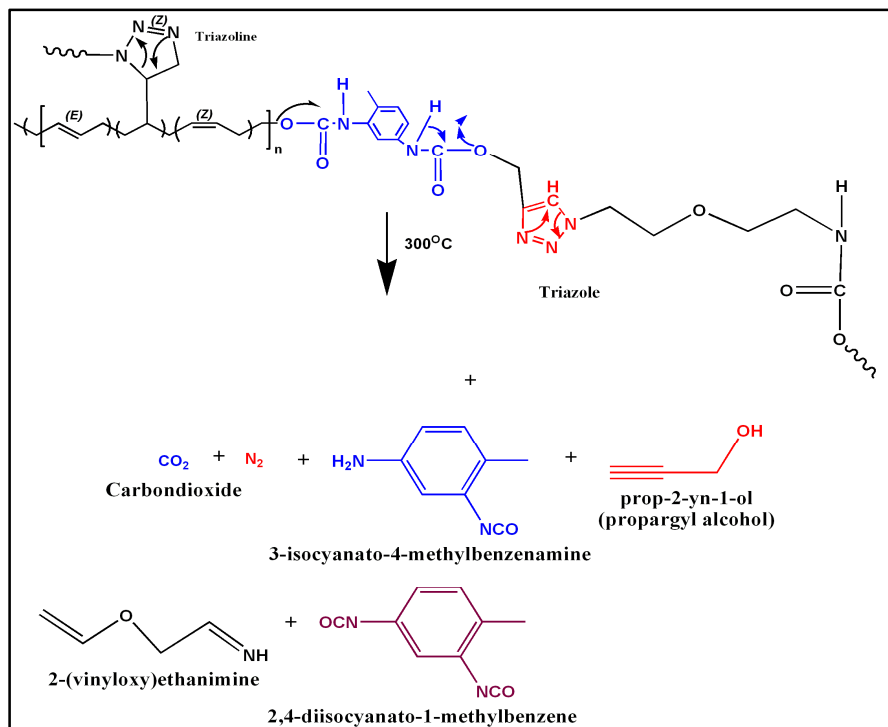
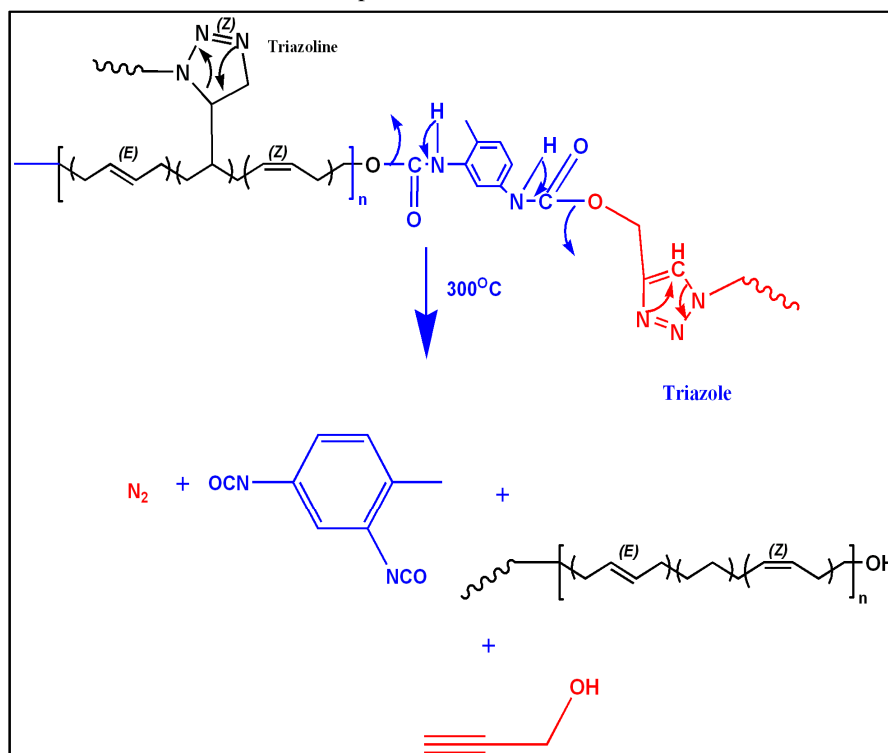


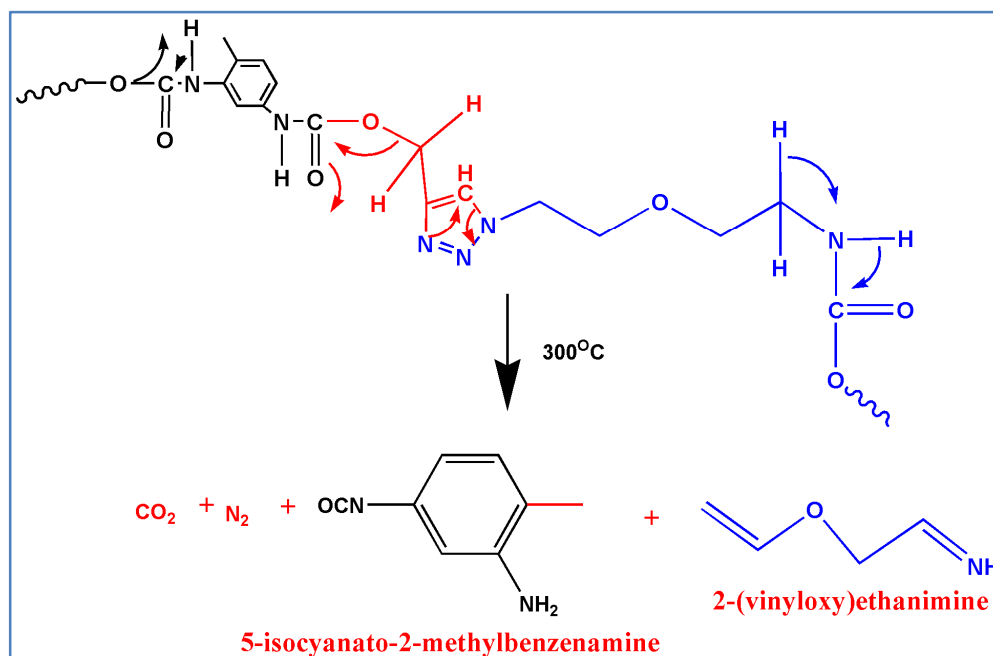
*Fig 4.11b) Pyrogram of cured PrTPB-AzTPB at 300°C*



**Scheme 4.4a.** Mechanism of decomposition of PrTPB-AzTPB cured network and products



**Scheme 4.4b.** Cleavage of urethane in PrTB-AzTPB to yield alcohol and isocyanate along with triazole group breakdown



*Scheme 4.4c: Cleavage of urethane in PrTPB-AzTPB to yield alkene and amine along with triazole group cleavage*

### 4.3.8 Propellant Studies

#### 4.3.8.1. Thermochemical Measurements

The theoretical empirical formula can be calculated from the molecular weight of the polymer (Table 4.4). The combustion is an exothermic reaction and heat of combustion ( $\Delta H_c$ ) corresponds to the energy liberated when the chemical bonds are broken during combustion resulting in products of the initial compound. From the heat of combustion data, the heat of formation of the polymers were computed (Table 4.4) which was used for the theoretical performance evaluation of propellant.

*Table 4.4. Heat of combustion of PrTPB and AzTPB*

Polymer	Heat of combustion (kJ/g)	Empirical formula	Heat of formation (kJ/mol)
PrTPB	41.8	$\text{C}_{5.05}\text{H}_{6.9}\text{N}_{0.2}\text{O}_{0.4}$	+ 251.2
AzTPB	41.9	$\text{C}_{5.15}\text{H}_{7.4}\text{N}_{0.5}\text{O}_{0.5}$	+ 461.3

Theoretical performance evaluation as done using NASA CEA programme for a typical motor operating pressure of 6.93MPa and area ratio of 10 for low aluminised (with 2% aluminium) propellant system. The effect of solid loading (AP content) for a fixed aluminium content of 2% (by weight) was computed for propellants based on PrTPB-AzTPB as binder (Fig.4.12). From the graph, it is observed that the peak specific impulse (Isp) is obtained at ~85-90% solid loading. However, for use as gas generators, lower solid loadings are preferred. Hence, for a typical AP content of 77% (by weight), the performance of PrTPB-AzTPB-AP propellant were computed and compared with HTPB-AP propellant (Table 4.5). The comparison of the theoretical flame temperature and exhaust gases for the propellant indicates a higher flame temperature of 3032 K for the former. The major combustion products are CO, CO<sub>2</sub>, N<sub>2</sub>, H<sub>2</sub>, H<sub>2</sub>O, HCl, Al<sub>2</sub>O<sub>3</sub>. The performance of HTPB-AP propellant and the combustion mechanism of HTPB-AP propellant has been elucidated earlier.<sup>53-54</sup> The mass percentage of gaseous products namely CO and N<sub>2</sub> evolved during decomposition of PrTPB-AzTPB-AP propellant is higher compared to conventional HTPB-urethane propellant of the same composition. Interestingly the present system offers high flame temperature of 3032 K against 2421 K for the conventional one. The HCl emission for the propellant is also reduced. This is advantageous for gas generator or igniter applications.

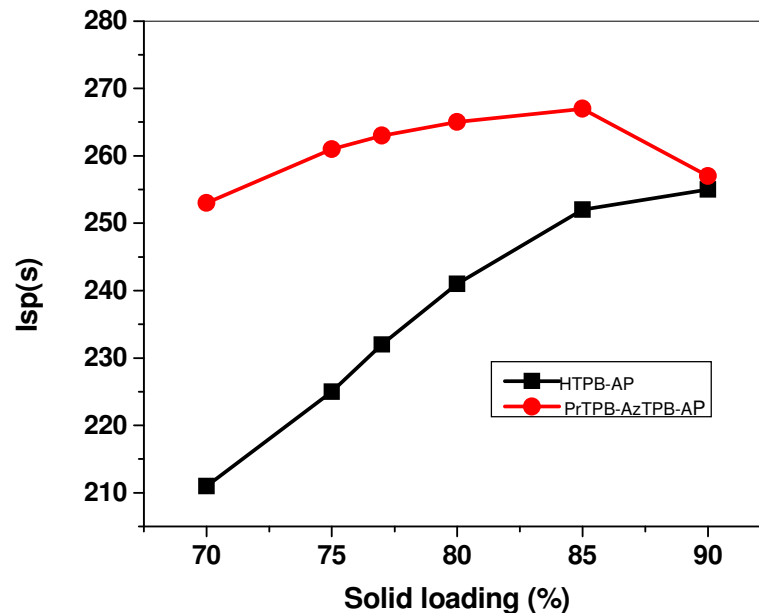


*Fig.4.12 Effect of solid loading on the Isp of PTPB-AzTPB and HTPB propellant (AP as oxidiser, 2% aluminium)*

**Table 4.5. Thermochemical Performance Parameters of PrTPB-AzTPB Propellant (AP: 77% with 2% Aluminium)**

Parameters	HTPB propellant	PrTPB-AzTPB propellant
Isp (s)	224.0	245.0
V.Isp (s)	241.4	261.0
Flame temperature (Chamber) (K)	2421	3032
<b>Combustion products (Mass , %)</b>		
CO	42.5	51.2
CO <sub>2</sub>	0.9	0.01
HCl	15.5	9.6
H <sub>2</sub>	5.1	5.4
H <sub>2</sub> O	1.6	0.08
N <sub>2</sub>	6.3	8.5
Al <sub>2</sub> O <sub>3</sub>	8.2	4.3

#### 4.3.8.2. Propellant processability, mechanical properties and burn rate

The propellant level studies were conducted using PrTPB-AzTPB binder (alkyne:azide molar stoichiometry of 0.85:1) as binder with ammonium perchlorate as oxidiser. For comparison, the properties of propellant processed using HTPB-TDI polyurethanes as binder were also evaluated (isocyanate: hydroxyl molar equivalence of 0.85:1, which is used conventionally).

Propellant based on AzTPB-PrTPB appears to give better mechanical properties than those based polyurethanes (Table 4.6). The tensile strength of the AzTPB-PrTPB propellant is 1.28 MPa in comparison to polyurethane which has 1.1 MPa, the elongation at break is 81 % against 63% for urethanes and Young's' modulus value is 4.41 MPa as against 3.5 MPa for urethane based propellant. The propellant tends to exhibit easy flow characteristics with low end of mix viscosity of 165 Pa.s at 40°C in comparison to urethane based system which has 352 Pa.s. The build up rate of viscosity is also lower compared to urethane based propellant which is advantageous for processing. The burn rate (Table 4.7) of the PrTPB-AzTPB propellant was evaluated for at 6.93 MPa using cured propellant strands and compared with HTPB-



urethane propellant, of the same composition. The burn rate of the two propellants is comparable which indicates that functional modification does not deteriorate the ballistics. The safety characteristics of PrTPB-AzTPB and HTPB-TDI propellant were evaluated and it was found that the impact and friction sensitivity data are marginally better for PrTPB-AzTPB propellant.

**Table. 4.6. Properties of PrTPB-AzTPB Propellant**

<b>Propellant</b>	<b>PrTPB-AzTPB</b>	<b>HTPB-TDI</b>
<u>Viscosity (Pa.s) at 40°C</u>		
End of mix	165	352
After 3 hours	312	864
<u>Mechanical Properties</u>		
Tensile strength (MPa)	1.28	1.10
Elongation (%)	81	63
Modulus (MPa)	4.0	3.51
<u>Safety Properties</u>		
Impact sensitivity (kg.cm)	90.0	82.0
Friction sensitivity (kgf)	28.8	23.4
<u>Burn rate (mm/s) at 6.93MPa</u> (for five samples)	16.29 ±0.03	16.31 ±0.01

#### **4.3.8.3. Thermal Decomposition of the propellant**

The thermal decomposition of PrTPB-AzTPB propellant was studied by TG-DSC at a heating rate of 1°C/min (Fig.4.13). The propellant undergoes two-stage decomposition, similar to HTPB-TDI propellant<sup>55-56</sup>. The first stage decomposition occurs in the temperature range of 225-315 °C with a weight loss of 10%. This is attributed to the cleavage of urethane-triazole-triazoline bonds in the binder along with low temperature decomposition of AP. The second stage occurs in temperature range of 316-350°C, binder-AP second stage decomposition with a weight loss of 75%. The residue obtained at 400°C is 15%. Thermal stability of both the propellant systems is comparable.

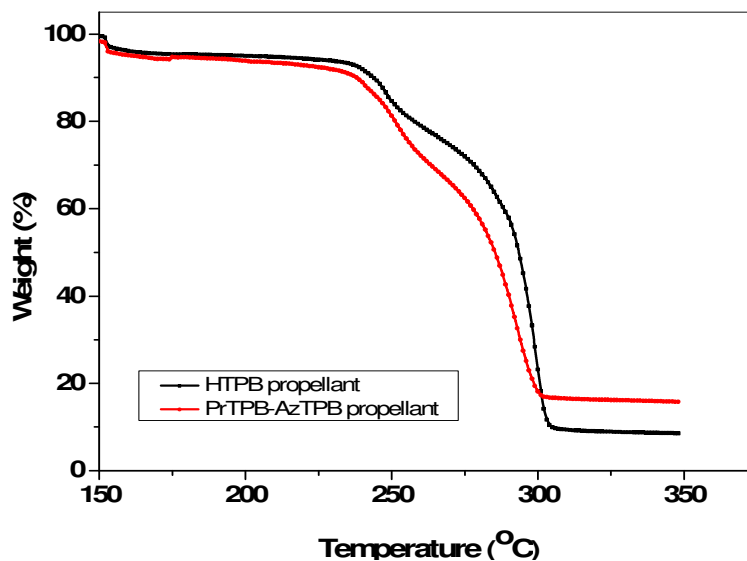


*Fig 4.13. Thermal decomposition of PrTPB-AzTPB propellant (Heating rate 1°C/min, in N<sub>2</sub>)*

#### 4.4. CONCLUSIONS

Azide and alkyne terminated polybutadienes were synthesised from HTPB and crosslinking was effected through 1, 3- dipolar cycloaddition. The curing of the two polymer systems was effected to form triazole-triazoline network and the curing was monitored by DSC. The related kinetic parameters were useful for predicting the cure profile of the system. The mechanical properties of triazoles based on PrTPB and AzTPB were found to be superior to that of urethanes prepared from HTPB-TDI. DMA of the network showed a biphasic transitions and a higher storage modulus for triazole-triazoline networks when compared to HTPB-urethane system. The biphasic characteristics observed in DMA was corroborated by morphological changes using SPM. The thermal decomposition studies indicate that thermal stability for triazole-triazoline crosslinked networks are decided by the polyurethane network in the low temperature regime of 300<sup>0</sup>C and by the polybutadiene backbone in high temperature regime. However, in the propellant level, the crosslink's have only a subtle role in the thermal decomposition pattern. The propellant processed using this binder has the advantages of improved 'pot life' as indicated by the end of mix viscosity which is 165 Pa.s against 352 Pa.s for polyurethane propellant along with a slow build up rate. The mechanical properties of the propellant are superior to polyurethane with an improvement of 14% in tensile strength, 22% enhancement in elongation and 12% in modulus. Thus '1, 3 -dipolar addition' offers a synthetic

means for cross linking the versatile HTPB binder resulting in triazole networks with superior mechanical properties than polyurethanes without affecting the ballistics of the propellant. This is the first ever attempt to crosslink HTPB by '1, 3 -dipolar addition' reaction.

.

---

## 4.5. REFERENCES

1. Davenas, A. *J. Propulsion and Power* **2003**, 19, 1108-1128
2. Caveny, LH; Geisler, RL; Ellis, RA; Moore, TL. *J. Propulsion and Power* **2003**, 19, 1038-1066.
3. DeLuca, LT; Galfetti, L; Maggi, F; Colomb, G; Merotto, L; Boiocchi, M; Paravan, C; Reina, A; Tadini, P; Fanton, L. *Acta Astronautica.*, **2013**, 92, 150-162.
4. Abhay, MK; PD Devendra. *Res J. Chem. Environ*, **2010**, 14, 94-103.
5. Guery, JF; Chang, IS; Shimada, T; Glick, M; Boury, D; Robert E. *Acta Astronautica* **2010**, 66, 201-219.
6. Badgujar, DM; Talawar, MB; Asthana, SN; Mahulikar, PP. *J. Hazardous Materials* **2008**, 151, 289-305.
7. Assink, RA; Lang, DP; Celina, M. *J. Appl. Polym. Sci.*, **2001**, 81, 453-459.
8. Celina, M; Graham, AC; Gillen, KT; Assink, RA; Minier, LM. *Rubber Chem. Techn.*, **2000**, 73, 678-693.
9. Hailu, K; Guthausen, G; Becker, W; König, A; Bendfeld, A; Geissler, E. *Polymer Testing* **2010**, 29, 513-519.
10. Daesilets, S; Villeneuve, S; Laviolette, M; Auger M. *J. Polymer Science, Part A: Polymer Chemistry*, **1997**, 35, 2991-2998.
11. Gopala Krishnan, PS; Ayyaswamy, K; Nayak, SK. *J. Macromolecular Science, Part A: Pure and Applied Chemistry*, **2012**, 50, 128-138.
12. Fabio, LB; Marcio, AA; Bluma, GS. *J. Appl. Polym. Sci*, **2002**, 83, 838-849.
13. Ji, H; Sato, N; William, KN; Mays, JW. *Polymer*, **2002**, 43, 7119-7123.
14. Wang, Y; Hillmyer, MA. *Macromolecules*, **2000**, 33, 7395-7403.
15. Eroglu MS; Hazer B; Guven O. *Polym. Bull.* **1996**, 36, 695-701.
16. Subramanian, K; Sastri, KS. *J. Appl. Polym. Sci*, **2003**, 90, 2813-2823.
17. Cho, BS; Noh, ST. *J. Appl. Polym. Sci*, **2009**, 121, 3560-3568.
18. Saravanakumar, D; Sengottuvelan, N; Narayanan, V; Kandaswamy, M; Varghese TL. *J. Appl. Polym. Sci*, **2011**, 119, 2517-2524.
19. Barcia, FL; Thiago, PA; Bluma, GS. *Polymer*, **2003**, 44, 5811-5819.
21. Murali, MY; Raju, MK. *Designed Monomers and Polymers*, **2005**, 8, 159-175.
22. Shankar, RM; Roy, TK; Jana, T. *J. Appl. Polym. Sci*, **2009**, 114, 732-741.
23. Huisgen, R. *Angew. Chem. Int. Ed.*, **1963**, 2, 633-645.
24. Fireston, R. *J. Org. Chem.*, 1968, 33, 2285-2290.
25. Rostovtsev, VV; Green, LG; Fokin, VV; Sharpless, KB. *Angew. Chem. Int. Ed* **2002**, 41, 2596-2599.
26. Binder, WH; Sachsenhoer, R. *Macromol. Rapid Commun.*, **2007**, 28, 15-54.
27. Binauld, S; Damiron, D; Hamaide, Pascault, JP; Fleury, E; Drockenmuller, E.. *Chem. Commun.*, **2008**, 35, 4138-4140.
28. Döhler D; Michael P; Wolfgang HB. *Macromolecules*, **2012**, 45, 3335-3345.

- 
29. Tsarevsky, NV. Bencherif, SA; Matyjaszewski, K. *Macromolecules*, **2007**, 40, 4439-4445.
  30. Jung, JH; Lim, YG; Lee, KH; Koo, BT. *Tetrahedron Lett* .**2007**, 48, 6442–6448.
  31. Keicher, T; Kuglstatter, W S. Eisele, T. Wetzler, H. Krause. *Propellants Explos. Pyrotech.* **2009**, 34, 210–217.
  32. Min, BS; Park, YC; Yoo, JC. *Propellants Explos. Pyrotech.* **2012**, 37, 59 –68.
  33. Rahm, M *Green Propellants*, PhD Thesis, Royal Institute of Technology, Stockholm, Sweden, **2010**
  34. Ding, Y; Hu, C; Guo, X; Che, Y; Huang, J. *J. Appl. Polym. Sci* **2014**, doi:10.1002/APP 40007.
  35. Nair, PR; Nair, CPR; Francis, DJ. *J. Appl. Polym. Sci*, **1999**, 71, 1731-1738.
  36. *Urethane foam polyol raw materials testing*. In *ASTM D 2849-69*, 1980.
  37. Li, Y; Yang, J; Benicewicz, BC. *J. Polym. Sci.: Part A: Polym. Chem.*, **2007**, 45, 4300-4308.
  38. Flory, PJ. *Principles of polymer chemistry*. Cornell University Press, **1953**.
  39. Frankland, J A.; Edwards, HG M.; Johnson, AF; Lewis, IR; Poshyachinda, S, *Spectrochimica Acta.*, 1991, .47A, 1511-1524
  40. Pham, QT. *Proton and carbon NMR spectra of Polymers*, Florida, **1991**.
  41. Sreelatha, SP; Ninan, KN. *J. Appl. Polym. Sci.*, **1995**, 56, 1797-1804.
  42. Bräse, S; Gil, C; Knepper, K; Zimmerman, V. *Angew. Chem. Int. Edn*, **2005**, 44 5188-5240.
  43. Katritzky, A; Christopher, AR; Joule, JA; Zhdankin, VV. *Handbook of Heterocyclic Chemistry*, 3<sup>rd</sup> Edition, Elsevier, Netherlands, **2010**.
  44. Kissinger, H. *J Res. Nat. Bur. Stand*, **1956**, 57, 217-221.
  45. Sekkar, J. *J. Appl. Polym. Sci.*, **2010**, 117, 920-925.
  46. Jain, SR.; Sekkar, V; Krishnamurthy, VN. *J. Appl. Polym. Sci*, **1993**, 48, 1515-1523.
  47. Wingborg, N. *Polymer Testing*, **2002**, 21, 283-287
  48. Nielsen, LE.; Landel, F. *Mechanical properties of polymers and composites*. Marcel Dekker: Newyork, **1994**.
  49. Voorhees, KJ; Lattimer, RP. *J. Polym. Sci.: Part A: Polym. Chem*, **1982**, 20, 1457-1467
  50. Paabo, M; Levin, BC. *Fire and Materials*, **1987**, 2, 1-29
  51. Nagle, DJ; Ceina M, Rintoul, L, *Polymer Degradation and Stability*, **2007**, 92, 1446-1454.
  52. Lattimer, RP; Williams, RC. *J. Anal. Appl. Pyro.*, **2002**, 63, 85-104.
  53. Arisawa, H; Brill, TB. *Combustion and Flame*, **1996**, 106, 131-143.
  54. Kubota, N. *Propellant and Explosive: Thermochemical Aspects of Combustion*, Wiley VCH, Weinheim, Germany, **2007**.
  55. Cai, W; Thakre, P; Yang, V. *Combust. Sci. and Tech.*, **2008**, 180, 2143-2169.
  56. Rocco, JAFF; Lima, JES; Frutuoso, AG; Iha, K; Ionashiro, M; Matos, JR; Suarez-ha, MEV. *J. Thermal Analysis and Calorimetry*, **2004**, 75, 551-557.
-

*Chapter 5*

**Propargyloxy Telechelic Binders: Synthesis  
and Curing through ‘Click Reaction**

---

*A part of the results from this chapter is being patented.*

*S.Reshmi, Nair, CPR. Patent application entitled “Telechelic binders with  
‘Clickable groups’ and solid propellants thereof”: submitted*

### Abstract

*This chapter describes the investigations on functional modification of hydroxyl terminated polybutadiene (HTPB) and polytetramethylene oxide (PTMO) to derive propargyloxy terminated polybutadiene (PTPB) and propargyloxy terminated polytetramethylene oxide (PTMP) by a route different from that described in Chapter 4. The polymers were synthesised and characterised by spectroscopic as well as chromatographic techniques. The polymers were then cured by 'Click Chemistry' approach to form triazole network using an azide bearing polymer viz. glycidyl azide polymer (GAP). The curing parameters were studied using Differential Scanning Calorimetry (DSC). For PTPB-GAP system, curing occurs only for an alkyne:azide molar equivalence of 1:0.1 and beyond this stoichiometry, phase separation occurs. In the case of PTMP-GAP system, the maximum properties are achieved for an alkyne:azide molar equivalence of 1:1. DSC studies were carried out for PTMP-GAP system and the kinetic parameters derived were used for predicting the cure profile at a given temperature. Rheological studies of PTBP-GAP and PTMP-GAP systems were carried out and the properties were compared with HTPB-tolylene diisocyanate (TDI) based urethane system (based on hydroxyl: isocyanate). The studies revealed that the gel time for curing through the 1, 3 dipolar addition is higher for triazole curing route than that for urethanes based indicating a higher 'pot life'. The mechanical properties of the triazole mediated networks were evaluated. The mechanical properties of the resultant triazole networks obtained from PTPB-GAP and PTMP-GAP were comparable to those of HTPB-urethanes. Thermo gravimetric analysis (TG) of the triazoles derived from these polymers were investigated and the mechanism of decomposition of PTMP-GAP with AP as oxidiser was elucidated by pyrolysis GC-MS and TG-MS studies for the first time.*

*The propellant level properties of PTPB-GAP triazole and PTMP-GAP triazole were evaluated and compared with propellants based on HTPB- urethane system. The studies reveal that propellant based on PTPB-GAP triazole, PTMP-GAP triazole provides acceptable mechanical properties, superior processability than HTPB-urethanes and improved ballistic properties in terms of higher gas generating species during combustion.*

### 5.1. INTRODUCTION

Telechelic polymers find an important role as binders in solid propellants wherein the reaction of the end groups with suitable curative gives rise to a crosslinked three dimensional network capable of holding the other ingredients in solid propellants like oxidiser and metallic fuel. Typical functional groups of choice of oligomers are hydroxyl, carboxyl, amine, epoxy, thiol etc.<sup>1-6</sup> The polymer backbone can be crosslinked by either hydrocarbons like polybutadienes or polyalkylene ether. Amongst this, hydroxyl terminated polybutadiene (HTPB) is the most popular binder used in solid propellants both for boosters and upper stage motors.<sup>6-7</sup> Polytetramethylene oxide (PTMO) is another binder used for specific applications such as gas generators and pyrogen igniter propellants.<sup>9-10</sup> For both HTPB and PTMO, the reaction of hydroxyl groups with polyisocyanate resulting in polyurethanes is the mode of the crosslinking.<sup>10</sup> Though such systems are currently the most widely used, they have the short comings in terms of limited pot life and possibility of intervention of extraneous side reactions causing microvoids and deterioration of mechanical properties in the cured propellant matrix. A carboxyl functional polymer needs polyepoxy curative which generates a good amount of hydroxyl groups in the matrix rendering the system hydrophilic with associated problems. Same is the case with amine or thiol end groups that need epoxy or aziridine curatives. These curatives being oxygen/amine rich do not add to the fuel value either.<sup>11-18</sup> Hence, it is always desirable to have end groups that can undergo addition reaction to give crosslinked matrices particularly if the addition product adds to the energy and ballistics of the cured polymer network. ‘Click’ reaction between certain azide-alkyne groups assumes great importance in this context.<sup>19-25</sup> There have been few reports<sup>26-30</sup> on alkyne-azide ‘click reaction’ through a 1,3-dipolar cycloaddition to form 1,2,3-triazole networks for crosslinking polymers as well as propellant binders including a recent paper<sup>31</sup> on synthesis and characterisation of PTPB. However, in all these cases, the aspects of processability, mechanical properties and propellant energetics have not been addressed.

The present chapter reports modification of the hydroxyl groups of HTPB and PTMO to ‘clickable group’ alkyne groups which can be crosslinked using azides to yield triazoles. In Chapter 4, HTPB functionalisation was attempted through an isocyanate intermediate while in this chapter, a direct method of propargylation has



been attempted. The chapter details the synthesis and characterisation of propargyl oxy terminated polybutadiene (PTPB) and polytetramethylene oxide (PTMP). The alkyne functional polymers were then cured with azide containing polymer glycidyl azide polymer (GAP) to give triazoles. The curing kinetics, thermal decomposition mechanism, mechanical characterisation and dynamic mechanical characteristics of the cured triazole network in neat polymer, processability, mechanical properties, energetics, burn rate and thermal decomposition of the propellant with ammonium perchlorate (AP) as oxidiser has been investigated.

### 5.2. EXPERIMENTAL

#### 5.2.1 Materials

HTPB, PTMO, sodium hydride, propargyl bromide ammonium perchlorate (AP) and aluminium powder were used for the studies. The solvents namely methanol, toluene, pentane and tetrahydrofuran (THF) of high purity (AR grade) were used. The characteristics of the materials are described in Chapter 2.

#### 5.2.2 Instrumental

The methods and equipments used for characterisation are described in Chapter 2. FTIR,  $^1\text{H}$  and  $^{13}\text{C}$  NMR analyses of the samples were done. Curing was monitored using differential scanning calorimeter. Thermal decomposition was studied using a simultaneous TG-DSC. Mechanical properties viz. tensile strength, elongation and modulus were evaluated using Universal Testing Machine. Dynamic mechanical analysis (DMA) was done. The morphological studies of the sample were carried out using a Scanning Probe Microscope. GC-MS studies were conducted using a Thermo Electron Trace Ultra GC directly coupled to a mass spectrometer and SGE pyrolyser. TG-MS studies were conducted using TGA attached with Quadruple mass spectrometer at heating rate of  $5^\circ\text{C}/\text{min}$  for cured polymer and at  $2^\circ\text{C}/\text{min}$  for the propellant samples. Heat of combustion were measured using bomb calorimeter. Burn rate measurements were done using acoustic emission technique mentioned.

### 5.2.3.Synthesis

#### 5.2.3.1 Synthesis of propargyloxy terminated polybutadiene (PTPB)

Propargyloxy terminated polybutadiene (PTPB) was synthesised from HTPB by treating with propargyl bromide in presence of sodium hydride (NaH) (*Scheme 5.1*). In a typical reaction, 15g (0.006 mol) of moisture free HTPB was dissolved in THF and reacted with 1.25g (0.052 mol) of NaH at 40°C for 3 hours using magnetic stirring in nitrogen atmosphere. To the mixture, 5 ml (0.03 mol) of propargyl bromide was added and reaction was continued for 24 hrs. Following the reaction, 30 ml of methanol was added to remove excess NaH. The product was washed with hot water, followed by methanol. The product was dried at 60°C to remove methanol and water. The product was extracted using pentane and dried under reduced pressure at 80°C for 6hrs. Yield: ~89%.

#### 5.2.3.2 Synthesis of propargyl oxy terminated polytetramethylene oxide (PTMP)

Propargyloxy terminated polytetramethylene oxide (PTMP) was synthesised from PTMO by reaction with propargyl bromide in presence of sodium hydride (*Scheme 5.2*) as in the case of HTPB. In a typical reaction, 15g (0.0075 mol) of moisture free PTMO was dissolved in THF and reacted with 1.4g (0.0067 mol) of NaH at 40°C for 3 hours. To the mixture, 5 ml (0.03 mol) of propargyl bromide was added and reaction was continued for 15 hrs. Following the reaction, 30 ml of methanol was added to remove excess NaH. The product was washed with hot water, followed by methanol. The product was dried at 60°C to remove methanol and water. After drying, the product was extracted using THF and was dried under reduced pressure at 60°C for 5hrs. Yield ~80%.

#### 5.2.4. Curing Procedure

PTPB and PTMP were cured using glycidyl azide polymer (GAP). PTPB was cured using GAP at an alkyne: azide molar ratio of 1: 0.1 and PTMP-GAP was cured at an alkyne: azide molar ratio of 1: 1. The mixtures were then cast in aluminium moulds and the curing reaction was carried out at 60°C for a period of 5 days.

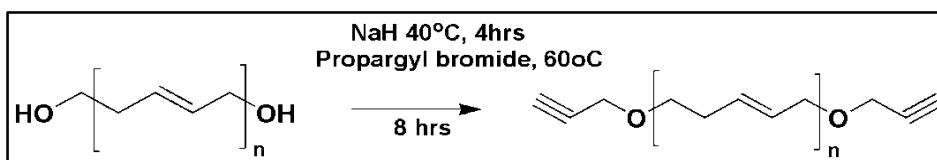
### 5.2.5. Propellant Processing

Propellant studies were done using PTPB-GAP and PTMP-GAP as binder, ammonium perchlorate as oxidiser (77% by weight) and aluminium as metallic fuel (2%). The properties were compared with propellant based on HTPB-TDI and AP. For this thermochemical performance evaluation of the propellant was carried out using NASA-CEA programme and the results are compared with conventional HTPB propellant having the same formulation. For processing the propellant, the alkyne-azide molar ratio for PTPB-GAP was maintained at 1:0.1 and PTMP-GAP system was maintained at 1:1 and for HTPB-TDI system, the isocyanate-hydroxyl ratio was maintained at 0.85:1. For computing the thermochemical performance, the heat of formation of the polymers were computed for the two polymers from the heat of combustion data. The propellant mixing studies were carried out in a 1 kg scale in a Guitard horizontal mixing system at 40°C for average mixing time of three hours. The resulting slurry was cast under vacuum (10mmHg). For comparison, HTPB with TDI as curing agent was also processed in the same manner. End of mixing (EOM) viscosity and build up values were measured using Brookfield Viscometer. The propellant slurry was cured at 60°C for 5 days. Burning rate measurements were conducted at pressures 6.93 MPa using an acoustic emission strand burner using cured strands (size:80x6x6 mm). The bomb was pressurised using nitrogen and burning was detected by acoustic emission detector.

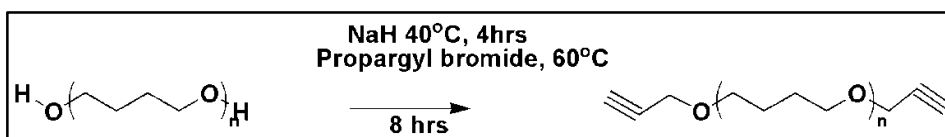
## 5.3 .RESULTS AND DISCUSSION

### 5.3.1. Functionalisation of HTPB and PTMO

Incorporation of ‘clickable’ groups were realised through transformation of HTPB and PTMO to propargyl terminated by conversion of the polymers to their sodium salt and thereafter to PTPB and PTMP by reaction with propargyl bromide as given below in Scheme 5.1 and 5.2. Both the polymers were characterised by FTIR, NMR and GPC techniques. The method reported in literature<sup>31</sup> for the synthesis of PTPB is condensation of HTPB using propargyl bromide using potassium ter-butoxide.



*Scheme 5.1 Typical Synthesis Scheme for PTPB*



*Scheme 5.2 Typical Synthesis Scheme for PTMP*

For PTPB, the presence of propargyl group was confirmed by FTIR (Fig 5.1) by the characteristic absorption at  $2130\text{ cm}^{-1}$  corresponding to  $-\text{C}\equiv\text{C}-\text{H}$ , absorption at  $3307\text{ cm}^{-1}$  due to alkenyl C-H stretch and absence of broad peak at  $3400\text{--}3600\text{ cm}^{-1}$  corresponding to hydroxyl groups. The spectra of HTPB and PTPB are compared in Fig 5.1a and b respectively. The double bond and microstructures of the butadiene<sup>32</sup> remains unaltered even after the modification of the polymer backbone.

$^1\text{H}$  NMR of PTPB (Fig 5.2) showed all the chemical shifts as that of HTPB<sup>32</sup> and the microstructure of PTPB was found to be identical to that of HTPB. In addition, the chemical shifts at 2.5 ppm due to  $-\text{C}\equiv\text{C}-\text{H}$  and the one at 4.2 ppm due to  $\text{O}-\text{CH}_2-$  bonded to the propargyl group confirms the anchoring of propargyl oxy groups to HTPB and this matches with reported literature<sup>30</sup>.

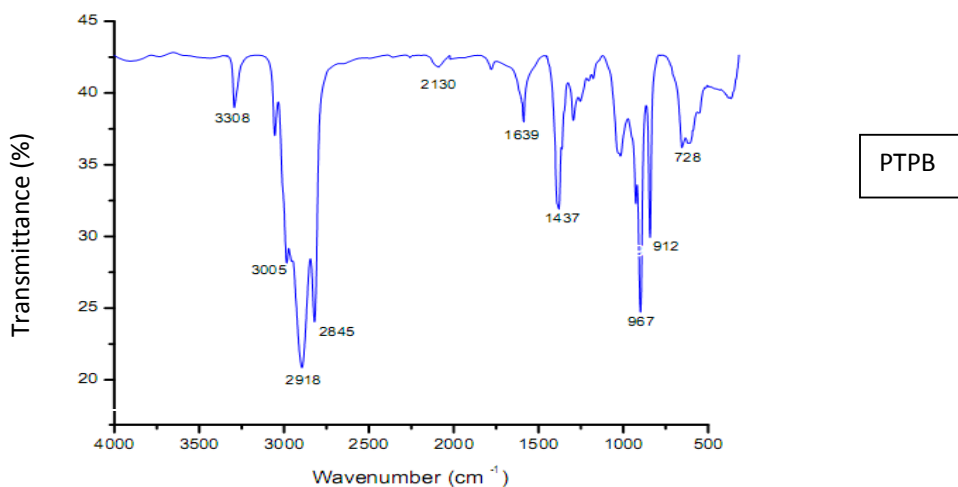


*Fig.5.1 FTIR spectrum of PTPB*

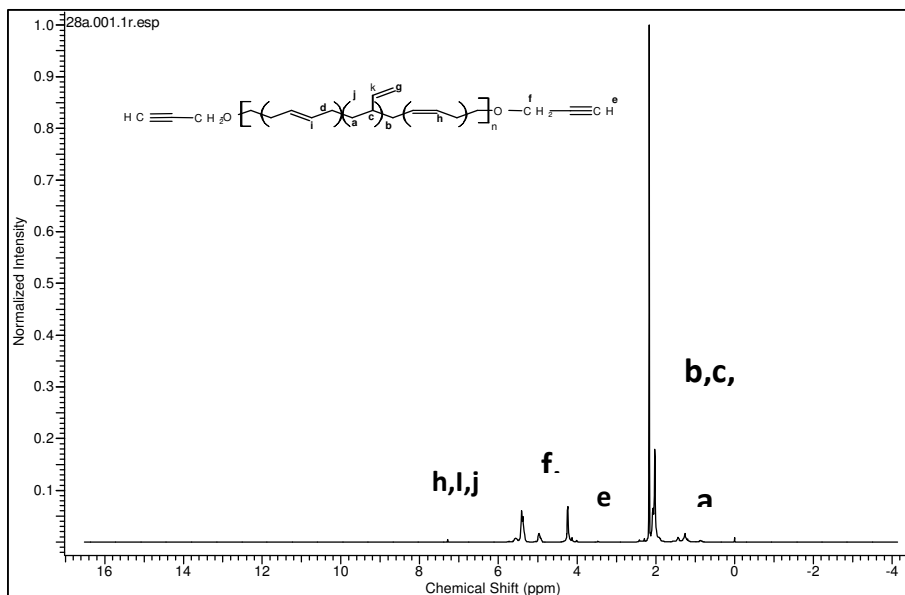


**Fig.5.2.**  $^1\text{H}$  NMR spectrum of PTPB (in  $\text{CDCl}_3$ )

In the case of PTMP, the presence of propargyl group was confirmed by characteristic peak of acetylene group ( $\nu\text{-C}\equiv\text{C-H}$ ) at  $2130\text{ cm}^{-1}$  in the FTIR spectrum (Fig 5.3) with the absence of absorption due to hydroxyl groups at  $3400\text{-}3600\text{ cm}^{-1}$  in the spectra.

$^1\text{H}$  NMR (Fig 5.4) of PTMP, showed all chemical shifts of PTMO. The chemical shifts at  $0.7\text{-}1.8\text{ ppm}$  is due to  $\text{-CH}_2$  groups, the peak at  $2.5\text{ ppm}$  is due to  $\text{-C}\equiv\text{C-H}$ , the one at  $3.5\text{-}3.7\text{ ppm}$  corresponds to  $\text{O-CH}_2\text{-}$  groups and peak at  $4.3\text{ ppm}$  is due to  $\text{O-CH}_2\text{-}$  bonded to the propargyl group in PTMP.

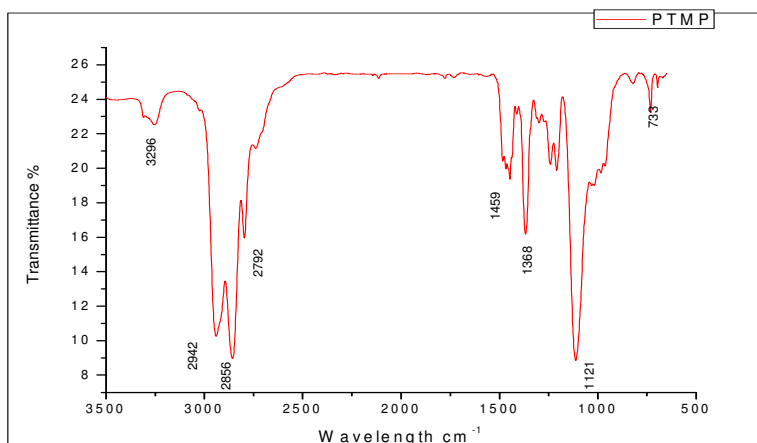


**Fig.5.3** FTIR spectrum of PTMP

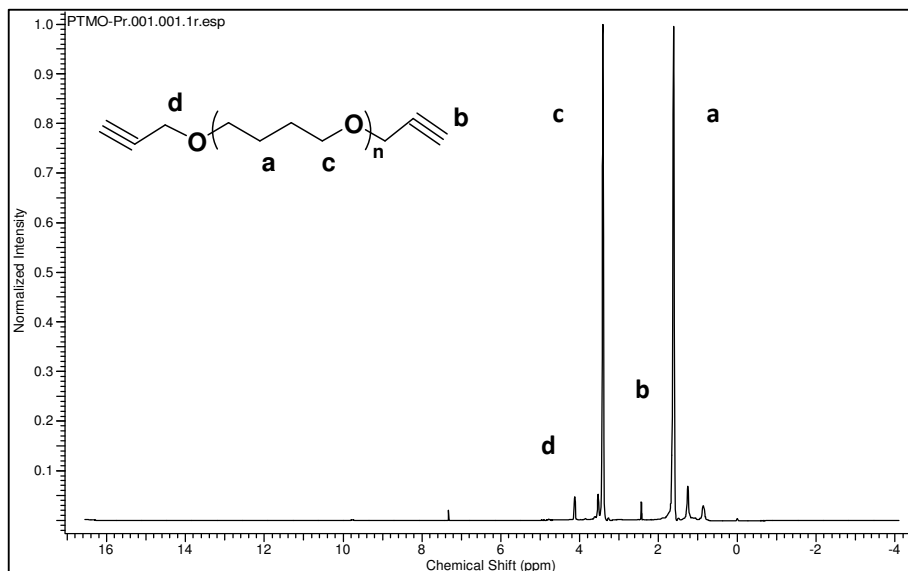


**Fig.5.4.**  $^1\text{H}$  NMR spectrum of PTMP (in  $\text{CDCl}_3$ )

GPC traces of the PTPB and PTMP corrected for hydrodynamic volume are given in Fig 5.5& 5.6 respectively. The calculated number average molecular weight for PTPB and PTMP are 3627 and 3618, weight average molecular weights (Mw) of PTPB and PTMP are 15551 and 16150 respectively and the polydispersity indices (PDI) are 2.4 and 1.8 respectively. Unlike in the case of urethane mediated end functionalisation, the process does not add to any change in molecular weight.

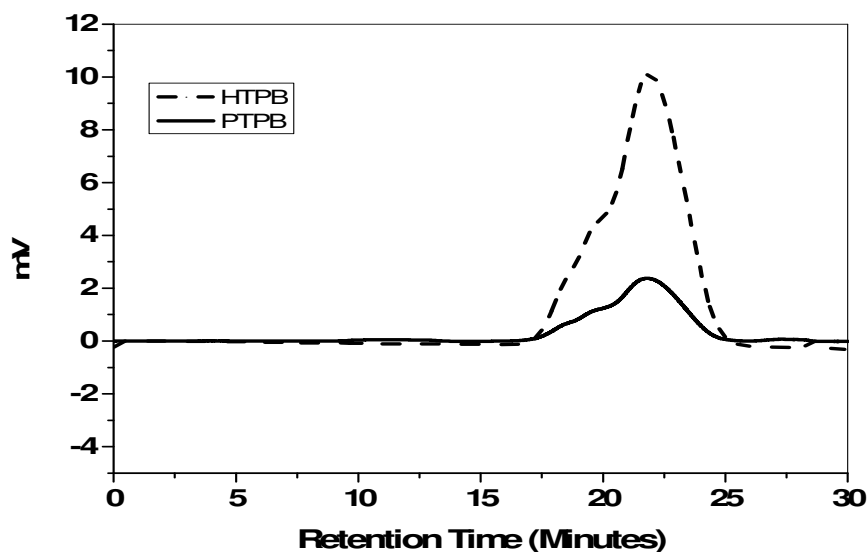


**Fig. 5.5.** GPC chromatogram of HTPB, PTPB

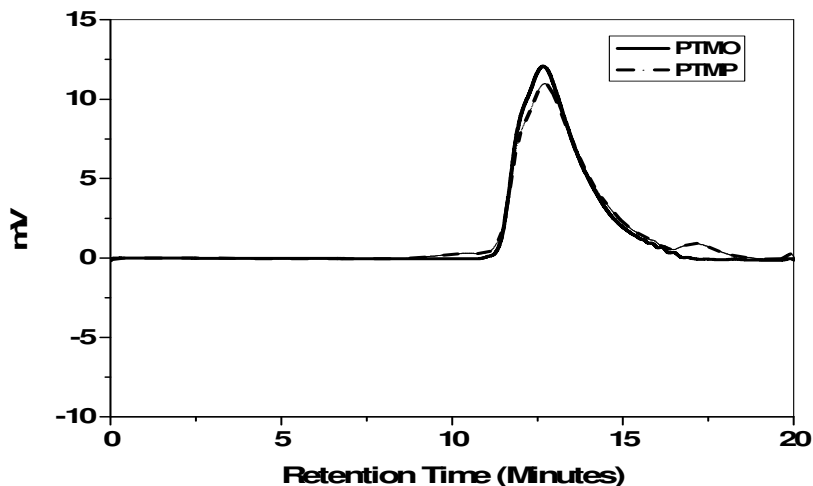
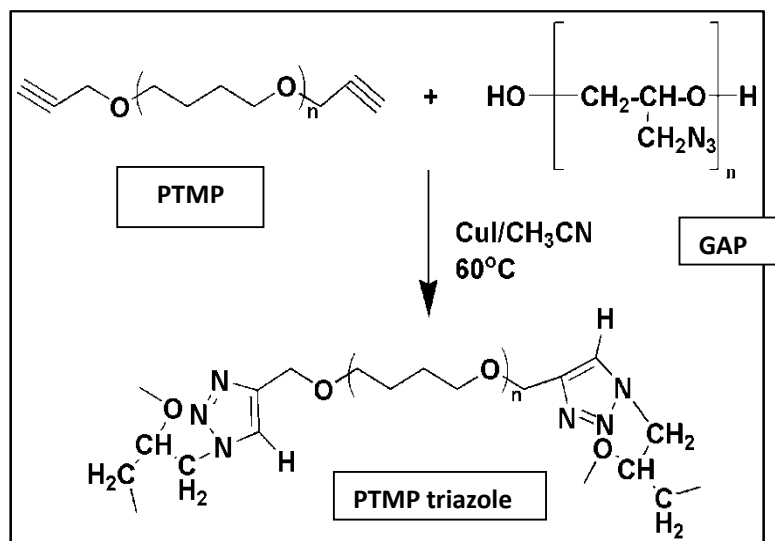


Fig. 5.6. GPC chromatogram of PTMO, PTMP

### 5.3.2. Cure Characterization

In a typical reaction, the alkyne groups of PTMP or PTPB reacts with the azide groups of GAP resulting in triazoles through ‘Click reaction’ (Scheme 5.3).



Scheme 5.3. Cycloaddition reaction between PTMP and GAP giving triazole

#### 5.3.2.1. PTPB-GAP Curing

The curing of PTPB with GAP results in the formation of triazole. To study the curing of PTPB-GAP system, non-isothermal differential scanning calorimetry (DSC) analysis was done at a heating rate of 5°C/min. Initially DSC study was carried out for an azide to alkyne molar equivalence of 1:1. It was observed that at this composition completion of cure does not occur. Instead, azide decomposition is

more predominant (Fig 5.7a). Curing is found to occur only for an alkyne-azide molar equivalence of 1:0.1 and beyond this, phase separation occurs. This can be attributed to the difference in the solubility parameters of the polymers. HTPB<sup>33</sup> has a solubility parameter of  $17.6 \text{ MPa}^{1/2}$  and that of GAP<sup>34</sup> is  $22.8 \text{ MPa}^{1/2}$  which causes miscibility issues beyond a certain concentration. The poor compatibility between GAP and HTPB due to polar nature of azide groups and non polar nature of HTPB backbone has been reported by Ding et al.<sup>31</sup> also. The cure reaction of PTPB with GAP resulting in the formation of triazoles for alkyne-azide equivalence of 1:0.1 occurs in the temperature range of  $110\text{--}185^\circ\text{C}$  with an associated enthalpy of  $50 \pm 2 \text{ J/g}$ . This is followed by decomposition of the residual azide at  $\sim 186^\circ\text{C}$  (Fig.5.7b) as the reaction is not complete in a DSC cell.

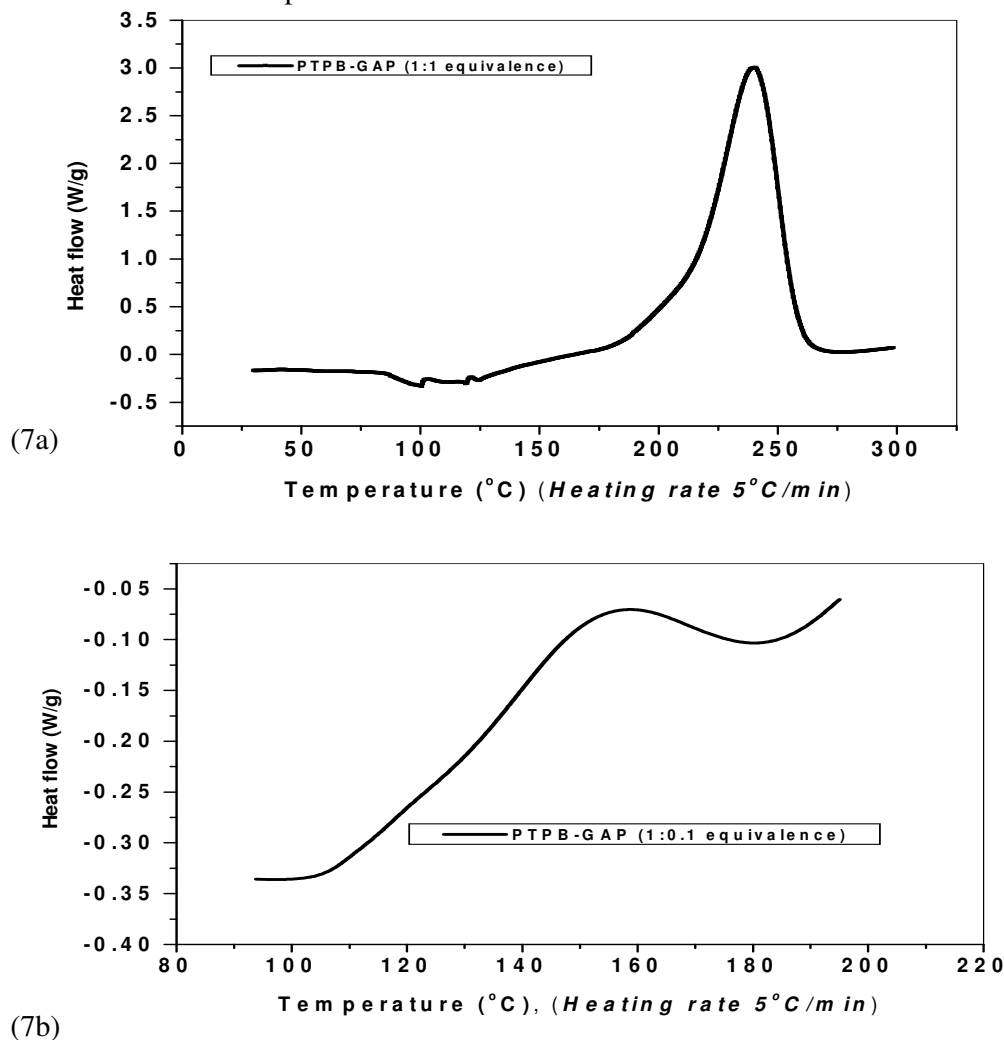


**Fig. 5.7.** DSC Traces of Curing of PTPB with GAP **a)** Azide-alkyne equivalence 1:1  
**b)** Azide-alkyne equivalence (1:0.1)



### 5.3.2.2. PTMP-GAP Curing

The curing of PTMP with GAP was evaluated using DSC for both uncatalysed and catalysed, for a typical heating rate of 10°C/min. The uncatalysed cure reaction occurs in the range of 110-236°C and is not conducive for propellant applications as the safe operational temperatures for curing of solid propellants is in the range of 40-60°C. Hence, curing of PTMP was effected by reacting with glycidyl azide polymer (GAP) to yield crosslinked triazole network in the presence of cuprous iodide (CuI) with acetonitrile as catalyst. DSC studies were carried out by varying the catalyst concentration (0, 0.1, 0.3 and 0.5 weight % CuI) to investigate the influence of catalyst concentration (Table 1) on cure temperature. In the presence of catalyst, curing of PTMP with GAP to yield triazoles occurs in the temperature range of 53-210°C with an enthalpy of 75 ±2 J/g (Fig 5.8). It is seen that, increase in catalyst concentration facilitates curing. Cure initiation systematically shifts to lower temperature with increased catalyst concentration. However, the presence of copper catalyst lowers the decomposition of azide from 210 to 189°C. Hence, for further studies, a catalyst concentration of 0.1% was chosen. Unlike PTPB-GAP system, in PTMP-GAP system has no problems related to phase separation. This is because of the fact that solubility parameters of GAP (22.8 MPa<sup>1/2</sup>) and PTMO<sup>35</sup> (20.9 MPa<sup>1/2</sup>) are close enough and are conducive for high miscibility between the polymers at all proportions.

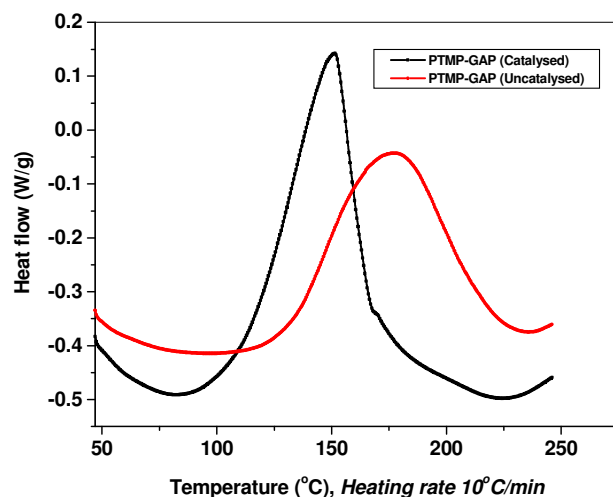


*Fig. 5.8. DSC Traces of Curing of PTMP with GAP (Heating rate 10°C/min)*

**Table 5.1** Phenomenological Details of Curing –Effect of Catalyst (Heating rate 10°C/ minute)

Catalyst Content (CuI in acetonitrile) (%)	Initial temperature, T <sub>i</sub> (°C)	Peak temperature, T <sub>m</sub> (°C)	Final temperature, T <sub>f</sub> (°C)
0	110	176	236
0.1	78	147	210
0.3	56	93	194
0.5	53	87	189

### 5.3.3. Cure kinetics

The cure kinetics for PTMP-GAP system was followed for the catalysed reaction by non-isothermal DSC method based on varying heating rates at 3,5 7 and 10°C/min for a catalyst (CuI) content of 0.1% by weight . The peak reaction temperatures (T<sub>m</sub>) obtained are 132, 137, 141 and 147°C for heating rates of 3, 5,7 and 10° C respectively and the phenomenological details of the curing at different heating rates are given in Table 5.2.

**Table 5.2.** Phenomenological Details of Curing-Effect of heating rate

Heating rate (°C/min)	Initial temperature, T <sub>i</sub> (°C)	Peak temperature, T <sub>m</sub> (°C)	Final temperature, T <sub>f</sub> (°C)
3	56	132	196
5	60	137	200
7	67	141	205
10	78	147	210

The kinetics of cure reaction was evaluated by the variable heating rate method of Kissinger<sup>36</sup> based on heating rate as a function of the temperature maxima (T<sub>m</sub>) in DSC. The activation energy (E) is obtained from the slope of the plot of log ( $\phi/T_m^2$ ) against 1/T<sub>m</sub> (Fig.5.9) where  $\phi$  =heating rate, E= Activation energy, R= Universal gas constant, T<sub>m</sub>= Peak maximum temperature. For the computations, T<sub>m</sub> is the average of the T<sub>max</sub>. The pre-exponential factor (A) was calculated using the relation given in equation 1 .

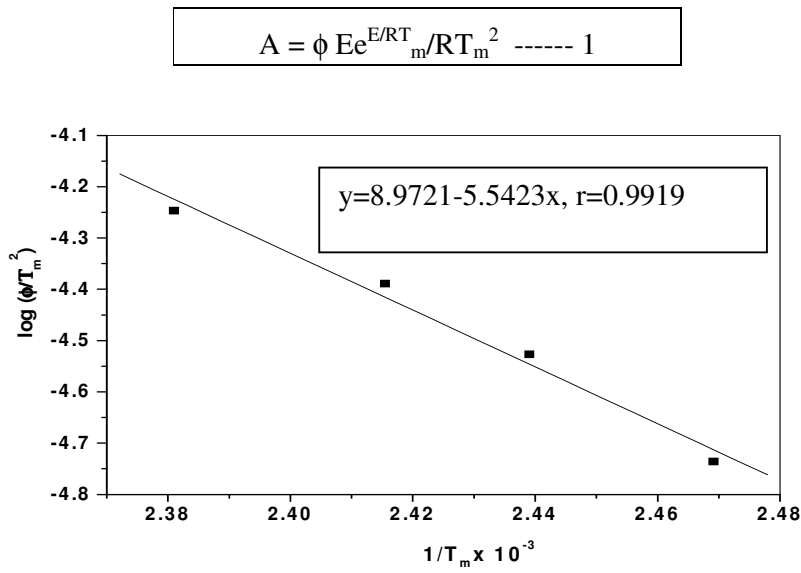


**Fig. 5.9.** Kissinger plot for determination of activation energy (E) for PTMP-GAP system

The activation energy (E) computed by Kissinger method is 106.1 kJ/mol. The pre-exponential factor (A) is  $1.893 \times 10^{11} \text{ s}^{-1}$  and rate constant at a temperature of  $60^\circ\text{C}$  (computed by the relation  $k=Ae^{-E/RT}$ ) is  $4.3 \times 10^{-6} \text{ s}^{-1}$ . From this, the isothermal cure profile for the system can be predicted for any given temperature using equation 2 relating time (t), temperature (T) and fractional conversion ( $\alpha$ ). A typical example for the conversion is given in Fig.5.10 for a temperature of  $60^\circ\text{C}$ ,

$$\alpha = 1 - \{1 - A(1-n) t e^{-E/RT}\}^{1/1-n}, n=2 \text{ --- 2}$$

n=order reaction, E=activation energy, R=universal gas constant, T=temperature in absolute scale

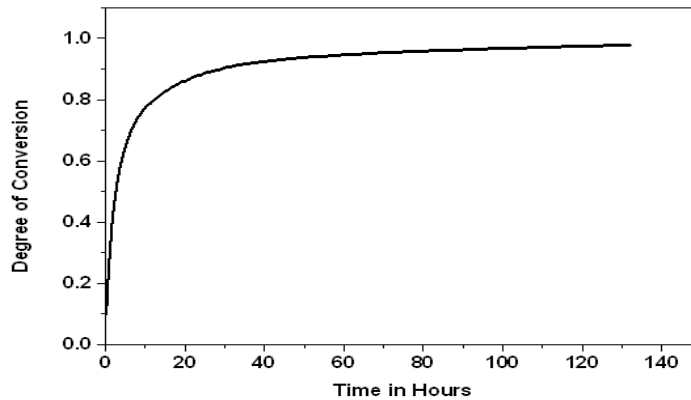


**Fig. 5.10.** Prediction of Isothermal Cure Profile (at  $60^\circ\text{C}$ ) for PTMP-GAP system

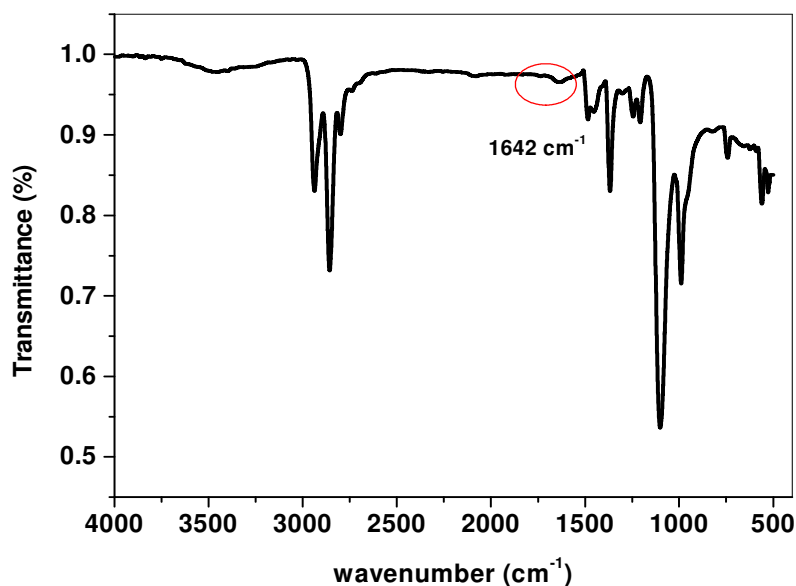


*Fig. 5.11. FTIR Spectra of cured PTMP-GAP (ATR)*

For the cure reaction a conversion of 95% is achieved after 120 hours. The triazole formation in PTMP was confirmed by FTIR, by the appearance of a peak at  $1642\text{ cm}^{-1}$ , due to double bond of triazole<sup>37</sup>, which is absent in the neat polymer and the disappearance of azide peak at  $2108\text{ cm}^{-1}$  (Fig 5.11).

The rheological behaviour of the curing reaction of PTPB and GAP (molar stoichiometry of 1:0.1) and PTMP-GAP (molar stoichiometry of 1:1) were investigated at  $80^{\circ}\text{C}$ . The isothermal evolution of storage modulus ( $G'$ ) and loss modulus ( $G''$ ) vs. reaction time for the curing reaction for PTPB-GAP is given in Fig 5.12 and that of PTMP-GAP is given in Fig 5.13. Both moduli (storage and loss) increase as a result of the increase in crosslinking as observed in the rheogram. The cross over point of loss modulus with storage modulus is considered as the gel point. The gel point for PTPB-GAP system occurs after 190 minutes. In this case, a higher modulus build up may be attributed to triazole and triazoline (due double bond-azide reaction<sup>38</sup>) formation. For PTMP-GAP system, the gel point is reached after 280 minutes and the modulus build up is benign compared to PTPB-GAP system. The gel point is higher than for HTPB-TDI system which is 120 minutes. This indicates a higher 'pot-life' for the cure reaction involving PTPB-GAP and PTMP-GAP systems.

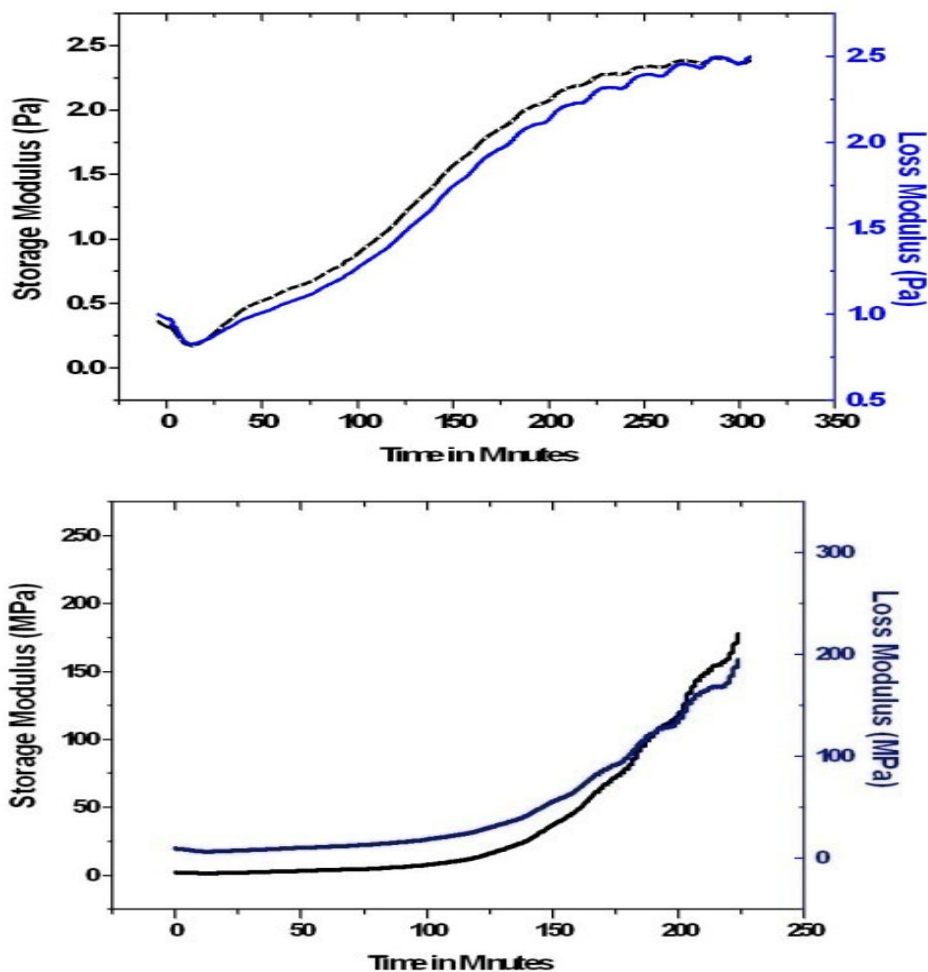


*Fig.5.12. Rheogram of PTPB with GAP at 80°C*

*Fig. 5.13. Rheogram of PTMP with GAP at 80°C*

#### 5.3.4. Mechanical properties

The mechanical properties viz. tensile strength (T.S), elongation and modulus of the cured polymers (PTPB-GAP and PTMP-GAP) were determined. The tensile strength of the PTPB-GAP triazole-triazoline for an azide –alkyne molar equivalence of 1:0.1 is 1.18 MPa, elongation at break is 21 % and the modulus is 0.88 MPa. Ding et al.<sup>31</sup> have reported the mechanical properties of PTPB-GAP system for various stoichiometries of alkyne: azide and a tensile strength of 2.7 MPa, elongation break ~47 % and modulus of 5.36 MPa. However, they have not discussed the problems related to miscibility and phase separation between PTPB and GAP during the preparation of composite.

The mechanical properties of HTPB urethanes cured using different isocyanates like isophorone diisocyanate, hexamethylene diisocyanate are reported<sup>39-40</sup>. The tensile strength is reported to be in the range 0.3-0.7MPa, elongation at break is in the range 170-400% and Young's modulus in the range 0.3-1.04 MPa. For triisocyanate based HTPB-urethane, the reported values of 0.4-1.18 MPa and elongation at break is 90-140%. The decrease in elongation may be due the increase in the rigidity of the networks formed from the triisocyanates. Similar is the present observation wherein the rigid triazole groups are decreasing the elongation characteristics of the cured polymer.

For PTMP-GAP based triazoles (an azide –alkyne molar equivalence of 1:1) the tensile strength obtained is 0.29 MPa with elongation at break of 53% and modulus of 0.15 MPa (Table 5.3). In literature<sup>41-42</sup>, it is reported that using an isocyanate like TDI or isophorone diisocyanate (IPDI), curing of PTMP is not effected and is not converted to a solid as the functionality of the polymer is 1.8-2.0. Hence for improving this, various crosslinkers like glycerine and glycerol propoxylate, have been used for curing of PTMO-IPDI. The reported values for tensile strength for these systems are in the range 0.9-7 MPa with elongation at break in the range 700-800%. These values have been generated for various degrees of crosslinking. In the present case, for PTMP-GAP system curing is effected without any crosslinkers which may be due to the large number of azide groups and rigid nature of triazole groups.

***Table. 5.3. Mechanical Properties of cured PTPB and PTMP polymer***

<b>Mechanical Properties</b>	<b>PTPB-GAP</b> (-C≡CH:N <sub>3</sub> =1:0.1)	<b>PTMP-GAP</b> (-C≡CH:N <sub>3</sub> =1:1)
Tensile strength, (MPa)	1.18	0.29
Elongation at break (%)	21	53
Modulus (MPa)	0.88	0.15

### **5.3.5. Dynamic mechanical characterisation**

DMA of triazoles based on PTPB-PTMP were evaluated for an alkyne-azide molar stoichiometry of 1:0.1. A biphasic transition with two glass transitions ( $T_g$ ) is obtained. The first transition occurring at -40.5 °C is due to the butadiene backbone and the second one at 18.4 °C, likely due to the triazole-triazoline network

(Fig.5.14). The dynamic mechanical characteristics of PTMP-GAP were not evaluated as the samples were too brittle. The reported values of  $T_g^{42}$  for PTMO based urethanes are in the range  $-57$  to  $-3$  °C.

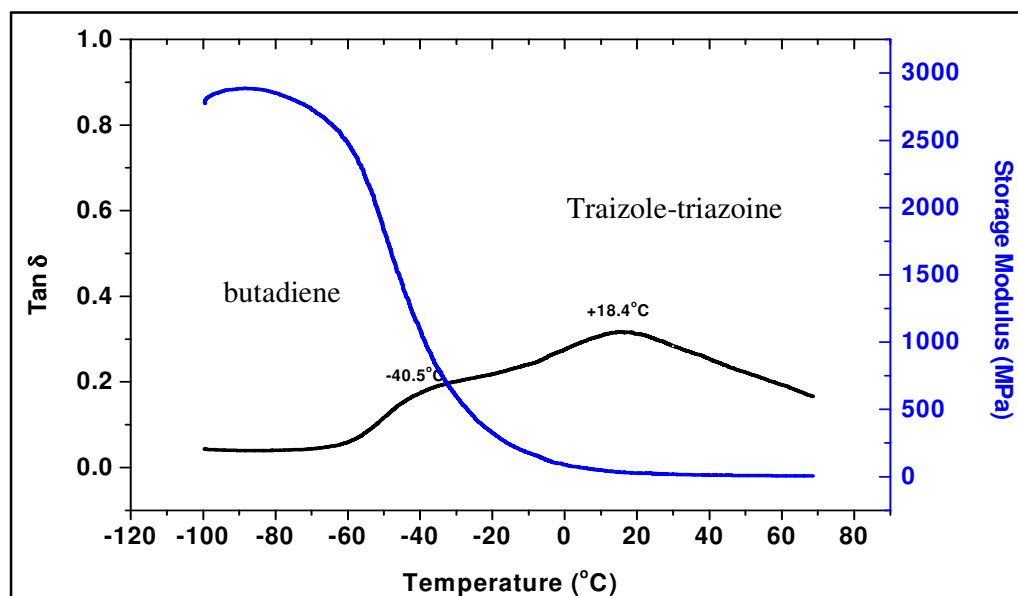


*Fig. 5.14. Tan  $\delta$  and Storage modulus of Cured PTPB-GAP Polymer*

### 5.3.6. Thermal decomposition studies

The thermal decomposition characteristics of triazole-triazoline of PTPB-GAP and PTMP-GAP were studied using thermogravimetric analysis (TGA). TGA was done at a heating rate of  $5^{\circ}\text{C}/\text{min}$  in nitrogen atmosphere. The cured PTPB-GAP undergoes a single-stage decomposition (Fig.5.15 a). The decomposition occurs in the temperature range of  $250$ - $460^{\circ}\text{C}$  with a weight loss of  $94\%$ . The peak reaction temperature is  $452^{\circ}\text{C}$ . The residue left over at  $600^{\circ}\text{C}$  is  $6\%$ . This is different from HTPB-TDI urethane system where two-stage decomposition is reported<sup>43</sup>. The mechanism of HTPB urethane has been studied by flash pyrolysis<sup>44</sup> and it is reported that initially the cleavage of urethane bond occurs liberating the curing agent which vaporises. This is followed by decomposition of polymer back bone. The mechanism of the decomposition reaction was investigated using pyrolysis GC-MS and TG-MS. The pyrolysis studies at  $300^{\circ}\text{C}$  gave butylated hydroxyl toluene (BHT) which is the antioxidant used in HTPB. Unlike in HTPB-TDI, in cured PTPB-GAP, the cleavage of triazole-triazoline group occurs along with degradation of polymer backbone which is supported by the pyrolysis data. Further, the pyrolysis characteristics were

studied at a higher temperature of 500°C. This revealed that at 500°C, cleavage of the triazole group occurs (Fig 5.15b) liberating N<sub>2</sub> (retention time, RT 1.74) in addition to the degradation of polybutadiene back bone giving rise to butadiene (RT 1.83), cyclohexadiene (RT 2.03), 4-vinyl cyclohexene (RT 4.99), xylene (RT 5.93), methyldiene (RT 10.05) and BHT (RT 14.90) as reported in literature.<sup>44-45</sup>

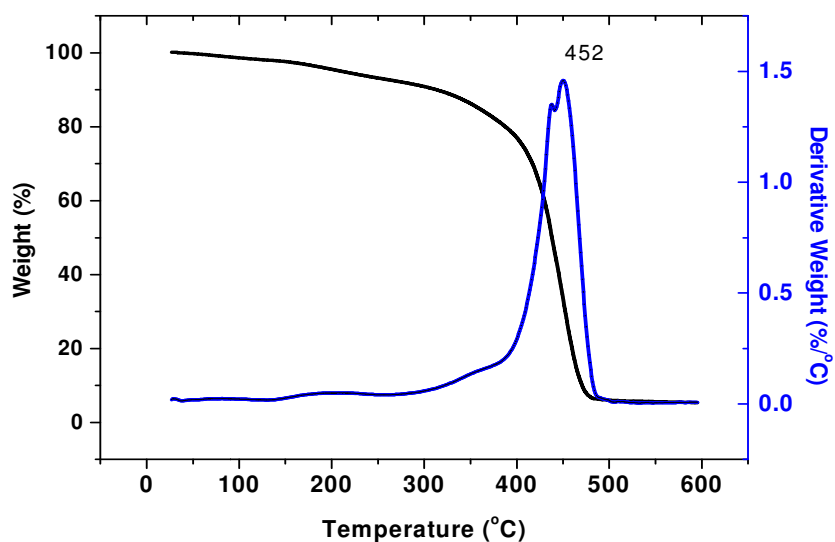


Fig 5.15a. TGA-DTG trace of PTPB triazoles (Heating rate 5°C/min)

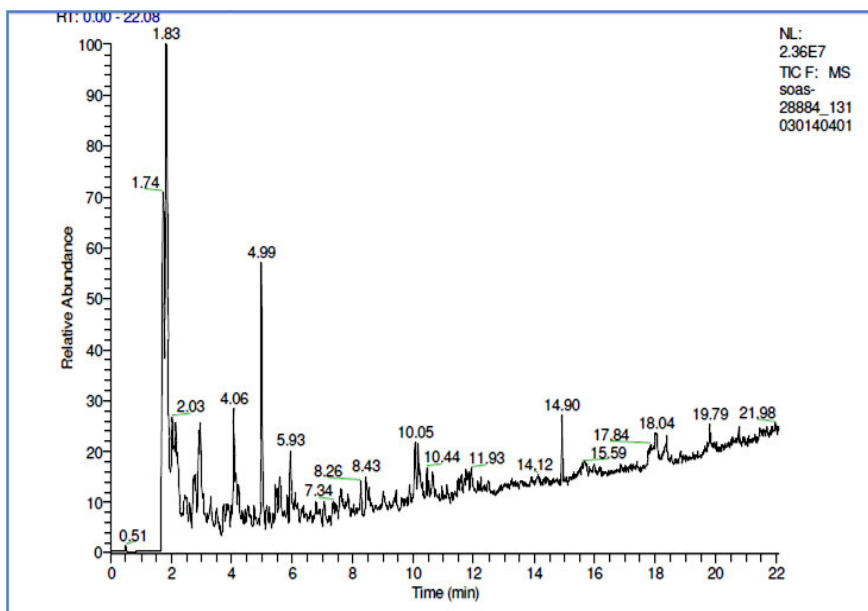
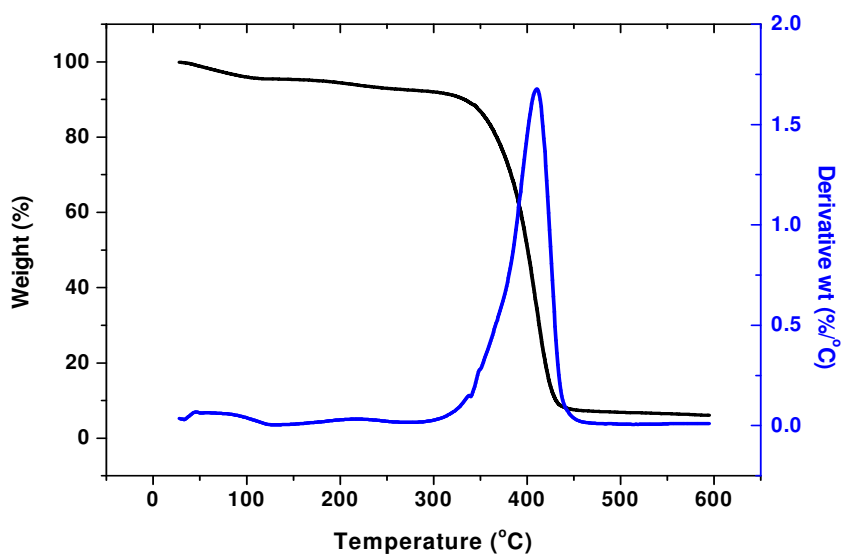


Fig 5.15b. Pyrogram of of cured PTPB-GAP at 500°C





**Figure 5.16 a** TGA-DTG trace of PTMP triazoles (Heating rate 5°C/min)

The cured PTMP-GAP also undergoes a single-stage decomposition (Fig.5.16 a). The decomposition occurs in the temperature range of 220-460°C with a weight loss of 92% with peak reaction temperature at 412°C. The residue left over at 600°C is 8%. The mechanism of the decomposition reaction was investigated using pyrolysis GC-MS and TG-MS. Pyrolysis GC-MS studies at 300°C detected the evolution of adsorbed water and BHT only. Hence, the pyrolysis characteristics were studied at a higher temperature of 500°C. This revealed that at 500°C, cleavage of the triazole group liberating N<sub>2</sub> (RT 1.29) in addition to the degradation of the polyether back bone resulting in the formation of butane (RT 3.86), 1-butoxybutane (RT 7.95), 4-butoxy butanal (RT 11.12), 1-(3-butoxypropoxy)butane (RT 15.05), 4-(3-butoxypropoxy)butanal (RT 17.58), 1-(3-(3-butoxypropoxy) propoxy)butane (RT 20.51), 4-(3-(3-butoxypropoxy) propoxy) butanal (RT 22.6) and 1-(3-(3-(3-butoxypropoxy) propoxy) propoxy) butane (RT 24.91). The decomposition products are similar to those reported in literature for the decomposition of PTMO<sup>46</sup>. Kohga<sup>41-42</sup> et al have reported the thermal decomposition behavior of PTMO cured with various crosslinkers like glycerine and glycerol propoxylate, where the polymers cured using isophorone diisocyanate and decomposition is found to proceed through a single stage in the temperature range of 290-470°C. Lattimer et al.<sup>47</sup> have reported the pyrolysis products from a polyether-based polyurethane by matrix-assisted laser desorption/ionization mass spectrometry (MALDI-MS), direct probe chemical

ionization mass spectrometry (CI-MS), and ATR-FTIR. The degradation was explained based on three decomposition pathways. The first one is mainly due to dissociation to isocyanate and alcohol, the second one being dissociation to amine, olefin, and carbon dioxide followed by oligomeric decomposition to yield alkyl and aldehyde end groups. Though the decomposition temperature range is similar, the mechanism is different as there is no cleavage of urethane bonds in the present case.

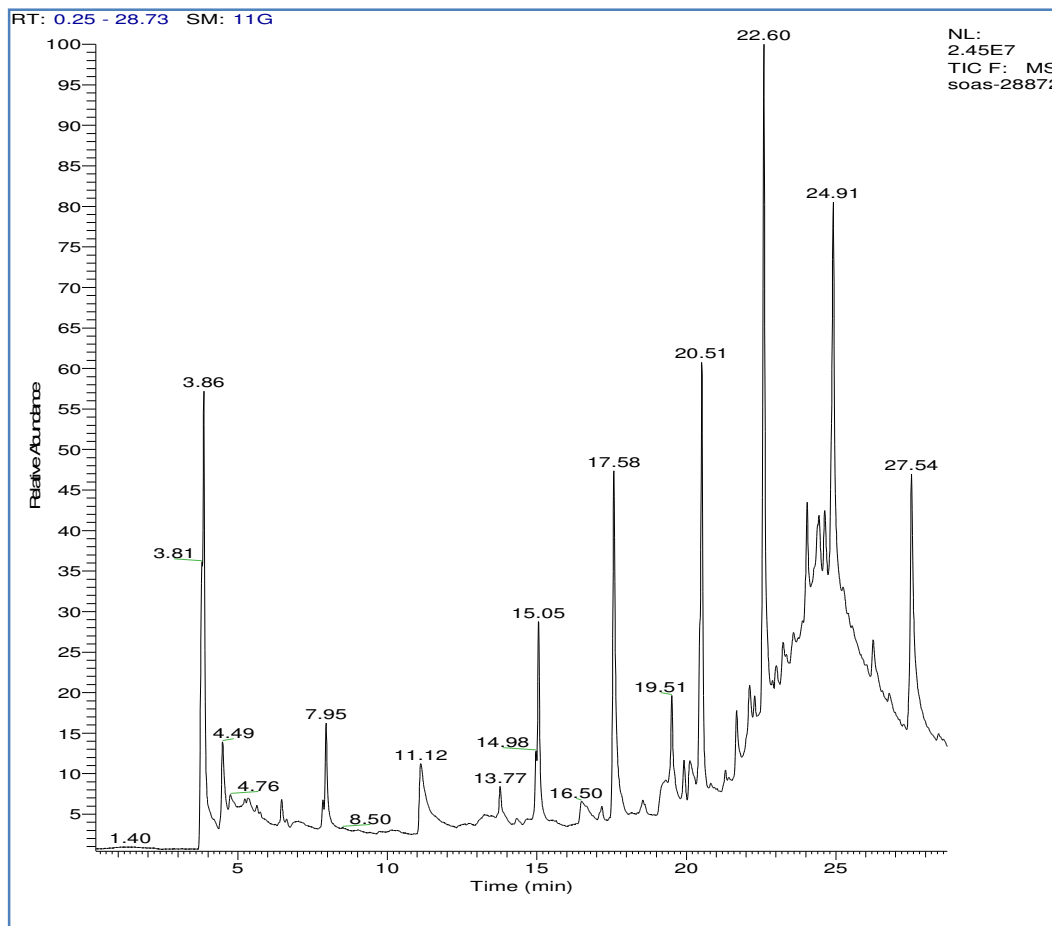


**Figure 5.16b.** Pyrogram of cured PTMP-GAP at 500°C

In order to study the interaction of ammonium perchlorate (AP) with PTMP, the PTMP-AP triazole propellant (with AP content-77%) were processed. The thermal decomposition of PTMP-AP triazole occurs in three stages. The first stage occurs in the temperature range of 219 -293°C with a weight loss of 32%. The second stage decomposition occurs in the temperature range of 294 -333°C with a weight loss of 10% and the third stage occurs in the temperature range of 334 -

395°C with a weight loss of 57%. The residue left over at 600°C is 1%. It is observed that in the presence of AP, the thermal stability of PTMP triazoles is lowered due to the interaction of AP with the polymer. The mechanism of decomposition was investigated using pyrolysis GC-MS and TG-MS studies. Pyrolysis GC MS studies at 250°C (Fig 5.17), resulted in the evolution of tetrahydrofuran (RT 5.83), 1-(4-chlorobutoxy)-4-chlorobutane (RT 13.62) and BHT (RT 14.86). The studies indicate that the hydrochloric acid (HCl) liberated during decomposition of AP induces cleavage of the polyether back bone in PTMP resulting in the formation of cyclic tetrahydrofuran as given in Scheme 5.4. However, the triazole ring is not affected at lower pyrolysis temperature. The cleavage of polyether backbone results in formation of 5-(pent-4-enyloxy) pent-1-ene which reacts with HCl giving rise to 1-(4-chlorobutoxy)-4-chlorobutane which may be occurring by free radical addition.

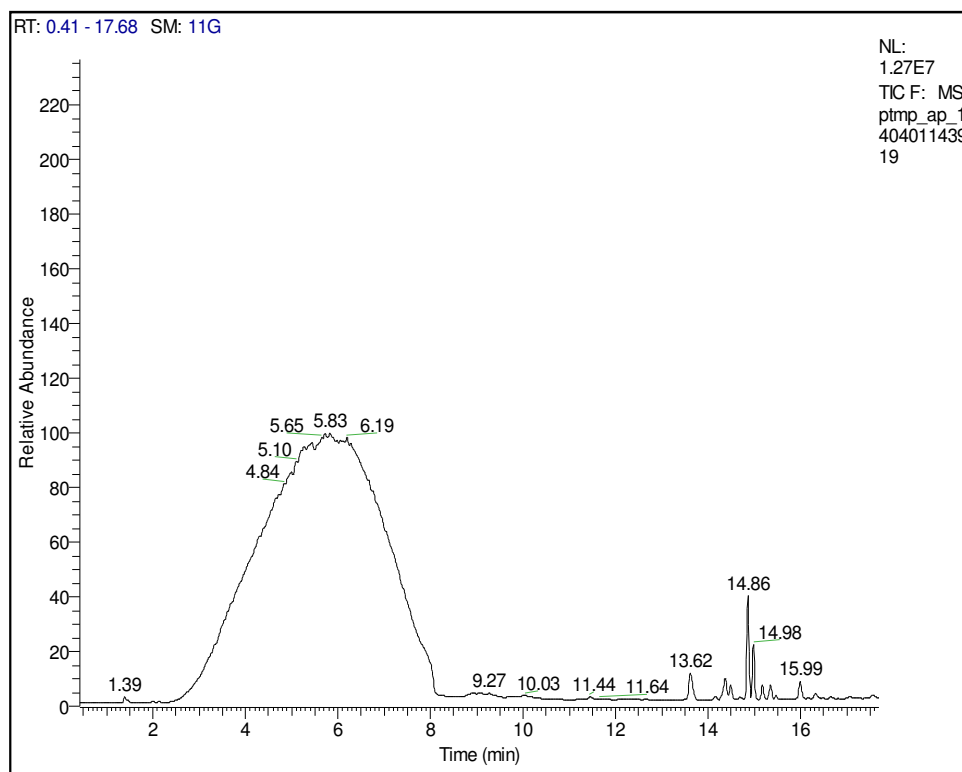
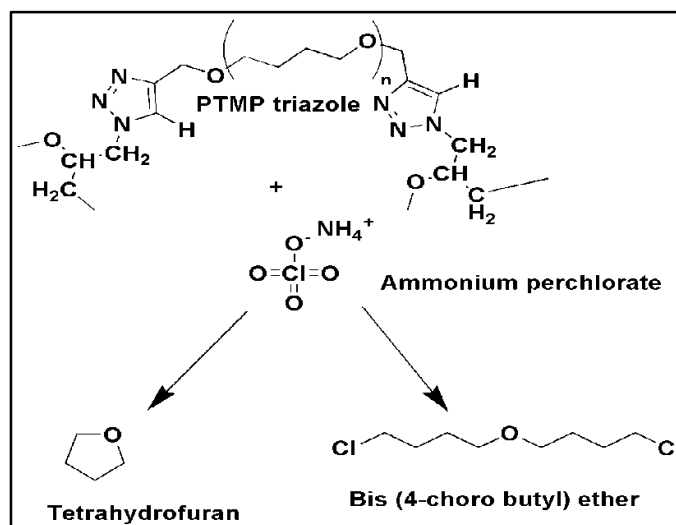


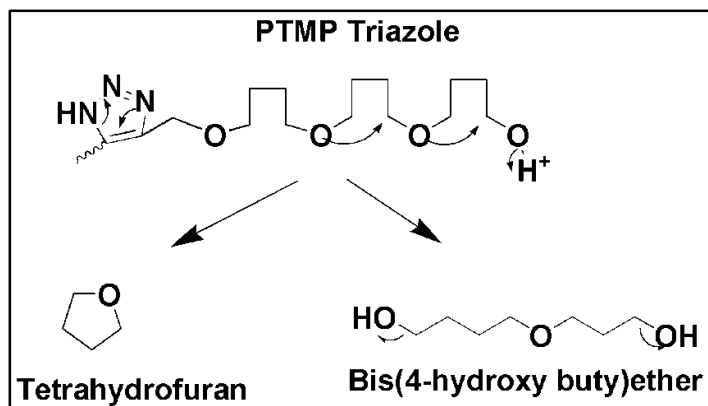
*Figure 5.17* Pyrogram of PTMP triazole-AP at 250°C



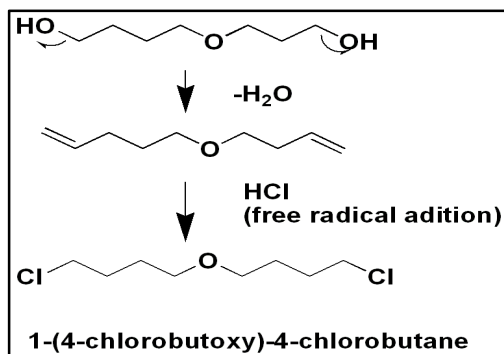
**Scheme 5.4. a)** Low temperature decomposition of PTMP triazole with AP (General Scheme)

Pyrolysis GC MS studies at 450°C, resulted in the evolution of H<sub>2</sub>O, N<sub>2</sub>O, N<sub>2</sub> (RT 1.65), Chloroethene (RT 1.74), Acrylonitrile (RT 2.00), t-butylchloride (RT 2.09), dichloroethene (RT 2.17), THF (RT 2.55), benzene (RT 2.80), chloro benzene (RT 5.18) and cyanobenzene (RT 7.43). The pyrolysis GC-MS at a higher temperature of 450°C, results in the degradation of the triazole ring along with polymer back bone and at higher temperatures, the presence of AP induces formation of aromatic compounds. The decomposition mechanism of PTPB-GAP-AP was found to be similar HTPB-AP pyrolysis reported in literature<sup>44</sup>. Hence, it is not discussed further.

#### 5.4 b Step 1



## 5.4 c) Step 2



*Scheme 5.4. Low temperature decomposition mechanism of PTMP triazole with AP (at 250°C)*

### 5.3.7. Propellant Studies

Propellant studies were done using PTPB-GAP and PTMP-GAP as binder, ammonium perchlorate as oxidiser and aluminium as metallic fuel (2%) for oxidiser loading of 77% by weight. For this, thermochemical performance evaluation of the propellant was carried out and the results are compared with conventional HTPB propellant of the same formulation. In order to compute the thermochemical performance, the heat of formation of the polymers were computed for the two polymers from the heat of combustion data.

#### 5.3.7.1. Thermochemical measurements

The heat of combustion of PTPB and PTMP were measured using bomb calorimeter. The theoretical empirical formula can be calculated from the molecular weight of the polymer. From the heat of combustion data and molecular weight of the polymer, the heat of formation of the polymer as computed. (Table 4).

*Table 5.4. Heat of formation of PTPB and PTMP*

Polymer	Empirical formula	Heat of formation (kJ/mol)
PTPB	$C_{4.1}H_6O_{0.1}$	-290.5
PTMP	$C_4H_8O$	-268.5

Theoretical performance evaluation using NASA CEA programme of low aluminiumised (with 2% aluminium) propellant was completed at an operating pressure

of 6.93MPa and area ratio of 10. The effect of solid loading (AP content) for a fixed aluminium content of 2% (by weight) was computed (Fig.5.18). From the graph, it is observed that peak Isp and flame temperature (Tc) are obtained at ~85%. But for use as gas generators, lower solid loadings are preferred and Isp is not a concern. Hence, for a typical AP content of 77% AP, the performance of PTPB-AP and PTMP-AP propellant were computed and compared with HTPB-AP propellant ( Table 5.5). It is observed that PTPB-AP and PTMP-AP propellant releases higher N<sub>2</sub> and H<sub>2</sub>O content than conventional HTPB urethane-AP propellant. Kohga et al.<sup>48</sup> have reported the performance of PTMO-AP based propellant for a solid loading of 80% where the curing of PTMO was done using IPDI as curing agent through urethane groups. In their computations, the mole fractions of H<sub>2</sub> and H<sub>2</sub>O of the PTMO-AP propellant are different from those of the AP/HTPB propellant. The mole fraction of H<sub>2</sub> for the PTMO-AP propellant is smaller and the fraction of H<sub>2</sub>O for the AP/PTHF propellant is greater than that for the AP/HTPB propellant. In the present case the results obtained for PTMP-AP system is similar although the concentration of gases are different which may be due to the end group modification and difference in AP content. In PTPB-GAP-AP system also, the concentration of H<sub>2</sub>O, N<sub>2</sub> and CO<sub>2</sub> are higher than conventional HTPB-AP propellant.

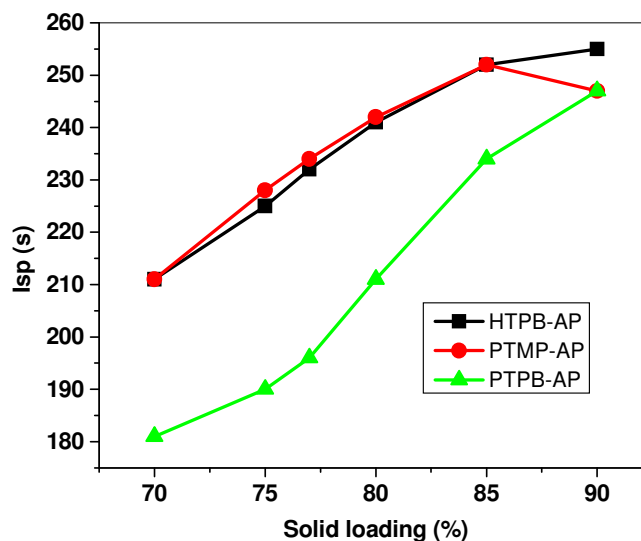


*Fig.5.18. Variation of Isp with solid loading for PTPB, PTMP and HTPB propellant (2% aluminium)*

**Table 5.5. Thermochemical Performance Parameters of PTPB and PTMP Propellant**

(Aluminium content 2%)

Parameters	HTPB-AP (urethane)	PTPB-AP	PTMP-AP
Isp (s)	241.4	235.6	250.6
V.Isp (s)	224.0	220.0	235.1
Flame temperature (Chamber) K	2421	2293	2460
Combustion products , (mass %)			
CO	42.5	7.8	8.6
CO <sub>2</sub>	0.8	16.2	19.9
HCl	15.5	15.5	15.5
H <sub>2</sub>	5.1	1.3	1.3
H <sub>2</sub> O	1.6	12.9	14.2
N <sub>2</sub>	6.3	15.6	15.5
Al <sub>2</sub> O <sub>3</sub>	8.2	8.2	8.2

**5.3.7.2. Propellant processability, mechanical properties, thermal decomposition and burn rate**

The viscosity build up of PTPB-GAP as well as PTMP-GAP propellant were evaluated and compared with HTPB propellant. The ‘end of mix viscosity’ of PTPB-GAP propellant is 173 Pa.s and that of PTMP-GAP propellant is 123 Pa.s as against HTPB-TDI propellant which is 480 Pa.s. The build up rate is lower (Table 5.6) which brings out the obvious advantage of the azide-alkyne curing reaction with respect to processability over the conventional reaction involving diisocyanate-hydroxyl groups of PTPB-GAP and PTMP-GAP propellant.

**Table 5.6** Viscosity build up of PTPB and PTMP propellant

<i>Time in hrs</i>	<i>Propellant Viscosity in Pa.s at 40°C</i>		
	<b>HTPB-TDI</b> <i>(NCO:OH=0.85:1)</i>	<b>PTPB-GAP</b> <i>(-C≡CH:N<sub>3</sub>=1:0.1)</i>	<b>PTMP-GAP</b> <i>(-C≡CH:N<sub>3</sub>=1:1)</i>
0	480	173	123
2	540	368	156
3	900	235	280

The mechanical properties of propellant based on PTPB-triazole and PTMP-triazole were evaluated and compared with HTPB-TDI urethanes (Table 5.7). It is observed that propellant based on PTPB-GAP has a higher tensile strength and lower elongation than HTPB-urethane based propellant. In the case of PTMP triazole propellant, though the tensile strength of the propellant is comparable to HTPB based propellant, the elongation is lower. This could be due to the rigid characteristics of the triazole groups in comparison to urethanes. In literature<sup>49</sup>, the problems of curing of PTMO using isocyanates are elaborated wherein the formation of voids, longer cure time etc are described that can affect the quality of the propellant. The above said problems can be totally overcome by curing through the new triazole route.

**Table 5.7** Mechanical Properties of PTPB and PTMP propellant

<b>Mechanical Properties</b>	<b>HTPB-TDI</b> <i>(NCO:OH=0.85:1)</i>	<b>PTPB-GAP</b> <i>(-C≡CH:N<sub>3</sub>=1:0.1)</i>	<b>PTMP-GAP</b> <i>(-C≡CH:N<sub>3</sub>=1:1)</i>
Tensile strength, (MPa)	0.49	0.80	0.59
Elongation at break (%)	35	10	10
Modulus (MPa)	3.92	2.94	1.96



The thermal decomposition of PTPB-GAP-AP propellant was studied by TG-DSC at a heating rate of 1°C/min (Fig.5.19). The propellant undergoes two-stage decomposition which is similar to HTPB-TDI-AP propellant. The first stage decomposition occurs in the temperature range of 205-265°C corresponding to the decomposition of AP with a weight loss of 23%. The second stage decomposition occurs in the temperature range of 267-312°C which is due to the decomposition of binder and second stage decomposition of AP with a weight loss of 65% and residue obtained at 356°C is 12%. The thermal stability of both the propellant PTPB-GAP and HTPB-TDI-AP propellant are comparable.

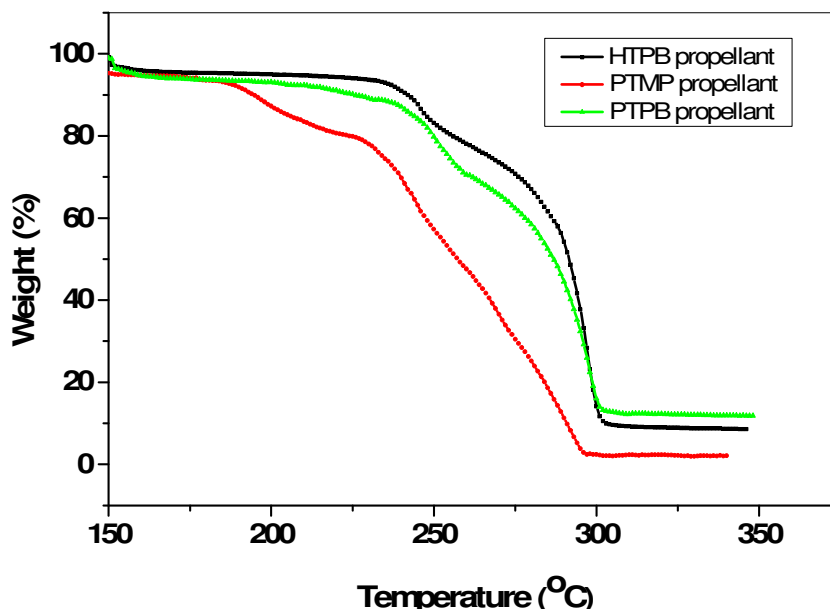


**Fig 5.19.** TGA of PTPB, PTMP-AP and HTPB-TDI-AP propellant

The thermal decomposition of PTMP-GAP propellant was also studied by TG-DSC at a heating rate of 1°C/min (Fig.5.19). PTMP-AP propellant undergoes three-stage decomposition similar to PTMP triazole –AP decomposition. The first stage decomposition occurs in the temperature range of 173-231°C corresponding to binder degradation with a weight loss of 14%. The second stage decomposition occurs in the temperature range of 232-278°C which is due to the combined decomposition of binder and first stage decomposition of AP with a weight loss of 28%. The third stage decomposition occurs in the temperature range of 279-300°C due to second stage decomposition of binder along with AP (52%) and residue at 300°C is 6%.

The burn rate of the PTPB-triazole and PTMP-triazole propellant were evaluated (Table 5.8) and compared with HTPB-TDI urethane based propellants at 6.93 MPa. The burn rate values are found to be comparable for all the propellants at the present solid loading that were used. Kohga et al.<sup>49</sup> have reported the burn rate and Isp of PTMP-AP based propellant, with a solid loading of 80% and that use of PTMO can enhance the Isp. However, the present formulation has been designed for gas generator/igniter application and Isp is not of concern. From the study, it can be concluded that the triazole formation has no adverse effects on the ballistic properties of the propellant and is advantageous with respect to the combustion products.

*Table 5.8 Burn rate of the PTMP and PTPB propellant*

Burn rate (mm/s)	HTPB-TDI	PTPB-GAP	PTMP-GAP
at 6.93 MPa	16.09±0.08	16.10±0.12	15.89±0.05

#### **5.4. CONCLUSIONS**

The end functionalisation of hydroxyl terminated polybutadiene and polytetramethylene oxide by alkyne functional groups through a direct method to yield PTPB and PTMP was carried out. The curing of the two polymers were effected through ‘click mechanism’ by reaction of the alkyne groups with an azide containing polymer namely GAP to form triazole network in the presence of cuprous iodide as cure catalyst. The curing reaction was monitored by DSC. While, curing of PTPB with GAP at higher alkyne-azide molar equivalence phase separation occurs due to difference in solubility parameters of PTPB and GAP. For this system, curing occurs only at an alkyne-azide ratio of 1:0.1. However, PTMP-GAP system is miscible at all concentrations as there solubility parameters are comparable and curing was effected at an alkyne-azide ratio of 1:1. The related kinetic parameters were derived for PTMP-GAP system and were used for predicting the cure profile of the system. The rheological studies reveals that gel point for PTPB-GAP system occurs after 190 minutes (at 80°C) and for PTMP-GAP system, the gel point is reached after 280 minutes in comparison to 120 minutes for HTPB-TDI system, which is advantageous for processing. The mechanical properties of the triazoles

based on PTPB and PTMP systems were evaluated and compared with HTPB-TDI urethanes. DMA studies indicate a biphasic transition for PTPB-GAP with two glass transitions ( $T_g$ ) occurring at  $-40.5^\circ\text{C}$  which may be due to the butadiene backbone and the second one at  $18.4^\circ\text{C}$  may be due to the triazole network. DMA studies of PTMP-GAP triazoles were not done as the samples were brittle.

The thermal decomposition studies indicate that the thermal stability of the neat polymers is improved by triazole formation. The mechanisms of decomposition of the triazoles were elucidated by pyrolysis GC-MS/TG-MS studies. It is observed that the degradation of the polymer does not occur at lower temperature of  $250^\circ\text{C}$ . At higher temperatures, the decomposition is complete and proceeds with cleavage of triazole groups and the polymer back bone. The decomposition of the polymers in the presence of AP was evaluated as oxidiser. The decomposition pattern of PTPB-GAP-AP system is similar to HTPB-TDI-AP decomposition. Unlike in the neat polymer, due to the presence of AP, the decomposition of PTMP-GAP system occurs at a lower temperature with formation of cyclic intermediates mainly tetrahydrofuran. The decomposition at higher temperatures yielded chloro compounds. These are formed by the reaction of AP with the primary pyrolysis product of the polymer. The propellant level studies indicate that better processability with a low end-of mix viscosity and slow build up profile. The mechanical properties and burn rates of the propellant based on PTPB-GAP-AP and PTMP-GAP-AP are comparable to conventional HTPB-TDI-AP propellants. Propellants based on these binders yield more gaseous products which are conducive for specialised applications such as gas generator or as pyrogen igniter propellant.

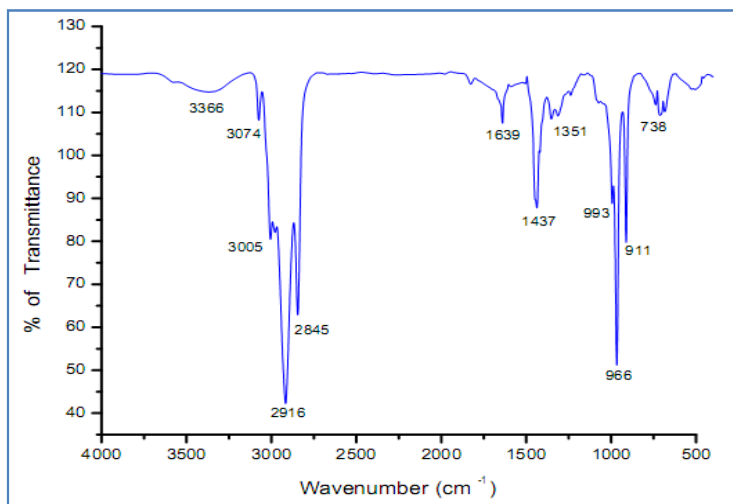
**5.5. REFERENCES**

1. Knifton, JF; Marquis, ET. Texaco Chemical Company. USA, **1992**, *US Patent 5159123*.
2. Ladmiral, V; Mantovani, G; Clarkson, J; Cauet, S; Irwin, JL; Haddleton, DM. *J.Am. Chem. Soc*, **2006**, 128, 4823–4830.
3. Van Caeter, TRIP. **1995**, 3, 227-233.
4. Aoshima, V. *J. Polym. Sci., Part A: Polym. Chem*, **1984**, 22, 2443-2453.
5. Kennedy, N. *J. Polymer Sci. Part A: Polym. Chem*, **1982**, 20, 2809-2817
6. Fraser, R. *Macromolecules*, **1995**, 28, 7256-7261
7. Andrea, BD; Lillo, F; Faure, A, Perut, C. *Acta Astronautica*, **2000**, 47, 103-112.
8. Bruno, C; Accettura, AG; *Advanced Propulsion Systems and Technology Today to 2020*, Vol.223, AIAA, Reston, VA, **2008**
9. Kohga, M; Okamoto, K. *Combustion and Flame*, **2011**, 158,573-582.
10. Kohga, M; Naya, T; Shioya, S. *J.Appl.Polym. Sci*, **2013**, 128, 2089-2097.
11. Fabio, LB; Marcio, AA; Bluma, GS. *J.Appl.Polym. Sci*, **2002**, 83, 838-849.
12. Latha, PB; Adhinarayanan, K; Ramaswamy, R. *Int.J.Adhes.Adhes*, **1994**, 14, 57-61.
13. Milla, R; Colclough, W; Golding, ME; Honey, PJ; Paul, NC;Sanderson, AJ; Stewart, MJ. *ACS Symp Series*, **1992**, 623, 97-102.
14. Chien JWC; Kohara, T; Lilliya, CP; Sarubbi, T; Su, BH;Miller, RS. *J.Polym Sci. Part A: Polym. Chem*, **1980**, 18, 2723-2729.
15. Lugadet, F; Deffieux, A; Fontanille, M. *Eur. Polym J*, **1990**, 26, 1035-1040.
16. Wang, Q; Wang, L; Zhang, X; Mi, Z, *J.Hazardous Material*, **2009**, 172, 1659-1666.
17. Boutevin, G; Ameduri, B; Boutevin, B; Joubert, JP. *J.Appl.Polym. Sci*, **2000**, 75, 1655-1666.
18. Gopala Krishnan, PS; Ayyaswamy, K; Nayak, SK. *J. Macromolecular Science, Part A: Pure and Applied Chemistry*, **2012**, 50,128-138.
19. Huisgen, R. *Angew. Chem. Int. Ed*, **1963**, 2, 633–645.
20. Fireston, R. *J. Organic Chemistry*, **1968**, 33, 2285–2290.
21. Rostovtsev, VV; Green, LG; Fokin, VV; Sharples, KB. *Angew. Chem. Int. Ed*, **2002**, 41, 2596-2599.
22. Binder, WH; Sachsenhoer, R. *Macromol. Rapid Commun*, **2007**, 28, 15-54.
23. Binauld, S; Dameron, D; Hamaide, T; Pascault, JP; Fleury, E; Drockenmuller E. *Chem. Commun*, **2008**, 35, 4138-4140.
24. Aronson, J. *The synthesis and characterization of energetic materials from sodium azide*, PhD Thesis, Georgia Institute of Technology, **2004**.
25. Opsteen, JA, Hest, JCM-v. *Chem.Commun.*,**2005**, 6,57-59.
26. Rahm, M. *Green Propellants*. Stockholm, Sweden.: Royal Institute of Technology; **2010**.
27. Jung, JH; Lee, KH; Koo, BT. *Tetrahedron Letters*, **2007**, 48, 6442-6448.

28. Wang, L; Song, Y; Gyanda, R; Sakhuja, R; Nabin, K; Hanci, C; Gyanda, K; Mathai, S; Sabri, F; Ciaramitaro, DA; Bedford, CD; Katritzky, AR; Duran, RS *J.Appl.Polym. Sci.*, **2010**, 117, 2612-2621
29. Song, Y; Wang, L; Gyanda, R; Sakhuja, R; Cavallaro, M; Jackson, DC; Meher, NK; Ciaramitaro, DA; Bedford, CD; Katritzky, AR; Duran, RS. *J.Appl.Polym. Sci.*, **2010**, 117, 473-478
30. Lee, DH; Kim, KT; Jang, Y; Lee, S; Jeon, HB; Paik, H; Min, BS; Kim, W. *J.Appl.Polym. Sci.*, **2014**, DOI: 10.1002/APP.40594
31. Ding, Y; Hu, C; Guo, X; Che, C; Huang, J. *J.Appl.Polym. Sci.*, **2014**, doi: 10.1002/app.40007
32. Frankland, J A.; Edwards, HG M.; Johnson, AF; Lewis, IR, Poshyachinda, S, *Spectrochimica Acta.*, **1991**,.47A,1511-1524
33. Huang, S; Lai J-Y. *J.Membrane Science*, **1995**, 105, 137-145.
34. Min, BS; Baek, G; Ko, SW. *J.Ind.Chem.Eng.*,**2007**, 13, 373-379.
35. Mark, JE. *Polymer Data Hand Book*, Oxford University Press, New York, **1999**.
36. Kissinger, HE. *J ResNatBurStand*, **1956**, 57, 217-221.
37. Sun, S; Wu, P. *J Phys Chem A*, **2010**, 114, 8331-8336
38. Bräse, S; Gil, C; Knepper, K; Zimmermann, V. *Angew. Chem. Int.Edn*, **2005**, 44, 5188-5240.
39. Eroglu, MS. *J.Appl.Polym. Sci.*, **1998**, 70, 1129-1135.
40. Wingborg, N. *Polymer Testing*, **2002**, 21, 283-287
41. Kohga, M. *Propellants, Explos.Pyrotech.*, **2013**, 38, 366-331
42. Kohga, M; Naya, T; Shioya, S. *J.Appl.Polym. Sci.*, **2013**, 128,2089-2097.
43. Catherine, KB. *Thermoanalytical investigations on curing and decomposition of polyol binders*. Thiruvananthapuram: University of Kerala. India; **2003**
44. Arisawa, H; Brill, TB. *Combustion and Flame*, **1996** 106, 131-143.
45. Yang, V; Brill, TB; Ren, -Z. *Solid Propellant Chemistry, Combustion and Motor Interior Ballistics*, Vol 185, Progress in Astronautics and Aeronautics, AIAA.Inc, Virginina, **2000**.
46. Lattimer, RP. *J.Anal.Appl.Pyrol.*, **2001**, 57, 57-66.
47. Lattimer, RP; Williams, RC. *J.Anal.Appl.Pyrol*, **2002**, 63, 85-104.
48. Ganesh, K; Sundarrajan, S; Kishore, K, Ninan, KN; George, B, Surianarayanan, M. *Macromolecules*, **2000**, 33, 326-330.
49. Kohga, M; Miano, W; Kojima, T. *J.Prop.Power*, **2006**, 22, 1418-1421.

## SUPPORTING INFORMATION

5A.1 a



5A.1 b

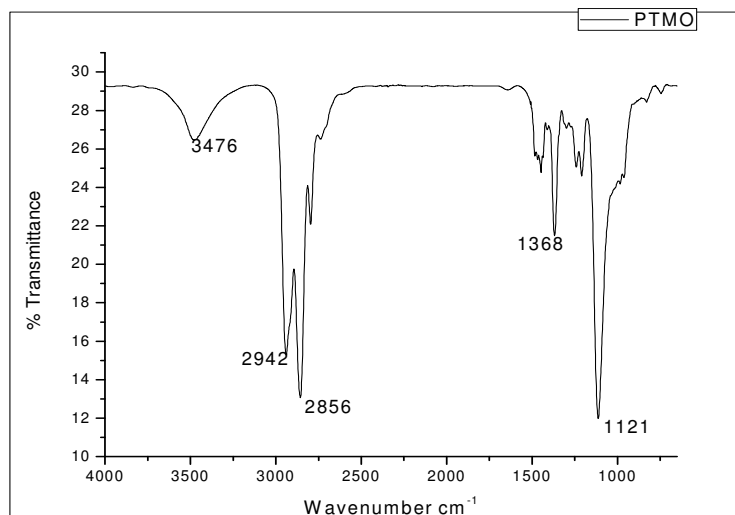
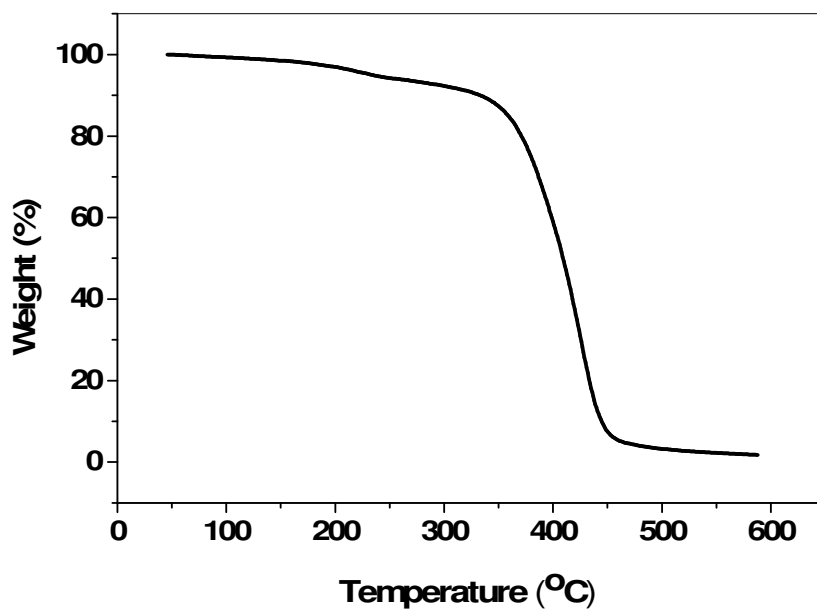


**Fig.5A.1** FTIR spectrum of a) HTPB b) PTMO



50-650,10c/min

ptmp-gap-ap 2170 (22.702) Cm (1796:2301-(11117:1638+2462:2671))

50-650,10c/min/min, 08-Apr-2014 + 15:02:12

1: Scan EI+  
8.82e8

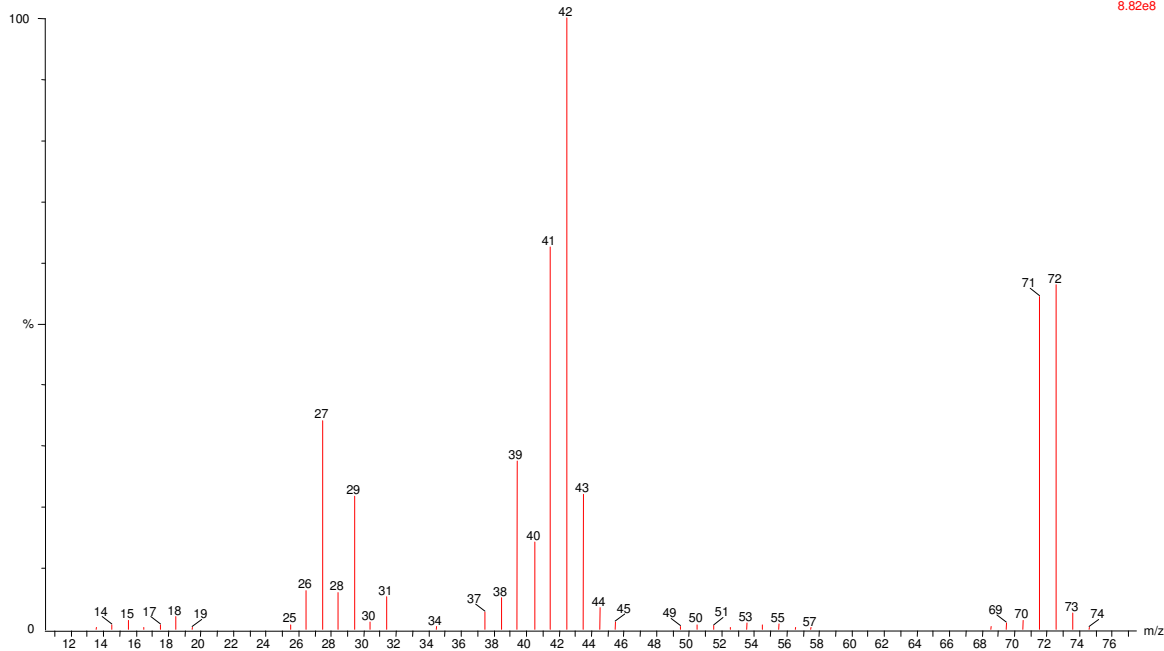


*Fig.5A.2. Typical TG-MS Curve for PTMP-GAP-AP System (First stage)*

*(Heating rate 5°C/min)*

*Chapter 6*

**Thermal Decomposition Aspects of a Diazido Ester**

---

❖ *A part of the results from this chapter has been published in*

***Reshmi, S; Vijayalakshmi, KP; Thomas, D; George, BK; Nair, CPR. Thermal Decomposition of a Diazido Ester: Pyrolysis GC-MS and DFT Study, J. Analytical and Applied Pyrolysis, 2013, 104, 603-608***



### Abstract

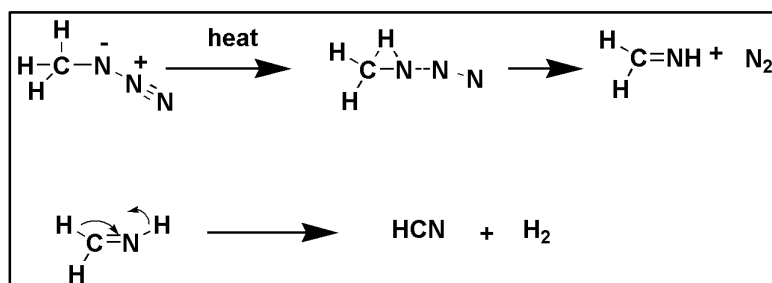
*Azides are versatile compounds with wide applications in organic synthetic reactions, as described in previous chapters. Thermal stability of azides, their derivatives and their decomposition products have a direct bearing on the performance of these molecules in propellants binders. In the present chapter, the thermal decomposition of a typical diazido ester 1, 6-bis (azidoacetoxy) hexane (HDBAA) was investigated by thermogravimetric–differential scanning calorimetric studies. The mechanism of decomposition was elucidated using pyrolysis gas chromatography-mass spectrometric techniques. At 230°C, HDBAA, preferentially form the corresponding diimine by elimination of N<sub>2</sub>. The decomposition of the diazido ester was complete at 500°C yielding N<sub>2</sub>, CO, CH<sub>2</sub>NH and HCN with the concurrent formation of diols and dienes. The experimental findings were rationalized through density functional theory (DFT) based computational analysis.*

## 6A.1 INTRODUCTION

In recent years, azides are finding wide application as building blocks in organic synthetic chemistry,<sup>1</sup> biological field for photo affinity labelling<sup>2</sup> and as energetic additives for solid propellants formulations.<sup>3-7</sup>

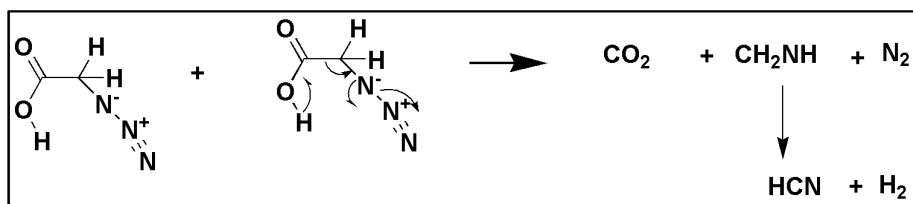
Thermal decomposition, thermodynamic properties and the chemical nature of the decomposition products of energetic materials are key factors in the ignition and combustion processes.<sup>8-9</sup> The basic understanding of these processes may also aid in identifying any toxic and hazardous molecule that can emanate during its decomposition and hence, essential for assessing the hazard characteristics of energetic materials and to develop reliable models for their risk analysis.

Azides are important in propellant formulations because of the exothermic release of nitrogen, often explosively on heating.<sup>10-11</sup> Since, azides are heterogeneous in nature, the mechanism of decomposition, their decomposition pathways and products vary greatly. Studies<sup>12</sup> on the thermal decomposition of methyl azide by photoelectron spectroscopy (PES) and infrared matrix isolation spectroscopy report that there are two distinct decomposition pathways. The initial step is elimination of N<sub>2</sub> to form a nitrene, which subsequently isomerise to the imine by a 1, 2-hydrogen shift. The imine can further dissociate to HCN and H<sub>2</sub> as shown in Scheme 6a.1.



*Scheme 6a.1 Imine formation in azides by 1, 2 H shift*

In the case of organic azido carboxylic acids, CO<sub>2</sub> and CH<sub>2</sub>NH are released followed by the release of HCN (Scheme 6a.2) and during decomposition of methyl 2-azidopropionate, the imine formed in the first step, further decomposes to form CH<sub>3</sub>OH, CO, and CH<sub>3</sub>NH<sub>2</sub> through accessible energy barriers. The second route yields CO<sub>2</sub>, CH<sub>4</sub> and CH<sub>3</sub>CN as decomposition products.<sup>13-15</sup>



**Scheme 6a.2.** Decomposition mechanism of an azido carboxylic acid

Though azides like ethylene glycol bis(azidoacetate) (EGBAA), diethyleneglycol bis(azidoacetate) (DEGBAA), trimethylol nitromethane tris(azidoacetate) (TMNTA), pentaerythritol tetrakis (azidoacetate) (PETKAA) etc.<sup>16-19</sup> have been used in propellant formulations, until now there have been no reports on the thermal decomposition mechanism of diazido compounds, where one azide group may influence the decomposition of the other.

The present chapter discusses the thermal decomposition characteristics of a diazido ester namely 1,6-bis (azidoacetoyloxy) hexane (HDBAA). The mechanism for the thermal decomposition has been suggested and has been rationalized using density functional theory calculations (DFT).<sup>20-23</sup> The diazido ester HDBAA can be used as energetic plasticiser in composite solid propellants or as curing agents for alkene hydrocarbon binders such as hydroxyl-terminated polybutadiene (HTPB).

## 6A.2. EXPERIMENTAL

### 6A.2.1 Materials

1,6-hexanediol, sodium azide, toluene-4-sulfonic acid and monochloroacetic acid were used for the study as described in Chapter 2. Dimethyl sulphoxide, toluene and dichloromethane were the solvents used.

### 6A.2.2 Instrumental

FTIR spectra and <sup>1</sup>H NMR analyses were done. Thermal decomposition was studied using a simultaneous TG-DSC at a heating rate of 5°C/min in nitrogen atmosphere. Pyrolysis GC-MS studies were conducted using a Thermo Electron Trace Ultra GC directly coupled to a Thermo Electron Polaris Q (Quadrupole ion trap) mass spectrometer and SGE pyrolyser as described in Chapter 2.

**6A.2.3. Synthesis and characterization of HDBAA**

HDBAA was synthesised following a two-step procedure.<sup>26-27</sup> In the first step, 1,6-bis(chloroacetoxy) hexane (HDBCA) was synthesized by esterification reaction of 1,6-hexanediol with monochloroacetic acid in toluene in the presence of toluene-4-sulfonic acid. This reaction was carried out in a flask equipped with reflux condenser and a Dean-Stark water trap was placed with 11.1 g (0.094 mol) of 1,6-hexane diol, 19.3g (0.204 mol) 1-chloroacetic acid, 0.0035 g toluene-4-sulfonic acid-monohydrate, and 35 ml toluene. The mixture was heated under reflux (130°C) with stirring until no more azeotrope from toluene-water separated in the Dean-Stark trap. Then the solution was cooled down to room temperature and washed with 5% sodium bicarbonate solution, two times with water, and dried with sodium sulphate. The solvent was then distilled off and the product HDBCA was isolated. Yield: ~61%.

HDBCA was converted to the azide derivative HDBAA by reaction with sodium azide in dimethyl sulphoxide at 50°C (Scheme 6a.3) in a three necked flask under nitrogen blanket. For the reaction, typically 5.0 g (0.019 mol) of HDBCA was reacted with 2.3 g (0.035 mol) sodium azide in 20 ml dimethylsulphoxide (DMSO) solvent for 20 hrs. The product was isolated by extracting with dichloromethane and concentrated under reduced pressure. Yield: ~85%.

**HDBCA FTIR** (NaCl plates): 2942  $\text{cm}^{-1}$  and 2863  $\text{cm}^{-1}$  (-CH-), 2947  $\text{cm}^{-1}$  (-CH), 2129  $\text{cm}^{-1}$  (-C≡C), 1755  $\text{cm}^{-1}$  (-COO), 788  $\text{cm}^{-1}$  (-C-Cl), . <sup>1</sup>H NMR (300 MHz $\delta$ , ppm, CDCl<sub>3</sub>): 1.4, 1.7 (-CH<sub>2</sub>-);, 4.08, (-CH<sub>2</sub>-Cl -); 4.2 (-CH<sub>2</sub>-COO-);4.75 (t, 2H, CH<sub>2</sub>-O).

**HDBAA FTIR** (NaCl plates): 2942  $\text{cm}^{-1}$  and 2863  $\text{cm}^{-1}$  (-CH-), 2947  $\text{cm}^{-1}$  (-CH s), 2129  $\text{cm}^{-1}$  (-C≡C), 1755  $\text{cm}^{-1}$  (-COO), 2108  $\text{cm}^{-1}$  (-C-N<sub>3</sub>), . <sup>1</sup>H NMR (300 MHz $\delta$ , ppm, CDCl<sub>3</sub>): 1.4, 1.7 (-CH<sub>2</sub>-);, 3.85, (-CH<sub>2</sub>-N<sub>3</sub> -); 4.2 (-CH<sub>2</sub>-COO-);4.75 (t, 2H, CH<sub>2</sub>-O).

**6A.2.4. Computational calculations**

Geometry optimizations were performed with BLYP functional in conjunction with 6-31G(d,p) basis set as implemented in the program package Gaussian09<sup>28</sup>. During geometry optimization no symmetry constraints were

imposed. Default settings of SCF and geometry convergence criteria were used for all the calculations. No corrections were made for the basis set superposition errors (bsse). In general, DFT methods give negligible values for bsse. More accurate energies were obtained from single point calculations using BLYP/6-311++G(d,p) method and these energies were subsequently used in the analyses of chemical mechanisms. All transition states were confirmed by their characteristic single imaginary frequency in the normal vibrational mode.

## 6A.3. RESULTS AND DISCUSSION

### 6A.3.1. Synthesis and characterisation of HDBAA

The diazido ester HDBAA (the molecular structure of HDBAA is depicted in Fig. 6a.1) was synthesised based on a reported procedure<sup>26-27</sup> by a two step process. The first step involves esterification of 1,6-hexane diol with chloroacetic acid resulting in the formation of 1,6-bis (chloroacetoxy) hexane (HDBCA). HDBCA was then converted to HDBAA by azidation using sodium azide. (Scheme 6a.1)

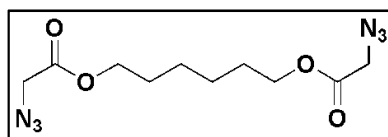
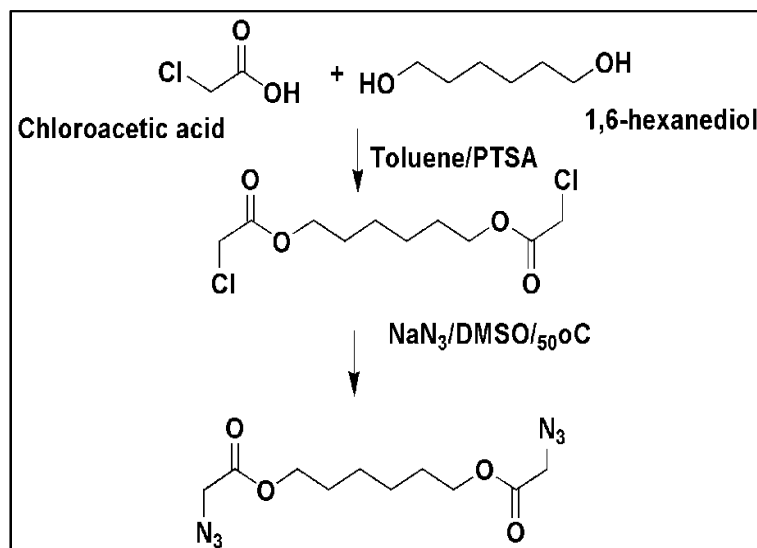


Fig. 6a.1. Structure of the HDBAA



Scheme 6a.1 Synthesis Scheme of HDBAA

### 6A.3.2 Thermal decomposition studies of HDBAA

Thermogravimetric analysis (TGA) of HDBAA was done at a heating rate of 5°C/min in nitrogen atmosphere. HDBAA undergoes three-stage decomposition as shown in Fig. 6a.2. The first stage decomposition occurs in the temperature range of 138-262°C with a weight loss of ~61 %. The second stage degradation occurs in the temperature range of 263-337°C and is associated with a weight loss of 16%. The third stage occurs in the temperature range of 338-494°C with a mass loss of 16%.

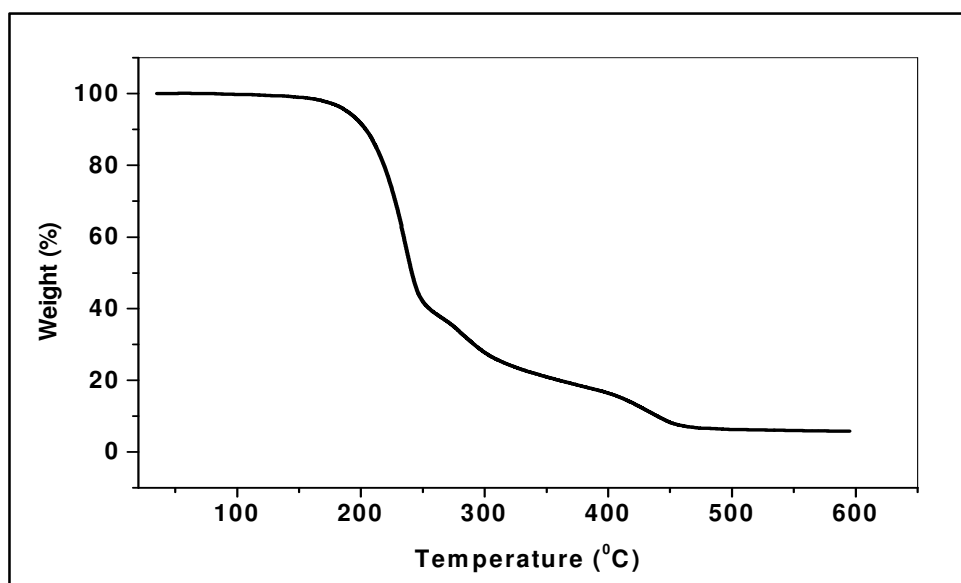


*Fig. 6a.2. TGA curve of HDBAA (Heating rate 5 °C/min in N<sub>2</sub> atmosphere)*

### 6A.3.3 Pyrolysis GC-MS Studies

Pyrolysis GC-MS experiment was done at 230°C and 500°C. The pyrogram (Fig. 6a.3a) at 230°C showed two major peaks, one at retention time (RT) 20.86 corresponding to unreacted HDBAA and the other at RT 15.99 corresponding to the decomposition product. The pyrogram at 500°C (Fig. 6a.3b) showed four major peaks corresponding to RT 1.63, 2.32, 5.53 and 10.11. Some minor peaks are also observed which could be due to secondary pyrolysis products formed by recombination reactions.

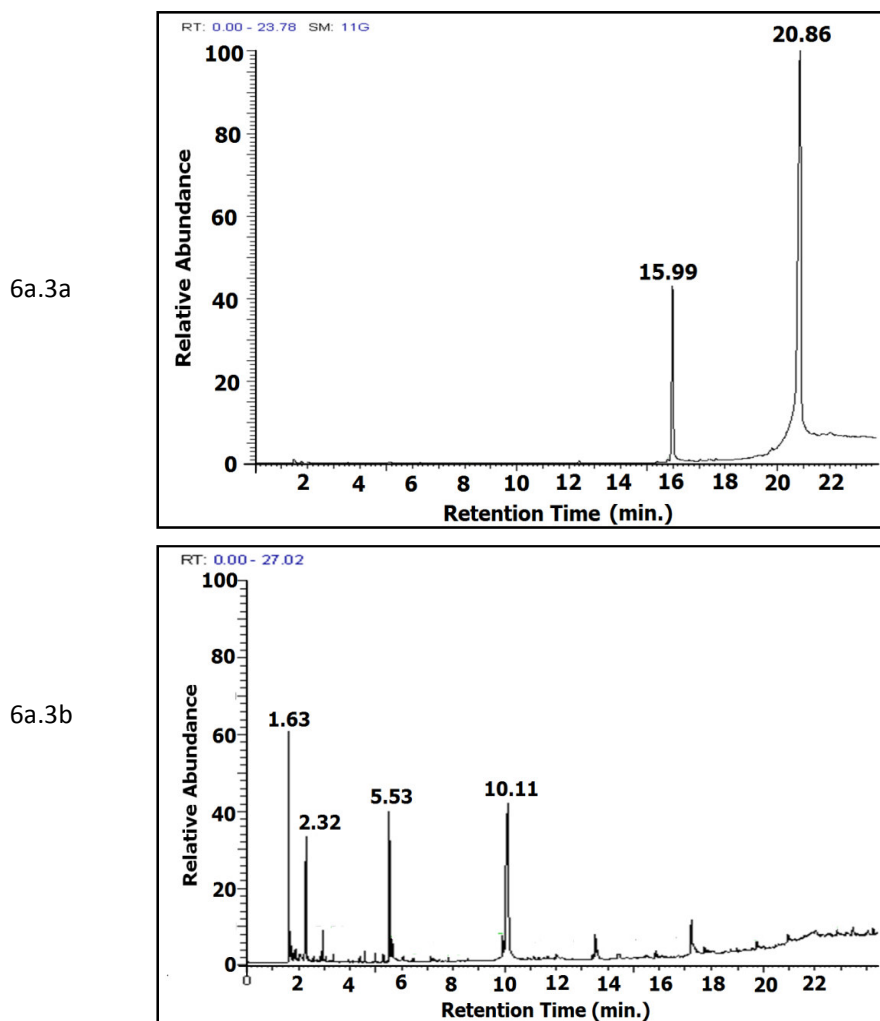
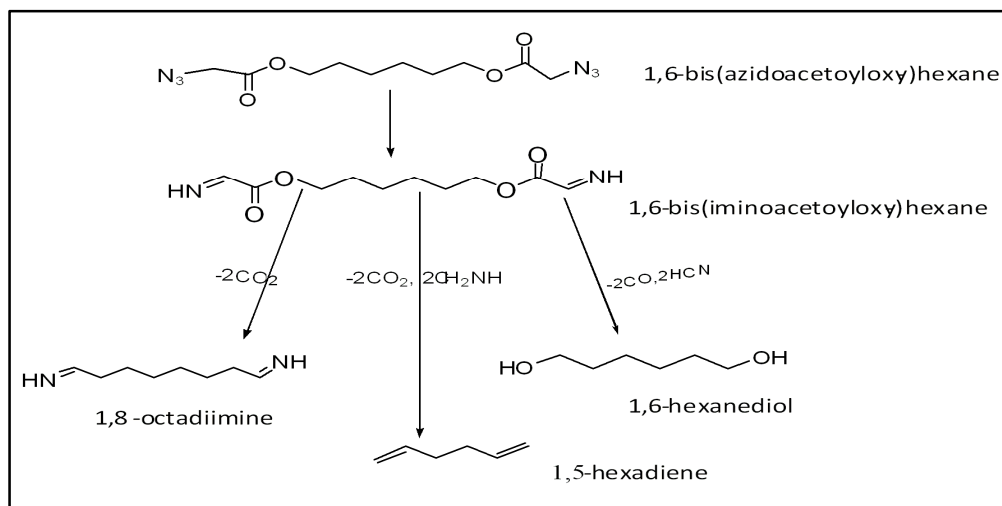


*Fig. 6a.3. Pyrogram of HDBAA at (a) 230°C and (b) at 500°C*

A probable mechanism for the thermal decomposition is depicted in Scheme 6a.4. At 230°C, elimination of  $N_2$  can occur from the terminal azido groups to yield 1,6-bis(iminoacetoxy) hexane (HDBIA) and this corresponds to RT 15.99 (Fig. 6a.3a). At 500°C, (Fig. 3b) HDBIA undergoes further decomposition to yield 1, 8-octadiimine (RT 2.32) by eliminating  $CO_2$  (RT 1.63). Two other well defined products, 1, 5-hexadiene (RT 5.53) due to elimination of  $CO_2$ ,  $CH_2NH$  and 1,6-hexanediol (RT 10.11) by evolution of  $CO$  and  $HCN$  are also detected in the pyrogram. This corroborates the three stage decomposition observed in TG-DSC studies. The observation related to formation of imine and also elimination of  $CO_2$ ,  $CH_2NH$  are in concordance with literature<sup>14-15</sup>.



**Scheme 6a.4.** Mechanism for thermal decomposition of HDBAA

DFT study results discussed in the following studies given in the following section support the mechanism given in Scheme 6a.4. The transition state (TS1) for the elimination of  $\text{N}_2$  from one of the terminal azido groups is depicted in Fig 6a.4a. The transition state is characterized by breaking of N-N bond (N...N distance 2.21 Å) and a simultaneous 1, 2-hydrogen shift from carbon to nitrogen (N...H distance 1.70 Å), with an initial activation energy ( $E_{\text{act}}$ ) of 155.1 kJ/mol. The same mechanism holds true for elimination of the second  $\text{N}_2$  from the other azido group (Fig 6a.4b. TS2) to yield HDBIA. However elimination of the second  $\text{N}_2$  requires much lower activation energy of 163.9 kJ/mol. Energy profile for this two step reaction is presented in Fig.6a.5. The reaction is highly exothermic yielding 387.9 kJ/mol of energy.

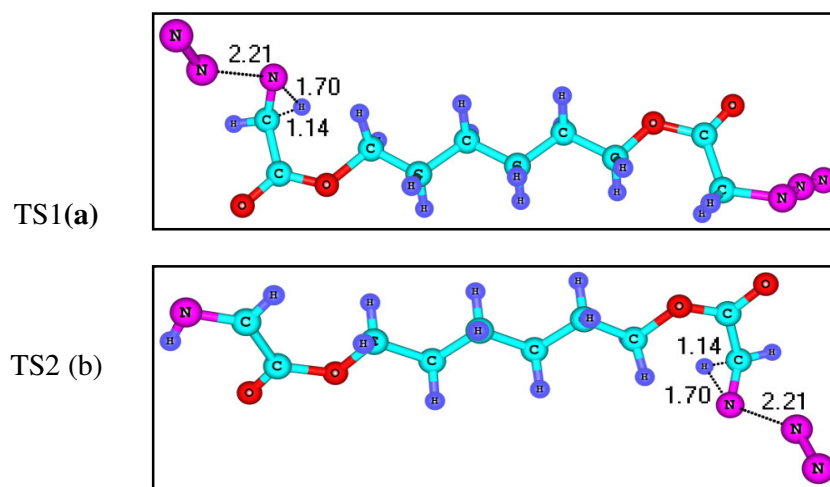


**Fig. 6a.4.** (a) TS1 for elimination of first  $\text{N}_2$  from HDBAA and (b) TS2 for the elimination of  $\text{N}_2$  from mono-imine intermediate.



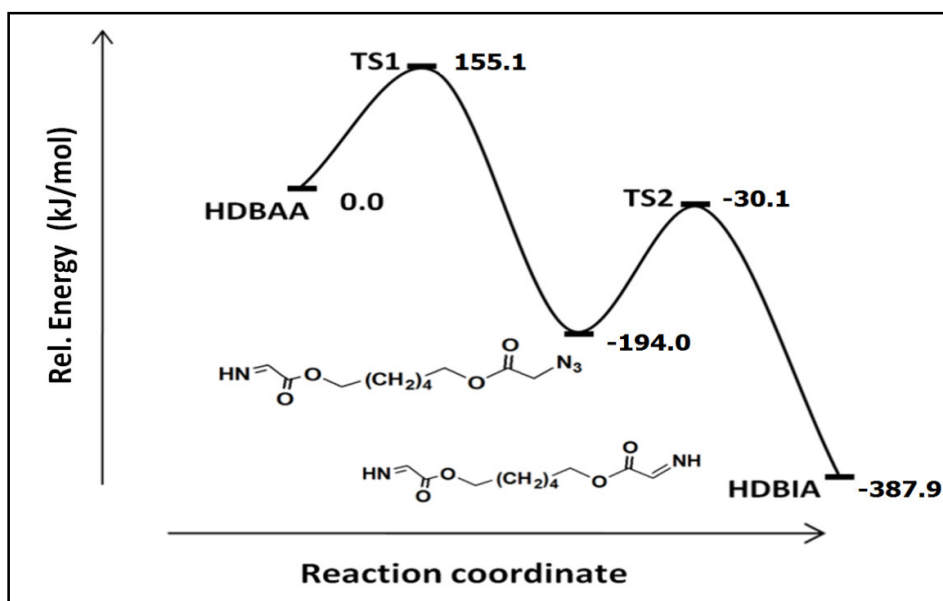
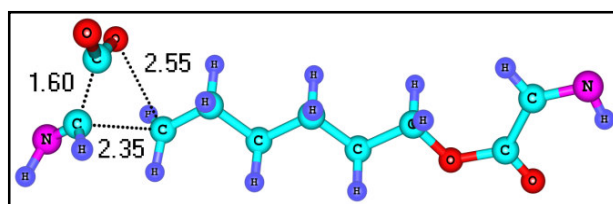
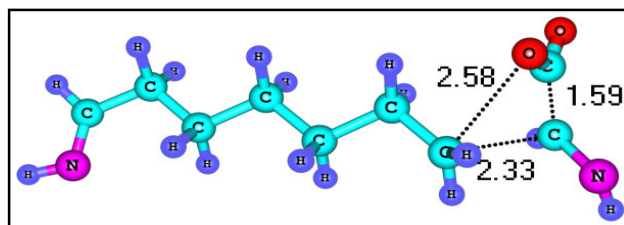


Fig. 6a.5 Energy profile diagram of  $N_2$  elimination reactions of HDBAA

All other products found in the pyrogram at higher temperature arise from the decomposition of HDBIA. Formation of 1,8-octadiimine is through elimination of two  $CO_2$  molecules from HDBIA. The transition states viz. TS3 and TS4 in Fig 6a and 6b corresponds respectively to the elimination of each  $CO_2$  from HDBIA. The energy profile diagram (Fig. 6a.7) indicates that the overall reaction is 255.4 kJ/mol exothermic. HDBIA further decomposes at high temperature ( $500^\circ C$ ) only due to the high energy barrier (281.3 -276.7 kJ/mol).

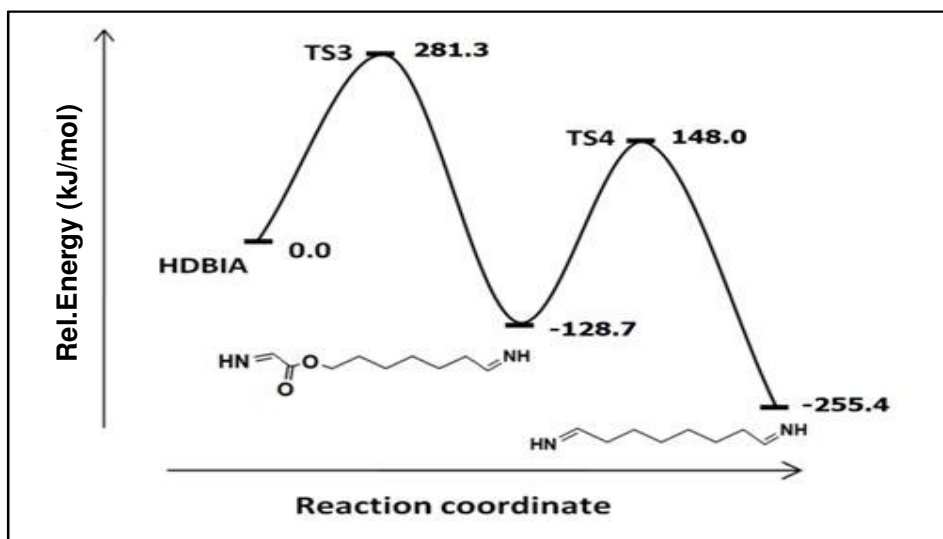


TS3 (a)



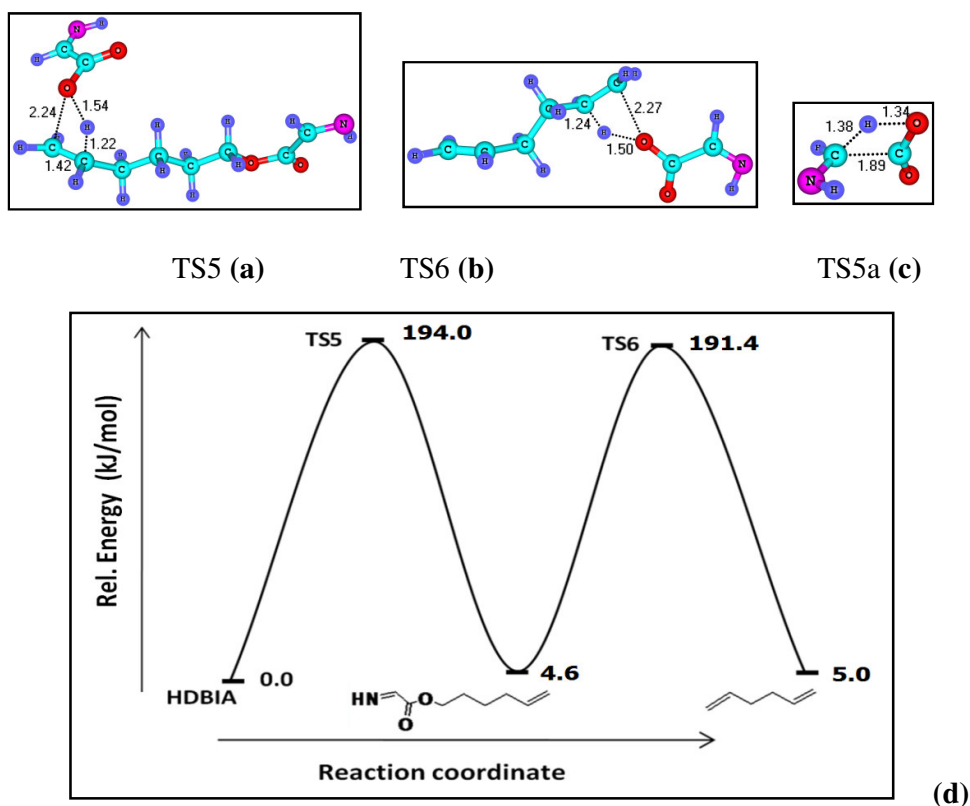
TS4 (b)

Fig. 6a.6 (a) TS3 & (b) TS4 for elimination of two  $CO_2$  molecules from HDBIA



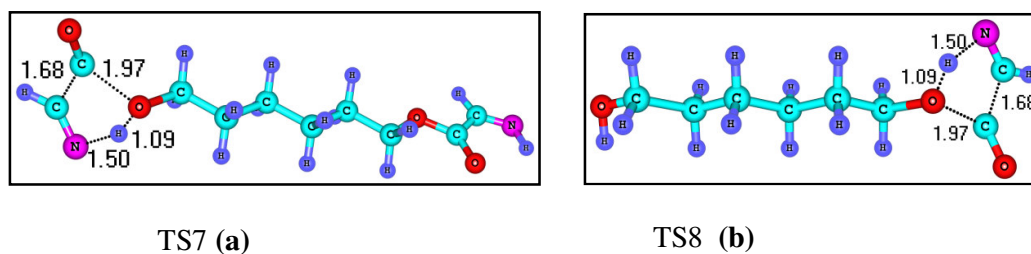
**Fig. 6a.7.** Energy profile diagram for decomposition reaction of HDBIA to octadiimine

1,5-hexadiene is formed by elimination of iminoethanoic acid (NHCHCOOH) from HDBIA, while removal of CO and HCN from HDBIA can yield 1,6-hexanediol. DFT studies suggest that step-by-step elimination of two molecules of NHCHCOOH can take place from HDBIA (Fig.6a.8c). Iminoethanoic acid (NHCHCOOH) may undergo decomposition via TS5a to yield CO<sub>2</sub> and CH<sub>2</sub>NH. NHCHCOOH elimination from HDBIA takes place through the four-membered cyclic transition state TS5 (Fig 6a.8a) and the decomposition product, being an olefinic intermediate undergoes further decomposition via TS6 (Fig. 6a.8b) to yield 1, 5-hexadiene. TS5 and TS6 have similar structural features at the activated cyclic region as both essentially describe similar reactions. The energy profile diagram given in Fig. 6a.8d shows that TS5 requires E<sub>act</sub> of 194 kJ/mol while that of TS6 is 186.8 kJ/mol. The reaction leading to intermediate monoene and the next step leading to 1, 5-hexadiene is slightly endothermic with enthalpy change of 4.6 and 5.0 kJ/mol respectively. The decomposition of NHCHCOOH is exothermic by 43.5kJ/mol and requires E<sub>act</sub> of 283.3kJ/mol. The products CO<sub>2</sub> and CH<sub>2</sub>NH from TS5a are detected in the pyrogram.



**Fig. 6.a8** (a) TS5 (b) TS6 (c) TS5a for elimination of  $\text{CO}_2$  and  $\text{CH}_2\text{NH}$  from HDBIA (d) Energy profile diagram for the formation of 1,5-hexadiene from HDBIA.

Formation of 1,6-hexanediol from HDBIA is energetically demanding as it has to pass through five-membered cyclic transition states TS7 and TS8 which are described in Fig. 6a.9a and 9b respectively. These transition states describe concerted bond breaking processes which lead to simultaneous expulsion of CO and HCN. In TS7, O-CO (1.97 Å) and C-CO (1.68 Å) bonds are partially ruptured which facilitates the formation of CO. While this happens, the alkoxide moiety accepts the migrating hydrogen from the imine functionality to form the alcohol derivative. Very similar bond breaking and bond forming sequences are seen in TS8 too.



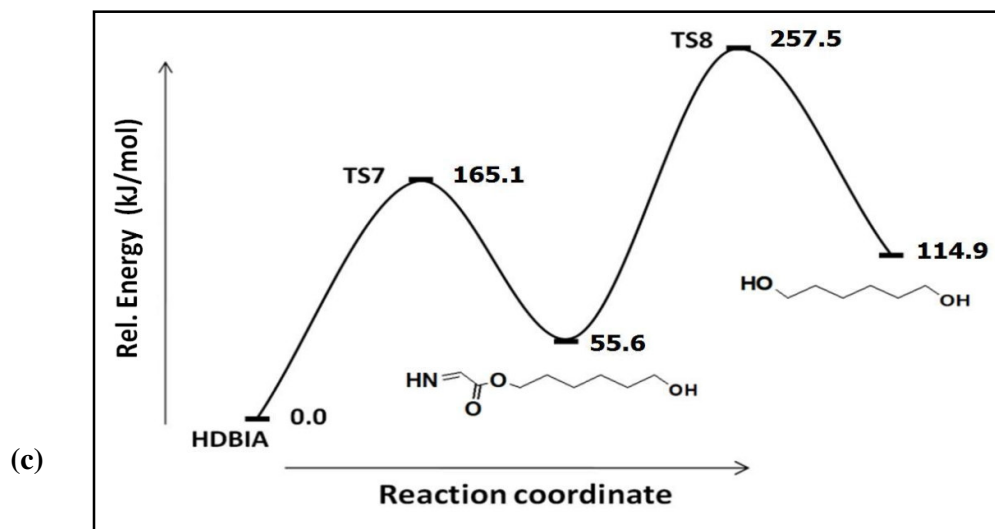


**Fig. 6a.9.** Formation of CO and HCN via (a) TS7 and (b) TS8. (c) Energy profile diagram for 1, 6-hexanediol formation from HDBIA.

The intermediate product formed by mono elimination of CO and HCN is 55.6kJ/mol higher in energy than by the reactant diimine while the final product is 114.9 kJ/mol higher in energy than diimine (Fig.6a.9c). The first step requires a lower activation barrier 165.1kJ/mol compared to the second elimination. Since the  $E_{act}$  for the second step is 201.9kJ/mol, the reaction can take place only at high temperature which rationalizes its formation at 500°C during pyrolysis.

#### 6A.4. CONCLUSIONS

Thermal decomposition of a diazido ester HDBAA which can be used as an energetic plasticiser or curing agent in solid propellants was investigated by pyrolysis GC-MS studies and DFT calculations. The diazide undergoes highly exothermic decomposition by elimination of nitrogen leading to the formation of imine (HDBIA) initially at 230°C. HDBIA decomposes at higher temperature of 500°C to form diimines by elimination of CO<sub>2</sub>, diol through elimination of CO<sub>2</sub> and HCN and dienes due to CO<sub>2</sub>, CH<sub>2</sub>NH elimination. The insight into the thermal decomposition mechanism of HDBAA provides valuable inputs for assessing their thermal stability and decomposition products for risk analysis as well as for application in solid propellants.

**6A.5. REFERENCES**

1. Bräse, S; Gil, C; Knepper, K; Zimmermann, V. *Angew. Chem. Int. Ed.*, **2005**, 44, 5188-5240
2. Schuster, GB; Platz, MB. *Adv. Photochem.*, **1992**, 17, 69-143.
3. Abhay, KM; Pathak, D. *Res.J. Chemistry and Environment*, **2010**, 14, 94-103.
4. Bunte, G; Pontius, H; Kaiser, M. *Propellants, Explos. Pyrotech.*, **1999**, 24, 149-155.
5. Guery, JF; Chang, IS; Shimada, T; Glick, M; Boury, D; Robert, E, Napior J, Wardle R, Perut C, Calabro M, Glick R, Habu H, Sekino N, Vigier G, d'Andrea B, *Acta Astronautica*, **2010**, 66, 201-219.
6. Nair, UR; Asthana, SN; Rao, AS; Gandhe, BR. *Defence Science Journal*, **2010**, 60 137-151.
7. Cumming, AS. *J.Aerospace Technology and Management*, **2009**, 1, 161-166.
8. Manelis, GB. *Thermal Decomposition and Combustion of Explosives and Propellant*, Taylor & Francis Inc., New York, **2003**.
9. Naik, NH; Gore, GM; Gandhe, BR; Sikder, AK. *J.Hazardous Materials*, **2008**, 159, 630-635.
10. Damse, RS; Singh, A. *Defence Science Journal*, **2008**, 58, 86-93.
11. Brochu, S; Ampleman, G. *Macromolecules*, **1996**, 29, 5539-5545.
12. Nguyen, MT; Sengupta, D; Ha, TK. *J. Physical. Chem A*, **1996**, 100, 6499-6503.
13. Dyke, JM; Levita, G; Morris, A; Ogden, JS; Dias, AA; Algarra, M; Santos, JP; Costa, ML; Rodrigues,P; Barros, MT. *J. Physical. Chem. A*, **2004**, 108, 5299.-5264
14. Dyke, JM; Levita, G; Morris, A; Ogden, JS; Dias, AA; Algarra, M; Santos, JP; Costa ML; Rodrigues, P; Andrade, MM; Barros, MT. *Chemistry – A European Journal*, **2005**, 11, 1665-1676.
15. Pinto, RM; Dias AA, Costa, ML, Rodrigues P, Barros MT, Ogden JS, Dyke JM, *J. Physical Chemistry A*, **2011**, 115, 8447-8457.
16. Oyumi, Y. *Propellants, Explos. Pyrotech.*, **1992**, 17, 226-231.
17. Feng, Z; Hou, Z; Li, Z. *Beijing Ligong Daxue Xuebao/Transaction of Beijing Institute of Technology*, **1996**, 16, 138-145.
18. Fujimura, K. *Science and Technology of Energetic Materials*, **2006**, 67, 33-39.
19. Gaur, B; Lochab, B; Choudhary, V; Varma, IK; *J. Macromolecular Science - Polymer Reviews*, **2003**, 43, 505-545.
20. Becke, AD. *J. Chem. Phys A*, **1993**, 98, 5648-5652.
21. Arenas, JF; Marcos, JI; Otero, JC; Tocón, IL; Soto, J. *Int. J. Quantum Chemistry*, **2001**, 84, 241-248.
22. Chen, FF; Wang, F. *Molecules*, **2009**, 14, 2656-2668.
23. L'Abbe, G. *Chemical Reviews*, **1969**, 69, 345.
24. Pearson, AWH; *The chemistry of heterocyclic compounds, Vol.59, Synthetic applications of 1,3 dipolar cycloaddition chemistry towards heterocycles and natural product, edited by, John Wiley & Sons. Inc.*, **2002**.

25. Manzara, PA, *Azido polymers having improved burn rate*, US 5681904 A **1996**
26. Ou Y, Chen B, Yan H, Jia H, Li J, Dong S, *J. Prop.Power*, 1995,11, 838.
27. Agrawal JP, Hodgson R, *Organic Chemistry of Explosives*, John Wiley & Sons Ltd, England, **2007**.
28. Frisch, M; Trucks, GW; Schlegel, HB; Scuseria, GE; Robb, MA; Cheeseman, JR; Scalmani, G; Barone, V; Mennucci, B; Petersson, GA; Nakatsuji, H; Caricato, M; Li, X; Hratchian, HP; Izmaylov, AF; Bloino, J; Zheng, G; Sonnenberg, JL; Hada, M; Ehara, M; Toyota, K; Fukuda, R; Hasegawa, J; Ishida, M; Nakajima, T; Honda, Y; Kitao, O; Nakai, H; Vreven, T; Montgomery, J; Peralta, JE; Ogliaro, F; Bearpark, M; Heyd, JJ; Brothers, E; Kudin, KN; Staroverov, V; Kobayashi, R; Normand, J; Raghavachari, K; Rendell, A;Burant, JC; Iyengar, SS; Tomasi, J; Cossi, M; Rega, N; Millam, J M; Klene, M; Knox, J E; Cross, JB; Bakken, V;Adamo, C; Jaramillo, J; Gomperts, R; Stratmann, RE; Yazyev, O;Austin, AJ; Cammi, R; Pomelli, C; Ochterski, JW; Martin, RL; Morokuma, K; Zakrzewski, VG; Voth, GA; Salvador, P; Dannenberg, JJ; Dapprich, S; Daniels, AD; Farkas, O; Foresman, JB; Ortiz ,J V; Cioslowski, J; Fox, DJ. *Gaussian 09*. Revision A02; Gaussian, Inc. Wallingford, CT **2009**.

*Chapter 6B*

**Reaction of Azides with Olefinic  
Compounds**

---

**Abstract**

*Hydroxyl terminated polybutadiene (HTPB) was cured using a diazide 1,6-bis (azidoacetoyloxy) hexane (HDBAA) via a 1,3 -dipolar cycloaddition reaction between the azido group of HDBAA and double bonds in HTPB to form 1,2,3-triazolines in the presence of Cu(I) a catalyst. The mechanism of Cu(I) catalysed azide-alkene cycloaddition reaction was analysed by density functional theory (DFT) using model alkenes namely cis-3-hexene, trans-3-hexene and 2-methyl pentene. This way a new isocyanate free route was evolved for curing HTPB.*



## **6B.1.INTRODUCTION**

1,3 -dipolar cycloadditions are used extensively for the functionalization of polymers.<sup>1-4</sup> These reactions are categorized into a series of reactions named ‘click’ reactions, which is defined by a gain of thermodynamic enthalpy of at least 84 kJ/mol. These reactions are also characterized by high yield, simple reaction conditions, fast reaction times, and high selectivity. In spite of the numerous reports on cycloadditions in alkyne/azide click reactions<sup>5</sup> olefin/azide reactions remains a least explored area. This is of significance when extended to conventional binders used in solid propellant such as hydroxyl-terminated polybutadiene (HTPB).

Conventionally, HTPB is cured with diisocyanates to form polyurethane networks wherein the terminal hydroxyl groups in HTPB undergo reaction with polyisocyanates to form the polyurethane network. The urethane formation reaction is plagued by other side reactions as described previously and in this chapter, an alternate approach of exploiting Cu(I) catalysed azide-alkene 1,3 -dipolar addition reaction between an azides and the double bonds of HTPB is reported. The reaction yields 1,2,3- triazolines. Though azide-alkene reaction have been reported in literature<sup>6-7</sup> for many applications, the mechanism of the Cu (I) catalysed reaction has never been studied. Thus the chapter also reports the mechanism of this reaction validated using density functional theory (DFT) calculations in isomers of hexene (cis-3-hexene, trans-3-hexene and 2-methy pentene: model compound of HTPB) where 1,6-bis (azidoacetoxy) hexane (HDBAA), is the azide. To the best of our knowledge this the first ever report on an isocyanate free curing of HTPB using an azide.

## **6B.2. EXPERIMENTAL**

### **6B.2.1. Materials**

HTPB and cuprous iodide (CuI) were used for the study and their characteristics are described in Chapter 2. Acetonitrile is the solvent used for the study.

### **6B.2.2. Instrumental**

FTIR spectra were recorded and pyrolysis studies were conducted using a Thermo Electron Trace Ultra GC directly coupled to a Thermo Electron Polaris Q

(Quadrupole ion trap) mass spectrometer and SGE pyrolyser as described in Chapter 2.

### **6B.2.3. Synthesis and characterization of HDBAA**

HDBAA was synthesised following a two-step procedure as described in the previous chapter 6A.<sup>8-9</sup>

### **6B.2.4. Curing of HTPB using HDBAA**

HTPB was cured using HDBAA by mixing HTPB with HDBAA in the presence of CuI catalyst (1% by weight of binder) at a molar equivalence of 1:1 at 50<sup>0</sup>C in a rotary flash evaporator. The mixtures were then cast in aluminium moulds and cured at 60<sup>0</sup>C for 5 days.

### **6B.2.5. Computational calculations**

Geometry optimizations were performed with BLYP functional in conjunction with 6-31G(d,p) basis set as implemented in the program package Gaussian 09.<sup>10</sup> During geometry optimization no symmetry constraints were imposed. Default settings of SCF and geometry convergence criteria were used for all the calculations. No corrections were made for the basis set superposition errors (bsse). In general, DFT methods give negligible values for bsse. More accurate energies were obtained from single point calculations using BLYP/6-311++G(d,p) method and these energies were subsequently used in the analyses of chemical mechanisms. All transition states were confirmed by their characteristic single imaginary frequency in the normal vibrational mode.

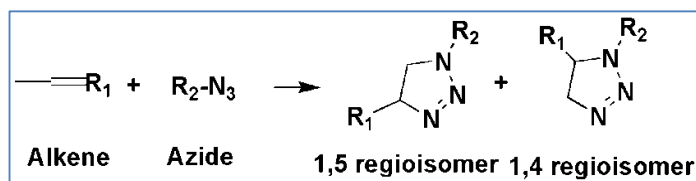
The mechanism of curing of HTPB was investigated using HDBAA as curing agent using hexene as model compound of HTPB for the analysis. The cis, trans, and vinyl form of olefin part in HTPB are represented by cis-3 hexene (Cis3H), trans 3-hexene (Trans3H) and 2-methyl 1- pentene (2MP) respectively.

## **6B.3. RESULTS AND DISCUSSION**

### **6B.3.1. Reaction of HDBAA with HTPB**

1,3 -dipolar cycloaddition between an azide and alkene results in formation 1,4 and 1,5 regioisomers of 1,2,3-triazoline as given in Scheme 6b.1. An azide group of a compound like HDBAA can undergo reaction with HTPB to form triazoline

networks as shown in Fig 6b.2. The reason for not exploring the reaction mechanism of copper catalysed azide-alkene reaction may be due to the fact that triazoline differs markedly in the stability as a function of the substituent groups that are attached. Their isolation is also reported to be challenging.<sup>6</sup>



*Scheme 6b.1* Azide-alkene 1,3 -dipolar cycloaddition

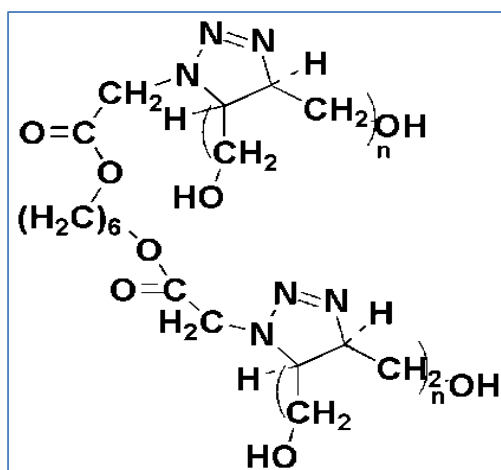


*Figure 6b.1.* HTPB and HDBAA crosslinked to yield triazoline

### 6B.3.2. Uncatalysed cycloaddition of HDBAA with hexene

The chemical properties of azides can be explained by the mesomeric structures shown in Figure 6b.2. The electronic effects of the alkene substituent on the orientation of azide is well studied in literature and in general, the strained and electronically activated alkenes display faster reactions with azides.<sup>8-9</sup> Except in cases where overriding steric effects operate, azide addition to alkenes has always been observed to take place in a Markownikoff's fashion initiated by electrophilic attack by the terminal azide nitrogen on the alkene. In the case of HTPB-HDBAA addition reactions, the activating factor is the electron withdrawing acetate moiety in the azido compound.

HTPB has a zig-zag molecular arrangement due to its cis-trans-vinyl types of double bonds as given in Fig 6b.3. The cis, trans and vinyl form of HTPB are represented by cis-3 hexene (cis3H), trans 3-hexene (trans 3H) and 2-methyl 1-pentene (2MP) respectively (Fig 6b.4) and the optimised structures of these compounds are given in Fig.6b.4.

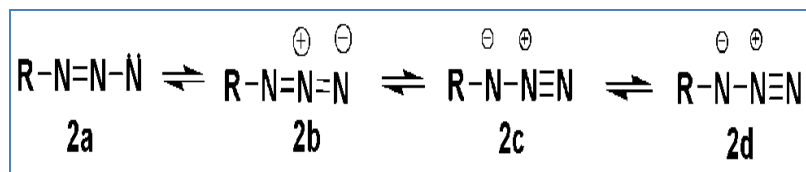


Fig 6b.2. Mesomeric structure of azide

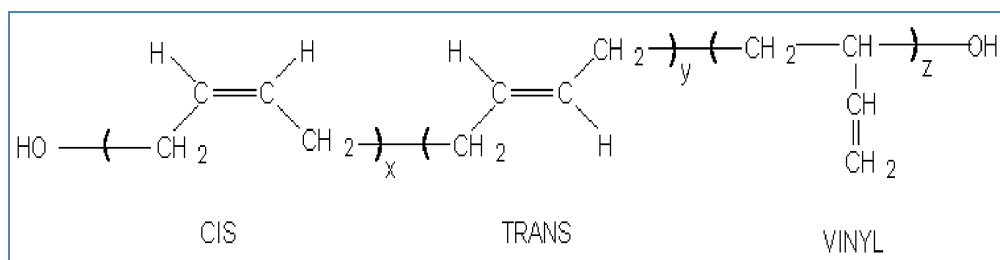


Fig 6b.3. Types of double bonds in HTPB

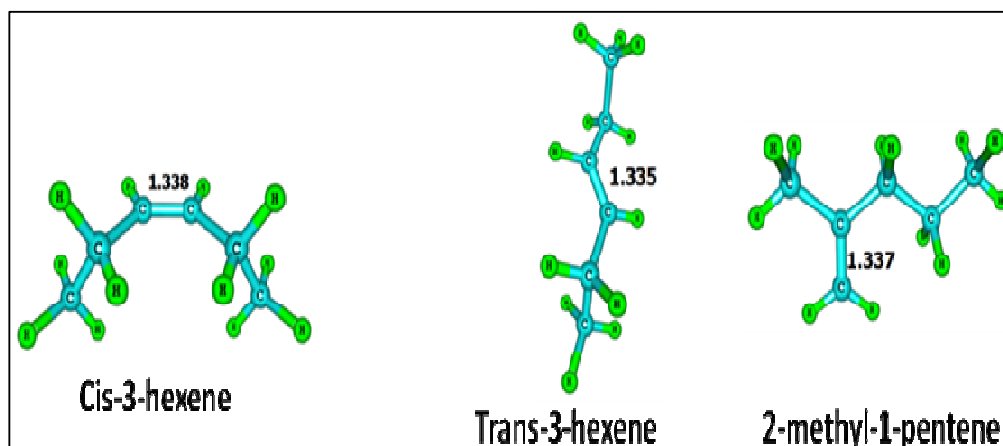


Fig. 6b.4 Optimized Structure of cis-3 hexene, trans 3-hexene, 2methyl pentene

The thermal cycloaddition of organic azide to olefin (cis3H, trans3H, 2MP) allows the synthesis of 1, 2, 3 triazolines. The computed reaction energy and activation barriers for hexene-HDBAA reactions are given in Table 6b.1. The olefin bond changes to saturated bond. Consequently the bond length changes from 1.384 to 1.553 Å. (Fig.6b.5)

**Table 6b.1.** Computed heat of reaction and activation barrier of alkene-HDBAA reactions

Compounds with HDBAA	Heat of reaction (kJ/mol)		Activation Barrier (kJ/mol)
	Monoadduct	Diadduct	Monoadduct
Cis3H	-85.7	-191.0	84.8
Trans3H	-96.1	-210.3	76.0
2MP (1,4 addition)	-109.5	-201.1	87.8
2MP (1,5 addition)	-81.1	-177.7	72.7

The computed parameters suggest that all addition reactions are exothermic in nature. In general, the heat of reaction of monoadduct formation ranges from 81.1 to 109.5 kJ/mol.

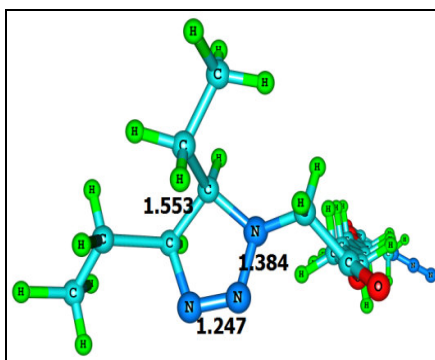


**Fig 6b.5.** Transition state for Monoadduct of cis-3-hexene with HDBAA

Among various isomeric double bonds, trans3H is associated with relatively more negative heat of reaction as well as a lower activation barrier of 76 kJ/mol. The unreacted azide in the monoadducts can further undergo cycloaddition with available double bonds. The predicted heat of reaction of diadduct clearly suggests a facile reaction with HTPB. The interactions of hydroxyl end groups do not affect the computed energies of addition reactions. Since the major part of olefin content in HTPB is trans type, theoretical studies predict HDBAA as a viable curative for HTPB type polymers on thermal activation.

The unsymmetrical structure in 2MP can give either 1, 4 adduct or 1,5 adduct as described in the Figure 6b.6. Although 1,3-dipolar cycloaddition of azides to alkene is classified as a concerted reaction, the distinct preference for the orientation of addition is explained by the transition state depicted. In the cycloaddition, the formation of bond C4-N3 is considered to proceed more rapidly than bond C5-N1 in the 1, 5 addition pattern. Substituents on C5, which stabilize the incipient positive charge at this position, should facilitate addition. The lowest activation barrier of 72.7 kJ/mol obtained for 1,5 regioisomer is explained by the higher stabilization of the positive charge at the C5 compared to the C4. In the case of 1, 4 addition, the formation of N3- C5 bond, induces positive charge on unsubstituted CH2 which leads to a higher activation barrier of 87.8 kJ/mol. The geometrical parameters of transition states are comparable to that of alkyne-azide cycloaddition reactions.<sup>11-13</sup>

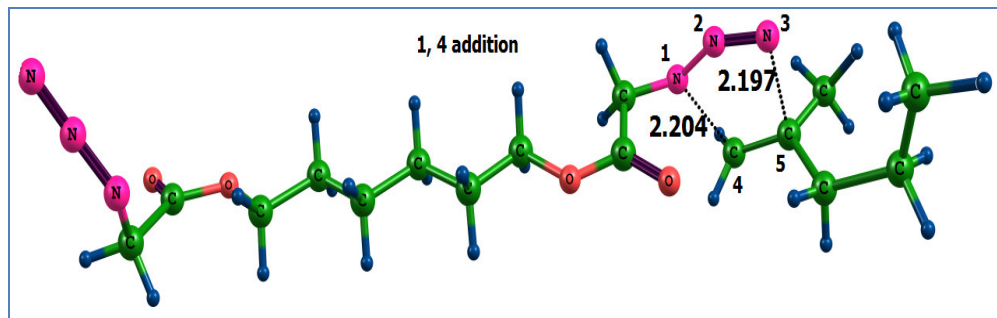


Fig 6.b.6.a

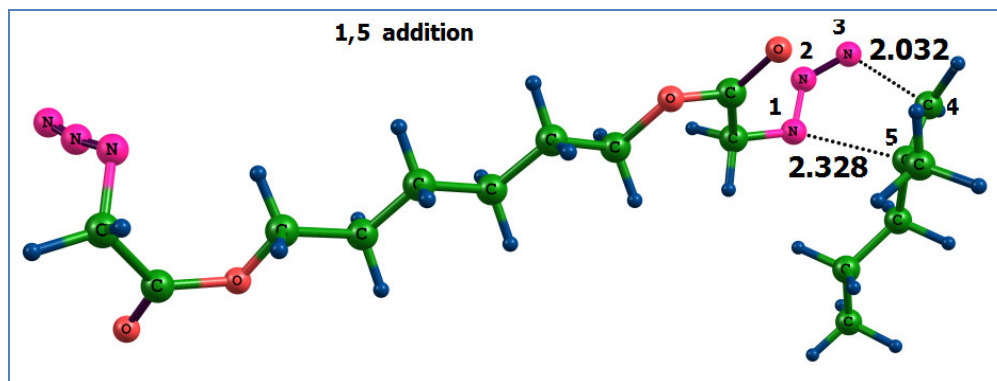


Fig 6b.6.b.

**Figure 6.b. 6.** Transition states located for a) 1, 4 and b) 1,5 cycloadditions of 2-methyl pentene.

### 6B.3.3. Catalyzed cycloaddition of HDBAA with Hexene

The catalytic effect of CuI in the curing reaction of HTPB was analyzed using solvated Cu(I) ions represented by Cu(CH<sub>3</sub>CN) as model compound. As a first

step, Cu acetonitrile complex might be coordinating with the olefin. A general description on metal olefin coordination is made using Dewar Chatt- Duncanson model<sup>14</sup> as given in Figure 6b.7. Though there are reports on copper mediated azide-alkene reaction resulting in triazolines<sup>15-18</sup>, the mechanism of this reaction has not been reported previously.

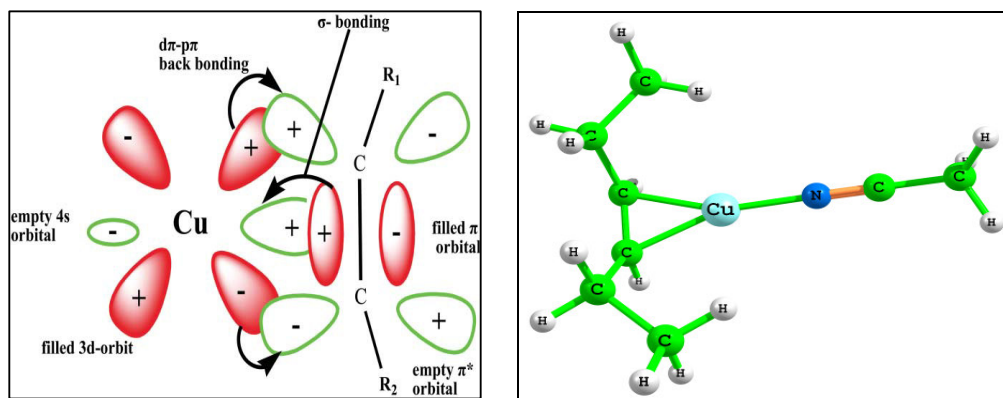


**Figure 6b.7** Schematic orbital description of Cu-alkene coordination (b) optimized structure of Cu [ CH<sub>3</sub>CN, Cis3Hexene ]<sup>+</sup>

The  $\pi$ -bond consists of two components: one is arising from overlapping of the occupied olefin  $\pi$  orbital and the unoccupied 4s<sup>0</sup> orbital of the Cu (I) atom which is dominant in the bond, and the other is formed by the back donation from the 3d<sup>10</sup> Cu(I) orbitals to the unoccupied antibonding orbital of the alkene-group. The computed energy parameters suggest that the olefin complexes of Cu(I) is exothermic by 300.9 kJ/mol. Hence the intermediate ternary complex depicted can be formed from hexene Cu(I) complex intermediate complex. (Fig 6b.8) In the identified ternary intermediate Cu acetonitrile complex acts as a link between the reactants, trans-3-hexene and HDBAA (Fig 6b.8).

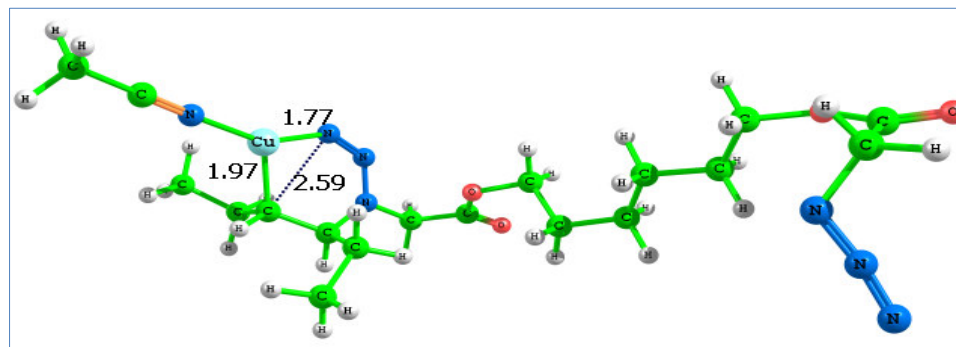
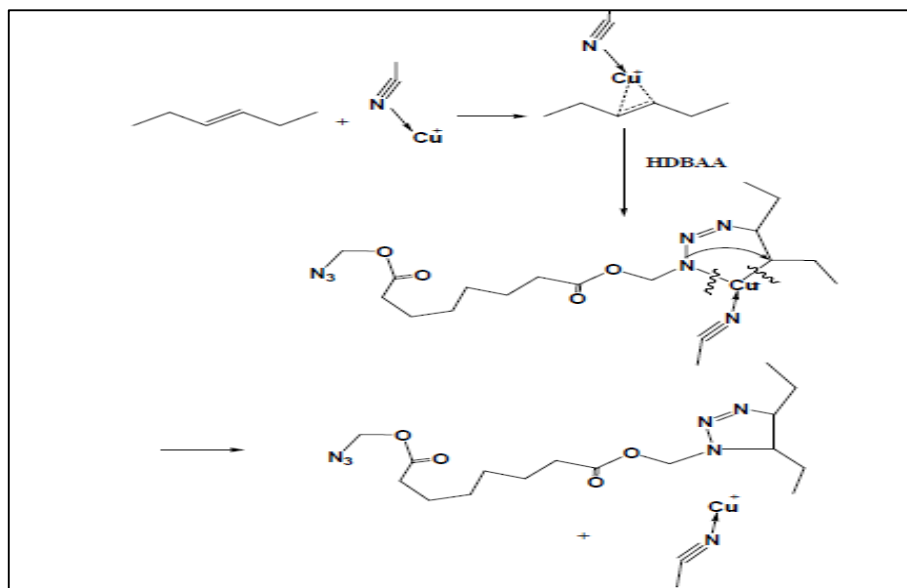


**Figure 6b.8.** Ternary complex of Cu(I) acetonitrile, trans-3- hexene and HDBAA.

The formation of the above complex is found to be exothermic by 74.4 kJ/mol for trans3H in first pathway mechanism. This complex regenerates the catalyst forming the final cured product by passing through the transition state shown in Figure 6b.8. The computed activation barrier for this process is 21.3 kJ/mol (Table 6b.2). The easy decomposition of the complex to the product of triazolines is well reflected in the calculated activation barriers which range from 21.3 – 36.4 kJ/mol depending on the type of olefin. This is much less than the computed activation barrier of ~ 84 kJ/mol in the uncatalysed system. The overall reaction of Cu(I) catalyzed HDBAA addition to hexene reaction pathway can be summarized as in scheme 6b.2.

**Table 6b.2** Computed energy parameters for the formation of Cu [CH<sub>3</sub>CN, Hexene, HDBAA]<sup>+</sup> and its decomposition to triazolines

Olefin	Heat of reaction of Cu [CH <sub>3</sub> CN, Hexene, HDBAA] complex ( kJ/mol)	Activation barrier (kJ/mol)
Trans 3H	-74.4	-21.3
Cis 3H	-53.9	-36.4
2MP (1,4)	-56.4	-33.0
2MP (1,5)	-67.3	-25.5



**Scheme 6b.2.** Proposed reaction pathway for Cu(I) catalyzed HTPB curing using HDBAA.



The same strategy was adopted for curing HTPB using HDBAA through the unsaturation in HTPB in the presence of catalyst CuI, resulting in the formation of triazoline. The formation of triazoline was confirmed by FTIR analysis of the cured product (Fig 6b.9a and b) where the characteristic peak corresponding to the N=N stretching of triazoline ring ( $1591\text{ cm}^{-1}$ ) was detected with disappearance of peak at  $2095\text{ cm}^{-1}$  corresponding to azide group. Pyrolysis GC-MS studies of the cured polymer, (Fig 6b.10) at  $300^\circ\text{C}$ , showed elimination of  $\text{N}_2$  (RT 1.35), confirming triazoline formation. The elimination of nitrogen from triazoline resulting in aziridine proceeds through the reaction pathway given in Scheme 6b.3. In literature synthesis of 1,2,3-triazole from azide-alkene reaction has been reported<sup>19-20</sup>. However, the mechanism was not elucidated.

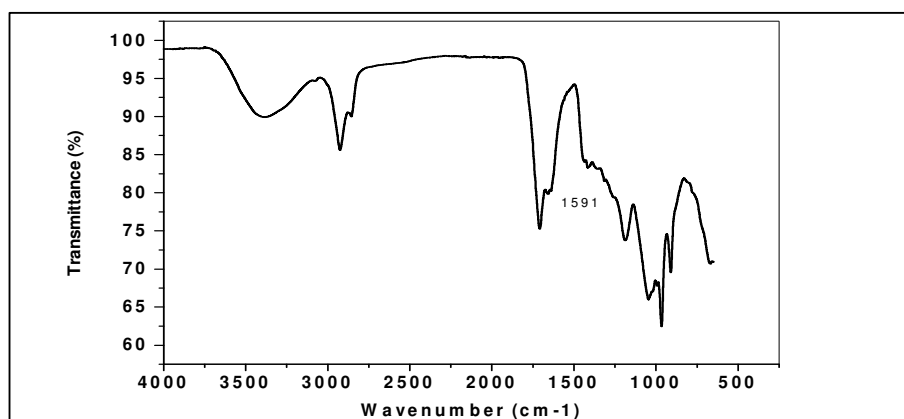


**Figure 6b.8** FTIR spectra of HTPB-HDBAA Cured polymer (ATR)

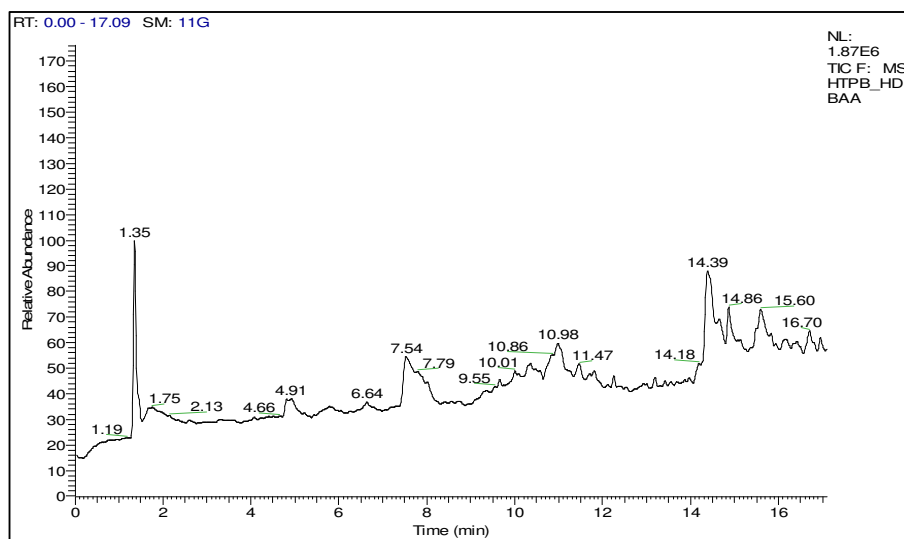
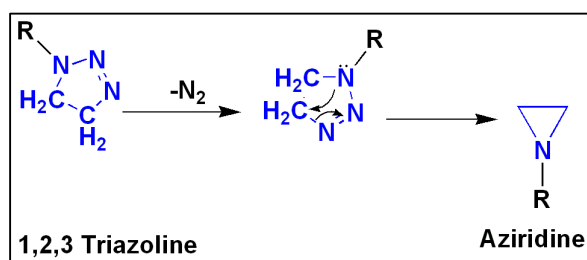


**Fig 6b.10.** Pyrogram of HTPB cured using HDBAA ( $300^\circ\text{C}$ )



*Scheme 6b.3 Elimination of nitrogen from triazoline*

## 6B.4. CONCLUSIONS

The computed energetic properties of hexene-HDBAA reactions suggest that an isocyanate free curing of HTPB is feasible using HDBAA, on thermal activation ii) among the isomeric olefin bonds, azide addition to trans type bonds are energetically more favourable (iii) when Cu(I) salt is used as catalyst the activation barrier reduces from  $\sim 84$  kJ/mol to  $\sim 38$  kJ/mol suggesting the feasibility of curing of HTPB under ambient temperature. HTPB was thus cured through an isocyanate free route by reaction with the azide HDBAA to yield triazoline crosslinked polymer network. The formation of triazoline was confirmed using FTIR and pyrolysis GC-MS studies. This reaction supports the observation reported in the chapter 4 where azide terminated HTPB undergoes self curing reactions. The higher crosslink density observed on co-curing of propargyl terminated HTPB with azide polymers (in chapter 4 and 5) is also due to this cycloaddition process. This recognition opens the possibilities for realising molecules, cross linking polymers and synthetic openings.

**6B.5. REFERENCES**

1. Itsuno, S. *Progr. Polym. Sci.* **2005**, 41, 540-547
2. Trost, BM; Fleming, I; Semmelhack, M. *Comprehensive organic synthesis, Addition and Substitution at C-C,  $\pi$ -bond*, Vol. 4, Pergamon Press, Netherlands, **1991**.
3. Ru, K; Braun, CK; Freysoldt, THE; Wierschem, F. *Chem. Soc. Rev.* **2005**, 34, 507-511
4. Goodall, GW; Hayes, W. *Chem. Soc. Rev.* **2006**, 35, 280-289
5. Binder, WH; Sachsenhofer, R. *Macromol. Rapid Commun.*, **2007**, 28, 15-54
6. Pearson, AWH. *The chemistry of heterocyclic compounds, Vol.59, Synthetic applications of 1,3 -dipolar cycloaddition chemistry towards heterocycles and natural product*, edited by, John Wiley & Sons. Inc, **2002**.
7. Manzara, AP. *Azido polymers having improved burn rate*, US 5681904 A, **1996**.
8. Ou, Y; Chen, B; Yan, H; Jia, H; Li, J; Dong, S. *J. Propulsion and Power*, **1995**, 11, 838-842.
9. Agrawal, JP; Hodgson, R. *Organic Chemistry of Explosives*, John Wiley & Sons Ltd, England, **2007**, p. 333.
10. Frisch, M; Trucks, GW; Schlegel, HB; Scuseria, GE; Robb, MA; Cheeseman, JR; Scalmani, G; Barone, V; Mennucci, B; Petersson, GA; Nakatsuji, H; Caricato, M; Li, X; Hratchian, HP; Izmaylov, AF; Bloino, J; Zheng, G; Sonnenberg, JL; Hada, M; Ehara, M; Toyota, K; Fukuda, R; Hasegawa, J; Ishida, M; Nakajima, T; Honda, Y; Kitao, O; Nakai, H; Vreven, T; Montgomery, J; Peralta, JE; Ogliaro, F; Bearpark, M; Heyd, JJ; Brothers, E; Kudin, KN; Staroverov, V; Kobayashi, R; Normand, J; Raghavachari, K; Rendell, A; Burant, JC; Iyengar, SS; Tomasi, J; Cossi, M; Rega, N; Millam, J M; Klene, M; Knox, J E; Cross, JB; Bakken, V; Adamo, C; Jaramillo, J; Gomperts, R; Stratmann, RE; Yazyev, O; Austin, AJ; Cammi, R; Pomelli, C; Ochterski, JW; Martin, RL; Morokuma, K; Zakrzewski, VG; Voth, GA; Salvador, P; Dannenberg, JJ; Dapprich, S; Daniels, AD; Farkas, O; Foresman, JB; Ortiz, J V; Cioslowski, J; Fox, DJ. *Gaussian 09. Revision A02*; Gaussian, Inc. Wallingford, CT **2009**.
11. Agard, NJ; Prescher, JA; Bertozzi, CR. *J. Am. Chem. Soc.* **2004**, 126, 15046-15047
12. Himo, F; Lovell, T; Hilgraf, R; Rostovtsev, VV; Noodleman, L; Sharpless, KB; Fokin, VV. *J. Am. Chem. Soc.* **2005**, 127, 210-216
13. Lopez, SA; Houk, KN. *J. Org. Chemistry*, **2013**, 78, 1778-1783
14. Catt, J; Duncanson, LA. *J. Chem. Soc.* **1953**, 21, 2939-2947
15. Yang, CH; Lee, LT; Yang, JH; Wang, Y; Lee, GH. *Tetrahedron*, **1994**, 50, 12133-12140
16. Prager, RH; Razzino, P. *Aust. J. Chem.* **1994**, 47, 1375-1382
17. Anderson, GT; Henry, JR; Weinreb, SM. *J. Org. Chem.*, **1991**, 56, 6946-6952
18. Husinec, S; Porter, A; Roberts, JS; Strachan, CH. *J. Chem. Soc. Perkin Trans.* **1984**, 1, 2517-2523.

19. Miguel, ID; Herradón, B; Mann, E. *Advanced Synthesis & Catalysis*, **2012**, 354, 1731–1736
20. Janreddy, D; Kavala, V; Kuo, C; Chen, W; Ramesh, C; Kotipalli, T; Kuo, T; Chen, M; He, C; Yao, C. *Advanced Synthesis & Catalysis*, **2013**, 355, 2918–2927

SUPPORTING INFORMATION

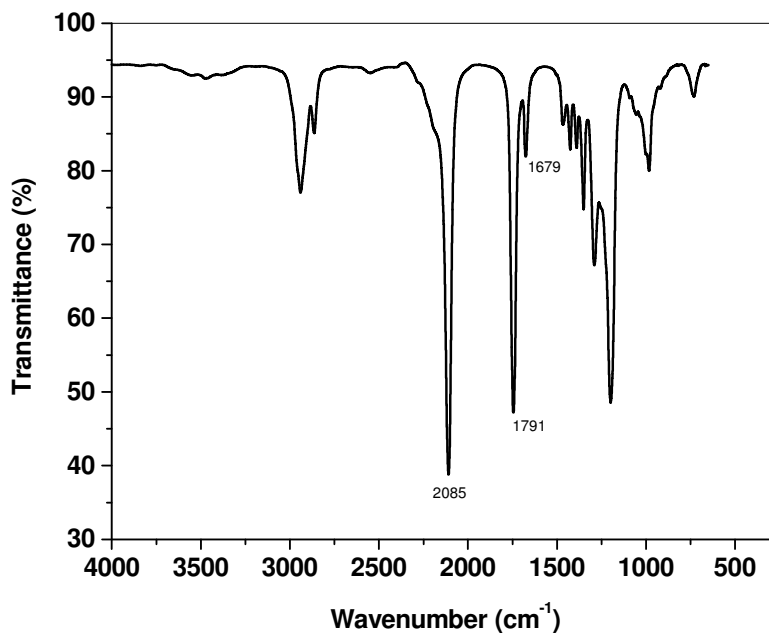


**Fig.6B.1A.** *FTIR spectra of mixture of HTPB with HDBAA (Before curing), NaCl plates*

*Chapter 7*

**Summary and Conclusions**

---

This chapter highlights summary of the important conclusions drawn from the research work. Solid propellants continue to be indispensable part of launch vehicles and missiles owing to their high reliability, ease of manufacturing, high thrust levels achieved etc. Lot of research efforts has been dedicated for the continual improvement in performance of solid propellants by means of improving the oxidizers and binders. Such innovations are focused towards realizing high performance and eco friendly propellants. The search for environment friendly molecules is aimed at the development of chlorine-free propellant compositions to alleviate problems associated with the much discussed perchlorate and hydrochloric acid contaminations.

Development of new generation chlorine free, high energy oxidizers like ammonium dinitramide (ADN) /hydrazinium nitroformate (HNF) have the added advantage of imparting high performance in terms of specific impulse with various solid propellant binders like hydroxyl terminated polybutadiene (HTPB), glycidyl azide polymer (GAP), polytetramethylene oxide (PTMO) etc.

In all composite solid propellants currently in use, polymers perform the role of a binder for the oxidiser, metallic fuel and other additives. It performs the dual role of imparting dimensional stability to the composite and provides structural integrity and good mechanical properties to the propellant. This is established by the reaction of the hydroxyl groups with suitable curative that gives rise to a crosslinked three dimensional network capable of holding together the other ingredients in solid propellants

HTPB, GAP and PTMO being hydroxyl telechelics, are conventionally cured with isocyanates like tolylene diisocyanate (TDI) or isophorone diisocyanate (IPDI) to form polyurethane networks. However, curing with an isocyanate leading to polyurethane has the inherent drawback of extraneous reaction with moisture causing evolution of carbon dioxide during curing that induces voids in the system. The inherent incompatibility of energetic oxidizers like ammonium dinitramide (ADN) and hydrazinium nitroformate (HNF) with isocyanates also warrants an isocyanate-free cure chemistry to be evolved for processing high performance, energetic composite solid propellants.

Alkyne-azide and alkene-azide ‘click reaction’ through a 1, 3-dipolar cycloaddition reaction forms the respective 1, 2, 3-triazole and 1, 2, 3 triazoline networks. The chemistry is relatively simple, needs low activation, catalysable and less prone for side reactions. Thus, the curing of GAP, PTMO and HTPB through ‘click chemistry’ offers an alternate route for processing of solid propellants wherein, the matrix resins and their cured networks are endowed with improved processability, superior mechanical properties, better thermal stability and improved ballistic properties in view of the higher heat of decomposition of the triazole/triazoline groups. In the present thesis, ‘Click chemistry’ has been explored for obtaining binders crosslinked through triazole/triazoline networks. Thus curing of GAP binder and that of HTPB and PTMO after functional modification is discussed in the thesis after a detailed literature survey in Chapter 1 and description of the experimental methodologies in Chapter 2.

Chapter 3 deals with GAP binder wherein GAP is crosslinked through ‘Click chemistry’ by reacting with the azide group with alkyne containing compounds to yield triazoles. For this, various alkynyl compounds including bis propargyl succinate (BPS), bis propargyl adipate (BPA), bis propargyl sebacate (BPSc.) and bis propargyloxy bisphenol A (BPB) were synthesized and characterized. The curing of the systems was monitored by differential scanning calorimetry (DSC) and the derived kinetic parameters were used for predicting the cure profile of the system. The mechanism of the curing reaction of GAP with these alkynyl compounds was studied using appropriate model compound (2-azidoethoxyethane, AEE) and the reaction mechanism has been modelled using density functional theory (DFT).

DFT studies done using model compound implied marginal preference for 1, 5 addition over 1, 4 addition. Rheokinetic studies indicated that the use of a catalyst enhances the rate of reaction substantially and leads to complete curing, as indicated by a higher storage modulus. For the GAP-triazole systems, the tensile strength and modulus increased while elongation decreased on increasing the crosslinking as expected. The properties were compared with those of polyurethane derived by reaction of GAP with TDI. Dynamic mechanical analysis (DMA) of the GAP-triazole exhibited biphasic transitions corresponding to both polyether back bone in



GAP and triazole groups through crosslinking of azide with alkynes. The thermal decomposition studies indicate higher thermal stability for triazole-crosslinked GAP in comparison to GAP-urethane. Pyrolysis gas chromatography –mass spectroscopy (GC-MS) and TG-MS studies were used for elucidating the mechanism of thermal decomposition, which indicated that the decomposition initiates through the cleavage of ester groups of the curing agent (BPSc) followed by the scission of the triazole groups, substantiating the superior thermal stability of triazole crosslinks. Propellant level studies of GAP-triazole indicated better processability for the propellant, good mechanical properties, higher thermal stability as well as better safety characteristics for the cured propellant based on GAP-AP in comparison to GAP urethanes.

In Chapter 4, the concept of ‘click chemistry’ was further extrapolated to the versatile solid propellant binder, HTPB. For this, HTPB was chemically transformed to derive azide terminated polybutadiene (AzTPB) and propargyl terminated polybutadiene (PrTPB) through a urethane group. Both the polymers were characterized by spectroscopic and chromatographic techniques. The blend of these two polymers underwent curing under mild temperature (60°C) conditions predominantly through 1, 3-dipolar cycloaddition reaction. The cure reaction was monitored using Fourier transform infrared spectroscopy (FTIR), DSC and the derived kinetic parameters including activation energy and rate constant were used for predicting the cure profile at a given temperature. Properties of the cured triazole polymer network were evaluated and compared with conventional polyurethane networks prepared from HTPB cured using tolylene diisocyanate (TDI) as curing agent. Mechanical properties of the triazole containing polybutadiene network were superior to those of polyurethanes with similar backbone. Closer evaluation of crosslinking reaction revealed that additional reactions involving azide groups and the ethylenic unsaturation in polybutadiene backbone resulting in triazoline formation occurs in conjunction with triazoles. The cured triazoline-triazole polymer network exhibited biphasic morphology in contrast to the polyurethane which exhibited a single transition. This was corroborated by associated morphological changes as observed by Scanning Probe Microscopy (SPM). Thermal decomposition of the cured PrTPB-AzTPB polymer was investigated using TGA, pyrolysis GC-MS

and TG-MS techniques. The decomposition is found to occur through two-stage mechanism wherein the cleavage of the urethane groups (used for end capping) occurs initially. The cleavage of urethane groups triggers the decomposition of the triazole groups also, unlike GAP-triazoles. The second stage decomposition leads to the degradation of the polybutadiene backbone. The addition of AP does not alter the decomposition pattern and gives out products that are similar to those reported in literature.

Rheological studies revealed that curing through the 1, 3 dipolar addition imparts longer 'pot-life' to polybutadienes in contrast to conventional curing through the urethane route. Thus, propellant level studies using this binder indicated superior mechanical properties, with of insensitivity to moisture, improved 'pot-life' and comparable burn rate with lower pressure index to that of conventional HTPB urethane propellants.

While Chapter 4 describes that HTPB was end functionalized with propargyl group through an isocyanate route, the fifth chapter describes the direct etherification of the terminal hydroxyl groups of HTPB and PTMO to end cap with propargyl groups. Both the polymers were cured by 'Click Chemistry' to form triazole network using an azide polymer viz. glycidyl azide polymer by 'click chemistry' in the presence of cuprous iodide as catalyst. The associated cure profiles were generated using DSC and the related kinetic parameters of curing were derived. The phase separation in PTPB-GAP system restricts the possibility for varying the alkyne-azide molar stoichiometry beyond 1:0.1. However, in the case of PTMP-GAP system, maximum properties could be achieved for an alkyne-azide molar stoichiometry of 1:1. Rheological studies revealed that the curing through 'click chemistry; imparts longer 'pot life' to the system. Thermal decomposition mechanism of the cured polymers as well as the cured polymer-AP (PTPB and PTMP) system was elucidated by using TGA, TG-MS and Pyrolysis GC-MS studies. The decomposition pattern of PTPB is similar to that reported literature. However, the presence of AP causes the formation of cyclic and aromatic products during decomposition of PTMP triazoles. Propellant level studies using these binders with ammonium perchlorate as oxidiser were also carried out. It was

observed that the mechanical properties and burn rate characteristics of the propellants are comparable to HTPB-urethane based systems with the advantage of improved 'pot-life'.

The azide containing molecules are potential additives or curatives in propellants binder systems in solid propellants and it was of interest to study their decomposition mechanism. In this background, the work in the sixth chapter has been subdivided into two sections. In the first part, the synthesis, characterization and thermal decomposition mechanism of a diazido ester 1, 6 –bis (azidoacetoxy) hexane (HDBAA) have been reported. In the second part of the chapter, the possibility of using this diazido ester as a curing agent for alkene and alkyne - hydrocarbon binders in composite solid propellant has been explored. This study revealed that for curing polymers like HTPB by 1, 3-dipolar addition, triple bonded functional groups are not mandatory. They can be cured through reaction of unsaturation with azide though it is a slow process.

The thermal decomposition characteristic of HDBAA was investigated by thermogravimetric studies. The mechanism of decomposition was elucidated using pyrolysis gas chromatography-mass spectrometric techniques. At 230°C, HDBAA preferentially forms the corresponding diimine by elimination of N<sub>2</sub>. Decomposition of the diazido ester was complete, at 500°C yielding N<sub>2</sub>, CO, CH<sub>2</sub>NH and HCN with the concurrent formation of diols and dienes. The experimental findings were rationalized through density functional theory (DFT) based computational analysis.

In the subsequent section, DFT methods were employed to understand the reaction mechanism through olefin-azide 'click reaction' resulting in 1,2,3 triazoline using isomers of hexene (cis-3-hexene,trans-3-hexene and 2-methyl pentene) as model compounds of HTPB with HDBAA as curing agent. The computed energetic properties of hexene-HDBAA reactions suggested that an isocyanate-free curing of HTPB is feasible using HDBAA, on thermal activation. Among the isomeric olefin bonds, azide addition to trans type bonds is energetically more favourable for an uncatalysed reaction. In the case of vinyl type double bonds, isomeric 1, 4 and 1, 5 type addition products are predicted where the formations of latter possess the lowest activation barrier of 72.7 kJ/mol vis-a-vis 87.8 kJ/mol for the 1, 4 addition.

The catalytic activity of Cu(I) salts in the reaction is examined and a lower energy pathway is identified for all the isomeric double bonds. The presence of Cu (I) salts as catalysts reduces the activation barrier from ~85 kJ/mol to ~21 kJ/mol suggesting the feasibility of curing of HTPB under ambient temperature.

Important conclusions drawn from this thesis work are

1. GAP can be crosslinked through 1, 3-dipolar addition of the azide groups to various aliphatic and aromatic alkynes. DFT studies done using model compound implied marginal preference for 1, 5 addition over 1, 4 addition for the uncatalysed reaction.
2. GAP-triazole based networks exhibited biphasic transitions. Rheokinetic studies indicate that catalyst enhances the rate of reaction substantially and leads to completion of curing.
3. Thermal decomposition studies indicate higher thermal stability for triazole crosslinked GAP in comparison to urethane. Mechanism of decomposition was also elucidated.
4. The propellant level studies of GAP-triazole with AP as oxidizer indicate better processability for the propellant with superior mechanical properties, thermal stability as well as safety characteristics than GAP urethanes.
5. Propargyl and azide end capped polybutadienes were synthesised for the first time and characterised. Curing of these two polymer systems was effected through '1,3-dipolar addition' to form triazole –triazoline network.
6. 'Click chemistry' offers a versatile means for crosslinking. The propellant level studies of the polybutadiene containing triazole-triazoline networks with AP as oxidizer indicate better processability, good mechanical properties and comparable burn rates with respect to HTPB-AP propellant.
7. Curing of the propargyl oxy telechelic polymer systems was effected through 'click mechanism' by a polyazide, to form triazoles. Detailed characterisations

of these triazoles were done with respect to the curing kinetics, thermal decomposition, mechanical and dynamic mechanical properties.

8. The propellant based on the new binders in combination with AP as oxidiser offer better performance in terms of evolving large volumes of low molecular weight gaseous products. The propellants based on these systems also have lower viscosity and lower rate of viscosity build-up with acceptable mechanical properties and burn rates.
9. Thermal decomposition studies of a diazide ester HDBAA provided insight into the thermal decomposition mechanism of HDBAA, as well as on the feasibility of curing of HTPB through triazole networks.

This thesis brings to light the fundamental aspects of functional modification and curing of three propellant binder's viz. GAP, HTPB and PTMO by 'click chemistry' approach. The mechanism of curing and thermal decomposition of these binders has been elucidated. Comparison of mechanical and dynamic mechanical properties as well as rheological characteristics has been done with conventional polyurethane systems both in polymer well as in composite propellant. This work also conveys that 'Click chemistry' offers an alternate route for processing of propellants, wherein the cured resins offer insensitivity to moisture resulting in defect free propellants, improved 'pot-life', better thermal stability and mechanical properties and possess higher ballistic properties in view of the favorable enthalpy of decomposition.

### **OUTLOOK FOR FUTURE WORK**

Development efforts by international space community are focused on reducing cost and increasing performance while maintaining or improving the mechanical and ballistic properties and safety characteristics of the propellant. New propellants are required not only to increase the available energy of a propellant and raise the specific impulse (Isp), but also to meet environmental constraints and improved safety. There is scope for achieving the goal by innovation in propellant binders as the current approaches based on propellants are risk assisted. For solid propellant motors, the goal is to improve the overall performance by 5 to 8% while

reducing the adverse environmental impact. ADN (ammonium dinitramide) and hydrazinium nitroformate (HNF) are powerful chlorine free oxidisers which have substantially higher heat of formation than AP leading to superior Isp (10-15 s higher than HTPB-Al-AP) in combination with energetic polymers.

Specific areas that need further attention are:

1. Studies of 'click cured' propellants with ADN/HNF as oxidizers wherein the approach of 'green chemistry' can be exploited by using a non-isocyanate route.
2. Improving the mechanical properties of the triazole-triazoline based binders by design of suitable crosslinkers.
3. Synthesis and characterization of triazole based energetic plasticisers in place of non-energetic plasticisers which give immense scope for lowering the glass transition, viscosity and improving the processability of the propellant with enhanced mechanical properties as well as ballistic properties.

## LIST OF PATENTS/PUBLICATIONS/CONFERENCE PAPERS

### Patents

1. S.Reshmi, S.Gayathri and C.P.Reghunadhan Nair, "A process for high burn rate solid propellants based on azide polymer binder crosslinked through triazoles" (Filed).
2. S.Reshmi and C.P.Reghunadhan Nair, "Telechelic binders with 'Clickable groups' and solid propellants thereof" (to be submitted)

### Publications

1. S.Reshmi, K.P.Vijayalakshmi, Deepthi Thomas, E.Arunan and C.P.Reghunadhan Nair, "Glycidyl Azide Polymer Crosslinked Through Triazoles by Click Chemistry: Curing, Mechanical and Thermal Properties" **, Propellants, Explosives, Pyrotechnics**, Volume 38, Issue 4, 525-532, 2013
2. S.Reshmi, K.P.Vijayalakshmi, Deepthi Thomas, Benny.K.George and C.P.Reghunadhan Nair, "Thermal Decomposition of a Diazido Ester : Pyrolysis GC-MS and DFT study, **J. Analytical and Applied Pyrolysis**, 104, 603-608, 2013
3. S.Reshmi, E.Arunan and C.P.Reghunadhan Nair, "Azide-Alkyne Polybutadienes: Synthesis, Crosslinking and Propellant Studies", **Industrial and Engineering Chemistry**, 453, 16612-16620, 2014

### Conference Papers

1. **S.Reshmi**, C.Sreekumaran Nair and C.P.Reghunadhan Nair "Mechanical and Thermal Characterization of Glycidyl Azide Polymer Based 1,2,3 Triazole Networks" , MACRO-2010, New Delhi.
2. S.Reshmi, Vijayalakshmi.K.P, G.Viswanathan Asari, Benny.K.George, and C.P.Reghunadhan Nair, "Glycidyl Azide Polymer Cured with Bis Propargyl Oxy Bisphenol A: Rheological, Thermal and DFT Studies" Hemce 2011, TBRL, Chandigarh.
3. Reshmi, S.Gayathri and C.P.Reghunadhan Nair, "Triazole Crosslinked Propargyl Terminated Polytetramethylene as Solid Propellant Binder: Thermal and Mechanical Characterisation" MACRO-2013, Bangalore
4. Vijayalakshmi.K.P, S.Reshmi, Benny.K.George, and C.P.Reghunadhan Nair "Theoretical studies on curing reactions of HTPB using azido-functionalized, curing agent, HEMCE-2014, Thiruvananthapuram.
5. S.Reshmi, Vijayalakshmi K.P, R.Sadhana, Elizabeth John, Benny.K.George and C.P.Reghunadhan Nair, "Mechanistic Insights into Azide-Hydroxyl Competitive Reactions with a Diisocyanate in Glycidyl Azide Polymer" HEMCE-2014, Thiruvananthapuram.